Th-Pos1

SIGNAL TRANSDUCTION ACROSS VOLTAGE-DEPENDENT ION CHANNELS OF ALAMETHICIN IN THE PRESENCE OF EXTERNAL NOISE. ((S.M. Bezrukov[1] and I. Vodyanoy[1,2])) [1]DCRT & NIDDK, NIH, Bethesda, MD 20892; [2]ONR, Europe, London, NW1 5TH, UK

Voltage-dependent ion channels of alamethicin reconstituted into an artificial lipid bilayer membrane that separates two electrolyte solution baths are studied from the point of view of signal transduction. It is demonstrated that such a system is a nonlinear amplifier that can amplify low-frequency periodic signals of several millivolts with a gain factor of 20 - 30 dB. The effects of external electrical input noise on the system gain and the output signal-to-noise factor were studied. Our results show that over a certain range of parameters the voltage-dependent ion channels are robust to the input noise - addition of 10 mV rms white noise to a 5 mV sine-wave signal at the input increases output signal by about 20 dB conserving, or even slightly increasing, the signal-to-noise factor at the system output. Alamethicin channels in a lipid bilayer seem to be the simplest model found so far for studies of mechanisms of biological signal transduction. They show important features of signal amplification and tolerance to external noise sources.

Th-Pos2

CORRELATIONS OF THE BEHAVIOR OF CONDUCTANCE BURSTS OF ALAMETHICIN SINGLE CHANNELS WITH THE TIME BETWEEN BURSTS. ((S.L. Keller and S.M. Gruner)) Princeton University, Princeton, New Jersey, 08544.

At low concentrations, the peptide alamethicin formed single ion-channels in a lipid (for example, DOPE) bilayer. Single alamethicin ion-channels accessed several conductance levels in a burst which was monitored by voltage clamping (130mV) the membrane. The burst duration,T, the integrated conductance of the burst over time, $\int^T$conductance·dt, and the average conductance over time, $1/T \int^T$conductance·dt,were plotted vs. the time before each burst. Single channels with very high burst duration, integrated conductance, and average conductance appeared after short times between bursts. Following V. and I. Vodyanoy (1988. *Biophys. J.* 53:505a) we used an autocorrelation function to analyze the bursts. Since different peptide concentrations and transmembrane voltages alter the time between bursts (and therefore the behavior of the burst itself), these variables should be carefully monitored in any experiment reporting burst characteristics.

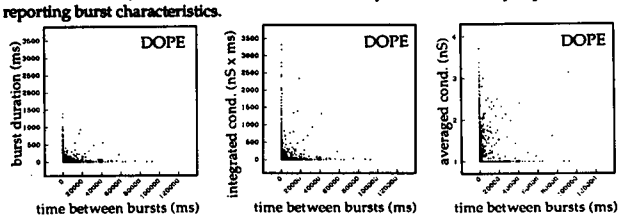

This work has been supported by the N.I.H. and the D.O.E.

Th-Pos3

THE STRUCTURE AND MOLECULAR DYNAMICS OF A VOLTAGE-GATED PEPTIDE CHANNEL ((J.R. Lewis, J.F. Ellena and D.S. Cafiso)). Department of Chemistry and Biophysics Program, University of Virginia, Charlottesville, VA 22901.

A molecular modeling and ^{1}H NMR study was carried out on alamethicin, a small 20 aa voltage-gated peptide channel. A set of structures is obtained from high-resolution NMR data in detergent that are interconvertible by rotation of the backbone angles of residues 10, 11 and/or 12 (Biochemistry 33, 4036 (1994)). Most structures were either linear or had a large backbone bend at residues 10 and/or 11. We have calculated the dipole moments of the NMR-derived structures and the crystal structure. Molecular dynamics simulations were used to examine the rate of interconversion during 50 ps simulations run at room temperature. Interconversion takes place at higher temperatures and these results were used to estimate the room temperature interconversion rate. The above structural data is interpreted in terms of the mechanism of voltage-dependent ion channel formation by alamethicin.

Th-Pos4

MECHANISM OF VOLTAGE-GATING IN A PEPTIDE ION CHANNEL. ((C.L. North, M.R. Barranger, J.F. Ellena and D.S. Cafiso)). Department of Chemistry and Biophysics Program, University of Virginia, Charlottesville, VA 22901. (Spon. by R.G. Bryant)

Alamethicin is a small 20 aa peptide that forms voltage-gated channels in lipid bilayers. A combination of high-resolution NMR, solid state NMR, and site directed spin labeling was used to determine the dynamics and membrane structure of this peptide-channel. The peptide which is predominantly α-helical undergoes large amplitude bending motions about MeA 10 (α-methylalanine), as revealed by paramagnetic enhancements of nuclear relaxation. The flexibility of this peptide appears to be due to the presence of proline in position 14. Solid state NMR spectra of oriented bilayer samples indicate that the N-terminal segment of the peptide is inserted into the membrane hydrocarbon along the bilayer normal. The membrane insertion and pitch of the helix is also indicated in collision-gradient EPR experiments which are performed on site directed spin-labeled alamethicin analogs. A model consistent with our experimental and computational data is proposed which involves the voltage-dependent linearization of the peptide across the lipid bilayer. The transmembrane field converts the peptide from a bent form where the polar Gln residues are protected to a linear form that is laterally amphipathic. This laterally amphipathic structure then assembles to form a conductive pore.

Th-Pos5

COLICIN E1 ION CHANNEL BINDING WITH MEMBRANE: AN OPTIMUM ELECTROSTATIC INTERACTION IS REQUIRED FOR ACTIVITY. ((S. D. Zakharov, Y.-L. Zhang, J. B. Heymann and W. A. Cramer)) Department of Biological Sci., Purdue Univ., W. Lafayette IN 47907. (Spon. by M. Laskowski, Jr.)

The binding of the 190-residue colicin E1 channel polypeptide, P190, to artificial membranes was studied using fluorescence resonance energy transfer from three intrinsic tryptophans to trinitrophenyl-phosphatidylethanolamine, incorporated at low stoichiometry into DOPG/DOPC vesicles. Binding was modeled as a bimolecular reaction of free P190 with n lipid molecules. The dissociation constant, K_d, and the lipid:protein stoichiometry, n, were determined from titration of P190 with membrane vesicles. A major role for electrostatic interactions in the initial binding of the polypeptide to the membranes was inferred from the dependence of the binding parameters on (a) ionic strength (0.1-0.3 M), (b) net positive charge of the channel polypeptide (pH 3.5-4.5), and (c) negative surface charge density (PG content) of the vesicles. The binding is characterized by a dissociation constant, K_d = 3-8 nM, and a lipid binding stoichiometry, n = 30-80 lipids/polypeptide. The small extent of the reversal of P190 binding caused by increase of pH and ionic strength indicated the presence of a significant non-electrostatic binding component that appears within 0.5 min of the initiation of binding. The monotonic decrease in K_d and n with increasing content of anionic (PG) lipid contrasted with a maximum for *in vitro* channel activity at 30-50% PG. A comparison of these data lead to the conclusion that colicin activity requires an optimum, not a maximum, strength of electrostatic interaction. Surface electrostatic interactions that are too strong are associated with lower activity and possibly preclude insertion of the hydrophobic helical hairpin anchor of the channel. The acidic lipid content associated with optimum activity is close to the physiological level of 30% found in the wild-type *E. coli* cytoplasmic membrane. (Supported by NIH GM-18457)

Th-Pos6

SINGLE CHANNEL COMPARISON OF COLICIN E1 AND ITS C-TERMINAL POLYPEPTIDE. ((B. Deriy, W. Cramer, & F. Cohen)) Dept of Molec Biophys & Physiol, Rush Medical College, Chicago, IL 60612 & Dept of Biol Sci, Purdue Univ, W Lafayette, IN 47907. (Spon. by D. Pepperberg)

Patch clamp experiments were used to characterize channels formed by colicin E1 and its channel-forming 190 residue (p190) C-terminal polypeptide in asolectin membranes in 1 M KCl, pH 3.5. Channels were activated by trans-negative voltages, -20 to -60 mV, and deactivated with trans-positive potentials. Properties of both proteins were qualitatively similar, quantitatively different. For colicin, initial conductances were 20 pS. After 1-30 min, 40 and 60 pS channels appeared. For p190, the earliest conductances were 7-13 pS. 25 and 50 pS appeared later. The 50-60 pS channels often exhibited 20-30 pS substates. Larger channels, with conductances multiples of the earliest, were not stable and would soon disappear. Channels exhibited rapid (> 5 KHz) flickering, more common for larger channels and for p190. If larger channels had not yet flickered, high deactivation voltages (e.g. 150 mV) induced it. The probability of open vs. closed while rapidly flickering was weakly voltage-dependent. Channels increasingly inactivated with time. Deactivation voltages induced recovery. Inactivation could become so pronounced that the apparent voltage dependencies for opening and closing reversed, as if protein had fully translocated across the bilayer. The quantal increases in conductance with time suggest that individual channels stably associate into dimers and trimers; usually all the individual associated channels simultaneously gate open and closed. When nonsimultaneous gating occurs, substates appear. (NIH GM47828 and GM18457).

Th-Pos7

THE CRYSTAL STRUCTURE OF THE CHANNEL-FORMING DOMAIN OF COLICIN E1.

Patricia Elkins, Amy Bunker, William Cramer, and Cynthia Stauffacher, Department of Biological Sciences, Purdue University, West Lafayette, IN 47907.

Colicin E1 is a bacterial toxin secreted by *E. coli* which kills rival strains of bacteria by forming a channel in the inner cell membrane. Colicin E1 (MW = 58 kD) consists of three functional domains that are involved in receptor binding, translocation across the outer cell membrane and channel-formation. Crystals of the channel-forming polypeptide, which diffract to 2.2 - 2.4 Å, have been grown in space group I4. Crystals of a proteolytic polypeptide and an engineered polypeptide differ in unit cell parameters (a=102.8 Å, c=35.6 Å and a=87.2 Å, c=59.3 Å, respectively).

The structure of the engineered polypeptide was solved by multiple isomorphous replacement using four heavy atom derivatives with anomalous scattering from a diphenyl mercury derivative. The initial electron density map, calculated from a set of MIR phases with an overall figure-of-merit of 0.49 to 3.0 Å, had clearly interpretable helical and loop regions. An atomic model is being built into the 3.0 Å solvent-flattened electron density map. Phase extension and refinement will produce a 2.5 Å resolution structure.

The structure of the colicin E1 channel-forming domain is a sandwich of 10 helices in three layers, similar to the known structures of other members of the colicin family, colicin A and colicin Ia. A major difference is seen in the N-terminal helix of this domain. While this helix lies close to the molecule in other colicins, in colicin E1 the helix makes an angle of greater than 30° with the molecular axis. We propose that the opening of this angle may serve as a communication signal between the colicin E1 functional domains.

Th-Pos8

A REVERSIBLE PROBE FOR THE ACCURATE LOCATION OF SPECIFIC RESIDUES IN THE VOLTAGE-GATED COLICIN Ia CHANNEL.

((K. S. Jakes, X.-Q. Qiu, A. Finkelstein and S. L. Slatin)) Albert Einstein College of Medicine, Bronx, N.Y. 10461

We recently showed that channel gating by the bacterial protein toxin colicin Ia involves the reversible movement of a substantial portion of the protein across the lipid bilayer. This was established by showing that biotin moieties attached covalently to unique cysteine residues bound streptavidin on the *cis* or *trans* side of the bilayer in a fashion dependent on whether the channel was closed or open (Nature (1994), 371, 158-161). The spatial resolution of these experiments was limited to as much as 16 Å by the length of the spacer arm used to attach the biotin to the genetically introduced cysteines in the protein. Here, we report the use of a reversible biotinylation reagent, HPDP-biotin (Pierce), which attaches directly to the cysteine sulfhydryl via a disulfide bond which can later be reduced. Colicin Ia with unique cysteines in the translocating region was biotinylated with HPDP-biotin and tested for its susceptibility to streptavidin. *Trans* streptavidin interfered with channel closing in much the same way as for colicin biotinylated with NEM-biotin. However, this effect could be reversed by the membrane impermeant reducing agent, cysteine. Thus, the disulfide bond between the colicin's cysteine and the biotin reagent was directly accessible to the *trans* solution and not buried in the bilayer, a spacer arm's length away from the aqueous phase. Similar experiments with *cis* streptavidin confirm that the translocating region crosses the entire thickness of the membrane as the channel gates.

Th-Pos9

THE HIGH-RESOLUTION CRYSTAL STRUCTURE OF COLICIN IA.

((M.C. Wiener, P. Ghosh, R.M. Stroud)) Dept. of Biochemistry & Biophysics, University of California, San Francisco, 94143-0448.

The formation of ion-permeable channels in target cell membranes is a general mechanism of cytotoxicity The process involves secretion of a soluble protein which inserts into the plasma membrane of the target cell and forms pores. The *Escherichia coli* toxins, colicins, are a well-characterized example of this functional class of proteins. A low-resolution structure of the soluble form of colicin Ia has been determined by our laboratory [Ghosh et al. (Nature Structural Biology, **1**, 597-604, 1994)]. We have subsequently: i) extended resolution from 3.4 to 2.35 Å by using cryocrystallographic methods, and ii) obtained isomorphous derivatives (to 3.0 Å) by reaction of mercurials with three different single-cysteine colicin mutants (wild-type colicin has no cysteines). We are currently interpreting the electron-density maps; the status of the structure determination will be described.

Th-Pos10

HYDROPHOBIC HAIRPIN OF THE PORE-FORMING DOMAIN OF COLICIN E1: SOLUTION AND MEMBRANE STRUCTURE AS STUDIED BY SITE-DIRECTED SPIN LABELING.

Łukasz Salwiński and Wayne L. Hubbell, Jules Stein Eye Institute and Department of Chemistry and Biochemistry, UCLA, Los Angeles, CA; (Sponsor Z. Farahbakhsh)

In order to study the structure and membrane localization of the hydrophobic hairpin of the C-terminal fragment of colicin E1 (helices 8 and 9, *fig*), a series of single cysteine mutants at positions 492-507 was prepared and each modified with a sulfhydryl specific nitroxide spin label.

In solution, the EPR spectra reveal that the nitroxides are immobilized in a nonpolar environment and are inaccesible to collisions with nonpolar (oxygen) and polar (NiEDDA) paramagnetic species in solution. This results are generally consistent with the colicin A-based model of colicin E1 (*fig*), in which helix 9 is buried within the structure, except that the helix likely extends to at least residue 507.

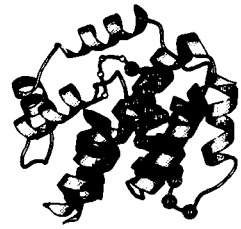

model of colicin E1

Upon membrane binding, major changes in the tertiary structure are evident. The localization of the residues in the membrane will be discussed within the scope of the current models of the membrane bound form of colicin E1.

Th-Pos11

A "BUTTERFLY" MODEL OF THE VOLTAGE-ACTIVATED HYDROGEN ION CONDUCTANCE.

((V. S. Markin#, V. V. Cherny*, and T. E. DeCoursey*)) #Department of Cell Biology and Neuroscience, University of Texas SWMED, Dallas, TX 75235, and *Department of Physiology, Rush Medical Center, Chicago, IL 60612.

To explain the gating of voltage-activated H^+ currents (see accompanying abstract) we propose a "butterfly" model of proton channel that is visualized as a multimeric structure consisting of a few motile protomers, or "wings" (Fig.1). The transition between open and closed states of the channel is regulated by proton adsorption to a site that is accessible from only one side of membrane at a time. The wings can move across membrane only in deprotonated form, changing accessibility of the regulation sites. The voltage dependence of gating may arise from proton adsorption or wing movement, or both. The model predicts that the voltage-activation curve depends on ΔpH only, rather than on pH_o and pH_i independently, and it accurately simulates the time course of proton currents and the tail currents. Curve fitting provided parameters of the model.

Supported by NIH and AHA.

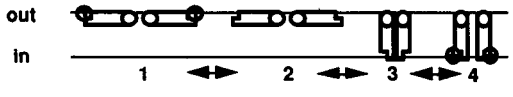

Fig. 1

Th-Pos12

THE VOLTAGE-ACTIVATED PROTON CONDUCTANCE IS DETERMINED BY THE pH GRADIENT

((V.V. Cherny, V.S. Markin*, T.E. DeCoursey)) Dept. Physiology, Rush Medical Center, Chicago, IL, *Dept. Cell Biol/Neurosci, U. Texas SWMED, Dallas, TX.

Voltage-activated H^+ currents were studied in rat alveolar epithelial cells using tight-seal whole-cell voltage-clamp recording and highly buffered, EGTA-containing solutions. The tail current reversal potential was close to the Nernst potential, varying 52 mV/unit pH over pH gradients, ΔpH, spanning four units (pH_o 5.5-8.0, pH_i 5.5-7.5). Therefore H^+ channels are extremely selective, $P_H/P_{TMA} > 10^7$, and both pH_i and pH_o were well controlled. The H^+ current amplitude, I_H, was practically constant at fixed ΔpH, in spite of 100-fold symmetrical changes in H^+ concentration. The rate-determining step in H^+ permeation must be pH-independent, localized to the channel (entry, permeation, or exit), and not due to *bulk* diffusion limitation. I_H-V and g_H-V relations were shifted along the voltage axis by ~40 mV/unit pH by changes in pH_i or pH_o. The activation rate (maximum rate-of-rise of I_H) shifted ~45 mV/unit ΔpH, but also increased at higher ΔpH. The deactivation rate (τ_{tail}) shifted ~20 mV/unit pH. If internal and external protons regulate the voltage-dependence of g_H gating at separate sites, these sites must be equally effective. A simpler interpretation is that gating is controlled by ΔpH. We propose a simple model to account for the observed ΔpH dependence (accompanying abstract). In summary, within the physiological pH range, both the amplitude and the voltage dependence of H^+ currents depend only on ΔpH and not on the absolute pH.

Supported by the American Heart Association and by the N.I.H.

Th-Pos13

VOLTAGE-ACTIVATED PROTON CURRENTS IN MEMBRANE PATCHES ((T.E. DeCoursey and V.V. Cherny)) Dept. of Physiology, Rush Medical Center, Chicago, IL 60612. (Spon. by Fred N. Quandt)

Voltage-activated H^+-selective currents are present in excitable cells, epithelium, and phagocytes. We studied voltage-gated H^+ currents in cell-attached, inside-out, and outside-out patch configurations in rat alveolar epithelium. Most patches contained H^+ currents. The pH_o- and pH_i-dependence in patches was identical to that of whole-cell currents. Therefore, the regulation by pH of the voltage-dependence of H^+ channel gating is exerted at a local level. Locally low pH_i could activate H^+ currents in a small area of membrane without activating the g_H in the entire cell membrane. For example, activating the g_H at the apical surface of an epithelial cell monolayer could extrude protons vectorially. In phagocytes the g_H could be activated in the phagocytic vacuole in response to a local outward proton gradient produced by NADPH oxidase. Single-channel H^+ currents are too small to have been resolved directly. The figure shows slowly-activating H^+ currents in a cell-attached patch, with pH 7.5 in the pipette. There is an obvious opening of a delayed rectifier K^+ channel (~10 pS) in one record. Their presence in cell-attached patches clearly demonstrates that H^+ currents are not the result of the peculiar ionic conditions often used to isolate them for study, but behave normally when the inside of the membrane is exposed to the cytoplasm of intact cells.

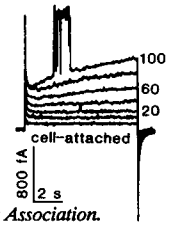

Supported by a Grant-in-Aid from the American Heart Association.

CHANNEL PERMEATION

Th-Pos14

WATER PERMEABILITY AS DERIVED FROM A MOLECULAR DYNAMICS SIMULATION OF A SINGLE-OCCUPANCY PORE. ((S.G. Kalko[1], J.A. Hernández[2], J.R. Grigera[1], and J. Fischbarg[3])). IFLYSIB, Univ. de La Plata, Argentina[1]; F. de Ciencias, Univ. de la República, Montevideo, Uruguay[2]; Coll. of Phys. & Surgeons, Columbia Univ., New York, U.S.A.[3].

We simulated the interactions between water molecules and a single-occupancy hydrophilic pore. The system consists of a rectangular box containing water molecules, some of which are positionally restrained so as to act as a membrane. One position in this membrane is initially vacant (the "pore"), but was dynamically occupied and vacated by the mobile molecules. We determined mean occupancy and vacancy times τ_o and τ_v at different temperatures. The system was represented by a two-state model, with kinetic constants directly determined from τ_o and τ_v; such model yielded the osmotic permeability coefficient per pore p_f for the site. The p_f value was of the order of 10^{-11} cm^3/s, a value significantly larger than the ones determined for CHIP28 (about 10^{-13} cm^3/s) and for gramicidin A (about 10^{-14} cm^3/s). From the p_f at different temperatures we computed an energy of activation consistent with that of single hydrogen bonds. These results are consistent with diverse theoretical analysis which predict that p_f should decrease with the number of molecules in the file. They also bring apparently the first estimate for the p_f of one of the simplest single-file pores.

Th-Pos15

MULTIPLE IONIZATION REACTIONS WITH DIFFERING pKs DETECTED FROM ION CHANNEL CURRENT FLUCTUATIONS. ((J.J. Kasianowicz † and S.M. Bezrukov ‡)) † NIST, Biotechnology Div., Gaithersburg, MD 20899; ‡ DCRT, NIH, Bethesda, MD 20892

The ion channel formed by *Staphylococcus aureus* α-toxin is large and relatively non-selective, yet its conducting properties are surprisingly pH dependent. Earlier, we studied the mechanism by which this channel's conductance decreases with an increase in pH and showed that for positive potentials (referenced to the side of protein addition), the conductance is controlled by several protonation sites in the channel lumen, each with an identical pK value of 5.5 (Bezrukov & Kasianowicz. 1993. *Phys.Rev.Lett.* 70:2352). In the present study, we address the cause of a marked asymmetry in the pH dependent current-voltage relationship. Specifically, we analyze the fluctuations in current through the fully open channel as a function of pH and the applied potential. In the presence of 1M NaCl and positive applied potentials, the low frequency noise exhibited a single well-defined peak between pH 3.5 and 7.5. In contrast, when the sign of the potential is reversed, a second, distinct peak with a pK ~ 4 emerges. Our results demonstrate that the total ionic current in the α-toxin channel is controlled by the state of ionization of different residues, and that the relative contribution of these distinct groups depends on the sign of the applied potential. One possible explanation is that the applied electric field causes a minor structural change in the channel, forcing additional residues into or out of the ion conduction pathway.

Supported by a NAS/NRC Associateship (JJK) and by an ONR grant (to V.A. Parsegian).

Th-Pos16

***PNP* THEORY FITS CURRENT-VOLTAGE *(IV)* RELATIONS OF A NEURONAL ANION CHANNEL IN 13 SOLUTIONS.** ((Duan Chen†, *Wolfgang Nonner, *and* Bob Eisenberg†)). Dept.'s of Physiology *at* †Rush Medical College, Chicago IL *and* *University of Miami, FL.

If a channel is described as a single distribution of permanent charge determined by the structure of the channel protein, the potential profile along its pore must change when concentration or potential is varied in the baths, because mobile charges (ions) in the pore and its boundaries change. ***PNP*** theory computes this profile by simultaneously solving Poisson and Nernst-Planck equations for a given structure of permanent charge. Diffusion constants in the pore (D_{Na} & D_{Cl}), and the permanent charge, determine *IV* relations at all concentrations. *IV* relations have been reported previously from a neuronal anion channel in 13 different NaCl solutions, symmetrical and asymmetrical (diluted), ranging from 59 to 785 mM. *IV* relations are predicted using *PNP* theory and a permanent charge distribution described by 4 parameters. Optimal values of D_{Na}, D_{Cl}, and those 4 parameters are determined by least squares fits to 1,722 data points. ***PNP theory fits the data, from all solutions, with 6 parameters*** and little error. In other words, data from one set of solutions can be used to predict measurements in other solutions, with little error. The computations show that ***potential profiles change significantly as solutions are changed.*** Theories that assume a potential profile (or rate constant) independent of bath composition are likely to have difficulty fitting data like this, taken over a wide range of concentrations, in symmetrical and asymmetrical solutions.

Th-Pos17

***PNP* THEORY FITS CURRENT-VOLTAGE *(IV)* RELATIONS OF A SYNTHETIC CHANNEL IN 7 SOLUTIONS.** ((D. Chen†, P. Kienker*, J. Lear‡ & R. Eisenberg†)) Dept.'s of Physiology, †Rush Medical Center, Chicago, *and* *Albert Einstein Medical College, New York *and* ‡Dept. of Biochemistry & Biophysics, University of Pennsylvania, Philadelphia.

The amphiphilic helical polypeptide Acetyl-(LeuSerSerLeuLeuSerLeu)$_3$-$CONH_2$ forms an asymmetrical channel of relatively simple and reasonably known structure. *IV* relations have been measured from single channels in 7 solutions, symmetrical and asymmetrical, ranging from 1 M to 63 mM KCl. The shape of the *IV* relation in asymmetrical solutions depends on which solution is on which side of the channel. With solutions oriented one way, the reversal potential V_{rev} = +14 mV; with the solutions interchanged, V_{rev} = −32 mV. ***PNP theory fits the data from all 7 solutions with 5 parameters:*** D_K, D_{Cl}, and the three parameters (two densities, one location) needed to describe permanent charge as a step function of position. More realistic descriptions of permanent charge allow better fits, as expected. Asymmetrical dependence of *IV* relations occurs because the potential profile in the pore depends on what solution is on what side: ***potential profiles change significantly as solutions are changed.***

Theories that assume how a potential profile (or rate constant derived from the potential) depends on bath composition have difficulty fitting data like this, taken over a wide range of concentrations, because mobile charges (ions) in the pore and on its boundaries vary so much. It seems likely that a theory must compute potential profiles in the channel's pore (e.g., from Poisson's equation), if it is to deal with large changes of concentration in the bath.

Th-Pos18

***PH* (POISSON-HYDRODYNAMIC) THEORY OF AN OPEN CHANNEL.** ((Duan Chen*, Bob Eisenberg*, Joseph Jerome† & Chi-Wang Shu‡)) *Physiology Dept., Rush Medical College, Chicago IL, †Dept. of Mathematics *at* Northwestern University, Evanston IL *and* ‡Brown University, Providence RI.

Most theories of open channels ignore heat generated by current flow, but that heat is known to be significant when analogous currents flow in semiconductors, as described by hydrodynamic theory, a combination of the continuity, Poisson, Euler-Navier-Stokes, and Fourier heat equations. If *PH* theory is used to describe current flow in an open ionic channel, ***substantial localized temperature changes (3-30°C) are predicted,*** for all the distributions of permanent charge and conditions that we examined. Temperature changes are generated (mostly) by transfer of energy from drift motion of ions (in the strong electric field in the channel's pore) to their random thermal motions, just as *V·I* heat is generated by drift motion of electrons in resistors. One parameter (saturation velocity) characterizes ionic motion as overdamped (*PNP* theory), intermediate ('adiabatic' theory of semiconductors), or unrestricted (*PH* theory). Experimental measurements have been reported (of Doppler shift of laser light) of the velocity of ions in gramicidin channels: the predicted saturation of velocity and temperature change should be observable in experimental measurements, as well as in molecular dynamics simulations of flux, at least in principle.

Temperature affects all types of ions, so fluxes are likely to co-vary and be coupled, in that sense. Heat generated (just outside a channel) by hydrolysis of ATP may be an important driving force for the fluxes of active transport.

Th-Pos19

PERMEATION PROPERTIES OF SELF-ASSEMBLING PEPTIDE NANOTUBES THAT FORM ION CHANNELS IN PLANAR LIPID BILAYERS. ((L.K. Buehler, J.R. Granja and M.R. Ghadiri)) The Scripps Research Institute, Chemistry Dept., La Jolla, CA 92037.

Synthetic cyclic peptides were designed that form short tubular structures (nanotubes) across phospholipid bilayers. Ion channel formation is based on self-assembling stacking processes of the ring shaped peptide units (spacing between rings 0.486nm) driven by the hydrophobic environment within the membrane. Single channel recordings show the formation of ion channel structures exhibiting varying conductances in the range of 40 to 150pS (in symmetric 500mM KCl). Using a five fold ion gradient, a permeability ratio of 3 to 4 for K^+ over Cl^- ions has been determined. A theoretical model was used to correlate different single channel conductances (and their increments) with different channel length. Both conductance and selectivity values obtained experimentally were compared with theoretical values calculated for K^+ and Cl^- fluxes. The Nernst-Planck electrodiffusion equation (assuming an electrical, but no chemical gradient) was applied to a cylindrical pore model (which is structurally relevant) in order to calculate the corresponding ion fluxes. A fit of theoretical with experimental conductances was obtained under the assumption of fully hydrated ions passing through the channel. Based on size differences of the permeating hydrated ions (Cl^- larger than K^+) a size selectivity rather than electrostatic interactions between ions and charged binding sites within the channel are predicted to be responsible for the observed permeability ratio.

Th-Pos20

GENERAL EFFECT OF RAPID FLUCTUATIONS ON PRACTICAL MEASUREMENTS OF UNITARY CHANNEL CURRENT AS DETERMINED BY COMPUTER SIMULATION. ((G.W.J. Moss and E. G. Moczydlowski)) Dept. of Pharmacology, Yale Univ. School of Medicine, New Haven, CT 06520.

Many ion channels exhibit open-state and/or substate noise that can compromise measurements of true unitary open channel current by standard methods of amplitude histogram analysis. This is a serious problem in mechanistic studies of ion permeation and selectivity since an underestimate of open channel current may lead to a distorted picture of the free energy profile for ion movement. In mutagenesis studies, this problem can lead to misinterpretation of the role of residues and domains in ion permeation. To systematically investigate the impact of fast fluctuations on unitary current measurements, we simulated single-channel data for a linear 3-state kinetic scheme of closed-open-substate. In this scheme, the model channel is allowed to make rapid transitions between the open state and a discrete subconductance level. Simulations were performed, systematically varying the rate constants for transitions to and from the subconductance state. Unitary channel current was measured by standard techniques described in the literature after filtering with a digital Gaussian filter. This exercise provides a general surface contour plot of apparent open channel current as a function of α (closing) and β (opening) rate constants between an open state and a particular substate. The results show that serious underestimates of unit conductance occur when α and β transition rates are both faster than ~10 times the filter frequency, f. At ~100f the errors reach a limiting plateau and the magnitude of excess noise is not a good indicator of the reliability of a conductance measurement. Under certain conditions, amplitude histograms are described by a β-function as observed for the effect of internal Kunitz inhibitors on maxi K(Ca) channels. (Supported by NIH, Donaghue Foundation.)

Th-Pos21

A PHYSIC MODEL OF ENERGY PROFILES OF IONS OR ION GROUPS PENETRATING A BIOLOGICAL MEMBRANE CHANNEL ((C.H. Zou and K. Cheng)) University of Miami School of Medicine, FL 33136.

To attempt to explain what determines an ion or an ion group penetration of a biological membrane channel, a physical model of energy profiles $V_2(x)$ is proposed, based on our previous study of one dimensional (1-D) steady state Schrödinger equation in a single particle system and in a time independent field (K. Cheng, et al., Biomedical Sciences Instrumentation, vol. 29, pp. 361-367, 1993). In this model, a $V_2(x)$ is simplified as an effective constant height of energy profile V_2 in a channel to obtain analytical solutions in mathematics. This model elucidates that: (1) Ion selectivities of a channel are determined by V_2. V_2 is defined as a V_{2c} for a cation and V_{2a} for an anion. $|V_{2c}|$ and $|V_{2a}|$ may be or may be not the same value depending on electrical characteristics of a channel. It is called a cation channel if a $|V_{2c}|$ is much lower than a $|V_{2a}|$ and vice versa. It is called a cation-anion cotranspoter if a $|V_{2c}|$ and a $|V_{2a}|$ are equal or almost equal. (2) Whether an ion can penetrate through or is reflected from a channel is mostly determined by the repulsion energies (barriers) rather than the attraction energies (wells). (3) A channel's conformation can be changed when it is stimulated strongly enough. The variation of the conformation could influence $V_2(x)$ and V_2, and eventually result in open or close of the channel.

Th-Pos22

A COMPUTER PROGRAM FOR THE MODELLING OF IONIC CONDUCTION BASED ON EYRING RATE THEORY. ((A. Tinker)) Dept. of Physiology, UCSF, San Francisco, CA 94143-0724.

A Windows™ based computer program has been developed for the modelling of ionic conduction founded on Eyring rate theory and standard treatments of surface charge. The channel conduction pathway is viewed as a series of binding sites separated by energy peaks over which the permeant ion must hop to traverse the pore. The program allows the user to select and edit a large number free parameters including number, valency and concentration of permeating ion, barrier number, energy levels for peaks and wells and the position of these elements in the electrical field. Separate algorithms handle calculations for single and multiple occupancy. For the latter it is possible to specify varying degrees of repulsion. In addition the influence of surface charge as formulated in the Gouy-Chapman and Debye-Huckel treatments can be examined. For any particular chosen model the variation of single-channel current with holding potential and concentration can be calculated, displayed and printed. Furthermore a variety of more specialised calculations are possible including reversal potential and simulations of biophysical experiments such as mole fraction. The program may prove a useful tool for modelling specific experimental problems and for teaching. The poster will consist of a demonstration of the program. *Supported by the Wellcome Trust.*

Th-Pos23

MOLECULAR DYNAMICS SIMULATIONS ON CATION CHANNEL MODELS ((Pamidighantam V. Sudhakar, Chandralekha Singh, Eric Jakobsson and Shankar Subramaniam)) Department of Physiology and Biophysics, Center for Biophysics and Computational Biology, Beckman Institute, Materials Research Laboratory, National Center for Supercomputing Applications, University of Illinois, Urbana, IL 61801.

Understanding ion selectivity and permeation in protein channels is of considerable biological interest. Molecular models that conform to sequence variability, mutagenesis experiments, toxin binding and electrophysiological studies have been built by Guy and Durell, and for sodium channels by Lipkind and Fozzard. These laboratories have graciously shared with us coordinates of channel models proposed by them. Computational methods can be used to validate and refine such models. Molecular dynamics simulations have been carried out on models of sodium and potassium channel fragments that are thought to comprise the selectivity filter and narrow part of the pores. In the models considered thus far, the potassium channel model is a symmetric tetramer containing 100 residues, while the sodium channel is a heteromeric tetramer with each monomer containing between 31 and 34 residues. The potassium channel pore model is lined by backbone carbonyl groups. The sodium channel is modeled as four helix-helix segments with polar residue side-chains lining the pore. Other structures will be considered. Using boundary conditions similar to those previously developed in our laboratory for studying the gramicidin channel, these model systems are subject to molecular dynamics simulations. A detailed study of water structure and movement in the pore region is presented and analyzed. Potentials of mean force are calculated for ion permeation in these channel models. [Supported by NSF]

Th-Pos24

IDENTIFICATION OF AMINO ACID SEQUENCES IN THE DIHYDROPYRIDINE RECEPTOR CYTOPLASMIC II-III LOOP THAT ACTIVATE THE SKELETAL MUSCLE CALCIUM RELEASE CHANNEL ((Xiangyang Lu, Le Xu and Gerhard Meissner)) Department of Biochemistry & Biophysics, Univ. of North Carolina, Chapel Hill, NC 27599.

We previously reported that the cytoplasmic II-III loop of dihydropyridine receptor (DHPR) α1 subunit (SDCL) activates the skeletal muscle sarcoplasmic reticulum calcium release channel (CRC). SDCL has been shown to contain a phosphorylation site (Ser^{687}) (Rohrkasten et al., 1988, *J. Biol. Chem.* 263, 15325). We determined the binding of phosphorylated SDCL to the CRC and tested the role of SDCL phosphorylation on activation of the CRC. SDCL was expressed in *E. coli* and phosphorylated at Ser^{687} by cyclic AMP-dependent protein kinase. The phosphorylated SDCL bound specifically to the skeletal, but not cardiac, muscle CRC and the binding could be displaced by the unphosphorylated SDCL. Phosphorylation of SDCL abolished activation of the CRC as determined in [^{3}H]ryanodine binding and single channel measurements. In addition, a mutant SDCL in which Ser^{687} was changed to Ala failed to activate the skeletal muscle CRC, but was still able to bind. These results suggest that Ser^{687} of the DHPR α1 subunit is important for SDCL activation of the skeletal muscle CRC. Furthermore, by testing the effects of smaller peptides derived from SDCL region of the DHPR α1 subunit, we identified a domain of 58 amino acid residues including Ser^{687} that potentiated [^{3}H]ryanodine binding to the skeletal muscle CRC.

Th-Pos25

THE β_1 SUBUNIT OF THE L-TYPE VDCC (CACNLB1) IS ESSENTIAL FOR EXCITATION-CONTRACTION COUPLING. ((R.G. Gregg, A. Messing#, R. Moss*, M. Behan#, R. Coronado*, C. Strube*, P.A. Powers)) Waisman Center, *Department of Physiology and #Veterinary Medecine, University of Wisconsin, Madison, WI 53705.

To determine the role of the β_1 subunit in skeletal muscle L-type calcium channel complex (α_1, α_2/δ, β_1 and γ), we have used gene targeting to produced a mouse line with a null mutation in the β_1 subunit gene (cacnlb1). Mice heterozygous (*cacnlb1*$^+$/*cacnlb1*$^-$) for the mutation develop normally, however, *cacnlb1*$^-$ homozygotes die at birth from asphyxia. The *cacnlb1*$^-$/*cacnlb1*$^-$ show marked deficiency of all skeletal muscles. Electron microscopy reveals a disorganized pattern of myofibrils in the *cacnlb1*$^-$/*cacnlb1*$^-$ mice compared to *cacnlb1*$^+$/*cacnlb1*$^?$ litter mates. Contraction of forelimb in response to electrical field stimulation is absent in the *cacnlb1*$^-$/*cacnlb1*$^-$ mice. Addition of caffeine to the bathing solution does elicit a contraction. These data indicate that the contractile machinery is present in *cacnlb1*$^-$/*cacnlb1*$^-$ mice, but that excitation-contraction coupling is absent. Whether the β_1 subunit is required for assembly, stability or state of the L-type channel remains to be determined. *(Supported by a grant to RGG and PAP from NSF).*

Th-Pos26

ABNORMAL CALCIUM CURRENT IN SKELETAL MUSCLE CELLS FROM MICE LACKING β_1 DIHYDROPYRIDINE RECEPTOR SUBUNIT. ((C. Strube, P.A. Powers*, R.G. Gregg*, R. Coronado)) Department of Physiology and *Waisman Center, University of Wisconsin, Madison, WI 53706, USA.

In skeletal muscle the dihydropyridine receptor complex is responsible for the L-type calcium current and is comprised of α_1, β_1, α_2/δ, and γ subunits. In myotubes from mice lacking β_1 subunit, we observed two types of inward currents carried by Ca^{2+} or Ba^{2+}. A fast-inactivated low threshold current was present in normal and mutant myotubes. A sustained high threshold current, named $I_{\beta 1}^-$, was present in mutant myotubes and was different from the L-type current of normal myotubes. The amplitude of $I_{\beta 1}^-$ was less than 10% of the amplitude of the normal L-type current. $I_{\beta 1}^-$ activated faster than, and deactivated slower than, the normal L-type current. In addition, $I_{\beta 1}^-$ was more sensitive to Bay K 8644 (2.5 fold increase) and to nifedipine (block) than the normal L-type current. Thus, the specific absence of the β_1 subunit during embryo development results in an abnormal dihydropyridine sensitive calcium current in skeletal muscles. β_1 could play an important role during myogenesis in the assembly, stability, and/or functional state of the dihydropyridine receptor complex.
(Supported by NSF, NIH, MDA, FRM and Philippe Foundation).

Th-Pos27

GTP$_\gamma$S DOES NOT DIRECTLY ALTER CA^{2+}-INDUCED CA^{2+} RELEASE IN SKELETAL MUSCLE FIBERS. ((L.V. Thompson, +S.K. Donaldson, and D.A. Huetteman)) University of Minnesota, Minneapolis, MN 55455; +Johns Hopkins University, Baltimore, MD 21205.

GTP$_\gamma$S has been shown to augment the excitation-contraction (EC) coupling Ca^{2+} release stimulated by TT depolarization. In mechanically peeled (sarcolemma removed) skeletal fibers, this GTP$_\gamma$S augmentation is selectively blocked by procaine, an inhibitor of Ca^{2+}-induced Ca^{2+} release (CaIR) (*Biophys. J.* 66(2):A340, 1994). CaIR can be stimulated independent of EC coupling by caffeine, which acts directly on the SR. The aim of this study was to test the hypothesis that there is a stimulatory effect of GTP$_\gamma$S directly on the CaIR mechanism. Mechanically peeled single rabbit adductor magnus fibers were studied. In this preparation, the TT are sealed and can be polarized or depolarized by ionic diffusion potentials created by varying bathing solution composition. SR Ca^{2+} release is manifested as an isometric tension transient. GTP$_\gamma$S (50 μM) does not alter the normalized peak magnitude of the contracture elicited by 0.5mM or 1.0mM bath caffeine under conditions for steady state depolarized TT. GTP$_\gamma$S also had no statistically significant effect on the time to 50% of peak magnitude of the submaximum caffeine contractures. Since submaximum caffeine contractures were not altered by GTP$_\gamma$S, GTP$_\gamma$S augmentation of SR Ca^{2+} release observed during peeled fiber EC coupling is not due to a direct effect on the CaIR of the SR. Supported by NIH AR 35132.

Th-Pos28

GTP$_\gamma$S REVERSES D600 BLOCK OF SKELETAL MUSCLE EXCITATION-CONTRACTION COUPLING. ((+S.K. Donaldson, L.V. Thompson, and D.A. Huetteman)) University of Minnesota, Minneapolis, MN 55455; +Johns Hopkins University, Baltimore, MD 21205.

G proteins affect excitation-contraction (EC) coupling in peeled (sarcolemma removed) rabbit skeletal muscle fibers. GTP$_\gamma$S augments sarcoplasmic reticulum (SR) Ca^{2+} release stimulated by TT depolarization; this GTP$_\gamma$S augmentation is selectively blocked by GDP$_\beta$S (*Am. J. Physiol.*, in press, 1994). G protein-specific nucleotides also reverse D600 block of EC coupling in the continued presence of bath D600 (*Biophys. J.*, 64(2):A36, 1993). The purpose of this study was to determine whether GTP$_\gamma$S reversal of D600 block is due to: 1) stimulation of SR Ca^{2+} release and/or elevation of myoplasmic [Ca^{2+}], or 2) an affect on the TT voltage sensors. To test between these two possibilities, 50μM GTP$_\gamma$S was added to the peeled bath only during the period of TT depolarization under conditions of D600 (10μM) block. In contrast to the reversal of D600 block that occurs when GTP$_\gamma$S is present during the complete EC coupling cycle, D600 block was not removed by addition of GTP$_\gamma$S only during the period of TT depolarization. Furthermore, since addition of GTP$_\gamma$S to the bath of D600-blocked fibers with depolarized TT elicited a small SR Ca^{2+} release, the GTP$_\gamma$S-reversal of D600 block cannot be explained by an elevation of myoplasmic [Ca^{2+}]. These data are consistent with a molecular binding site for GTP$_\gamma$S in the TT near the DHPR, perhaps on a G protein. Supported by NIH AR35132.

Th-Pos29

EVIDENCE FOR A MISSING LINK IN E-C COUPLING IN DYSGENIC MUSCLE CELLS ((G. Varadi, G. Mikala, P. Lory, M. Varadi, M. Pinçon-Raymond and A. Schwartz)) University of Cincinnati, Cincinnati, OH 45267 and INSERM Paris and Montpellier, France (Spon. by M. A. Matlib)

The expression of subunit genes of the calcium channel complex and other components of E-C coupling was studied in differentiating, immortalized mouse mdg cells. These cells showed expression of α_1, α_2/δ and γ transcripts of the skeletal muscle calcium channel genes and several known transcript variants of skeletal, cardiac and brain β genes. Although the expression of skeletal α_1 transcripts appeared at diminished levels compared to control cells, it was clearly detectable together with another α_1 transcript whose size matched with the cardiac α_1 transcript. PCR, cloning and sequencing showed that upon differentiation both skeletal and cardiac muscle calcium channel α_1 subunit genes are expressed. Using different RNA preparations (5 samples) and PCR products (3 reactions for each sample), we have shown that the mdg mutation occurs exclusively at nucleotide position 4009 where a cytosine residue is deleted. This mutation introduces a frameshift and a stop codon at 4169 thereby removing motif IVS_6 and the following part of the α_1 polypeptide. Interestingly, this mutation did not occur on the cardiac α_1 transcript. Consistent with the latter, in early stages of differentiation and fusion (1-3 nuclei/myotubes) we detected Ba^{2+} currents in dysgenic myotubes. The current-voltage relationships and kinetic parameters of these currents, termed previously "dysgenic current" resemble that of the cardiac L-type calcium currents. Furthermore, these currents were modulated by cAMP-dependent phosphorylation: stimulation with cAMP analogs or through activation of the β-adrenergic receptor, consistent with the results found in cardiac myocytes. These data establish the major phenotypic defect in mouse muscular dysgenesis. The enigma is the lack of E-C coupling in the presence of cardiac L-VDCC and all accessory subunits.

Th-Pos30

VOLTAGE AND TIME-DEPENDENT POTENTIATION OF DHP-SENSITIVE CALCIUM CHANNELS FROM T-TUBULE MEMBRANES OF SKELETAL MUSCLE. ((Rui Chen and Jianjie Ma)) Dept. of Physiol. & Biophys., Case Western Reserve, Cleveland, OH. (Spon. by T. Hoshiko)

Double pulse protocols were applied to the DHP-sensitive Ca channels from t-tubule membranes of rabbit skeletal muscle to study the effect of conditioning depolarization on the activation of the slow Ca channel. The conditioning-induced fast gating of the Ca channel (Ma et al., Biophys. J. 61: A130) was a steep function of the intermediate voltage (V_D) and the interval between the conditioning pulse and the test pulse (t_D) (Figure). With conditioning pulse, the time constant of activation (τ_m) at -20 mV was reduced from 390 ms (▽, reference) to 33, 42, 61 and 200 ms, when t_D = 50, 100, 200, and 500 ms, respectively (V_D = -50 mV). Hyperpolarization (V_D = -120 mV) eliminated the effect of conditioning pulse. D600 produced voltage dependent inhibition and prevented fast gating of the channel; it mainly reduced the occurrence of long open events (τ_{O2}= 25 ms) of the channel. Phosphorylation by PKA enhanced channel activity by shifting to the left the V-dependent activation and promoting long open events, resulting in potentiation of the conditioning effect. The results indicate that the slow Ca channel adopt fast gating via long open states of the channel. Supported by NIH, MDA and AHA.

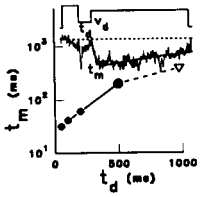

Th-Pos31

INVOLVEMENT OF DIHYDROPYRIDINE (DHP) RECEPTORS AND Mg^{2+} IN TERMINATING Ca^{2+} RELEASE IN CULTURED RAT SKELETAL MUSCLE ((N. Suda)) Max-Planck-Institut für biophysikalische Chemie, Am Fassberg D-37077 Göttingen, Germany

Combined patch-clamp and fura-2 measurements were performed to investigate the mechanism that terminates Ca release in rat skeletal myoballs. Ca release induced by 10 mM caffeine was terminated by depolarization (e.g. +20 mV for 1 s) and subsequent repolarization to -70 mV (RISC phenomenon)(Proc. Natl. Acad. Sci. USA, 91, 5725-5729, 1994). Extracellular perfusion of 0.5 to 1 μM (+)PN200-110 or nifedipine strongly inhibited RISC and also slowed [Ca]i decay after depolarization-induced Ca release (DICR). However, intracellular perfusion of DHPs did not. Ca channel tail current (currents other than Ca current were minimized) developed as the depolarizing pulse duration was increased and peaked around 0.7 s, 0.9 s and 1.1 s for depolarizing pulses of +70, +40 and +20 mV, respectively. These values are compatible with the activation time course of RISC (maximal effect took 0.5-1 s for +20 - +60 mV). Preconditioning depolarization (+70 mV, 25 -500 ms) markedly increased both inward pulse and tail currents evoked by stepping the membrane potential to +20 mV (100 - 200 ms) followed by repolarization to -70 mV, suggesting that the increase in the size of tail current is due primarily to the increased conductance of Ca channels during strong depolarizations. In the presence of 0.5 to 1 μM (+)PN200-110, both pulse and tail currents were strongly suppressed. The results suggest that slow activation of RISC may be associated with a slow conformational change in the DHP receptor and that the DHP receptor regulates closing of the release channel. When cells were perfused with 1 mM [Mg]i, RISC was present. However, RISC was abolished over a wide range of depolarizing potentials (-30 - +100 mV) by perfusing with 0.05 mM [Mg]i, although under the same conditions, repolarization still terminated DICR. Low [Mg]i did not shift either the voltage-dependence of DICR or Ca current-voltage relation. These results suggest that Mg-binding to the Ryanodine receptor via the DHP receptor plays a crucial role in repolarization-induced closing of the release channel.

Th-Pos32

THE EFFECTS OF MEMBRANE POTENTIAL ON THE ACTIONS OF DIHYDROPYRIDINES IN GASTROINTESTINAL SMOOTH MUSCLE ((O. Bayguinov, J.D.Campbell and K.M.Sanders)) Department of Physiology, University of Nevada School of Medicine, Reno, NV 89557.

Nifedipine (1μM) partially inhibits the plateau phase of electrical slow waves in gastrointestinal muscles, but does not block the upstroke phase. This suggests that channels other than L-type Ca^{2+} channels are involved in the upstroke or that L-type Ca^{2+} channels are not entirely blocked under the conditions of intact muscles. To distinguish between these possibilities, we studied the inhibition of slow waves and inward currents by nifedipine in canine colonic muscles using microelectrodes, double sucrose gap and patch clamp techniques. Nifedipine (1μM) reduced the rate-of-rise and amplitude of the upstroke component under physiological conditions. Elevated $[K^+]_o$ depolarized membrane potential from -80.8 ± 3.9 to -56.9 ± 4.5 mV, decreased the amplitude of slow waves from 39.9 ± 7.4 to 24.6 ± 4.4 mV, diminished the rate-of-rise from 0.72 ± 0.2 to 0.12 ± 0.1 V/s and reduced the frequency of slow waves (n=29). Nifedipine completely inhibited slow waves in depolarized muscles and this effect was reversed by photoinactivation of nifedipine. Electrical depolarization of muscle strips in the double sucrose gap also allowed nifedipine to more completely inhibit slow waves. In single cell experiments, nifedipine reduced peak inward Ca^{2+} current by 31.7% when cells were held at -80 mV and stepped to 0 mV but by 90% when cells were held at -60 mV. Inward current block was restored to near control levels by photoinactivation of nifedipine. These results suggest that the inability of dihydropyridines to block slow waves in GI muscles may be due to the voltage-dependency of the block rather than a contribution from dihydropyridine insensitive channels. (Supported by DK41315.)

Th-Pos33

EVOLUTION OF CALCIUM CURRENT AND E-C COUPLING IN CULTURED AMPHIBIAN SKELETAL MUSCLE CELLS ((Ruth Cordoba-Rodriguez, Donald R. Matteson, Hugo Gonzalez-Serratos)) Department of Biophysics, University of Maryland School of Medicine, Baltimore, Maryland 21201

Adult frog skeletal muscle cells exhibit slow inward Ca^{2+} currents (I_{Ca}) which are not essential for excitation-contraction coupling (e-c coupling) (Nature 298, 292-294, 1982). We are investigating whether I_{Ca} may have a role in e-c coupling during early stages of skeletal muscle cell development. The experiments were performed on embryonic skeletal muscle cells from Xenopus Laevis maintained in culture for one day to two weeks. Slow inward currents were recorded with Ba^{2+} as the current carrier, using the patch-clamp technique in the whole-cell configuration. As early as one day in culture, these cells had inward currents that increased in magnitude as $[Ba^{2+}]_o$ was increased, and were blocked by external Co^{2+}. These currents increased in amplitude from about 50pA to 2000pA with the age of the cells. One day old cells showed a threshold for contractures induced with caffeine of about 12mM while in one week old cells the caffeine contracture threshold was about 1mM. Preliminary experiments with the calcium indicator Calcium Green-1 show that the increase of intracellular $[Ca^{2+}]$ during stimulation was lower in young cells when compared to adult cells. Fluorescence intensity in young cells increased continuously during 700 ms depolarizing pulses. In old cells the fluorescence increase was biphasic with an early rise followed by a steady phase of lower fluorescence intensity. The above results suggest that in the early stages of development the function of the sarcoplasmic reticulum is not well developed and I_{Ca} may be important in e-c coupling. Supported by NIH grant NS17048.

SR Ca^{2+}-RELEASE CHANNELS: GATING

Th-Pos34

EFFECTS OF RAPAMYCIN ON RYANODINE RECEPTORS FROM SKELETAL AND CARDIAC MUSCLE. ((E. Kaftan, A. R. Marks*, and B. E. Ehrlich)) Univ. of CT, Farmington, CT and *Mount Sinai School of Medicine, New York, NY

To investigate the interactions between the ryanodine receptor (RyR) and FKBP12, we compared the effects of rapamycin, a drug that inhibits the peptidyl-prolyl isomerase activity of FKBP12, on RyR function. Native SR vesicles from skeletal muscle were fused with planar lipid bilayers for single channel analysis. Rapamycin (1μM) increased the open probability of skeletal RyR (Po=3.8% ± 0.78, control; 16.8% ± 1.01, treated). The increased open probability observed at the single channel level was correlated with enhanced ^{3}H-ryanodine binding to SR vesicles (45% increase, bilayer conditions) as expected because ryanodine binds preferentially to the open channel. Rapamycin also increased the open probability of cardiac RyR (Po=3.04% ±0.72, control; 12.04%±1.25, treated); in contrast, this increase in open probability was associated with a 50% decrease in single channel current amplitude. Unlike the skeletal SR, ^{3}H-ryanodine binding to cardiac SR decreased by 56% in the presence of rapamycin which may reflect an inability of ryanodine to bind the partially opened channel. These results support the hypotheses that FKBP12 is functionally associated with the RyR and that this association may differ among tissues.

Th-Pos35

BIOCHEMICAL AND BIOPHYSICAL CHARACTERIZATION OF THE DIAPHRAGM SR Ca^{2+} RELEASE CHANNEL. ((A. Decrouy, S. Proteau and E. Rousseau)) Dept. of Physiologiy and Biophysics, Univ. of Sherbrooke, Sherbrooke, Quebec, Canada J1H 5N4.

The displacement and saturation curves of [^{3}H]-ryanodine binding performed on microvesicles enriched in diaphragm SR membranes from mongrel dogs indicated that the alkaloid binds to its receptor, the SR Ca^{2+} release channel, with a 6.8 nM K_D. Our polyclonal antibodies raised against the canine cardiac isoform of the ryanodine receptor cross react with the diaphragm high molecular weight Ca^{2+} release channel proteins.

To further characterize the diaphragm SR Ca^{2+} channel, the ryanodine receptor protein complex was purified from SR vesicules and incorporated into planar lipid bilayer (PLB), the Ca^{2+} release channel displays a conductance of 610 pS in symetrical 200 mM KCl, 10 mM HEPES-Tris and 100 μM free $[Ca^{2+}]$, pH 7.4. The conductance was decreased to 183 pS when 50 mM Ca^{2+} was added on the luminal side of the channel. Native SR vesicles were also fused into PLB, and studied in asymmetrical Cesium Methane Sulfonate buffer and symmetrical free Ca^{2+} (100 μM) conditions, the recording currents displayed a mean conductance value of 320 pS. Likewise its cardiac and skeletal congeners, Po increases with depolarizing voltage, and the activity of either native or purified channel proteins is modulated by addition of 2 mM of Na-ATP on the cytoplasmic face of the ryanodine receptor.

Supported by an MRC grant. ER is a FRSQ Scholar

Th-Pos36

THE ROLE OF MODAL BEHAVIOR IN THE INACTIVATION OF CARDIAC Ca^{2+}-RELEASE CHANNELS. ((A. Zahradníková and I. Zahradník)) Institute of Molecular Physiology and Genetics, Slovak Acad. Sci., Bratislava, Slovak Republic

Cardiac Ca release channel gating was studied in planar lipid bilayers at intermediate activating Ca^{2+} concentrations (5 - 15 μM). The existence of three modes of activity was proved. In ***mode 0*** the channel is not available for opening. ***Mode 1*** has low openness (0.021 ± 0.004) and a large proportion of short openings (90 ± 2% of τ_{c1} = 0.38 ± 0.03 ms, 10 ± 2% of τ_{c2} = 2.86 ± 0.26 ms) which form unit bursts (88% of bursts). ***Mode 2*** has ten times higher openness (0.20 ± 0.04) and increased number of long openings (56 ± 4% of τ_{c1} = 0.41 ± 0.06 ms vs. 44 ± 4% of τ_{c2} = 2.77 ± 0.39 ms) which form aggregated-opening bursts (80 % of bursts). Transitions between modes 1↔0 and 1↔2 are frequent while direct mode 2↔0 transitions are probably not allowed. The lifetimes of modes 0, 1, and 2 were found to be τ_0 = 0.61 s, τ_1 = 1.60 s, and τ_2 = 0.86 s, respectively. These findings are compatible with a simple Markovian gating scheme (Fig. 1) according to which the channel enters ***fast-access states*** of mode 2 (*full ellipse*) upon Ca binding and afterwards slowly equilibrates into ***slow-access states*** of modes 1 and 0 (*dashed ellipse*). Based on these findings, a kinetic model was developed that simulates the known dynamics of Ca release channel, activation and inactivation, during sequential calcium step increases (Fig. 2), as well as the main features of single-channel behavior on activation and in steady state.

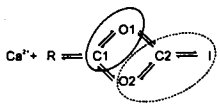

Fig. 1. Channel gating scheme

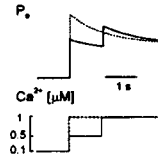

Fig. 2. Simulated time course of open probability (*top*) after a step (*bottom*) from *cis*-Ca^{2+} of 0.1 μM to 1 μM without (*dashed line*) and with (*full line*) a 1 s long "*cis*-Ca^{2+} prepulse" to 0.5 μM.

Th-Pos37

QUINIDINE-INDUCED SUBCONDUCTANCE ACTIVITY IN PURIFIED CARDIAC SR Ca^{2+} RELEASE CHANNELS.
((Robert G. Tsushima, James E. Kelly and J. Andrew Wasserstrom)) Department of Medicine, Northwestern University Medical School, Chicago, IL 60611.

We examined the effects quinidine on purified cardiac SR Ca^{2+} release channels incorporated into planar lipid bilayers and recorded under symmetrical 250 mM KCl (pCa 4.3). Quinidine (50 - 500 μM) reduced single-channel open probability in a voltage and concentration dependent manner. Quinidine block was observed only at positive holding potentials where current flow was from the cytoplasmic to the luminal side of the channel. A more pronounced effect was the appearance of a subconductance state at positive potentials. The single-channel current-voltage relationship in the absence of quinidine displayed an ohmic relationship with a slope conductance of 721 ± 4 pS (n=6), while the quinidine-induced substate exhibited inward rectification at positive potentials with a slope conductance of 204 ± 9 pS (n=6) (28% of control). Analyses of the open and substate dwell-time histograms were best fit to single exponentials functions and yielded k_{on} and k_{off} for quinidine binding. Both the on and off rates were dependent on voltage with k_{on} increasing *e*-fold per 63 mV of depolarization and k_{off} decreasing *e*-fold per 48 mV depolarization. Fits of the voltage dependence of k_{on} and k_{off} to a Boltzmann distribution revealed equivalent valences for the on and off rates of 0.62 and 0.84, respectively. The concentration dependence of quinidine block displayed positive cooperativity suggesting at least two molecules bind in the channel pore. The stereoisomer of quinidine, quinine, elicited a similar blocking behaviour on SR Ca^{2+} release channels implying a lack of stereospecificity in the blocking reaction. These findings suggest that the quinidine-induced subconductance may be the result of a partial occlusion of the channel pore interfering with ion conduction.
Supported by NIH, AHA Chicago Affiliate and MRC of Canada

Th-Pos38

MITOXANTRONE ANTAGONISM OF DOXORUBICIN AT CARDIAC SR CHANNELS IN THE PLANAR LIPID BILAYER. ((E.D. Buck and I.N. Pessah)) Department of Molecular Biosciences, University of California, Davis, CA, 95616

The competitive interaction between doxorubicin (DXR) and mitoxantrone (MTX) in rat cardiac sarcoplasmic reticulum (SR) has been investigated in the planar lipid bilayer. DXR, an anthraquinone, and MTX, an anthracenedione, are both clinically useful antineoplastic agents in use today, however, DXR's usefulness is limited by a dose and time dependent cardiotoxicity. Previous results (Kim, *et. al.*, 1994, Holmberg and Williams, 1990) have shown that under conditions which promote activation of SR Ca^{2+} channels MTX inhibits [^{3}H]ryanodine binding. We show that under conditions promoting closure of SR Ca^{2+} release channels (1μM Ca^{2+} and 1mM mg) DXR, but not MTX, stimulates [^{3}H]ryanodine binding to SR vesicles in a concentration dependent manner. When assayed in combination, MTX inhibits DXR stimulated ryanodine binding and shifts DXR induced binding without altering B_{max}, indicating a competitive interaction. These results are cooberated with active Ca^{2+} transport measurements in SR vesicles. Measurements performed in the planar lipid bilayer show that at low free Ca^{2+} (< 10μM), 10μM DXR stimulates single channel activity by dramatically increasing P_o. At these Ca^{2+} concentrations, MTX only slightly alters P_o. Pre-exposure of channels to 10μM MTX inhibits the DXR stimulated increase in P_o. Addition of 10μM MTX after DXR treatment reverses DXR stimulated channel activity. These results suggest that combination therapy with DXR and MTX may provide a rational basis for combination therapy aimed at extending the current limits of DXR.

Th-Pos39

ACTIVATION OF THE SKELETAL MUSCLE CALCIUM RELEASE CHANNEL BY CHLOROCRESOL. ((A. Herrmann-Frank, M. Richter and F. Lehmann-Horn)) Department of Applied Physiology, University of Ulm, D-89069 Ulm, F.R.G.

Chlorocresols, preservatives often added to commercial preparations of succinylcholine, have been shown to activate ryanodine receptor-mediated Ca^{2+} release in both skeletal muscle and cerebellum (Zorzato et al., Mol. Pharmacol. 44, 1192-1201, 1993). We tested the effect of the most potent activator, 4-chloro-m-cresol , on the sarcoplasmic reticulum (SR) Ca^{2+} release channel/ryanodine receptor from rabbit skeletal muscle. [^{3}H]ryanodine binding was performed in the presence of 1 M NaCl, 1 μM free Ca^{2+}, and 6 nM [^{3}H]ryanodine, pH 7.0. 4-chloro-m-cresol activated [^{3}H]ryanodine binding with a half-maximal stimulatory concentration of 85 μM. Hill plot analysis revealed a Hill coefficient of 1.3. We also examined the effect of 4-chloro-m-cresol on the isolated Chaps-solubilized Ca^{2+} release channel reconstituted into planar lipid bilayers. 4-chloro-m-cresol increased the channel open probability without changing its conductance. In the presence of 1 μM Ca^{2+}, the threshold concentration for activation was 50 μM while saturating effects were observed at concentrations ≥ 500 μM 4-chloro-m-cresol. Comparing the effect of 4-chloro-m-cresol on the cis (cytoplasmic) and trans (luminal) side of the channel, we found that the threshold concentration for activation was 4 times lower on the trans compared to the cis side (50 versus 200 μM). It is therefore suggested that 4-chloro-m-cresol activates SR Ca^{2+} release by binding to regulatory sites of the ryanodine receptor different to those from nucleotide and caffeine binding sites.

Th-Pos40

FAST RELAXATION OF MULTIPLE CALCIUM RELEASE CHANNELS FROM RABBIT SKELETAL MUSCLE IN LIPID BILAYERS. ((Jiying Zhao, Meredith A. Albrecht and Jianjie Ma)) Department of Physiology and Biophysics, Case Western Reserve University, Cleveland, Ohio 44106.

Multiple Ca release channels (n = 4-7) were incorporated into planar bilayers from junctional SR membranes of rabbit skeletal muscle. The channels when bound to ryanodine exhibited asymmetric voltage-dependence of opening: more active channels were measured at positive (cis-minus-trans) than at negative voltages at steady state. The conversion from multiple channels to single channel took 0.15 s at -100 mV. This time constant was about 30 times faster than that of a single channel (τ = 3.9 s at -100 mV). The rate of relaxation was slower at less negative voltages. The inactivated channels at -100 mV had fast responses to open at positive potentials: upon changes of potential from -100 to +100 mV, most channels opened within 5 ms, while a small portion opened within 30 ms (Fig.). The native Ca release channels (without ryanodine) also exhibited fast relaxation, but occurred preferentially at positive voltages. Relaxation of the native Ca release channels had a time constant of 0.81 s at +80 mV. The data suggest a possible interaction among the Ca release channels in bilayer. It is likely that other junctional SR proteins may mediate this interaction. Supported by NIH, AHA and MDA.

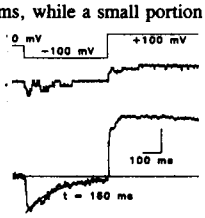

Th-Pos41

RESIDUAL CONDUCTANCE OF SKELETAL MUSCLE RYANODINE RECEPTOR. COMPARISON WITH GAP JUNCTION CHANNELS. ((Jianjie Ma)) Department of Physiology and Biophysics, Case Western Reserve University, Cleveland, Ohio 44106.

The skeletal muscle Ca release channel exhibits multiple conductance states. With 200 mM Cs-gluconate as the current carrier, the channel had a dominant conductance of 450 pS (O1). At positive voltages (current move from myoplasmic to SR), transitions between the full-open state (O1) and a sub-open state (O2, residue conductance of 95 pS) were frequently observed. The 95 pS residual conductance was sensitive to Ca and ATP activation, and could be promoted by the addition of 1 mM DCCD to the myoplasmic solution. In response to changes in membrane potential, some channels start opening from sub-conductance states (95 pS, 225 pS). Repetitive large test pulses drove the channel into desensitized state (Ma et al, Biophys. J. 66: A20), accompanied with the appearance of residual conductance. This residual conductance is similar to the gap junction channels (Bukauskas and Weingart, Biophys. J. 67: 613-625). The Ca release channels differed from the gap junctions in its unidirectional voltage dependence. In the presence of 100 uM myoplasmic [Ca], channel open probability (Po) as a function of voltage followed a Boltzmann distribution, with maximum Po = 22.9±4.7%, slop factor K = 25.9±5.0 mV, mid-point potential Vo = 96.4±11.8 mV, plus a basal open probability $P_{-\infty}$ = 2.4±0.3%. The data suggest that the Ca release channel had structure similar to a hemi-gap junction channel. Supported by NIH, MDA and AHA.

Th-Pos42

SINGLE CHANNEL MEASUREMENTS OF THE CALCIUM RELEASE CHANNEL (CRC) FROM FROG SKELETAL MUSCLE SARCOPLASMIC RETICULUM UNDER PHYSIOLOGICAL CALCIUM GRADIENTS ((James N. DeBritz and Philip M. Best)) Dept. of Physiology and Biophysics, University of Illinois, Urbana, IL, 61801.

The selectivity and conductance of the CRC of frog skeletal muscle was measured in native membrane under physiological calcium gradients. Single channel current was recorded from excised patches made from sarcoplasmic reticulum (SR) extruded to the surface of single muscle fibers whose surface membranes had been mechanically removed. The pipette solution (cytoplasmic face) contained 100mM triethanolamine methane sulfonate (TEAMS), 2mM EGTA, 85mM MOPS, and 0.78mM $CaCl_2$ (pCa=7.4) at pH=7.0, and the bath solution (luminal face) contained 100mM TEAMS, 2mM EGTA, 61mM MOPS, 0.78mM $CaCl_2$, and 4.82mM calcium gluconate (pCa=2.4) at pH=7.0. Under our experimental conditions, the CRC channel displays four conductance levels. Only two of these states are seen frequently enough to allow reliable determination of single channel conductance. Using a second-order polynomial fit to the current-voltage relationship, we report level 2 and level 4 conductances to be 29pS and 75pS, respectively. Current reverses at 14.8mV. Using the Goldman equation modified for divalent ions, this reversal potential gives a $P_{Ca}/P_{triethanolamine}$ of 15.5. The single channel calcium current for level 2, the most common conductance state, at 0mV, the presumed SR transmembrane potential during calcium release, was -0.615 ± 0.13 pA (n=4). (supported by AR32862).

Th-Pos43

RELEASED CA^{2+} HAS INITIALLY POSITIVE AND SUBSEQUENTLY NEGATIVE FEEDBACK EFFECTS ON THE TIME COURSE OF CA^{2+} RELEASE ((M. Yano[1], R. El-Hayek[1], B. Antoniu[1], and N. Ikemoto[1,2]). 1, Boston Biomed. Res. Inst.; 2, Dept. Neurology, Harvard Med. Sch., Boston, MA.

One of the important unsettled questions in muscle physiology is whether the transient increase in the sarcoplasmic Ca^{2+} ($\Delta[Ca^{2+}]$) produces *positive or negative feedback* on SR Ca^{2+} release. We addressed this question using our isolated triad preparation, which is devoid of the cytoplasmic components and hence would permit straightforward control of $\Delta[Ca^{2+}]$ as well as monitoring of Ca^{2+} release. The magnitude of $\Delta[Ca^{2+}]$ per released Ca^{2+} in the depolarization-induced release assay system was systematically varied using several approaches (e.g. changing [BAPTA] at constant $[Ca^{2+}]$). Then, its effects on the Ca^{2+} release time course were analyzed in Ca^{2+} release, ΔCa release, and $d(Ca^{2+}\text{ release})/dt$ curves. The increase in the magnitude of $\Delta[Ca^{2+}]$ led to (a) significant increase in the initial rate of Ca^{2+} release and (b) significant acceleration of the decay in the subsequent inactivation phase. The initial activation, but not the subsequent inactivation, paralleled $\Delta[Ca^{2+}]$, indicating that the accelerated inactivation took place spontaneously as a consequence of the initial hyper-activation by $\Delta[Ca^{2+}]$. Thus, it appears that $\Delta[Ca^{2+}]$ accelerates first the initial phase of Ca^{2+} release, then the subsequent spontaneous inactivation. This new model offers a reasonable explanation compatible with both of the two controversial views in the literature.(Supported by grants from NIH and MDA)

Th-Pos44

ENDOGENOUS PHOSPHORYLATION OF RAT BRAIN RYANODINE RECEPTOR CHANNELS. ((Li, X. and M. Fill.)) Department of Physiology, University of Texas Medical Branch, Galveston TX, 77555-0641. (Spon. by M. Jennings)

Single ryanodine receptor (RyR) channels isolated from rat brain were incorporated in planar bilayers by fusion of native ER vesicles. Single channel solutions contained (in mM): 250 $CsCH_3SO_3$, 10 CsHEPES (pH 7.4) and 0.01 free Ca^{+2}. Endogenous phosphorylation was done following a previously described protocol (Herrmann-Frank & Varsanyi, FEBS 332(3):237-, 1993). Bilayers were cast from a PE:PC decane mixture (8:2, 50 mg/ml). Single channel conductance, open probability, open and closed times were determined in control and endogenously phosphorylated RyR channels. Endogenous phosphorylation did not dramatically change these single channel parameters. Heavy intracellular membrane proteins isolated from rat brain, dog heart, and dog skeletal muscle were separated by SDS-PAGE. Western blots using antibodies recognizing inositol triphosphate receptor (IP_3R) and ryanodine receptor (RyR) were used to identify protein bands. Autoradiography of endogenously phosphorylated brain, cardiac and skeletal preparations indicate that the brain RyR was significantly phosphorylated. The cardiac and skeletal RyRs showed no evidence of endogenous phosphorylation. Thus, the brain preparation must retain endogenous kinase(s). More detailed single channel analysis is required to definitively establish the implications of endogenous phosphorylation of brain RyR. Supported by NIH NS-29640.

Th-Pos45

ADAPTATION OF SINGLE CARDIAC RYANODINE RECEPTOR CHANNELS MAY INVOLVE A CLOSELY ASSOCIATED REGULATORY PROTEIN. ((Velez, P., X. Li, R. Tsushima, M. Cortes-Gutierrez, A. Wasserstrom and M. Fill)) Dept. Physiology, Univ. of Texas Medical Branch, Galveston TX 77555-0641, & Reingold ECG Center, Northwestern University, Chicago IL 60611.

Single cardiac ryanodine receptor (RyR) channels isolated from dog ventricular muscle were incorporated into bilayers by fusion of native SR vesicles or liposomes containing purified RyRs. Free Ca^{+2} stimuli were applied by laser photolysis of caged-Ca^{+2} (DM-nitrophen). UV light was applied to a small area directly in front of the bilayer via a micro-positioned optic fiber. Solutions contained (in mM): 250 $CsCH_3SO_3$, 10 CsHEPES (pH 7.4) & 2 DM-nitrophen. Free $[Ca^{+2}]$ was titrated to pCa 7 and continuously monitored by a Ca^{+2} electrode. In parallel experiments, photolytic Ca^{+2} stimuli were calibrated by specialized Ca^{+2} electrodes and microfluorimetry. A standard photolytic Ca^{+2} stimulus was applied to native and purified RyRs. Ensemble currents were generated. Time constant of activation (τ_{act}) and adaptation (τ_{adp}) were determined by fitting exponential functions to ensemble currents. Adaptation was evident as a spontaneous decay in Po during a sustained Ca^{+2} stimulus (Science 260:807-,1993). The τ_{act} was identical ($\approx$1 ms) for native and purified RyRs. The τ_{adp} of native RyRs was $\approx$1 s. Purified RyRs (n=3) displayed no evidence of adaptation ($\tau_{adp} \rightarrow \infty$). These preliminary results suggests that single channel cardiac ryanodine receptor adaptation may involve a closely associated regulatory protein. (Supported by NIH AR-41197 & AHA).

Th-Pos46

STREAMING POTENTIALS INDICATES A SHORT SELECTIVITY FILTER IN CARDIAC Ca^{+2} RELEASE CHANNEL. ((Tu, Q., P. Velez, M. Brodwick and M. Fill.)) Department of Physiology, University of Texas Medical Branch, Galveston TX, 77555-0641.

Single cardiac ryanodine receptor (RyR) channels isolated from canine left ventricle were reconstituted into planar bilayers. Streaming potentials were measured in osmotically asymmetric solutions as a shift in reversal potential. Membrane potential changes induced by water movement through the bilayer (concentration polarization) and altered ion activities in concentrated nonelectrolyte solution were determined using valinomycin. In 400 mM symmetrical $CsCH_3SO_3$, the average streaming potential was 2.74±0.2 mV (n=5, mean±S.E.; 2 osmol/Kg) and independent of osmoticant used (sucrose or diglycine). Identical streaming potential magnitudes were obtained regardless of which side of the membrane the nonelectrolyte was placed. The RyR's streaming potential is comparable to values measured in a variety of surface membrane channels. Ryanodine-modified RyR channels had no measurable streaming potential, decreased Ba^{+2} permeability (P_{Ba}/P_{Cs} 8.2±0.7 to 1.8±0.5, n=4) and, increased $Tris^+$ permeability (P_{Cs}/P_{Tris} 5.1±1.1 to 1.7±0.3, n=3). Further, ryanodine-modified channels had identical cation/anion selectivity. These data suggests that the narrow region of the permeation pathway, perhaps the selectivity filter, is relatively short ($\approx$ 3 H_2O molecules long). and widens after ryanodine modification. Supported by NIH AR-41197 & AHA.

Th-Pos47

ACTIVATION OF SINGLE Ca^{+2}-ACTIVATED K^+ CHANNELS BY FLASH PHOTOLYSIS OF CAGED-Ca^{+2}. ((Velez, P., A. L. Escobar*, F. Cifuentes, J. L. Vergara* and M. Fill)) Department of Physiology, Univ. of Texas Medical Branch, Galveston TX 77555-0641, and Department of Physiology, UCLA School of Medicine, Los Angeles CA, 90024.

Free Ca^{+2} stimuli generated by photolysis of caged-Ca^{+2} (DM-nitrophen) were applied to single Ca^{+2}-activated K^+ (K_{Ca}) channels reconstituted in planar bilayers. These charybdotoxin-sensitive $\approx$300 pS (200/200 mM KCl, 10 HEPES, pH 7.5) channels were isolated from dog skeletal muscle T-tubes. Near maximal activity occurred at a steady state $[Ca^{+2}]$ of 10 μM (HP=+40 mV). Photolytic Ca^{+2} stimuli were precisely calibrated using a high temporal resolution confocal spot fluorimetry setup and Ca^{+2}-Orange-5N. Three Ca^{+2} stimuli were applied to the channels; #1) a large fast Ca^{+2} spike (half-width <30 μs) from low $[Ca^{+2}]$, #2) a compound Ca^{+2} stimulus consisting of a fast Ca^{+2} spike ($\approx$150 μs) and a step in free $[Ca^{+2}]$ (pCa 7 → 5) and, #3) a monotonic (no Ca^{+2} spike) stimulus where free $[Ca^{+2}]$ steps from pCa 6 → 5. Channels did not activate in response to Stimulus #1 (Ca^{+2} spikes alone). Channels activated equally fast ($\tau_{act} \approx 7$ ms) in response to Stimulus #2 or Stimulus #3. This suggests that the measured τ_{act} represents a maximum response time. Since K_{Ca} channels, fast cellular Ca^{+2} signalling effectors, were unable to respond to Ca^{+2} spikes, the Ca^{+2} spike induced by photolysis of DM-nitrophen may be too fast to introduce artifacts or to be applied as a probe to define biological phenomena. Supported by NIH AR-41197, AHA, and MDA.

Th-Pos48

IS RYANODINE RECEPTOR ADAPTATION TOO COMPLEX TO EXPLAIN WITH A SIMPLE MODEL?

((H. Cheng, M. Fill*, H. Valdivia†, W. J. Lederer)) Dept. of Physiology, Univ. of Maryland, Baltimore, MD 21201 and * Univ. of Texas Medical Branch, Galveston, TX 77555 and † Univ. of Wisconsin Medical School, Madison, WI 53706

We have proposed a simple Hodgkin-Huxley type of model that readily accounts for the complexities associated with ryanodine receptor (RyR) adaptation (S. Györke and M. Fill, *Science* **260**: 807 (1993)). The model is based on the established tetrameric RyR channel structure and biochemical data showing multiple high affinity Ca^{2+}-binding sites on each monomer. We postulated that one kind of binding site (O-domain) tends to **open** the channel when activated by Ca^{2+} and another (A-domain) tends to **adapt** (i.e. close) it. Thus, the tetramer would then have four O-domains and four A-domains. The model uses the following rules to describe the behavior of the channel. The channel opens when the number of active O-domains (O) on the tetramer exceed or equal the number of active A-domains (A), i.e., O≥A and closes when A>O, or when O= zero. In order for the model to fit the published experimental data, each O-domain must be cooperative (n=2) and have lower affinity and faster Ca^{2+}-binding kinetics than each A-domain. At high [Ca^{2+}] when both O- and A-domains are occupied, the data are best fit if the channel opens 75% of the time. This model predicts that steady-state P_O varies as a monotonic function of [Ca^{2+}] and that fast Ca^{2+} steps trigger transient bursts of channel activity well above the steady state level. Remarkably, our simple model accurately accounts for the experimental data which defines RyR adaptation. Thus, we propose that the complex adaptive channel behavior may arise from the assembly of simple interactive monomers.

Th-Pos49

INTERACTION OF THE *SHAKER* B INACTIVATION PEPTIDE WITH THE RYANODINE-MODIFIED SR Ca^{2+}-RELEASE CHANNEL.

((F. C. Mead, A. Tinker, D. Sullivan* and A. J. Williams)) National Heart and Lung Institute, University of London, LONDON, SW3 6LY, UK; *Graduate Department of Biochemistry, Brandeis University, Waltham, MA 02254.

In addition to its role in the inactivation of the *Shaker* B (*Sh*B) K^+ channel, the N-terminal peptide of this channel has been shown to act as a blocker of other forms of K^+ channel (see Beirão et al., J.Physiol., 1994; 474, 269-274). We now report that the *Sh*B peptide will block the sheep cardiac SR ryanodine receptor-channel. Purified receptor-channels were incorporated into planar phospholipid bilayers and gating of the channels was modified by the addition of 100nM ryanodine. With K^+ as charge carrier, μM concentrations of peptide, when added to the cytosolic face of the channel, produce well defined blocking events which reach a level indistinguishable from the normal closed level. The occurrence of block increases with concentration and increasing positive voltage, for example, with 20μM peptide, relative open probability at 20, 40, 60 and 80 mV was 0.9 ±0.04, 0.73 ±0.106, 0.413 ±0.09 and 0.185 ±0.073 respectively. Quantitative analysis of the blocking effect with 20μM peptide gives a $K_d(0)$ of 636.7 ±80.7μM and an effective valency of 1.57 ±0.06. The *Sh*B peptide is considerably less effective when added to the luminal face of the channel, producing only occasional blocking events to a level indistinguishable from the normal closed level. *Supported by the British Heart Foundation and the Wellcome Trust.*

Th-Pos50

Ca^{2+} ACTIVATION OF THE SHEEP CARDIAC SR Ca^{2+}-RELEASE CHANNEL ON A PHYSIOLOGICALLY RELEVANT TIMECOURSE.

((R. Sitsapesan, R.A.P. Montgomery & A.J. Williams)) NHLI, University of London, SW3 6LY, UK. ((Spon. by A.R.G. Lindsay))

Cardiac SR Ca^{2+}-release channels are activated by Ca^{2+} entering the cell during the action potential. Peak cytosolic "trigger" [Ca^{2+}] is reached within several milliseconds. Using a novel method permitting changes in cytosolic Ca^{2+} on a millisecond timescale we have investigated the gating behaviour of cardiac SR Ca^{2+}-release channels. Vesicles of heavy SR were incorporated into planar phospholipid bilayers painted on glass pipettes. The bilayer pipette (*trans* chamber) was placed in one of two parallel streams of solution flowing from a length of double-barrelled glass (theta) tubing. The theta tubing was then moved rapidly allowing the adjacent solution to flow over the bilayer pipette (solution change at bilayer surface ≤10 ms). Bilayers were voltage-clamped at ±40 mV in symmetrical 250 mM CsPIPES, pH 7.2 (luminal free [Ca^{2+}] 5 μM). The free cytosolic [Ca^{2+}] was increased from 0.1 μM up to 100 μM. We find that rapid activation of cardiac SR Ca^{2+}-release channels initiates gating which is no different to the steady state gating recorded using conventional bilayer techniques. At -40 mV no desensitization or inactivation was observed at [Ca^{2+}] up to 100 μM. However at +40 mV, rapid activation followed by inactivation of the channels by 100 μM Ca^{2+} was observed in a small proportion of channels.

This work was supported by the British Heart Foundation.

Th-Pos51

GATING OF THE CA^{2+} RELEASE CHANNEL (CRC) BY ATP OCCURS BY COOPERATIVE BINDING OF FREE ATP (N_H OF 3 TO 4), NOT REQUIRING CA^{2+} OR MG^{2+}

((A. Sonnleitner*, J. Copello*, S. Fleischer*, H. Schindler*)) *Institute for Biophysics, University of Linz, Austria; *Department of Molecular Biology, Vanderbilt University, Nashville, TN.

Terminal cisternae vesicles of sarcoplasmic reticulum from skeletal muscle were incorporated into planar lipid bilayers by vesicle fusion techniques. CRC's were activated by ATP (cis side), in the absence of Ca^{2+} (mM EGTA) and Mg^{2+} (50mM Ca^{2+} at the trans side). Activation was assayed by increase in open probability (p_o) of single channels. P_o reached half maximal values (EC_{50}) at about 0.2mM ATP in sigmoidal fashion, yielding Hill coefficients (n_H) of 3 to 4. Such dose-response curves, i.e. p_o as f[(ATP)] fitted a model by assuming that the channel opens in response to "all-or-none" cooperative binding of four free ATP's, according to $p_o=p_{o,max}/(1+(EC_{50}/[ATP])^4)$. Similar n_H values were found in mM free Mg^{2+} or μM free Ca^{2+}, while EC_{50} values shifted to higher values for Mg^2 and lower values for Ca^{2+}. Replacement of ATP by AMP-PCP gave similar results. The ATP-Mg complex did not activate as well as free ATP. Multi-channel data agreed qualitatively with single channel data, albeit with larger variation in n_H and EC_{50} values. The data provide two insights: (i) activation by ATP does not require Ca^{2+} and overcomes block by Mg^2 at sufficiently high ATP levels; and (ii) free [ATP] may modulate CRC activity. Small changes of [ATP] appear effective as a consequence of the high cooperativity (NIH HL 32711).

CHANNELS: LIGAND GATING AND CELL PROLIFERATION

Th-Pos52

SINGLE-CHANNEL KINETICS OF RECOMBINANT MOUSE AChR: EFFECTS OF MUTATION OF α-SUBUNIT RESIDUE Y190.

((J. Chen, Y. Zhang, G. Akk, S. Sine*, and A. Auerbach)) Dept. Biophysical Sciences, SUNY at Buffalo, NY 14214 and *Dept. Physiol Biophysics, Mayo Foundation, Rochester, MN 55905

In nicotinic AChR the residue αY190 is thought to be near the ACh docking site. Mutations to this residue causes large rightward shifts in the dose-response and equilibrium binding profiles. We have recorded and modeled single-channel currents from wt and mutant mouse AChR made of αβδγ subunits and expressed in HEK 293 cells.Y190F receptor currents occur in clusters at high ACh concentrations indicating that they undergo cycles of desensitization. With increasing [ACh] the effective opening rate saturates at 150 s^{-1} (400x slower than the wt); at low agonist concentrations the apparent closing rate is 500 s^{-1} (2x faster than the wt) and is the same for ACh, CCh, and TMA-activated receptors. The ACh association rates at the first and second agonist binding sites are 64x and 16x slower in the mutant. The ACh dissociation rates at these sites are 3x and 6x slower in the mutant. The ACh equilibrium dissociation constant at the two sites are 603 μM and 1380 μM. In energetic terms, the mutation makes binding to the first and second sites less favorable by 2.0 and 0.4 kcal/mol. The biggest energy cost is at the gating step as the open conformation is less favored in the mutant by 4.2 kcal/mol. For the overall reaction, activation requires an extra 6.6 kcal/mol in the mutant. Other substitutions at position Y190 (W,S, and T) result in channels that have closing rates up to 3x faster than the Y190F mutant. We can interpret the Y190F results as indicating that the mutation raises the free energy of the liganded-open state: the open conformation of the receptor makes more favorable contacts with the agonist than does the closed conformation, and these are disrupted by the mutation. The alignment of the mutant and wt reaction free energy profiles is undefined and we can alternatively interpret the results as indicating that vacant-closed receptors exist in a high energy conformation: the mutation lowers this energy thus increasing the energy required to reach the open state. This interpretation suggests a 'spring-loaded' gating mechanism for AChR (supported by grants from NSF, NIH and MDA to AA, and from NIH to SS)

Th-Pos53

A KINETIC MECHANISM FOR NICOTINIC ACETYLCHOLINE RECEPTORS BASED ON MULTIPLE ALLOSTERIC STATES

((O. Schaad, S.J. Edelstein, E. Henry♣, D. Bertrand and J.-P. Changeux§)) Université de Genève, CH-1211 Genève 4, Switzerland, ♣ NIDDK, NIH, Bethesda, Maryland 20892, §Institut Pasteur, 75734 Paris Cedex 15, France

Ionotropic receptors are characterized by interconversions between open and closed conformational states. Upon binding of agonists, receptor molecules in the closed but activatable resting state (the basal state, B) undergo rapid transitions to states of higher affinities with either open channels (the active state, A) or closed channels (the initial inactive and fully desensitized states, I and D). In order to represent the functional properties of such receptors, we have developed an allosteric-type kinetic model that links conformational interconversion rates to agonist binding. The linkage is based upon the position of the interconversion transition states on a hypothetical linear reaction coordinate. When the model is applied to the peripheral nicotinic acetylcholine receptor (nAChR), values of the parameters of the model are defined within narrow limits. As a result, the various ligand-gating properties, including single-channel recordings, can be represented and several new relationships are predicted. Simulations with the model justify the usage of dose-response curves under certain conditions, but predict channel activation with an A state affinity in the 50 nM range (in order to overcome the intrinsic stability of the B state and to produce the appropriate cooperativity), hence some 1000-fold stronger than the apparent affinity (EC_{50}) in the 50 μM range. Recovery from the desensitized states is predicted to occur via rapid transit through A states with minimal channel opening, thus without requiring a distinct "cyclic" recovery pathway as in the common phenomenological model. Transitions to the desensitized states by low concentration "pre-pulses" (with minimal IC_{50} values of about 20 nM) can also occur without significant channel opening, but the extent of desensitization is predicted to vary with the length of the pre-pulse.

Th-Pos54

INHIBITION OF ACH RECEPTOR CHANNELS BY BARBITURATES. ((R. Boguslavsky and J.P. Dilger)) Depts. of Anesthesiology, Physiology & Biophysics, SUNY, Stony Brook, NY 11794.

Barbiturates inhibit the acetylcholine receptor (AChR) channel; the mechanism for this action is unknown. We used patch clamp techniques to investigate the effects of pentobarbital (PB) and barbital (Barb) on $\alpha_2\beta\gamma\delta$-type nicotinic AChR channels from BC3H-1 cells. Single channel recording from outside-out patches reveals that both drugs cause AChR channel activity to occur in bursts. The mean duration of gaps within bursts is 2 ms for 0.1 mM PB and 0.05 ms for 1 mM Barb. Also, Barb reduces the apparent single channel current by 15%. One explanation for these results is that the drugs bind to the AChR protein and block the flow of ions through the channel. The gap duration would then be related to the dwell time of the drug at its blocking site. The more oil-soluble drug, PB, has the longer dwell time and the higher potency. If this is true, the single channel kinetics can be used to predict the time it takes for the drug to inhibit the channel after it is rapidly applied. To test this, we used a perfusion device capable of applying solutions to outside-out patches within 0.1 ms. We activate macroscopic currents by perfusing a patch with 10 mM ACh ± the drug. PB (0.1 mM) causes a 50% inhibition of the current with a time constant of 1.5 ms. Barb (2 mM) causes a 50% inhibition with a time constant <0.1 ms. These results support a channel blocking model for barbiturate action. This model also describes the action of volatile anesthetics and alcohols on the AChR. Supported by GM42095 (JPD).

Th-Pos55

ACETYLCHOLINE ACTIVATES TWO CURRENTS IN GUINEA-PIG OUTER HAIR CELLS. ((M.G. Evans)) Department of Physiology, School of Medical Sciences, University Walk, Bristol BS8 1TD, U.K.

Outer hair cells (OHC's) receive inhibitory efferent input from the medial olivo-cochlear system. The inhibitory transmitter is thought to be acetylcholine (ACh). Housley and Ashmore (Proc. R. Soc. Lond. B. 244:161. 1991) showed that ACh activated a K current in OHC's which was dependent on external Ca. The receptor was more effectively blocked by nicotinic antagonists than by muscarinic antagonists. In their model, ACh acting through a novel receptor, caused a rise in internal Ca which acted as a second messenger to activate a larger K current. Such a Ca rise was seen by Doi and Ohmori (Hearing Research 67:179. 1993). I now report that, in OHC's of about 30-60 μm, ACh activates an inward current of up to 20 pA at -70 mV, which precedes the larger outward K current recorded under whole-cell voltage clamp. The inward current is best seen in cells with resting potentials greater than -60 mV. The extrapolated reversal potential of the current is close to 0 mV. Both currents appear to be blocked by 200 nM α-bungarotoxin, but only the K current is dependent on external Ca. Thus the inward current is likely to be closely associated with the receptor and could provide the necessary pathway for Ca influx. A similar biphasic response has been reported in chick hair cells (Fuchs & Murrow, J. Neuroscience 12:800. 1992), and also in OHC's (Blanchet and Dulon, 21st IEB, Sept 1994, Montpellier, France), where similar models have been proposed. In broad agreement with these authors, I find that the steady-state I-V relation is N-shaped, as would be expected for a K current dependent on Ca influx.
Supported by the Wellcome Trust.

Th-Pos56

ALTERED GATING OF ACETYLCHOLINE RECEPTORS WITH CHANNEL-DOMAIN MUTATIONS. ((G. N. Filatov and M.M. White)) Dept. of Physiology, Medical College of Pennsylvania, Philadelphia, PA 19129.

Ligand-gated ion channels contain a conserved leucine in the middle of the M2 domain of each subunit (L251 in the muscle-type AChR) which has been proposed to serve as either the gate of the channel or the plug that blocks the pore in the desensitized state. Conversion of this leucine to a threonine in either the homomeric α7 neuronal AChR or the $5HT_3R$ leads to a decrease in the rate of desensitization and shifts the dose-response curve to lower concentrations. We have addressed the question as to whether all 5 leucines must be replaced for this effect to occur by using the mouse muscle AChR (which have a subunit stoichiometry of $\alpha_2\beta\gamma\delta$ and a defined geometrical arrangement of subunits) expressed in *Xenopus* oocytes and transfected mammalian cells. In AChRs in which any one leucine has been replaced by threonine (βL251T, γL251T, δL251T) the rate of desensitization is decreased > 5-fold and the EC_{50} for ACh activation is reduced from 20 μM to 1 μM; the effects are independent of which subunit contains the introduced threonine. Increasing the number of leucines at this position by using the αL251T mutant subunit and/or including more than one mutant subunit has little additional effect on the rate of desensitization, but shifts the dose-response curve even further to the left. These results are consistent with the notion that L251 in each subunit is involved in the gating of the channel, possibly through subunit-subunit interactions. Supported by NIH NS23885 and an AHA Established Investigatorship.

Th-Pos57

A CONFORMATIONAL CHANGE IN THE PEPTIDE BACKBONE OF EXTRA-MEMBRANOUS REGIONS OF THE NICOTINIC ACETYLCHOLINE RECEPTOR MAY LEAD TO CHANNEL INACTIVATION UPON DESENSITIZATION ((J.E. Baenziger, J.P. Chew and N. Méthot)) Dept. Biochemistry, University of Ottawa, Ottawa, Canada K1H 8M5

Changes in the secondary structure of the nAChR upon desensitization have been probed using a combination of FTIR difference spectroscopy and peptide hydrogen-deuterium exchange. Resting-to-desensitized difference spectra recorded in ^1H_2O buffer reveal a number of bands in the secondary structure sensitive amide I region (1600-1700 cm^{-1}) including an intense band near 1655 cm^{-1} which could reflect a change in the orientation of transmembrane α-helices upon desensitization. However, the 1655 cm^{-1} band shifts down in frequency to near 1640 cm^{-1} in ^2H_2O, a shift indicative of random coil structures. The down shift in frequency of this and other amide bands occurs within minutes of exposure of the nAChR to ^2H_2O. These results indicate that the majority of the changes in structure of the nAChR peptide backbone upon desensitization likely occur in regions of the protein involved in random coil structures hydrogen bonded to bulk solvent. Changes in the structure of extramembranous regions of the nAChR, possibly the ligand binding site, may therefore be responsible for channel inactivation upon desensitization.

Th-Pos58

STRUCTURE AND CONFORMATIONAL CHANGES OF THE NICOTINIC ACETYLCHOLINE RECEPTOR PROBED USING FTIR AND HYDROGEN EXCHANGE ((N. Méthot and J.E. Baenziger)) Dept. Biochemistry, University of Ottawa, Ottawa, Canada K1H 8M5

Both the secondary structure and the rate of exchange of peptide hydrogens for deuterium has been monitored by recording FTIR spectra of the nicotinic acetylcholine receptor (nAChR) as a function of time of exposure to ^2H_2O. Roughly 30% of the nAChR peptide N-^1H exchange for N-^2H within minutes of the addition of ^2H_2O. After several days, 75% exchange. The remaining 25% exchange only under conditions that lead to denaturation of the nAChR. Marked changes are observed in the amide I band, but the majority are complete within seconds of exposure to ^2H_2O and thus reflect the exchange of peptides hydrogen bonded to bulk solvent. The hydrogen-deuterium exchange behavior in the presence and absence of Carb as well as for the nAChR affinity purified and reconstituted into different lipid membranes suggests that neither Carb nor the absence of cholesterol or anionic lipids leads to a substantial change in nAChR secondary structure. Slight differences in the rates and/or the extent of exchange of peptide hydrogens for deuterium are detected which lead to minor changes in the shape of the secondary structure sensitive amide I band. The amide I band is very sensitive to peptide $^1H/^2H$ exchange and must be examined with caution when probing changes in protein secondary structure.

Th-Pos59

PHOTOINCORPORATION OF THE UNCHARGED HYDROPHOBIC PROBE [^{3}H] DIAZOFLUORENE INTO THE nAChR M2 REGION ((M.P. Blanton[1] L.J. Dangott[1],S.K. Raja[2], A.K. Lala[2], J.B. Cohen[1])) [1] Department of Neurobiology, Harvard Medical School, Boston, MA 02115; [2] Biomembrane Lab, Department of Chemistry, Indian Institute of Technology Bombay, India.

Photoincorporation of 2-[^{3}H] Diazofluorene ([^{3}H]DAF) into the *Torpedo* Nicotinic Acetylcholine Receptor (AchR) consists of two components: a non-specific component consistent with incorporation into residues situated at the lipid-protein interface[1] and a specific component inhibitable by non-competitive antagonists and localized to the M2 region of each subunit. In the absence of agonist [^{3}H]DAF labeled homologous residues in the M2 region of β- and δ-subunits (β-V-261 and δ-V-269) while no incorporation was detected in α-M2. A 10-fold excess of tetracaine (100 μM) reduced [^{3}H]DAF incorporation into these residues by greater than 90%. Interestingly there is a five-fold greater efficiency of photoincorporation into δ-V-269 than in β-V-261. These results indicate that within the resting ion channel the diazo group of [^{3}H]DAF is oriented towards the δ-subunit. The addition of agonist (100 μM carbamylcholine) results in a redistribution of [^{3}H]DAF labeled residues similiar to that observed previously with [^{125}I] TID[2]. These results provide important imformation about the structure of the channel both in the resting and desensitized states.

[1]Blanton, M.P., Raja, S.K., Lala, A.K. & Cohen,J.B. (1994) *Biophys J.* 66 A213.
[2]White, B.H. & Cohen, J.B. (1992) *J. Biol. Chem.* 267, 15770-15783.

Th-Pos60

BINDING DOMAINS FOR NONCOMPETITIVE ANTAGONISTS WITHIN THE nAChR ION CHANNEL ((Martin J. Gallagher and Jonathan B. Cohen)) Department of Neurobiology, Harvard Medical School, Boston, MA 02115

Pharmacological studies suggest that many noncompetitive antagonists (NCAs) of the *Torpedo* nicotinic acetylcholine receptor (nAChR) bind within its ion channel. The uncharged NCA [^{125}I]TID specifically photoincorporates into residues α-Leu-251, α-Val-255 and the homologous residues of the other subunits -- all of which lie on the pore-lining faces of the M2 transmembrane helices. However, [^{125}I]TID photoincorporation is allosterically, and not competitively, inhibited by the positively charged NCAs phencyclidine (PCP) and histrionicotoxin (HTX), which are presumed to bind within the pore. We have now examined the effect of three positively charged NCAs on the photoincorporation of [^{125}I]TID into the M2 ion channel domain in the resting (closed channel) state of the nAChR to determine how they shift the locus of [^{125}I]TID binding. Tetracaine (30 μM), an NCA that photolabels many of the same residues as TID, reduced the labeling of all M2 residues by 90% and did not introduce any new sites of labeling. This result is consistent with mutually exclusive binding of TID and tetracaine at a common site. PCP (50 μM) increased [^{125}I]TID incorporation into δ-Leu-265 by 2-fold, but decreased labeling of the homologous residue in the alpha subunit (α-Leu-251) by 70%. Photolabeling of the residues in the adjacent helical turn (α-Val-255 and δ-Val-269) was inhibited by < 20%. HTX (30 μM) inhibited [^{125}I]TID labeling of δ-Leu-265 by 65%, α-Leu -251 by 85%, and reduced incorporation into δ-Val-269 and α-Val-255 by 85% and 60% respectively. These results indicate that in the presence of PCP or HTX, [^{125}I]TID is still bound at the rings of aliphatic residues, but its binding domain is perturbed by asymmetric conformational changes of the M2 segments. In each case, [^{125}I]TID binding is preferentially oriented toward δ-Leu-265 and away from α-Leu-251.

Th-Pos61

CHEMICAL KINETIC MEASUREMENTS IN THE μS-MS TIME REGION OF THE NICOTINIC ACETYLCHOLINE AND OTHER NEUROTRANSMITTER RECEPTORS. ((L. Niu, R. Wieboldt, [1]D. Ramesh, [2]K.R. Gee, [3]B.K. Carpenter and G.P. Hess)) Section of Biochemistry, Molecular and Cell Biology, Cornell University, Ithaca, NY, 14853-2703. (Spon. by G. Hess)

A superfamily of receptor proteins in the membranes of cells of the nervous system regulates signal transmission between the cells. A new laser-pulse photolysis technique with a μs time resolution allows one to determine rate constants for the opening and closing of the receptor-channel, the dissociation constant for the ligand-binding site that controls channel opening, the concentration of the open-channel receptor form, and constants for the binding of inhibitors to the closed- and open-channel receptor forms independently, and gives information about the rate of receptor desensitization. The new technique is based on the synthesis of photolabile, biologically inactive precursors of neurotransmitters that can be equilibrated with a single cell. A laser pulse liberates the neurotransmitter and the resulting current can be recorded by the whole-cell recording technique. The time resolution of the technique for investigation of the acetylcholine receptor is 100 μs and of the glutamate, NMDA, and GABA receptors 50 μs. A new photolabile blocking group (2-methoxy-5-nitrophenol) for neurotransmitters containing carboxyl groups is photolyzed within 3 μs.

This work was supported by grants from the National Institutes of Health.
[1]Present address: CalBiochem-Nova Biochem, San Diego CA
[2]Molecular Probes, Inc., Eugene OR.
[3]Department of Chemistry, Cornell University

Th-Pos62

O-METHYLATION OF D-TUBOCURARINE AFFECTS SITE-SELECTIVE BINDING TO THE NICOTINIC ACETYLCHOLINE RECEPTOR **((Steen E. Pedersen)) Dept. of Mol. Physiology and Biophysics, Baylor College of Medicine, Houston, TX 77030**

The effects of methylation at the amines and phenols of d-tubocurarine on the affinity for the two acetylcholine (ACh) binding sites of the nicotinic acetylcholine receptor (AChR) were determined. The two ACh sites differ in their affinity for d-tubocurarine ~300 fold as shown by inhibition of [^{3}H]ACh binding. N-methylation and demethylation had little effect on affinity for either site. Thus, a quaternary ammonium is not required for high affinity binding to the ACh sites. Methylation at both the 7' and 12' phenoxides reduced the affinity for the higher affinity site 10 fold, the same change seen when comparing d-tubocurarine with its trimethylated derivative, metocurine. Two new compounds were prepared: 7'-O-methyl chondocurarine and 12'-O-methyl chondocurarine. Methylation of the 7' phenoxide decreased the affinity at both acetylcholine binding sites while methylation of the 12' phenoxide increased the affinity at the lower affinity site only. When both phenoxides are methylated, the changes at the low affinity site are compensatory and leave no net affinity change while the affinity at the high affinity site is reduced 10 fold. The effects of phenoxide methylation on affinity were additive indicating independent effects. Substitution of bromine or iodine at the 13' position reduced the affinity for the low affinity site only. Thus the 12' and 13' positions specifically affect binding at the low affinity site which is comprised of the α,δ-subunits of the AChR and not at the high affinity site comprised of the α,γ-subunits while 7' modification affects affinity at both sites. l-Bebeerine, a stereoisomer, shows no appreciable binding to the ACh binding sites but binds the noncompetitive antagonist binding site of the AChR as shown by inhibition of [^{3}H]phencyclidine binding with concomitant allosteric reduction of ACh affinity. Thus proper stereochemistry at the 1 position is critical for binding to the ACh binding sites.

Th-Pos63

INTERACTION OF OPEN CHANNEL BLOCKERS WITH NICOTINIC RECEPTOR CHANNELS - A MOLECULAR MODELLING STUDY. ((R. Sankararamakrishnan and M.S.P. Sansom)) Laboratory of Molecular Biophysics, University of Oxford, Oxford, U.K.

We have employed simulated annealing via restrained molecular dynamics simulations (Kerr et al., 1994) to model the pore domain of chick α7 nicotinic acetylcholine receptor. Site-directed mutagenesis and chemical labelling data have identified those M2 sidechains which line the central pore. Such data have been used to derive the Cα templates and distance restraints used in our simulations. Several models are compared, differing in which residues line the central pore and in the tilt angle of their helix axes relative to the pore axis. Interactions of the channel blocking compound QX-222 and the permeant organic cation isobutylamine with these models are evaluated via calculation of potential energy profiles as the drugs are moved through the pore. At each point along the pore the channel sidechains plus the drug molecule are energy minimized. With parallel M2 helices there is a barrier preventing entry of QX-222 into the pore which prevents the channel blocker from contacting those residues implicated in QX-222 binding by site-directed mutagenesis. Tilting the M2 helices by ca. 3°, such that the synaptic mouth of the pore is wider, allows QX-222 to enter the pore and bind midway down the M2 helices. These studies emphasize the need to consider sidechain flexibility when modelling the geometry and interactions of ion channel pores.

Kerr, I.D., Sankararamakrishnan, R., Smart, O.S. & Sansom, M.S.P. (1994) Parallel helix bundles and ion channels:- molecular modelling via simulated annealing and restrained molecular dynamics. *Biophys. J.* 67:1501-1515.

Th-Pos64

TRANSGENIC MICE CARRYING A SINGLE MUTATION IN THE M4 REGION OF THE MUSCLE ACETYLCHOLINE RECEPTOR ALPHA SUBUNIT SHOWED MARKED PROLONGATION OF CHANNEL OPEN TIME. ((R. Maselli, M. Chao, C. Gomez* and M. McNamee)) Univ. of Calif. Davis, Davis, CA 95616 *Univ. of Minn. (Spon. by R. Fairclough)

Site directed mutagenesis has identified the M2 transmembrane segment as the most important contributor to the permeation wall of the acetylcholine receptor (AChR) channel. Initial experiments have indicated less conspicuous involvement of the M4 (protein-lipid interface) domain in channel permeation. However, using the Xenopus oocyte system we have recently shown that a substitution of Cys 418 for Trp 418 in the M4 domain of the α-subunit of *Torpedo Californica* results in a dramatic prolongation of the channel open time. We have now, constructed a transgenic mice expressing the M4 α-subunit substitution to investigate the effect of this mutation in the whole neuromuscular junction. Mice expressing the M4 α-subunit mutation (αM4-mice) were studied with on-cell single channel recordings of the flexor digitorum muscle and intracellular voltage clamp of diaphragm muscle end-plates. α-M4-mice showed a two fold increase of channel open time with no change of channel conductance. Miniature end-plate currents had normal amplitudes but a six-fold increase of the time constants of decays. We conclude that changes in protein structure at the M4 transmembrane domain of the AChR alpha subunit can drastically affect receptor function and neuromuscular junction physiology.

Th-Pos65

ACTIVATION MECHANISM OF HOMOMERIC ρ_1 GABA CHANNELS. ((D. S. Weiss and J. Amin)) USF College of Medicine, 12901 Bruce B. Downs Blvd., Tampa FL 33612-4799.

We have recently identified several amino acids of the ρ_1 subunit (isolated from human retina) that are crucial for GABA-mediated activation of homomeric ρ_1 GABA channels expressed in *Xenopus* oocytes. Mutation of two of these identified amino acids, Y198S and Y247S, produced a ≈2500- and >30,000-fold reduction in GABA sensitivity. Evidence suggests these two residues are part of the GABA binding site. In this study, we coinjected wild type subunits with each of these mutant subunits (at different cRNA ratios) in order to examine the activation features of channels with fewer then normal binding sites. Assigning one binding site per subunit, and the subunits arranged in a symmetrical, pentameric structure, we set out to determine the number of binding steps required to open the channel. Our initial working hypothesis was a five binding step concerted activation mechanism; five GABA molecules must bind to open the channel. The experimentally-observed GABA dose-response relationships were inconsistent with predictions of the five binding step model. Our data suggests that there are five binding sites, of which only three need to be occupied by GABA for the channel to open. The two additional binding sites may help stabilize the open states of the pore and underlie both the slow deactivation of the GABA-activated current observed in oocytes expressing recombinant ρ GABA channels and the long-lasting GABA-mediated inhibition observed in retinal neurons.

Th-Pos66

THE STOICHIOMETRY OF CYCLIC NUCLEOTIDE-GATED ION CHANNELS. ((D.T. Liu, G.R. Tibbs, & S.A. Siegelbaum)) Center for Neurobiology & Behaviour, Columbia University, NY, NY 10032

To determine the subunit stoichiometry of cyclic nucleotide-gated (CNG) ion channels, we have coexpressed bovine retinal channels (RET) with a chimeric retinal channel containing an olfactory channel H5 domain (RO133). RO133 and RET show identical cyclic nucleotide selectivity and P_{max} (Goulding et al., Nature 364:61-64, 1993). However, when expressed alone, RET subunits form a channel with a conductance of 20pS, while the RO133 subunits form a channel with a larger conductance of 85pS (-80mV, pH9.0). Assuming that RET and RO133 assemble to form heteromultimers and the conductance levels of heteromultimers are determined by the subunit composition, the total number of conductance levels should be equal to the number of subunits plus one. When cRNAs of both RO133 and RET are injected in *Xenopus* oocytes, intermediate conductances are indeed observed in an excised inside-out patch with multiple channels. This suggests that heteromultimers can form. In patches with a single channel, the intermediate sizes are stable. At least four conductance levels have been observed so far. The total number of conductance levels is currently being investigated.

Fig.1 The figure shows a patch with two channels, one with the conductance level of RO133 and the other with an intermediate conductance level. Lines indicate closed, RET and RO133 conductance levels.

Th-Pos67

CLONING AND FUNCTIONAL EXPRESSION OF TWO ALTERNATIVE SPLICE VARIANTS OF A MOUSE 5-HT3 RECEPTOR
((M. Glitsch and A. Karschin)) Mol. Neurobiology of Signal Transduction, Max-Planck-Institute for Biophysical Chemistry, 37077 Goettingen, Germany

5-HT3 receptors are ligand gated cation channels that mediate rapidly depolarizing currents in central and peripheral neurons and thus play an important role in fast signal transduction. Here we report the cloning, functional expression and electrophysiological characterization of two alternative splice variants of a 5-HT3 receptor isolated from the mouse embryonic hippocampus x neuroblastoma fusion cell line HN 9.10e. Whole cell recordings in wildtype HN 9.10e cells identified a prominent 5-HT-induced current with properties typical of 5-HT3R-mediated currents. mRNA isolated from the cells was reverse-transcribed and subjected to PCR amplification using nondegenerate primers for the 5' and 3' ORF end of the mouse 5-HT3R-A sequence (Maricq et al., 1991, Science 254, 432). Sequencing of the amplified fragments identified a short version 5-HT3R-S with a six amino acid deletion in the second cytoplasmic loop, two amino acid insertions and one amino acid substitution (Hope et al., 1993, Eur. J. Pharmacol. 245:187). Restriction analysis also indicated the existence of the longer version in these cells which was PCR amplified using 5' and 3' primers spanning the deletion segment. As suggested by sequence analysis of genomic mouse DNA, both variants were the result of alternative splicing. Poly(A)$^+$ RNA transcribed from the two clones was successfully expressed in *Xenopus laevis* oocytes. In injected oocytes, 0.5 - 10 µM 5-HT evoked dose-dependent inward currents (V_H= -80mV). In the maintained presence of agonist the currents decreased rapidly, suggesting pronounced receptor desensitization. Bath-applied Ca^{2+} and Mg^{2+} (0.9-2 mM) decreased the amplitude of the currents with Ca^{2+} being the more potent inhibitor. The channels were permeable to both Na^+ and K^+ (E_{Rev} ~ 0 mV), whereas $Tris^+$ did not seem to permeate. Further characteristics and possible differences between the two splice variants are currently being investigated.

Th-Pos68

THE EFFECTS OF TAURINE ON SINGLE ION CHANNEL ACTIVITY IN RAT CEREBELLAR GRANULE CELLS ((M.-L. Linne[1], S.S. Oja[1] and T.O. Jalonen[2])) [1]Univ. of Tampere, 33101 Tampere, Finland, and [2]Albany Medical College, Albany, NY 12208, USA. (Spon. by C.P. Scholes).

Taurine (2-aminoethanesulphonic acid) has been proposed to act as a neuromodulator or neurotransmitter in the CNS, but as yet its role in the brain is not well understood. We have now investigated ionic currents activated and modulated by taurine in 7-day-old rat cerebellar granule cells after 5-7 days in culture using the single-channel patch-clamp technique. The activation/ inactivation of channels, the current magnitude at different membrane potentials and the open/closed kinetics were studied by using nanomolar to millimolar concentrations of taurine at pH 6.8, 7.4 and 8.0. Taurine was either applied to the bath or to the recording pipette solution. In the cell-attached recording configuration the activation of an inward current at the cell resting potential is seen at different taurine concentrations and pH. At hyperpolarized potentials (V_m < -70 mV) the single-channel activity and the current magnitude were increased. The reversal potentials of the current measured at different chloride concentrations and various chloride channel blockers are used to a more detailed ion channel characterization. Further studies are made using specific receptor antagonists as it has been suggested that taurine acts through GABA, glycine or specific taurine receptors.

Th-Pos69

EFFECTS OF CALCIUM ON NORADRENALINE EVOKED CATION CURRENT IN RABBIT PORTAL VEIN SMOOTH MUSCLE CELLS.
((Helliwell, R.M., Greenwood, I.A. and Large, W.A.)) Department of Pharmacology and Clinical Pharmacology, St. Georges Hospital Medical School, Cranmer Terrace, London, SW17 ORE, U.K. (Spon. T.B. Bolton)

Under conditions where the calcium current and calcium-activated conductances were suppressed, bath application of noradrenaline (100µM) produced a sustained noisy inward current (holding potential, -50mV) of 29 ±3pA (n=17). This is a cation current (I_{cat}) and has been described previously (Wang & Large 1991). The current/voltage relationship displayed inward rectification at voltages positive to +10mV and outward rectification at potentials negative to -40mV. The current reversed direction at +9 ±2mV in normal Ca^{2+} (1.5mM) extracellular solution and shifted -4 ±0.7mV, n=7, on addition of Ca^{2+} free extracellular solution. This procedure also enhanced the amplitude of I_{cat} at negative potentials. For example in 8 cells noradrenaline evoked an inward current (holding potential -50mV) which peaked at 35 ±4pA before decaying to 22 ±2.8pA. This was followed by an increase of 72 ±11pA on exposure to Ca^{2+} free extracellular solution. The effect of intracellular Ca^{2+} on the amplitude of noradrenaline evoked I_{cat} was also investigated on the same population of cells at a holding potential of -50mV. The initial amplitude was 21 ±4.8pA and 10 ±3pA and the amplitude after 6 min was 5 ±1.2pA and 1±0.9pA using 14nM and 100nM buffered free intracellular Ca^{2+} respectively. These preliminary data suggest that extracellular Ca^{2+} may have an antagonistic effect on the inward movement of cations through this channel in addition to a degree of permeability. There is also evidence to suggest that this current is modulated by intracellular Ca^{2+}.

Wang, Q. and Large, W.A. *J. Physiol.* 435, 21-39.

Th-Pos70

EFFECT OF PENTACHLOROPHENOL ON CALCIUM ACCUMULATION IN MUSCLE CELLS. ((J.C. Nwoga[1], J.C Sniffen[1], C. Peña-Rasgado[2], V.A Kimler[2] and H. Rasgado-Flores[2])) [1]Dept. Biol. Florida A&M Univ, Tallahassee, FL, 32307; and [2]Dept. Physiol. FUHS/The Chicago Medical School. N. Chicago, IL. 60064.

Pentachlorophenol (PCP) is used extensively as a biocidal agent and wood preservative although it may have cytotoxic and carcinogenic effects. However, little is known about how it affects cells. The effect of extracellularly applied pentachlorophenol (PCP) was studied on the membrane potential (V_M) and Ca^{2+} uptake in isolated, voltage-clamped barnacle muscle cells. Ca^{2+} uptake was determined radiometrically. 0.1 PCP induced a depolarization of 9 mV and an increase in Ca^{2+} uptake of 2.3 nmoles/mg dry weight with respect to control cells. The PCP-induced depolarization was respectively reduced by 11% and by 50% by removal of external Ca^{2+} (Ca_o) and by the simultaneous replacement of extracellular Ca^{2+} and Na^+ by $Tris^+$. Verapamil (0.1 mM) completely inhibited the PCP-induced Ca^{2+} uptake as well as the membrane depolarization in either the absence or presence of Ca_o. In cells whose V_M was maintained clamped, PCP induced a Ca^{2+} uptake which was identical as the one observed when accompanied by depolarization. This suggests that PCP induces activation of verapamil-sensitive Ca^{2+} channels independent of V_M. Activation of these channels produces membrane depolarization as Ca^{2+} permeates through them. In the absence of Ca_o, PCP-induced activation of these channels produces a smaller depolarization as Na^+, and, to a lesser extend, $Tris^+$ permeate through them.

Th-Pos71

MODIFICATION OF DISULFIDES INCREASES THE AFFINITY OF THE NMDA RECEPTOR. ((X-G Wu and B.N. Christensen)) Department of Physiology & Biophysics, Univ. Tx. Med. Br, Galveston, TX 77555.

It is well known that treatment of the NMDA receptor with reducing agents that convert disulfides to sulfhydryls produces a marked increase in the membrane current in the presence of agonist. If alkylation with N-methylmaleimide (NEM) follows reduction, the potentiation of the membrane current is irreversible. We have studied the effect on the NMDA-induced membrane current following treatment of catfish cone horizontal cells with dithiothreitol (DTT) and alkylation with NEM. Concentration-response curves of the NMDA response before and following modification by DTT and alkylation by NEM demonstrated a decrease in the EC_{50}. In three cells, the average EC_{50} before treatment was 47.63±11.67 µM and the membrane current -0.96±0.36 nA. Following modification and alkylation, the EC_{50} decreased to 23.45±4.19 µM and the membrane current increased to -1.97±0.62 nA.

The interaction of receptor (R) and agonist (A) can be expressed as:

$$A + R \underset{k_2}{\overset{k_1}{\rightleftharpoons}} AR \underset{k_4}{\overset{k_3}{\rightleftharpoons}} AR^*$$

Where $KD_1=k_2/k_1$ and $KD_2=k_4/k_3$. KD_1 is the dissociation constant of the agonist and KD_2 is the conformational dependent constant. The EC_{50} is dependent on both KD_1 and KD_2.

$$EC_{50} = \frac{KD_1}{1+KD_2} * KD_1$$

The effect of DTT on the NMDA response is to decrease the EC_{50} and increase the maximum response. Although a decrease in KD_1 can account for the change in EC_{50}, this alone will not increase the response. We provide evidence from a model simulation that both of these changes can be accounted for by a decrease in KD_2. Supported by grant NEI-01897.

Th-Pos72

BLOCK OF CHLORIDE CHANNELS INHIBITS HUMAN MYELOBLASTIC LEUKEMIA CELL PROLIFERATION

(Bo Xu and Luo Lu) Department of Physiology & Biophysics, School of Medicine, Wright State University, Dayton, Ohio 45435

Ion channels play important roles in cell volume regulation, secretion, activation and division in nonexcitable cells. In our previous study, we have identified and characterized a cAMP-dependent protein kinase regulated Cl^- channel in human myeloblastic leukemia ML-1 cells (J. Membrane. Biol. 142, 1994). The relationship of the chloride channel function to ML-1 cell proliferation / differentiation has been investigated. In serum derived G_0-arrested cells, addition of serum initiates a cascade of events that result in DNA synthesis and mitosis. This serum induced cell proliferation, however, is inhibited by the Cl^- channel blocker, anthracene-9-carboxylic acid (9-AC) in a range that is not directly toxic to ML-1 cells as assessed by trypan blue exclusion. 9-AC effectively blocked proliferating cell growth monitored by counting cell number and [^{3}H] thymidine incorporation. The half maximum inhibitory concentration (ID_{50}) was 0.7 mM. Time course of the study revealed that the inhibition on DNA synthesis by 9-AC initiated as early as in the first 30 min and reached the maximum in 24 hours. Possible mechanisms of 9-AC inhibition on ML-1 cell growth were investigated. Our results indicated that 9-AC treatment alters the intracellular pH (pHi) 0.3-0.5 over controls. Expression of early differentiation gene MCL-1 (Kozopas et al, PNAS, 90: 3516-3520) has also been examined by using northern blotting. One day after 1 mM 9-AC treatment, the level of MCL-1 gene expression was not significantly changed comparing to that of proliferating ML-1 cells. It is more likely that blockage of Cl^- channels activated by second massage system coupled to the growth factor receptor reduces Cl^- eflux, which in turn speeds up Cl^- / HCO_3^- exchanger and causes cytoplasm alkaline. The increment in pHi inhibits cell cycle dependent kinases (CDKs) and traps ML-1 cells in G_0 / G_1 stages. Our results suggest that second massage system regulating Cl^- channels might be one of the component involving cell proliferation stimulated by growth factors.

Th-Pos73

FAS-INDUCED CELL DEATH BY INCOMPLETE PROLIFERATION SIGNALLING. ((G.L. Busch*, E. Gulbins*, K.M. Coggeshall**, K. Schlottmann**, B. Brenner*, A.E. Busch* and F. Lang*)) *Institute of Physiology, University of Tübingen, 72076 Tübingen, Germany; **Dept. of Microbiology, Ohio State University, 43210 Ohio, USA. (Spon. by A.E. Busch)

Stimulation of lymphocytes via the Fas receptor results in apoptosis, although the mechanisms involved are unknown. Stimulation with anti-Fas antibody (Fas-Ab) induces ceramide production, Ras activation, and generation of H_2O_2 (E. Gulbins et al, submitted). Since incomplete cell activation appears to induce cell death and the Ras pathway is important in regulation of cell proliferation, we tested whether other important signalling events, in particular intracellular Ca^{2+} release, are modified by the Fas receptor, ceramide and H_2O_2. Ca^{2+} was determined in Fura-2AM loaded Jurkat cells, a human lymphoma cell line, by microspectrofluorimetry. Treatment of the cells with 50 µM C_2- or C_6-ceramide resulted in a rapid and transient increase in Ca^{2+} (by 357 ± 59 nM, n=6, and 423 ± 116 nM, n=4, respectively) which was not blocked by removal of extracellular Ca^{2+}. Similarly, H_2O_2 treatment (100 µM) resulted in a transient increase in Ca^{2+} (by 183 ± 6 nM, n=7). Pre-treatment with Fas-Ab, however, blocked both C_2- and C_6-ceramide and H_2O_2-induced Ca^{2+} transients. Similarly, Ca^{2+} (459 ± 41 nM, n=9) and IP_3 (18.9 ± 4.2%) increases induced by treatment with anti-TCR/CD_3 antibody (OKT-3) were also blocked by pre-treatment with Fas-Ab. This Ca^{2+} block by Fas receptor stimulation was shown to be mediated by a phosphatase as it was effectively reversed by calyculin (25 nM), okadaic acid (500 nM) and phenylarsine oxide (2 µM). Therefore, the Fas receptor seems to regulate two pathways, i.e. ceramide production, activation of Ras and H_2O_2 synthesis as well as stimulation of a phosphatase which prevents Ca^{2+} and IP_3 release. As incomplete proliferation signals appear to play a key role in apoptosis, we suggest that Fas-induced cell death results from incomplete cell activation via ceramide, Ras and H_2O_2, in conjunction with a phosphatase-mediated inhibitory signal.

Th-Pos74

ACTION OF STAUROSPORIN AND PMA ON FIBROBLAST SPREADING AND INTERNAL PH.

((Irina Yu. Novikova))
A.N. Belozersky Institute of Physico-Chemical Biology,
Moscow State University, Moscow, Russia
(Spon. by S. Levy)

Spreading of fibroblasts on glass is mediated by the interaction of cell-surface proteins from the integrins family with fibronectin or vitronectin which can be absorbed on glass. We tested involvement of protein kinase C (PKC) in the fibroblast spreading and pH increase during spreading. Internal pH was determined in each cell using fluorescent pH-sensitive dye BCECF. The staurosporin concentration needed to completely inhibit PKC activity in the membrane and the PMA (phorbol myristate acetate) concentration needed to deplete cells of PKC were determined for NMF and DM-15 cells using the measurement of PKC activity. In these concentrations staurosporin and PMA had no influence on the cell spreading. On the other hand, internal pH increase during the cell spreading in serum containing media was completely abolished by staurosporin and PMA. Thus, PKC activation is not necessary for fibroblast spreading, while the increase in pH during spreading is due to PKC activation.

Th-Pos75

ION CHANNEL PHENOTYPE OF MELANOMA CELL LINES.

((Daniel H. Allen, Albrecht Lepple-Wienhues, Michael D. Cahalan)) Dept. of Physiology and Biophysics, UC Irvine, CA 92717.

Melanoma cells are transformed melanocytes of neural crest origin. K^+ channel blockers have been reported to inhibit melanoma cell proliferation. We used whole-cell recording to characterize ion channels in four different human melanoma cell lines (C8161, C8321, C8146, and SK28). Protocols were used to identify voltage-gated (K_V), Ca^{2+}-activated (K_{Ca}), and inwardly rectifying (K_{IR}) K^+ channels; swelling-sensitive Cl^- channels (Cl_{swell}); and voltage-gated Na^+ channels (Na_V). The presence of Ca^{2+} channels activated by intracellular store depletion was tested using thapsigargin to elicit a rise in $[Ca^{2+}]_i$.

Cell Type	K_V	K_{Ca}	K_{IR}	Cl_{swell}	Ca^{2+}	Na_V
C8161	no	yes (ap)	yes	yes	yes (22%)	yes (40%)
C8146	yes	no	no	yes	not studied	no
C8321	no	no	no	yes	not studied	no
SK28	no	yes (CTX)	yes	yes	yes (50%)	no

K_V channels activated at ~-20 mV and showed use dependence. K_{Ca} channels in C8161 cells were blocked by 10 nM apamin (ap), but were unaffected by charybdotoxin (CTX). K_{Ca} channels in SK28 cells were sensitive to CTX (K_d = 4 nM), but were unaffected by apamin. The whole cell conductance levels for K_{IR} differed between C8161 (.6 nS) and SK28 (100 nS). Cl_{swell} current developed at .03 nS/sec when the cells were bathed in 80% Ringer solution, and was strongly outwardly rectifying (4:1 in symmetrical Cl^-). The percentage of cells with depletion-activated Ca^{2+} current decreased as the culture approached confluence. We conclude that different melanoma cell lines express a diversity of ion channel types. Supported by NIH grant NS14609.

Th-Pos76

A MODEL FOR A POSSIBLE FUNCTIONAL LINK IN THE MODES OF ACTION OF 5-HYDROXYTRYPTAMINE AND GLUTAMINE ON MITOGENIC SIGNAL TRANSMISSION

((Mary N. Stamatiadou)) Institute of Biology, NCRNS Research Center "Demokritos", Aghia Paraskevi, Athens, Greece.

Mitogenic signal transduction in mammalian cells may be readily controlled by small perturbations in the network of nutrient requirements of the cell. Thus, while glutamine deficiency limits growth of cultured fibroblasts, increased concentrations of glutamine in the culture medium of the cells result in diminishing the response of resting 3T3 cells to serum growth factors. When glutamine concentration is increased up to 4fold, no mitogenic stimulation is observed and the cells remain quiescent but healthy. While the response of the cells to mitogenic stimulation in the presence of excess glutamine is thus abolished, the temporal profile of primary signal transduction to DNA synthesis remains unaltered. Hence, regulation of intracellular glutamine synthesis may well constitute a lateral controlling filter in mitogenic signal transduction. Endogenous synthesis of glutamine in mammalian cells through action of the enzyme glutamine synthetase (EC 6.3.1.2) is controlled by its end product glutamine and by various exogenous agents including 5-hydroxytryptamine (5-HT) which is known to inhibit *de novo* synthesis of glutamine synthetase (Stamatiadou, M. N., *Biochim. Biophys. Acta* (1973) 304, 169-180). 5-HT also inhibits the induction of DNA synthesis following mitogenic stimulation of resting cells. The possibility is examined that the regulatory system of glutamine synthetase in mammalian cells may offer a model for a functional link in the modes of action of 5-HT and glutamine on mitogenic signal transmission.

Th-Pos77

EVIDENCE FOR AN IMMISCIBLE CHOLESTEROL PHASE IN ARTERIAL SMOOTH MUSCLE CELL PLASMA MEMBRANES IN DIETARY ATHEROSCLEROSIS. TN Tulenko & RP Mason† Medical College of PA, Phila., PA and †Allegheny Campus, Medical College of PA, Pittsburgh, PA

Small angle x-ray diffraction was used to examine arterial smooth muscle (ASM) cell plasma membranes isolated from control and dietary-induced atherosclerotic rabbits. These studies demonstrated progressive changes in ASM plasma membrane structure as a function of time on the cholesterol diet (2%) which correlated directly with membrane unesterified cholesterol content and the development of atherosclerotic lesions. Plasma membranes obtained from animals with advanced atherosclerosis had a two-fold increase in the membrane cholesterol:phospholipid molar ratio. Meridional x-ray diffraction patterns indicated an immiscible cholesterol "bilayer" phase with a width of 34 Å coexisting with the membrane liquid crystalline lipid bilayer (56Å width) at 37°C. The effect of cholesterol enrichment on the formation of an immiscible cholesterol domain was reversible and reproduced with a reconstituted phospholipid/cholesterol binary lipid system derived from cardiac tissue. A marked increase (1.5-fold; $p<.001$) in Ca^{++} permeability was observed in ASM strips isolated from animals in which the immiscible cholesterol bilayer phase was found. This augmented Ca^{++} permeability was mediated by a membrane pathway which was not inhibitable by either organic or inorganic (Ni^+) Ca^{++} channel antagonists. We suggest that this increased membrane Ca^{++} leak is mediated by the cholesterol bilayer phase domain. These data provide direct evidence for changes in the lipid organization of both model and SMC plasma membranes as a result of cholesterol enrichment during the development of dietary atherosclerosis. This change in lipid bilayer structure may underlie alterations in ASM cell plasma membrane Ca^{++} permeability that is related to the genesis of atherosclerotic lesions.

Th-Pos78

Potentiation of Neuronal Nicotinic Receptor Responses by Sulfhydryl Reagents

J.A. Ramirez-Latorre, A. Berliner and L.Role. Center for Neurobiology & Behavior, Columbia University. 722W 168th St. New York, NY 10032

We have observed that the positively charged sulfyhdryl reagent MTSEA causes a potentiation of the ACh response in oocytes injected with $\alpha4\beta2$ nAChR subunit RNA. This effect is specific for MTSEA, because the larger MTS derivative MTSET does not produce this potentiation. We have mutated every extracellular Cys to Gly in $\alpha4$ and two Cys in the M1 to M2 loop. We have identified the cysteine which reacts with MTSEA causing the potentiation of the ACh response. This Cys is in the intracellular M2 region. Experiments are underway to analyze this potentiation at the level of single channel kinetics. The $\alpha7$ subunit lacks this critical cysteine. We are currently testing the effects of MTSEA on homomeric $\alpha7$ channels, to determine the amino acid requirements for this potentiation.

Ca^{+2} produces a potentation on the $\alpha4\beta2$ combination of similar magnitude to that produced by MTSEA. We have also observed that the MTSEA interferes with the potentiating effects of Ca^{+2} in the $\alpha4\beta2$ combinations. We are also studying this effect at the single channel level to determine if Ca^{+2} and MTSEA produce similar effects at the single channel level. We are also trying to determine if the cysteine at the same position in the β subunits is less effective in potentiating the response to MTSEA.

NEURONAL PHYSIOLOGY

Th-Pos79

THE PHASE-LOCKING OF THE NEURAL DISCHARGE TO A WEAK CYCLIC INPUT: STOCHASTIC OR CHAOTIC ?

((S. Chillemi, M. Barbi, D. Petracchi)) Istituto di Biofisica del C.N.R., Via S. Lorenzo 26, 56127 Pisa, Italy. (Spon. by C. Frediani)

Many types of neurons exhibit a form of stochastic phase-locking in which they fire near a preferred phase but not at every cycle of a stimulus. Because of the phase preference the interspike interval histograms (ISIH's) appear multimodal with peaks located at integer multiples of the driving period T. This phenomenon has been well explained by modelling the neurons as bistable systems embedded in noise [1]. Central neurons in the isolated brain of the pond snail *Lymnaea stagnalis* show a rather different behaviour. When stimulated by a weak periodic stimulus they exhibit ISIH's characterized by very few peaks, that could be described at a first glance as m:n phase-locking; however, the interval sequence looks quite irregular. The variability seen in the spontaneous activity can account for the lack of complicated phase-locked responses [2]. This apparent randomness could be ascribed to the incoherent synaptic inputs or to the system's dynamics. To answer this question analyses in the phase space, specifically designed to detect deterministic features in a noisy discharge, are useful. In this work such tools will be used and in particular recently suggested techniques which look very important working with biological preparations [3,4].

[1] A. Longtin, A. Bulsara and F. Moss. (1991). Phys. Rev. Lett., Vol. 67: 656-659.
[2] A.W. Holden and S.M. Ramadan. (1981). Biol. Cybern., Vol. 41: 157-163.
[3] S.J. Schiff, K.J. Jerger, D.H. Duong, T. Chang, M.L. Spano and W.L. Ditto.(1994). Nature, Vol. 370: 615-620.
[4] G. Sugihara and R.M. May. (1990). Nature, Vol. 344: 734-741.

Th-Pos80

PACEMAKER SYNCHRONIZATION BY WEAK ELF FIELDS: A CIRCUIT MODEL SIMULATION.

((L. J. Bruner and J. R. Harvey)) Department of Physics, University of California, Riverside, CA 92521

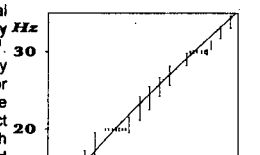

The possibility that repetitively firing neural (pacemaker) cells could be synchronized by regularly spaced synaptic input has long been recognized[1]. Synchronization of neural firing patterns by extremely low frequency (ELF) environmental electric or magnetic fields has also been considered[2]. While current densities of $\approx 10^{-3}$A-cm^{-2} are required for direct excitation of otherwise quiescent neural tissue, much lower peak current densities ($\approx 10^{-6}$A-cm^{-2}) generated by alternating ELF fields have been reported to entrain spontaneously firing molluscan pacemaker cells[2]. We have previously described a circuit model[3] which simulates repetitive spike generation by a space clamped patch of excitable membrane subjected to depolarizing current. Area of the simulated patch is 10^{-3}cm^2. The accompanying figure exhibits a smooth solid line graph of spike generator frequency *versus* dc depolarizing current. When 0.8 pA rms 60 Hz ac current is superposed, the discrete points with error bars indicating spike period dispersion are obtained. Subharmonic locking of the spike generator at 30, 20, and 15 Hz is evident. The corresponding simulated tissue current density is $\approx 10^{-9}$ A-cm^{-2}.

This work was supported by the Biological Sciences and Technology Program of the Office of Naval Research.

1. Perkel, D. H., Schulman, J. H., Bullock, T. H., Moore, G. P., and Segundo, J. P. *Science*, 145, 61-63 (1964).
2. Wachtel, H., *In*: Biological Effects and Dosimetry of Static and ELF Electromagnetic Fields. Grandolfo, M., Michaelson, S. M., and Rindi, A.,Eds, Plenum Press, New York. pp. 313-328 (1983).
3. Bruner, L. J., and Harvey, J. R., *Biophys. J.* **64 (No. 2; Pt 2)**, A99 (1993).

Th-Pos81

A CIRCUIT MODEL DEMONSTRATION OF STOCHASTIC RESONANCE.

((J. R. Harvey and L. J. Bruner)) Department of Physics, University of California, Riverside, CA 92521

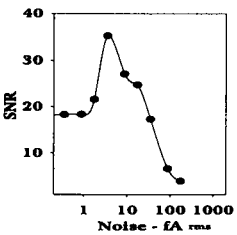

The presence of an optimum level of noise can actually enhance the signal to noise ratio of a detector under appropriate conditions, a phenomenon described as stochastic resonance[1]. Using a neural spike generator circuit model described previously[2], we have demonstrated stochastic resonance as illustrated in the accompanying figure. The spike generator is a relaxation oscillator of the van der Pol type. The signal to noise ratio (SNR) is defined as the ratio of oscillator mean period to oscillator period dispersion. The SNR is plotted linearly *versus* injected rms noise voltage plotted on a log scale. Injected noise is "white", covering a bandwidth of 0-10 kHz. Stochastic resonance illustrated by this example has its origin in period "chatter", inherent to the nominally noise free oscillator operating near cutoff, caused by variable duration momentary interruptions of movement around its limit cycle. These momentary cutoffs, which make the dominant contribution to period dispersion for the nominally noise free oscillator, are markedly reduced upon introduction of noise from an external source.

This work was supported by the Biological Sciences and Technology Program of the Office of Naval Research.

1. Moss, F., *Ber. Bunsenges. Phys. Chem.* **95** 303-311 (1991).
2. Bruner, L. J., and Harvey, J. R., *Biophys. J.* **64 (No. 2; Pt 2)**, A99 (1993).

Th-Pos82

PROPAGATION VELOCITY OF PERIODIC SYNCHRONIZED BURSTS IN CULTURED NETWORKS OF CORTICAL NEURONS.

((E. Maeda[1], H.P.C.Robinson[2] and A.Kawana[1]))
[1]NTT Basic Research Labs., Atsugi-Shi, 243-01, Japan and [2]Physiological Lab., University of Cambridge, CB2 3EG, U.K.

In order to study the basic mechanisms of synchronized firing in developing neuronal networks, the characteristics of periodic synchronized bursts in cultures of dissociated cortical neurons were studied using multisite recording through planar electrode arrays. The networks consisted of a sheet of cells of fairly uniform density (c. 10^4 cells/mm^2), and filling of cells with Lucifer Yellow revealed an average maximum extent of neuronal projections of approximately 200 μm from the cell body, compared to a network of approximately 1 cm in diameter. Therefore, the network may be considered as a collection of multiple overlapped local circuits, forming a 2-dimensional excitable medium. With maturation of the network (from 3 to 40 days after plating), not only the frequency but also the propagation velocity of bursts increased markedly (approximately from 5 to 100 mm/sec respectively). Partial sectioning of cultured networks by UV laser resulted in an increased propagation delay. These results indicate that the density of projections between areas is a major determinant of the propagation velocity. In addition, strong repetitive electrical stimulation evoking bursts over the whole network, led to a maintained increase in the propagation velocity. This suggests that the velocity is also determined by the efficiency of synaptic projections between cells, which may be modified by stimulation.

Th-Pos83

A NEW SIMULTANEOUS 1020-SITE OPTICAL RECORDING SYSTEM FOR DETECTING ELECTRICAL ACTIVITY AT A MICROSCOPIC SCALE. ((A. Hirota, K. Sato, Y. Momose-Sato, T. Sakai and K. Kamino)) Department of Physiology, Tokyo Medical and Dental University School of Medicine, Tokyo, Japan.

We have constructed a new optical 1020-site optical system for simultaneous recording of electrical activity, using a 34 x 34-element photodiode array. This recording apparatus has a major advantage over our present optical recording apparatus, based on a 12 x 12-element photodiode array, in that it permits a more detailed analysis of spatio-temporal patterning of neural activity/responses in central nervous systems. This new apparatus has now been used, for the first time, to detect regions of neural response to vagal stimulation in embryonic chick brainstem preparations, and our results have established that optical signals resembling intracellular membrane potential changes can be recorded simultaneously from 1020 adjacent loci in the same preparation with high spatial and temporal resolutions together with good signal-to-noise ratios. This apparatus is readily applicable to other systems and tissues.

Th-Pos84

EXCITABLE MOLECULES ARE ORIENTED IN NERVE AXONS. ((David Landowne)) Univ. of Miami Sch. of Medicine Miami, FL 33101.

A conspicuous property of the change in optical activity that accompanies nerve impulses in axons is it's polarity reversal when the propagation direction reverses with respect to the cell body. Optical activity is a result of photon-atom interactions and is thus subject to certain symmetry considerations. The existence of an optical activity signal means there is something about the changing molecules which has handedness. They must be arranged disymmetrically, without a center of inversion or reflection planes. If optically active proteins were inserted into the membrane with random orientations then whatever rotation was suffered by the light passing from extracellular to intracellular would be reversed on average as the light went intracellular to extracellular and there would be no net rotation.

An optical activity signal indicates the molecules lack a plane of symmetry in the molecular frame of reference and also in the arrangement of molecules in the cellular frame of reference. Others have shown that nerve sodium channels lack mobility in the membrane and associate with cytoskeletal elements. If the channel-cytoskeletal link and the cytoskeleton were polarised, one would expect the channels to be also. If excitable molecules were oriented with respect to the long axis of the nerve a molecular response proportional to dV/dx would reverse in sign with the propagation direction.

Orientation of channels would not be likely to alter impulse propagation but may be of consequence to growth and repair processes.

Supported by NIH grant NS26651.

Th-Pos85

INTRACELLULAR CALCIUM BUFFERING POWER MEASURED IN SNAIL NEURONS. ((C.J. Schwiening, H.J. Kennedy & R.C. Thomas)) Department of Physiology, University of Bristol, BS8 1TD, U.K.

We have used calcium-sensitive microelectrodes and injection of calcium buffer solutions to calibrate fura-2 in voltage-clamped snail neurons[1]. We then used the calibrated fura-2 signal and iontophoretic calcium injections to measure calcium buffering power. The holding potential was varied to change the resting free intracellular calcium concentration expressed as pCa_i. Calcium buffering power has been expressed in two different ways (see figures: Calcium buffering power plotted against pCa_i. Lines are the theoretical buffering power of the fura-2 used). Firstly by analogy to pH, β_{Ca} is equal to the equivalents of Ca^{2+} added per pCa unit change per litre of cell volume[2]. Secondly it can be expressed as B_{Ca}, the number of calcium ions injected per litre of cell volume to produce one free ion. We find that β_{Ca} is exponentially related to pCa_i while B_{Ca} is a linear function of pCa_i and both can be modelled[3] by 1mM of a calcium buffer with one binding site with a pK of 6.

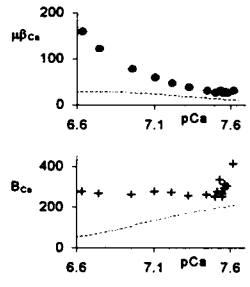

[1] see World Wide Web URL - http://www.bris.ac.uk /Depts/Physiology/curr_res.htm
[2] Ahmed Z & Connor JA (1988) *Cell Calcium* 9, 57-69
[3] Müller TH, Partridge LD & Swandulla D (1993) *Pflügers Arch.* 425, 499-505.

Th-Pos86

RAPID CALCIUM CONCENTRATION JUMPS MODULATE ACTION POTENTIAL PROPAGATION IN CULTURED DRG CELLS.

((CHR. LÜSCHER, P. LIPP, H.-R. LÜSCHER & E. NIGGLI))
Dept. of Physiology, University of Berne, Berne, Switzerland. (Sponsored by J.S. SHINER)

During a train of action potentials (AP) propagating in an axon of a DRG cell the safety factor for conduction gradually decreases. In an AP recorded in the cell soma this change is reflected by a decrease of the maximum upstroke velocity and an increased latency, eventually resulting in propagation failures at the entrance of the axon into the soma. - Cultured DRG cells of rat embryos were dialyzed with Fluo-3 and Fura-red as well as DM-nitrophen or diazo-2, respectively. Potentials were recorded in the current clamp mode of the whole cell patch clamp technique. APs were elicited by local field stimulation of the axon at a distance of 100-500 μm from the soma.- Ratiometric Ca measurements in the soma showed a rapid increase of the intracellular Ca concentration (approx. 100 nM) in response to a single invading AP. During AP trains (2-10 Hz, up to 100 stimuli) Ca accumulation reached values up to 1 μM. Simultaneously we observed the expected electrical changes and eventually failures. Flash photolysis of diazo-2 rapidly decreased the intracellular Ca concentration and transiently recovered the maximum upstroke velocity during a train of invading APs (5 Hz). A Ca concentration jump in the opposite direction (release of Ca from DM-nitrophen) increased the latency for a single AP at low stimulation frequencies (2 Hz).

These results suggest that in DRG axons intracellular Ca accumulation contributes to a decrease of safety factor for propagation during repetitive stimulation. Ca-induced Ca channel inactivation may be the underlying mechanism.

Th-Pos87

SINGLE L-TYPE CALCIUM CHANNEL CURRENTS RECORDED IN PHYSIOLOGICAL CALCIUM LEVELS. ((P.J. Church and E.F. Stanley)) SMS, NINDS, NIH, Bethesda, MD 20892.

Due to the relatively low conductance of calcium ions, biophysical studies of calcium channels are usually performed with high levels of barium or calcium ions as the charge carrier. Consequently, little is known about the behavior of these channels in physiological calcium levels. We have taken advantage of the relatively low noise recordings possible with the use of quartz glass electrodes to characterize L-type calcium channels from chick ciliary ganglion neurons in low external ion concentrations.

Ciliary ganglia from 15-day-old chick embryos were enzymatically dissociated in minimal essential medium at 37°C for 2 hours, triturated to single cells and plated onto coverslips. The bathing solution contained 140 KAsp to collapse the membrane potential. On-cell patch recordings were made with a range of external calcium and barium concentrations. Channel behavior was recorded in response to ramp and step depolarizations from a holding potential of -80 mV.

Single channel conductance was relatively independent of calcium concentration down to 2 - 4 mM. Maximum conductance approached 10 pS when calcium was the charge carrier and 25 pS when barium was the charge carrier.

Th-Pos88

ANALYSIS OF Ca^{2+} CURRENT FROM RAT CEREBELLUM EXPRESSED IN XENOPUS OOCYTES USING A GLASS FUNNEL TECHNIQUE. ((Y.M. Shuba, V.G. Naidyonov, and M. Morad)) Department of Pharmacology, Georgetown University, Washington, DC 20007. (Spon. by H. Tritthart)

Ca^{2+} channel expressed in Xenopus oocytes injected with mRNA extracted from rat cerebellum were studied using a new glass-funnel technique permitting voltage-clamping and intracellular perfusion of the oocytes. Ba^{2+} or Ca^{2+} currents were recorded in Cl^--free intra- and extracellular solutions and showed significant heterogeneity. Depolarizations from a holding potential of -120mV activated a low voltage activated (LVA) component of Ba^{2+} or Ca^{2+} currents. The LVA component activated at around -100mV, peaked at -40mV, and carried only 10-15% of the current compared to the high voltage activated (HVA) channels (peak current at +20mV). The presence of LVA current was also apparent from the two components of the steady state inactivation curve. The steady state inactivation component of HVA for Ba^{2+} and Ca^{2+} currents were fit by Boltzmann equation with half inactivation potential of -12mV and -10mV, slope factor 12.4mV and 12.2mV, and maintained level 0.62 and 0.58, respectively. HVA Ba^{2+} current inactivated monoexponentially with time constant of 2s while HVA Ca^{2+} current decayed biexponentially with time constants of 350ms and 2s indicating contribution of Ca^{2+}-dependent inactivation. Amplitude of HVA Ca^{2+} current was about 25% smaller than that of HVA Ba^{2+} current. HVA Ba^{2+} current was insensitive to dihydropyridines, but could be inhibited in voltage-dependent manner (22% at -10mV and 37% at +20mV) by Agelenopsis aperta venom (1:1000 dilution). 70% of this current could also be blocked by 20μM ωCgTx. Our data show the complex nature of Ca^{2+} channel currents expressed from rat cerebellum and demonstrate the adequacy of the glass funnel technique to critically analyze these currents in Xenopus oocytes. Supported by NIH HL16152.

Th-Pos89

IDENTIFICATION OF AN ISOFORM OF A B-CLASS CALCIUM CHANNEL IN RAT SYMPATHETIC NEURONS. ((Zhixin Lin, Edward Hawrot and Diane Lipscombe)), *Dept. of Molecular Pharmacology and Biotechnology and Dept. of Neuroscience, Brown University, Providence, RI 02912.*

The N-type channel expressed in sympathetic neurons is a relatively well characterized member of a large family of predominantly neuronal specific calcium channels. Whole-cell and single channel studies hypothesis that the N channel might be able to take on at least three different conformations with distinct characteristic open states. Modulators of channel gating, such as activated G-proteins, might act by stabilizing the channel in a particular conformation. Molecular studies, however, have also revealed that within each calcium channel family multiple isoforms exist which might also result in the expression of different functional channels. We were thus interested to determine whether multiple forms of the N channel might be expressed in sympathetic neurons. We have shown that five different α_1 subunit transcripts are present in sympathetic neurons with α_{1B} and α_{1D} being the most abundant, consistent with the high density of N and L channels in these cells. We have now extended these studies to show that two isoforms of α_{1B} have been detected. Using full length rbB-1 cDNA we screened our unidirectional rat superior cervical ganglia cDNA library (size selected to contain inserts of >4 kb). 67 positives were identified from screening 5 x 10^5 recombinants of which 54% were confirmed as B class, based on PCR screening with exact rbB-1 primers. Purification of five of these clones and subsequent restriction digest analysis revealed an isoform of rbB-1. The novel sequence, derived from a partial clone of 4.7 kb in length, differs from rbB-1 in two regions; (a) there is a four amino acid deletion within the proposed extracellular linker between IIIS3 and IIIS4 and, (b) the clone is 1.7 kb shorter in the 3' untranslated region with only 195 bases after the stop codon before the start of the poly $(A)^+$ tail. We are determining the relative abundance of this isoform of rbB-1 and have initiated expression studies to characterize its functional properties.

Th-Pos90

CALCIUM AND CAFFEINE DEPENDENCE OF SINGLE RYANODINE-SENSITIVE Ca^{2+} CHANNELS FROM ENDOPLASMIC RETICULUM OF CHICKEN CEREBELLUM (CB). ((Jimena Sierralta, B. A. Suárez-Isla, R Armisén and M. Fill*)) Dept. Fisiología y Biofísica, Univ. Chile, Fac. Med., Casilla 70005, Santiago 7 and Dept. Physiology & Biophysics, Univ. Texas Medical Branch, Galveston, TX 77555-0641.

Chicken cerebellum displays significant ryanodine binding associated with intracellular organelles. CB microsomes purified by sucrose gradient and fused into planar lipid bilayers (POPE:PS:PC 5:3:2 in decane) show high conductance ryanodine sensitive channels (300-500 pS in symmetric 400 mM $CsCH_3SO_3$, 20 mM TRIS-Hepes, pH 7.4)(Sierralta et al. BJ 64, A147, 1994). Caffeine activation (0.5-10 mM) was highly Ca^{2+} dependent, being higher at $[Ca^{2+}]$ above 1 μM. Two types of calcium dependencies were observed. A fraction of the channels that showed a bell-shaped dependence, were very active at 1 μM Ca^{2+} and were blocked by 100 to 500 μM Ca^{2+}. Others were activated at higher Ca^{2+} and displayed a sigmoidal activation curve that saturated above 10 μM Ca^{2+}. Both types of channels were ryanodine sensitive showing the characteristic substate induced by μM Ry. These results indicate that chicken cerebellum microsomes contain more than one type of ryanodine sensitive channel with different calcium dependencies. Supported by NIH R01NS29640, FONDECYT 293-0003.

Th-Pos91

KINETIC ANALYSIS OF SHAKER K-CHANNEL ACTIVATION. ((M.D. Rayner and Ken McCormack.)) School of Medicine, Univ. Hawaii, Honolulu, HI 96822 and Max-Planck Institut fur Experimentelle Medizin 11, Goettingen, FRG.

Kinetic analysis of macroscopic current activation, in *Xenopus* oocyte-expressed inactivation-removed *Shaker* channels, reveals three readily-differentiable time constants. When plotted against test potential, these time constants fall towards asymptotic values at positive potentials. These asymptotes are not explained by artifacts of filtering or as limitations imposed by clamp rise-time. By contrast, gating current rates do not appear to show equivalent, non-artifactual, limits at positive potentials. We conclude that the observed asymptotic limits in macroscopic current kinetics may reflect a coordinated conformational change which necessarily precedes entry into the open state. Although equilibrium properties of this conformational change are well represented by a first-order process, the kinetics appear considerably more complex. We explore strategies by which such kinetic data can be modeled more effectively, without the introduction of multiple additional states. We find that addition of a "delay time" within the rate equations is an effective modeling strategy and consider the biophysical implications of this approach.

(Supported by PHS grants #NS-21151, #NS-29204, NIH RCMI grant #RR-03061, with additional support from the Max-Planck Society.)

Th-Pos92

CLONING AND EXPRESSION OF HUMAN BK CHANNEL ALTERNATIVE SPLICE VARIANTS. ((S.I. Dworetzky, J.T. Trojnacki, M.C. McKay, D.J. Post-Munson, C.G. Boissard, J.T. Lum-Ragan and V.K. Gribkoff)) CNS Drug Discovery, Dept. 405 Bristol-Myers Squibb Co., Wallingford, CT 06492.

A putative BK channel was cloned from a human brain (substantia nigra) cDNA library by hybridization screening. The sequence of the clone (*hSlo*) shows high homology with the mouse BK clone, *mSlo*. Expression of *hSlo* in oocytes showed a family of outward currents, induced by step depolarizations, that were blocked by iberiotoxin. The *mSlo* and *hSlo* currents were virtually identical and had similar sensitivities to several activators and blockers of BK channels. Several alternative *hSlo* splice variants have been isolated. Thus far, there are two identified splice exons at junction A, 1 at junction B, and 1 at junction C. These splice junctions are found in the carboxyl terminus past the six membrane spanning domains. Splice exons A1 (3 aa) and B1 (27 aa) are identical to the *mSlo* exons. A 4 aa insert was located at a new splice junction designated C. The A2 splice exon, which codes for a 29 aa insert, is 62% homologous to the equivalent *mSlo* exon. The single channel conductance of the *hSlo* clone not containing any of the splice exons ($A^-B^-C^-$) and an isoform containing only the A2 exon ($A2B^-C^-$) was 285 pS. However, in comparing the Ca^{++}-dependence between the two variants, the $A2B^-C^-$ splice isoform demonstrated a much-reduced sensitivity to calcium.

Th-Pos93

CHANNEL FORMING ACTIVITY OF AMYLOIDOGENIC PEPTIDES. ((Meng-chin Lin[1], Tajib Mirzabekov[1], and Bruce Kagan[1,2])) [1]Neuropsychiatric Institute of UCLA Medical School and [2]Brentwood Veterans Administration Medical Center, Los Angeles, CA 90024.

The formation of amyloid has been implicated to play a role in the pathogenesis of Alzheimer's disease, type-2 diabetes mellitus, and spongiform encephalopathies. Alzheimer's disease related amyloid beta-peptide (Aβ) and its fragment Aβ25-35 have been found to be neurotoxic. We have demonstrated that Aβ25-35 can form voltage dependent ion channels with multiconductive levels in planar lipid bilayers. The Aβ25-35-containing membranes exhibit slight cation selectivity. We have examined the channel forming activity of different site-directed mutations of Aβ25-35. Replacing the C-terminal Met with Cys preserves both neurotoxicity and channel forming ability, but alters the voltage dependency. Deleting the C-terminal Met causes a loss of both neurotoxicity and channel forming activity. We have studied channel formation of another disease related amyloidogenic peptides: amylin and prion. It has been found that at concentrations of 10-100μg/ml, cytotoxic human amylin can increase the lipid membrane conductance 10^2-10^3 times, whereas nontoxic and nonamyloidogenic rat amylin can not. Like human amylin, prion (106-126) has been shown to interact with membranes, but no discrete channel function has yet been observed. We suggest that the mechanism which accounts for toxicity of amyloidogenic peptides is related to an ion leakage of cell membrane.

(Supported by grant from the Alzheimer's Association)

Th-Pos94

STRUCTURE OF NEUROMODULIN BASED PEPTIDES BOUND TO PHOSPHOLIPID BILAYERS USING MAGNETIC RESONANCE ((Stacey L. Wertz and David S. Cafiso)) Department of Chemistry, University of Virginia, Charlottesville, VA 22901.

Neuromodulin is a 25 kDa calmodulin-binding protein kinase C (PKC) substrate found in axonal growth cone membranes. It appears to bind membranes via an electrostatic interaction between the positively charged region near the N-terminus of the peptide and negative phospholipid headgroups. One basic seventeen residue segment of neuromodulin, which has the sequence Ace-KIQASFRGHITRKKLKG-Amide, contains the PKC phosphorylation site, the calmodulin binding site, and the membrane binding region. A complete series of cysteine substituted mutants were synthesized and derivatized with nitroxide spin labels. The orientation, the immersion depth, and the structure of the peptide on the membrane surface were determined using power saturation electron paramagnetic resonance techniques and lineshape analysis. High resolution nuclear magnetic resonance techniques were also used to determine the peptide's secondary structure in various solvents. Based on Cα chemical shifts, the peptide appears to be helical in methanol and more random in SDS micelles and in aqueous solution.

Th-Pos95

HAMSTER SCRAPIE PRION PROTEIN EXPRESSION IN A NOVEL MEMBRANE PROTEIN SPECIFIC EXPRESSION SYSTEM. ((G.J. Turner, I. Melhourn, R. Reusch, S. Pruisner and R.M. Stroud)) Department of Biochemistry and Biophysics, UCSF, San Franscisco, CA 94143.

We have converted the regulon which over-expresses bacteriorhodopsin, from the Archaebacterium *Halobacterium salinarium*, into a heterologous membrane protein expression system. Proof of concept is illustrated for the membrane associated Hamster Prion Protein (PrP^C). The PrP protein has both transmembrane and soluble domains and is normally found in the membranes of hamster brain tissue. The PrP constructions used are of two types and differ in the number of amino acids at the N-terminal region of the PrP protein. PrP gene coding regions were cloned, in frame, into the BR coding region in various configurations. pENDS·I·PrP fused the hamster PrP gene to the 13 amino acid Bop presequence. Two alternative forms including the entire *bop* gene and PrP were expressed; pENDS·V·PrP and pENDS·VI·PrP. Southern analysis indicated stably maintained plasmid copies of the Bop and PrP genes. Northern analysis failed to identify PrP specific mRNA, indicating transcripts with very short half times. Western analysis, performed on membrane fractions isolated from *H.salinarium* strains expressing the PrP gene, identified the appropriate fusions. pENDS·I·PrP demonstrates that the Bop presequence is sufficient to couple translation and membrane insertion. The pENDS·V and ·VI constructions generate chimeras with nearly full length BR resulting in chromaphorically tagged PrP protein. Spectral determinations allow an estimate of 1-3 mgs/liter of the fusion construction, consistent with PAGE analysis. A unique membrane-associated proteinase activity useful for cleavage of the pENDS·VI·PrP from BR sequences is demonstrated.

Th-Pos96

S100β IS A TARGET PROTEIN OF NEUROCALCIN δ, AN ISOFORM ABUNDANT IN GLIAL CELLS. ((K. Okazaki, N.H. Obata, S. Inoue and H. Hidaka))Department of Pharmacology, Nagoya University School of Medicine, 65 Tsurumai, Showa-ku, Nagoya 466, Japan.

Neurocalcin is a 3EF-hand type calcium-binding protein abundant in the central nervous system. This 23, 24 kDa protein was purified from bovine brain using W-77 affinity chromatography. At least six isoforms of neurocalcin have been identified from bovine brain. In immunohistochemistry, some isoforms of neurocalcin were expressed in cerebrum, cerebellum, spinal cord and adrenal medulla as well as sensory nervous system including retina, olfactory bulb, inner ear and muscle spindle. To clarify the function of neurocalcin δ, an isoform abundant in glial cells, we attempted to find target proteins by neurocalcin δ-affinity chromatography and an ^{125}I-neurocalcin δ gel overlay method. 10 kDa, 14 kDa, 27 kDa, 36 kDa and 50 kDa bands on SDS-PAGE were capable of binding to ^{125}I-neurocalcin δ. 10 kDa, 11 kDa, 19 kDa, 24 kDa, 36 kDa, 50 kDa and 70 kDa proteins were eluted from neurocalcin δ-affinity columns in a Ca^{2+}-dependent manner. Sequence analysis of proteolytic peptides identified these proteins as S100β (10 kDa), S100α (11 kDα), myelin basic protein (19 kDa), glyceraldehyde-3-phosphate dephydrogenase (36 kDa), and tubulin β chain (50 kDa). A zero-length cross-linking study indicated that S100β bound in an equimolar ratio to neurocalcin δ. Purified S100β protein had highest affinity to ^{125}I-neurocalcin δ than calmodulin or other members of the S100 family including calcyclin, calgizzarin or calvasculin. These findings suggest that neurocalcin δ may act in polymeric form bind to S100β and be involved in Ca^{2+}-signaling in glial cells.

Th-Pos97

THE ROLE OF MITOCHONDRIA IN GLUTAMATE - INDUCED NEUROTOXICITY. ((A.F. Schinder, E. Olson, N.C. Spitzer and M. Montal)) Dept. of Biology, Univ. of California, San Diego, La Jolla, CA 92093-0357.

Overstimulation of the N-methyl-D-aspartate (NMDA) subtype of glutamate receptors leads to massive Ca^{2+} influx and neuronal death. The underlying downstream mechanisms remain unclear. We postulate the mitochondrion as a central target for excitotoxic cell damage according to the following sequence of events: mitochondrial Ca^{2+} overload —> ATP depletion —> cell death. Cultured hippocampal neurons were challenged with 200 μM NMDA for a 20 min interval, and intracellular Ca^{2+} concentration ($[Ca^{2+}]_i$) was measured by imaging the fluorescence of the Ca^{2+} indicator Fluo-3. NMDA induced an increase in $[Ca^{2+}]_i$, with a complex time course: an initial peak (in the μM range), followed by a deep valley (Ca^{2+} buffering) which lasted several minutes, subsequent rise to a plateau, and return to baseline at the end of the stimulus. The number of cells returning to baseline decreased with longer challenges (>95% recovery for 20 min; 50% for 50 min). The role of mitochondria was assessed by using specific inhibitors of oxidative phosphorylation. A 15 min preincubation with antimycin A, an inhibitor of complex III, reduced Ca^{2+} buffering and recovery from overload in a dose-dependent fashion: a 1 nM dose inhibited only buffering, whereas 10 nM prevented both buffering and recovery. This biphasic pharmacological profile was reproduced by rotenone (inhibitor of complex I), although at a 10^3-fold higher concentration. FCCP at 0.1μM (proton ionophore) and oligomycin at 1μM (inhibitor of the ATP synthase) inhibited both buffering and recovery. In contrast, thapsigargin, an inhibitor of Ca^{2+} uptake in organelles, (≤ 500 nM) did not alter responses to NMDA. These results indicate that the functional integrity of the mitochondria is required for the neurons to properly handle intracellular free Ca^{2+} during an excitotoxic insult. Supported by DAMD 17-93-C-3100 and NIH NS15918.

Th-Pos98

A GENETIC BASIS FOR BRAIN ANEURYSMS. ((Austin,G., Schievenk,W., Dickson,D. & Richardson,S.)) Brain Aneurysm Research Laboratory, Neuroscience Institute, U.C.S.B., Santa Barbara, CA

Brain aneurysms (BA) are like a blister on an inner tube of a tire that has begun to wear. BA usually develop at a bifurcation area on a brain artery which has been weakened by a genetic defect. The protein structure of the artery begins to lose its normal three layer architecture and gradually the media and adventitia, composed of smooth muscle cells and collagen I, blend into one predominantly collagen layer. The causes of formation and rupture remain obscure; although, there is evidence for a genetic defect in the proteins of the arterial wall. In 130 cases at the Mayo Clinic of unruptured aneurysm less than 10 mm. in diameter none ruptured during a 8 1/2 year followup. The average size of rupture was 22 mm. Rupture occurs near the dome in 85% where the wall has become thinned from the effect of the pulse and pressure flow waves. Whenever there is one genetic defect, evidence points to a second. Adult polycystic kidney disease (APKD) is the most common genetic defect. Between 30% and 40% of patients with APKD develop BA. These are congenital and develop following birth. They enlarge and are picked up on the basis of suspicion, because they often resemble small tumors in and around the cranial nerves. They are detected by Magnetic Resonance Angiography. With pharmacologic control of blood pressure and use of pharmacologic agents to promote collagen synthesis, most aneurysms can be kept under 10 mm. in diameter.

VISUAL RECEPTORS

Th-Pos99

MICROSCALE CHARACTERIZATION OF VISUAL PIGMENT PHOTOLYSIS INTERMEDIATES WITH 10 NANOSECOND RESOLUTION ((J.W. Lewis[1], T.L. Mah[1], J. Liang[2], T.G. Ebrey[2], M. Sheves[3], F.F. Davidson[4] and D.S. Kliger[1])) [1]Univ. of California., Santa Cruz, [2]Univ. of Illinois, Champagne-Urbana, [3]Weizmann Inst., Israel, [4]MIT, Cambridge.

The general framework of intermediates formed after photolysis of visual pigments has been based on studies of their UV-VIS absorbance spectra. Due to the irreversible nature of visual pigment photolysis and the need for signal averaging, measurements with high time resolution have largely been confined to pigments such as bovine rhodopsin which can be prepared in large amounts (>>10 mg). Progress in understanding the nature of bovine rhodopsin intermediates has made it desirable to extend these measurements to cone-type pigments such as Tokay gecko P521 and to mutants of rhodopsin. The pigments of interest, however, are available only in submilligram quantities, requiring redesign of the metered flow system in an optical multichannel analyzer based kinetic spectrophotometer to operate with a 1μL sample. This system has been successfully applied to ~200 μg samples of P521 to resolve bi-exponential kinetic rates and spectra of intermediates which appear on the nanosecond to microsecond time scale. The results show an order of magnitude increase in the chloride dissociation constant between the Batho and BSI intermediates of P521. The optical system has also performed well with a mutant of rhodopsin expressed in COS cells, resolving significant differences in kinetics which appear in detergent suspensions on the millisecond time scale. This technology has been applied to artificial rhodopsins made from synthetic analogs of retinal. Higher signal-to-noise ratio measurements can be made in these systems as well, particularly when quantities of pigment available are limited.

Th-Pos100

EARLY PHOTOINTERMEDIATES OF ARTIFICIAL VISUAL PIGMENTS. ((T. L. Mah,[1] J. W. Lewis,[1] I. Pinkas,[2] M. Sheves,[2] M. Ottolenghi,[3] and D. S. Kliger[1])) [1]University of California, Santa Cruz, Santa Cruz, CA 95064, [2]Weizmann Institute of Science, Rehovot 76 100, Israel, [3]The Hebrew University of Jerusalem, Jerusalem 91 904, Israel.

Low temperature absorption techniques have been employed to probe the behavior of the artificial visual pigment, α-isorhodopsin. Previous studies of native rhodopsin and a variety of artificial rhodopsins have suggested that one of the photointermediates, bathorhodopsin (Batho), exists in equilibrium with another intermediate, BSI, which then decays to lumirhodopsin. The present study has confirmed this result in α-isorhodopsin by trapping Batho in this pigment. It has also been determined that the BSI formation temperature for this synthetic pigment is approximately 60 K, higher than that reported for 5,6-dihydroisorhodopsin. Experiments at room temperature with artificial visual pigments made from retinal analogs with bulky groups attached to the polyene chain have suggested that BSI formation depends on a barrier caused by steric interactions between the 5-methyl group and the 8-hydrogen of the chromophore. The results obtained in the present study are interpreted in terms of this barrier model.

Th-Pos101

ROOM TEMPERATURE TRAPPING OF RHODOPSIN PHOTOINTERMEDIATES. ((Sharon Sikora and T. Gregory Dewey)) Dept. of Chemistry, University of Denver, Denver, CO 80208.

Photointermediates in the light-activation process of bovine rhodopsin are trapped in trehalose-water glass films. This trapping is accomplished at room temperature due to the unusually high vitrification temperature of trehalose-water mixtures. Depending on experimental conditions, photointermediates resembling metarhodopsin I and metarhodopsin II are isolated. Ultraviolet circular dichroism spectra show that the metarhodopsin I product had no change in structure compared with unbleached rhodopsin. The metarhodopsin II product did show a significant decrease in α-helical content. Resonance energy transfer was measured from extrinsic probes located on each of the cytoplasmic cysteine residues to the retinal in the trapped photoproducts. The distances obtained for unbleached rhodopsin and metarhodopsin I are the same. Metarhodopsin II distances are considerably shorter. These results suggest large structural changes within the metarhodopsin II transition. Further structural investigations are performed using FTIR difference spectroscopy. The structural integrity of the rhodopsin in solution and in film is maintained as evidenced by FTIR spectroscopy.

Th-Pos102

LIGHT-ACTIVATED PROTONATION CHANGES OF *SENSORY RHODOPSIN II* FROM *NATRONOBACTERIUM PHARAONIS*. (M. Engelhard, B. Scharf and F. Siebert*) Max Planck Institut für Molekulare Physiologie, 44026 Dortmund and *Institut für Biophysik und Strahlenbiologie Albertstr. 23 79104 Freiburg, Germany

Sensory rhodopsin II the blue light receptor from *N. pharaonis* (pSR-II) has been purified and sequenced. The primary structure identifies pSR-II as a new member of the family of bacterial retinylidene proteins (R. Seidel et al., in press). The photocycle resembles that of bacteriorhodopsin and sensory rhodopsin I (SR-I) with an intermediate absorbing at around 400 nm indicating a deprotonated Schiff base.
FTIR-difference spectra between the ground state and this intermediate reveals a protonation of a carboxyl group which might be in analogy to bacteriorhodopsin Asp75. This protonation is independent of the pH at least in the range between pH 5 and pH 8. These results suggest that Asp75 is deprotonated in the ground state contrary to the finding in SR-I where a protonation of the corresponding Asp was postulated undergoing environmental changes upon light activation (Rath et al. 1994). An explanation for these discrepancies might be found in the different functions of the two light receptors with SR-I fulfilling a dual role (photo-attractant and in a two photon process photo-repellent) and SR-II being solely photo-repellent.

Th-Pos103

RESIDUE REPLACEMENTS OF BURIED ASPARTYL AND RELATED RESIDUES IN SENSORY RHODOPSIN I: D201N PRODUCES INVERTED PHOTOTAXIS SIGNALS. ((K.D. Olson, X.-N. Zhang, and J.L. Spudich)) Dept. Micro. and Mol. Genet., U. of Tx., Houston, TX 77030.

Sensory rhodopsin I (SR-I), a phototaxis receptor in *Halobacterium salinarium*, is structurally similar in its photoactive site to the proton pump bacteriorhodopsin (BR). SR-I also shares proton-transfer steps with BR during its photochemical reaction cycle. These proton movements result in active proton transport by SR-I in the absence of its transducer protein, HtrI. HtrI modulates the kinetics of SR-I photoreactions and their pH sensitivity, and prevents the release of protons from the membrane. To examine the possibility the proton transfers in SR-I may play a role in activating HtrI, we have mutated residues in SR-I that are in corresponding positions as residues in BR that participate in proton movements. The mutant receptors (D76N, D76A, D106N, D201N, R73N, Y87F) have been characterized with respect to their photoreactions in vitro, their phototaxis signaling responses in vivo, and whether they generate the pumping form in the absence of HtrI. The results confirm and extend our previous finding that D76 is not essential for phototaxis signaling but is critical for electrogenic transport. We identify the first residue in SR-I of vital importance to its attractant signaling function: D201. The D201N substitution converts the normally attractant signal of orange light to a repellent signal, which has strong implications for the transduction mechanism.

Th-Pos104

MAPPING THE SITES OF INTERACTION BETWEEN RHODOPSIN AND RHODOPSIN KINASE. ((Robin L. Thurmond and H. Gobind Khorana)) Departments of Chemistry and Biology, Massachusetts Institute of Technology, Cambridge, MA 02139.

Upon light-activation, rhodopsin binds and, presumably, activates rhodopsin kinase enabling phosphorylation to occur. We are investigating the role of the cytoplasmic peptide loops connecting helices C and D and helices E and F. Three rhodopsin mutants were used; two deletions mutants with deletions of amino acids 143-150 (CD loop) and of amino acids 237-244 (EF loop), respectively, and a third mutant in which the amino acids 235-250 (EF loop) were replaced by the "indifferent" sequence TSLHGYSVTGPTGSNL (Franke et al., J. Biol. Chem. **267**:14767). Upon expression in COS-1 cells, all three mutants formed opsins that regenerated the 500 nm absorbing chromophore with 11-cis retinal and the resulting mutant rhodopsins showed bleaching behavior identical to wild-type rhodopsin. The rates of phosphorylation were determined at pH 7.5 (10 mM bis-tris propane) in 0.02% lauryl maltoside and with 15 nM purified rhodopsin kinase. For wild-type rhodopsin, the maximum phosphorylation rate (1.1 pmol min^{-1} μg^{-1} kinase) was reached at rhodopsin concentrations above 0.1 μM. In contrast to the wild-type protein none of the mutants showed any phosphorylation activity over a 50-fold concentration range (0.01-0.5 μM). We are now studying if in the mutants, the binding and/or activation of the kinase by the mutants are affected. Supported by grants NIH GM 28289 (H.G.K.) and NIH EY06466-02 (R.L.T.).

Th-Pos105

DESENSITIZATION OF BLEACHED ROD PHOTORECEPTORS BY 11-*CIS* 13-DESMETHYL RETINAL. ((D.W. Corson, B. Katz and R.K. Crouch)) Medical University of South Carolina, Charleston, SC 29425.

Application of 11-*cis* retinal to isolated bleached rod photoreceptors normally results in the formation of visual pigment with a concomitant restoration of sensitivity resulting from relief of opsin desensitization and replenishment of photoactivatable pigment. We recently reported that 9-*cis* 13-desmethyl retinal formed a normal pigment that was capable of effectively restoring sensitivity to bleached rods (Corson *et al.*, 1994, *Biophys. J.66*:A245). This finding was in agreement with the results of a phoshodiesterase activation assay reported by Ebrey *et al.* (1980, *FEBS Lett. 116*:217-219). In addition, they reported that the 11-*cis* 13-desmethyl retinal isomer formed a photoactivatable pigment, but that this pigment produced substantial activation of phosphodiesterase in darkness. We have examined the activity of this analogue in isolated bleached photoreceptors by tandem spectroscopic measurements of pigment formation and sensitivity measurements by suction electrode recordings. Unlike the activity of all other analogues observed to date, the effect of the 11-*cis* isomer of 13-desmethyl retinal is to further depress the sensitivity of bleached rods and to reduce the maxmimum response amplitude for bright flashes from 46±.08% to 15±.04% (n=4) of the prebleach value. Preliminary experiments suggest that the depression of sensitivity is at least partially reversible by bleaching and application of 11-*cis* retinal. Although further experiments are required to characterize the mechanism of desensitization, the results are, so far, consistent with our expectations for an retinal analogue that forms a constitutively active pigment.

Supported by NIH Grants EY07543 & EY04939 and Research to Prevent Blindness.

Th-Pos106

LONGITUDINAL DIFFUSION COEFFICIENT OF A FLUORESCENT cGMP ANALOG IN THE SALAMANDER ROD OUTER SEGMENT. ((Y. Koutalos[1], R.L. Brown[2], J.W. Karpen[2] and K.-W. Yau[1,3])) [1]Dept. of Neuroscience and [3]Howard Hughes Medical Institute, The Johns Hopkins Univ. School of Medicine, Baltimore, MD 21205, and [2]Dept. of Physiology, Univ. of Colorado School of Medicine, Denver, CO 80262.

cGMP is the intracellular messenger mediating phototransduction in vertebrate rods, with its longitudinal diffusion in the outer segment likely to be a factor in determining light sensitivity. By analyzing the kinetics of cGMP-activated currents in truncated salamander rod outer segments (ROS), the cGMP diffusion coefficient was previously estimated to be ca. 60×10^{-8} cm^2 sec^{-1} (1). On the other hand, fluorescence measurements by Olson and Pugh (2) in intact salamander ROS using 8-(fluoresceinyl)thioguanosine 3',5'-cyclic monophosphate (fl-cGMP) led to a diffusion coefficient for this compound of 1×10^{-8} cm^2 sec^{-1}; after corrections for differences in binding to cellular components, this gave an upper limit of 11×10^{-8} cm^2 sec^{-1} for the cGMP diffusion coefficient. To properly compare the two sets of measurements, we have examined the diffusion of fl-cGMP in the truncated ROS. From the kinetics of fl-cGMP-activated currents, we have obtained a diffusion coefficient of $2-3\times10^{-8}$ cm^2 sec^{-1} for fl-cGMP, in broad agreement with the value in intact ROS. The cGMP diffusion coefficient measured from the same cells was 20–45 times higher ($40-95\times10^{-8}$ cm^2 sec^{-1}), suggesting a 20–45 fold correction for the differences in binding between cGMP and fl-cGMP.

1. Koutalos, Y., K. Nakatani & K.-W. Yau. 1994. Biophys. J. 66:A48.
2. Olson, A. & E.N. Pugh, Jr. 1993. Biophys. J. 65:1335–1352.

Th-Pos107

LIGHT-DEPENDENT PHOSPHOINOSITIDE METABOLISM IN THE MEMBRANES OF BOVINE ROS. THE SOURCES OF PHOSPHATE FOR PIP_2 SYNTHESIS.

((I.D. Volotovski, I.V. Grigorjev, A.N. Griz)) Institute of Photobiology, Academy of Sciences of Belarus, Minsk, 220733 Belarus

Light has been shown to controls the metabolism of phosphoinositides in retinal rods photoreceptor membranes. The synrthesis and hydrolysis of phosphatidilinositol 4,5-bisphosphate (PIP_2), the precursor of the lipid signal molecules, inositol 1,4,5-trisphosphate and 1,2-diacylglycerol, are stimulated by visible light absorbed by rhodopsin. The effect of light on phosphatidilinositol 4-monophosphate (PIP) and phosphatidic acid (PA) meta-bolism is negligible. Light was shown to exert its influence with help of βγ-transducin which appears to modulate the activities of PIP kinase and phospholipase C.

The special experiments has shown that PIP_2 synthesis was performing using not only γ-phosphate of ATP as it is generally agreed but also inorganic phosphate from $[^{32}P]H_3PO_4$ added into the medium. But PIP and PA formations occured only in ATP presence. $^{32}P_{in}$ incorporation into PIP_2 was stimulated by "cold" ATP with increment of 3. Hypotonic wash, treatment with with 2 M urea, 2 M LiCl and 20 mM p-chloromercuribenzoate of ROS membranes resulted in decrease and complete inhibition of PIP_2 synthesis. The discs isolated did not reveal any $^{32}P_{in}$ incorporation into PIP_2 even in presense of "cold" ATP. The data obtained indicated the possible existence of ATP-dependent PIP kinase regulator weakly associated with dics membranes and/or presumably the enzymic use of P_{in} for PIP_2 synthesis *in vivo*. The role of light dependence of PIP_2 metabolism in photoreseptor function is dissussed.

Th-Pos108

THE EFFECTS OF BACKGROUND ILLUMINATION ON THE PHOTORESPONSE OF RETINAL RODS AND THEIR RELATION TO INTERNAL CALCIUM. ((M.P. Gray-Keller and P.B. Detwiler)) University of Washington, Seattle, WA, 98195.

The relation between free internal calcium concentration (Ca_i) and effects of sustained background light on superimposed flash responses was examined in detached, functionally intact rod outer segments (ROS) from *Gecko* retina. ROS were dialyzed under whole-cell voltage clamp with solution containing 1mM GTP, 5mM ATP and 100μM Indo-dextran, a fluorescent calcium indicator. Background illumination that ranged from 4 to ~3600 Rh^*/s causes respectively a 6 to 85% reduction in circulating dark current (I_d) and has dramatic effects on sensitivity, rate of rise, time to peak and recovery time of superimposed dim flash responses (see figure). All four parameters decrease with increasing background intensity, however, sensitivity and rate of rise show a much larger fold reduction than either time to peak or recovery time. We have shown previously[1] that Ca_i in dark-adapted ROS is 550nM and reaches a minimum of 50nM after ~20s of saturating illumination. The reduction in Ca_i is substantially less during subsaturating illumination and is proportional to the amount of I_d. To determine the relationship between calcium and adaptation, experiments are underway to measure Ca_i in darkness and during the steady state response to the same backgrounds shown in the figure. A background intensity of 133 Rh^*/s causes a 40% decrease in I_d, which results in a 2-fold drop in Ca_i, a 7-fold reduction in sensitivity, a 4-fold decrease in the rate of rise and ~50% acceleration in both time to peak and recovery time of the dim flash response. [1]Gray-Keller and Detwiler, 1994, *Neuron* 13, 1-20.

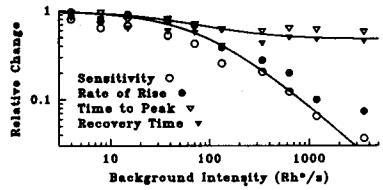

Th-Pos109

BLOCK OF CONE cGMP-GATED CHANNELS BY INTERNAL ORGANIC CATIONS.

((S.C. Stotz and L.W. Haynes)) Dept. of Medical Physiology and Neuroscience Research Group, University of Calgary, 3330 Hospital Dr. N.W., Calgary, Alberta, T2N 4N1, Canada

The cGMP-gated channel of rod photoreceptor outer segments is blocked by internal organic cations (*e.g.*, Picco and Menini, 1993, *J. Physiol.* 460:741-758). Here we report that the cGMP-gated channel of cone outer segments is blocked by the symmetrical tetra-alkylammonium compounds TMA, TEA, TPrA, and TBA, and by the buffer Tris when these compounds are applied to the internal side of the channel at mM to μM concentrations. Inside-out patches were excised from channel catfish (*Ictalurus punctatus*) cone outer segments. The pipet contained (in mM): 120 NaCl, 0.1 NaEGTA, 0.1 NaEDTA, 5.0 NaHEPES (pH 7.6). The bath contained either an identical solution or a solution in which of one of the blockers substituted on an equimolar basis for sodium. Channels were maximally activated by the addition of 1 mM cGMP to the bath solution. Current-voltage relations (obtained by applying 120 mV s^{-1} ramps between ±80 mV, averaging and subtracting to obtain the net cGMP-dependent current) were obtained in the absence or presence of a blocker. For each concentration of a blocker, the fractional block of the conductance was determined from the current-voltage relations at 10 mV increments. Plots of the conductance vs. concentration were fitted to obtain the K_D at each voltage. In all cases, Hill coefficients of 1 were obtained, indicating that a single molecule was sufficient to block the channel. The voltage-dependence of K_D was measured and the K_D at 0 mV determined. K_D(0 mV) decreased monotonically with increasing carbon chain length from ~70 mM (TMA) to ~0.4 mM (TBA). The addition of one carbon increased the binding energy by ~4 KJ mol^{-1}. The buffer Tris also blocked the channel, with K_D(0 mV) of ~23 mM. For all of the blockers, the fractional block increased monotonically with voltage, as expected for an impermeant blocker. Using the Woodhull formalism for the voltage-dependence of fractional block by an impermeant blocker, the location for the binding site was estimated to be ~40% across the voltage drop from the cytoplasmic side of the channel. Supported by MRC (Canada) and AHFMR.

Th-Pos110

THE CONTRIBUTION OF INWARD RECTIFICATION AND TRANSIENT Ca^{2+} CURRENTS TO MEMBRANE OSCILLATIONS IN *HERMISSENDA* PHOTORECEPTORS.

((L. Matzel[1], E. Yamoah[2] and T. Crow[2])) [1]Rutgers University, New Brunswick, NJ, 08903 and [2]Univ. of Texas, HSCH, Houston, TX 77225.

The eye of *Hermissenda* consists of two type A and three type B photoreceptors. Type A cells are typically quiescent in the dark, however dark-adapted type B photoreceptors undergo rhythmic spike activity. Light elicits a depolarizing generator potential that may be oscillatory and non-phasic in both types of cells. The differential sensitivity of the A and B cells to light may have important implications for light dependent behaviors. The electrophysiological differences between the two types of cells may result from differences in their synaptic inputs and/or from differential expression of membrane conductances in both cell types. Here we report differences in the properties of inward rectifier currents in the type A and B photoreceptors using the whole cell patch-clamp technique. Inward rectifier currents were activated with hyperpolarizing voltage pulses under conditions where voltage-gated Na^+, Ca^{2+} and outward K^+ and Cl^- currents were suppressed. The transient Ca^{2+} current (Ni^{2+} sensitive) was recorded as described previously (Yamoah and Crow, 1994). Both time-dependent and time-independent inward rectification was observed in the photoreceptors. The B cells expressed predominantly the time-dependent current and the A cells typically expressed the time-independent currents. The time-dependent inward rectification reversed around -25 to -35 mV and was blocked by 0.5 - 1mM external Cs^+. In contrast, the time-independent current reversed at more hyperpolarized potentials, -60 to -70 mV, and was sensitive to Ba^{2+}. Under current clamp 1mM Cs^+ produced a membrane hyperpolarization and reduced spike activity of dark-adapted B cells. In addition, 1mM Ni^{2+} reduced spontaneous spike frequency of B cells from about 2.5 Hz to 0.6 Hz and Ba^{2+} increased membrane oscillation in the type A cells in the dark. We propose that the differential expression of two distinct inward rectifiers in type A and B cells may contribute to differences in their intrinsic membrane properties.

EPITHELIAL PHYSIOLOGY

Th-Pos111

EVIDENCE FOR A NONSELECTIVE CHANNEL PERMEABLE TO BOTH Cl^- AND Ca^{2+} IONS AT THE APICAL MEMBRANE OF THE RABBIT DISTAL CONVOLUTED TUBULE.

((N. Denicourt, M. Gagnan-Brunette* and R. Sauvé)) Membrane Transport Research Group, Dept. of Physiology, Univ. Montréal and *Maisonneuve Hospital, Montréal, Canada H3C 3J7.

The distal convoluted tubule (DCT) is responsible for approximately 10% of the total Ca^{2+} reabsorption by the kidney. This process is entirely transcellular and involves a passive entry of Ca^{2+} at the apical membrane of DCT cells. The molecular basis of this Ca^{2+} entry process was investigated by fusion of vesicles prepared from apical membranes of isolated DCT onto a planar lipid bilayer (PE:PC; 1:1). Experiments carried out in 200 mM (cis)/50 mM (trans) $CaCl_2$ conditions led to the identification of a 14 pS (n=13) channel that appeared permeable to both Ca^{2+} and Cl^- ions (P_{Ca}/P_{Cl} = 0.4 on the basis of HGK equation). The open channel probability (P_o) showed a weak voltage dependency with higher P_o values at negative potentials (trans relative to cis), but was unaffected by a change in the trans Ca^2 concentration. Experiments in which Na^+ and $NMDG^+$ were used as charge carriers yielded $P_{Cl} > P_{Na} > P_{Ca} > P_{NMDG}$ with relative values of 1.0: 0.8: 0.4: 0.1. The channel could not blocked by cis or trans addition of Gd^{3+}, Cd^{2+}, Ni^{2+} or ruthenium red. Anions such as So_4^- failed to affect channel activity and Ca^{2+} channel blocking agents such as nefidipine were also ineffective. These results support previous $^{45}Ca^{2+}$ uptake measurements performed on these vesicles which showed that Na^+ (cis and trans) interferes with the Ca^{2+} influx. This channel may account for part of the passive entry of Ca^{2+} in resting DCT cells. Supported by the Canadian Kidney Foundation.

Th-Pos112

CALCIUM DYNAMICS IN A MATHEMATICAL MODEL OF THE PRINCIPAL CELL IN RABBIT CORTICAL COLLECTING TUBULE.

((Yuanhua Tang and John L. Stephenson)) Department of Physiology and Biophysics, Cornell University Medical College, New York, NY 10021

Intracellular calcium (Ca_i) regulation and oscillation are explored in an extension of a mathematical model of the principal cell in the cortical collecting tubule proposed by Strieter *et al.* (*Am. J. Physiol.*, 263:F1063-1075). There are ATP-driven Ca pumps and IP_3-sensitive Ca channels on the membrane of endoplasmic reticulum. Regulatory effects of Ca_i on the apical Na channels are introduced, based on experimental data by Palmer and Frindt (*Am. J. Physiol.* 253:F333-339). Ca_i shows excitable dynamics in responses to stimulatory hormones that raise IP_3 level, as shown experimentally with application of AVP and Endothelin-1 (Naruse *et al. Am. J. Phyiol.* 261: F720-F725). As the stimulatory level further increases, the model predicts sustained Ca_i oscillations. Na-free extracellular solutions also result in sustained Ca_i oscillations due to gradual Ca_i accumulation, as demonstrated experimentally by Koster *et al.*, (*Kidney Int.* 43:828-836). In the model, Ca_i oscillation effectively restores the intracellular homeostasis under temporal disturbances. Procedures that increase Ca_i or induce the onset of Ca_i oscillation decrease net Na absorption by the epithelium and cause the membranes to depolarize, through the down regulation of apical Na permeability by Ca_i. The feedback control mechanism proposed by Taylor and Windhager (*Am. J. of Physiol.* 236:F505-512) is shown to work in cases where there are changes in Na gradient across the epithelium. The model also agrees with the experimental observations on the application of ouabain to the basolateral side (Silver *et al. Am. J. Physiol.* 264: F557-564), and amiloride to the apical side (Frindt *et al. Am. J. Physiol.* 264: F565-574). Different hormones modulate the Na absorption rate by changes in the basal Ca_i level. Supported by NIH grant DK31550.

Th-Pos113

RECONSTITUTION OF A PASSIVE Ca^{2+}-TRANSPORT PATHWAY FROM THE BASOLATERAL PLASMA MEMBRANE OF RAT PAROTID GLAND ACINAR CELLS. **T. Lockwich, S.V. Ambudkar', J. Chauthaiwale, and I.S. Ambudkar.** CIPCB, NIDR, NIH, Bethesda, Md. and 'Division of Nephrology, Dept. of Medicine, Johns Hopkins School of Medicine, Baltimore, Md.

We have previously reported the presence of two Ca^{2+} permeabilities in rat parotid gland basolateral membrane vesicles (BLMV); a saturable, high affinity component and an unsaturable component (J. Membrane Biol.(1994) 141; 289-296). In this study, we have solubilized BLMV with octylglucoside (1.1%) in the presence of E.coli lipids and glycerol (20%) and have reconstituted the solubilized proteins into proteoliposomes (PrL) using a detergent dilution method. The PrL exhibited 3-5-fold higher $^{45}Ca^{2+}$ influx as compared to control liposomes (without protein). $^{45}Ca^{2+}$ influx in PrL was saturable and exhibited a single Ca^{2+} permeable component with an appparent K_{Ca}=142±32 μM. The K_{Ca} of Ca^{2+}-transport in PrL was similar to that of the high affinity Ca^{2+} influx component seen in BLMV and thapsigargin-treated, internal Ca^{2+} pool-depleted parotid acini; 117±19 μM and 70±20 μM, respectively. The V_{max} of Ca^{2+} influx in PrL (11.2 nmoles/mg protein/minute) was about 3-fold higher than in BLMV. The unsaturable Ca^{2+} flux component was not detected in PrL. Passive $^{45}Ca^{2+}$ influx in PrL, similar to that in BLMV, was inhibited by divalent cations in the order; Zn^{2+}>Mn^{2+}>Co^{2+}=Ni^{2+}, but appeared to be more sensitive to lower concentrations of Zn^{2+} and Mn^{2+}. Also consistent with our observations with BLMV and internal Ca^{2+} store-depleted acinar cells, the carboxyl group reagent N,N'-dicyclohexylcarbodiimide (DCCD) inhibited the reconstituted passive Ca^{2+} transport in PrL. Importantly, in both BLMV and PrL, DCCD induced a 40-50% decrease in the V_{max} of the high affinity site, without an alteration in K_{Ca}. These data strongly suggest that we have successfully reconstituted the high affinity Ca^{2+} transport pathway from BLMV into PrL.

Th-Pos114

THE EFFECT OF ASTHMA PROPHYLAXIS AGENTS ON AN AIRWAY EPITHELIAL CHLORIDE CHANNEL. ((1E.W.F.W. Alton, 1D.J. Kingsleigh-Smith, 1F.M. Monkonge, 1S.N. Smith, 2A.R.G. Lindsay, 3A. Norris, 1D.M. Geddes, 2A.J. Williams.)) 1Ion Transport Unit, 2Dept. of Cardiac Medicine, National Heart and Lung Institute, London, UK, 3Fisons Pharmaceuticals, Loughborough, UK. (Spon. by S.E. Harding)

A number of recent observations suggest that airway Cl^- transport may be involved in the pathogenesis of asthma. We have previously described the properties of a voltage- and Ca^{2+}-dependent chloride channel present in airway epithelium (Alton et al, J. Physiol. 443 137-159 (1991)). We have now studied whether agents used clinically in the prophylaxis of asthma (sodium cromoglycate, nedocromil sodium and frusemide) affect the properties of this channel. Membrane vesicles from airway epithelium were incorporated into planar phospholipid bilayers under voltage clamp conditions. Sodium cromoglycate and frusemide produced a dose-related reduction in single channel conductance with EC_{50}s of 4.63mM and 0.31mM respectively. Nedocromil sodium produced a dose-related reduction in channel open probability with an Ec_{50} of 0.52mM. Membrane fractionation showed that the channel is predominantly localised to the apical membrane, and these agents only produced effects from the presumed extracellular surface of the channel. We conclude that agents used clinically in the prophylaxis of asthma alter the properties of an apically localised airway epithelial chloride channel.

Th-Pos115

STIMULATION OF CL SECRETION BY APICAL GENISTEIN REQUIRES INTRACELLULAR cAMP IN COLONIC EPITHELIAL CELLS. ((Beate Illek and Terry E. Machen)). University of California, Berkeley, CA 94720.

The apical Cl conductance in colonic HT-29/B6 and T-84 epithelia is regulated by a cAMP-dependent PKA pathway. We have recently shown that the tyrosine kinase (PTK) inhibitor genistein is a potent stimulator of CFTR activity in CFTR-transfected fibroblasts without increasing intracellular cAMP levels. We further studied the functional significance of genistein during Cl secretion in HT-29/B6 and T-84 cells expressing native CFTR. Monolayers were basolaterally permeabilized with the cAMP-permeable pore former α-toxin (250 U/ml) to gain direct access to the cytosolic side, and gradient driven Cl current (I_{Cl}) (140:30 mM, mucosal-to-serosal) was monitored under short circuit conditions. In the absence of cytosolic cAMP, genistein had no effect. When monolayers were stimulated with cAMP (5-100 μM), subsequent mucosal but not serosal addition of genistein (50 μM) increased I_{Cl} further by 15-35%. When cAMP was removed, I_{Cl} remained stimulated as long as genistein was present. In contrast, another PTK inhibitor tyrphostin A23 (50 μM) completely blocked the cAMP-stimulated I_{Cl}. Besides the effects on apical Cl channels, both genistein and tyrphostin A23 blocked the basolateral K conductance in apically amphotericin-permeabilized monolayers. Therefore, in intact epithelia the overall secretory response to genistein is composed of stimulatory effects on the apical CFTR and inhibitory effects on basolateral K channels. We conclude that genistein stimulates CFTR activity via an apical genistein-sensitive tyrosine kinase-dependent pathway which interacts with the PKA system.

Supported by DFG, CFF, CFRI.

Th-Pos116

FEEDBACK REGULATION OF AN EPITHELIAL SODIUM CHANNEL IN PLANAR LIPID BILAYERS. ((I.I. Ismailov, B.K. Berdiev, D.J. Benos)) Department of Physiology and Biophysics, University of Alabama at Birmingham, Birmingham, AL., 35294.

Purified bovine renal epithelial Na^+ channels display a specific orientation when incorporated into planar lipid bilayer membranes formed from phosphatidylethanolamine: phosphatidylserine:cholesterol (2:1:2), namely, the *trans*-facing portion of the channel is "extracellular" (*i.e.*, amiloride-sensitive), while the *cis*-facing side is "intracellular" (*i.e.*, protein kinase A + ATP-sensitive). The channel has a main state unitary conductance of 40 pS and displays two subconductive states when bathed with symmetrical 100 mM NaCl solutions. Current-voltage curves of the main and subconductive states remain linear in the range of ±100 mV. Dwell time constants for the main and subconductive states were 50 and 10 ms, respectively. Closed time histograms had two exponentials with constants of 70 and 900 ms. In this study we directly tested the hypothesis that sodium regulates this channel by feedback inhibition. Application of a sodium gradient across the bilayer containing an incorporated channel, keeping the total osmolarity of each solution constant by substitutions with NMDG-Cl, resulted in a shift of reversal potential entirely consistent with that predicted for a cation selective channel. Elevation of the $[Na^+]$ gradient from the *trans* side increased single channel open probability (P_O) only when the *cis* side was bathed with solution containing a low (10 to 30 mM) $[Na^+]$ and 10-100 μM $[Ca^{2+}]$. Reducing $[Na^+]_{cis}$ increased P_O at any $[Na^+]_{trans}$. Buffering of the *cis* compartment with a zero-$[Ca^{2+}]$-EGTA solution increased the initial level of channel activity (P_O= 0.12 ± 0.017 versus 0.02 ± 0.009 in control), but eliminated the influence of both *cis*- and *trans*- $[Na^+]$ on P_O. Protein kinase C-induced phosphorylation shifted the dependence of P_O on $[Ca^{2+}]_{cis}$ from 10-100 μM to 1-3 μM. The relative probability of the channel being in a subconductive state remained unchanged in all circumstances. Supported by NIH Grant DK37206.

Th-Pos117

EVIDENCE FOR INTRINSIC VOLTAGE-DEPENDENT GATING OF THE VOLUME-ACTIVATED CHLORIDE CURRENT. ((A.P. Braun and H. Schulman)) Dept. of Neurobiology, Stanford University Medical Center, Stanford, CA 94305

Hypotonicity-induced increases in cell volume lead to the development of a volume-activated chloride current which is critically involved in a cell's regulatory volume decrease (RVD). Using whole cell patch clamp methodology, we have examined the biophysical properties of the non-voltage-gated, volume-activated chloride current in single human T84 epithelial cells. Following voltage-dependent inactivation, this chloride current displays clear voltage-dependent recovery from inactivation, as judged by tail current behavior, and the recovery of peak outward currents using a double pulse voltage clamp protocol. The time constants derived for these two recovery processes at different membrane potentials are identical, suggesting that a common molecular mechanism may underlie both recovery processes. These channels can further undergo a form of voltage-dependent, steady-state inactivation that appears to differ from the inactivation observed at positive potentials. Physiologically, these results suggest that the cell's membrane potential, acting through the channel's intrinsic voltage sensor, will influence RVD by determining the availability of chloride channels activated under cell swelling conditions.

Th-Pos118

THE STRUCTURE OF NEONATAL STRATUM CORNEUM LIPIDS: A SMALL-ANGLE X-RAY DIFFRACTION STUDY. ((L.B. Nonato[1,2], J.A. Bouwstra[3], G.S. Gooris[3], C. Cullander[2], and R.H. Guy[2])) [1]Graduate Group in Bioengineering, UCBerkeley and UCSF, [2]Department of Pharmacy and Pharmaceutical Chemistry, UCSF, CA, USA, and [3]Pharmaceutical Technology, Center for Bio-Pharmaceutical Sciences, Leiden University, the Netherlands.

The intercellular lipids of the stratum corneum (SC), the topmost layer of the skin, are believed to be the regulatory barrier of transport across the skin. Structural characterization of the stratum corneum lipids of premature neonatal skin may provide insight into its increased permeability. Small-angle X-ray diffraction was performed to determine the organization of the SC lipids of neonates of varying gestational and postnatal ages. From the diffraction pattern of the SC from an infant of 42 weeks estimated gestational age (EGA) and 35 days postnatal age, the lipid lamellar structure was characterized by repeat distances of 6.5 and 13.4 nm, similar to that found in adult SC. This suggests that the skin barrier of a neonate of this age may be equivalent to that of an adult. The repeat distances calculated from the diffraction curves of SC of less mature neonates (40 wks EGA, 7 days postnatal age; 34 wks EGA, 8 days postnatal age; 29 wks EGA, 10 days postnatal age) were different from those found in adult and from each other, indicating structures that vary with gestational and postnatal age. Interestingly, the sample from the 40 week EGA, 7 days postnatal age neonate did not produce a diffraction curve similar to that of adult SC, suggesting that even full-term infants may not have a structurally mature SC. Further X-ray diffraction studies and complementary biophysical techniques should provide additional information about the development of neonatal skin. Supported by NIH HD-23010, NSF, and NWO.

Th-Pos119

TISSUE DISTRIBUTION OF MIWC AND GLIP WATER CHANNEL HOMOLOGS DETECTED BY IMMUNOHISTOCHEMISTRY. ((A. Frigeri, M. Gropper and A.S. Verkman)) CVRI, UC San Francisco, CA 94143-0521, (Intro. by S. Bicknese).

We recently reported the cloning of two new members of the MIP26 family. In oocyte expression studies, MIWC (Mercurial Insensitive Water Channel) (JBC 269:5497-5500, 1994) conferred mercurial-insensitive water permeability and GLIP (JBC 269:21845-21849) conferred stilbene-inhibitable glycerol permeability. To examine tissue distribution and membrane localization, peptide-derived polyclonal antibodies were raised against the C-termini of MIWC and GLIP. Interestingly, these proteins localized to the same membranes in some tissues. MIWC and GLIP were expressed selectively in the basolateral membrane of kidney collecting duct principal cells, whereas the intercalated cells were unstained. Both cortical and medullary collecting duct were labeled. No significant increase in staining intensity was found in kidneys from dehydrated rats. In the gastrointestinal tract, MIWC and GLIP were detected on the columnar epithelium of colon but absent in stomach and small intestine. In the respiratory tract, both proteins were found on the tracheal epithelium. In brain, MIWC was found in the ependymal cells lining the ventricle surface and in thin layer closely adherent to the surface, while GLIP was strongly expressed on the brain surface. In eye, MIWC was present on the conjunctival epithelium and retina whereas GLIP was only found in conjunctiva. These results suggest the involvement of MIWC and GLIP in the urinary concentrating mechanism, cerebrospinal fluid regulation, and intestinal reabsorption.

Th-Pos120

PURINERGIC REGULATION OF ANION SECRETION IN CULTURED CYSTIC FIBROSIS PANCREATIC DUCT CELLS. *H.C. Chan, Y.L. Fung, W.T. Cheung & P.Y.D. Wong. Department of Physiology, Faculty of Medicine, The Chinese University of Hong Kong, Shatin, Hong Kong.*

Defective ß-adrenergic regulation of anion secretion across epithelia of various exocrine glands is the basic feature of cystic fibrosis (CF). The present study explored purinergic regulation of anion secretion across cystic fibrosis pancreatic ductal epithelium (CFPAC-1) by examining the effect of extracellular ATP on the short-circuit current (I_{SC}). CFPAC-1 cells grown on Millipore filters did not exhibit significant basal current nor respond to stimulation by either secretin or forskolin. However, large increase in I_{SC} could be induced by apical application of ATP in a dose-dependent manner (EC_{50} at 3 μm). Replacement of Cl^- in the bathing solution or treatment of DIDS markedly reduced the I_{SC}, indicating that large portion of the ATP-activated I_{SC} was Cl^--dependent. The effects of different adenosine nucleoside/nucleotides on I_{SC} were also studied to identify the type of purinoceptors involved. The order of potency was ATP = UTP > ADP > adenosine consistent with that for P_2-purionceptors. Reactive blue (100 μM), a specific antagonist for P_2 receptor, was found to inhibit 86% of the ATP-induced I_{SC}, further indicating the involvement of P_2 receptors. The ATP-induced I_{SC} was also inhibited by pretreatment of the cells with BAPTA-AM, indicating a role of intracellular Ca^{2+} in mediating the ATP response. Preliminary results from experiments in monolayers with nystatin-permeabilized basolateral membranes suggested that ATP-induced I_{SC} could be mediated by apical Cl^- channels. Our study indicates the presence of a P_2-linked regulatory mechanism for anion secretion in CF pancreatic duct cells which could have therapeutic potential.

Th-Pos121

MODE OF ACTION OF DIFFERENT INSECTICIDAL CRYSTAL PROTEINS OF *BACILLUS THURINGIENSIS* IN LEPIDOPTERAN MIDGUT ((I. Zimanyi, S.C. MacIntosh and B. Wilms)) Novo Nordisk Entotech, 1497 Drew Ave., Davis, CA 95616.

The parasporal inclusions of *Bacillus thuringiensis* (Bt)contain different Cry proteins, which have insecticidal activity. Recent studies suggest that the site and mode of action of these Cry proteins is quite complex. The Cryl proteins are active only against lepidopteran larvae. The Cry protein specifically recognizes and binds to a protein located in the brush border membrane (BBM) of the larval midgut. Most recently this binding protein was shown to possess aminopeptidase N activity. Studies also have shown that the binding of Cry protein to the receptor is necessary but not sufficient for its toxicity. Cry proteins block the cation-dependent amino acid transport systems of lepidopteran midgut, they also disrupt the well defined ion gradients of the BBM, and are capable of forming ion channels or pores in the BBM.

The present study investigates the mode of action of the inhibition of histidine (HIS) transport, membrane depolarization, and receptor binding by Cryl proteins of Bt in BBM Vesicles of *Spodoptera exigua*. We found that the receptor binding parameters of the different proteins correlate well with their toxicity in the field, however, there is no clear correlation between the inhibition of HIS transport. CrylA(c) inhibits the HIS transport in a concentration-dependent fashion, by significantly shifting the K_m of the transport without changing the V_{max}, suggesting a competitive type of interaction with the transporter. CrylA(b) binds to one population of high-affinity binding sites, its IC_{50} on the inhibition of HIS transport is in good correlation with its affinity to its binding site. The effect of Cryl proteins on the membrane potential of BBMV is studied using a membrane potential sensitive fluorescent probe. CrylA(b) can cause depolarization of the membrane at high concentrations, and can dramatically reduce the HIS-induced K^+ influx into the vesicles, which is in good correlation with its efficacy in inhibiting the transport of HIS. Possible link between the amino acid transport inhibition, the receptor binding and the pore-formation of Cryl toxins will be discussed.

ENDOTHELIA: NITRIC OXIDE AND ENDOTHELIN

Th-Pos122

THE INVOLVEMENT OF NITRIC OXIDE IN RAPID DESENSITIZATION TO α_1-ADRENOCEPTOR MEDIATED INCREASES IN INTRACELLULAR Ca^{2+} IN SINGLE SMOOTH MUSCLE CELLS. ((Xiao-Fang Li and C.R. Triggle)). Smooth Muscle Research Group, Faculty of Medicine, The University of Calgary, Calgary, AB, Canada T2N 4N1. (Spon. by E.A. AiELLO)

Desensitization, manifested as a decrease in the phasic (transient) elevation of intracellular Ca^{2+} ($[Ca^{2+}]_i$) following repeated exposure to cirazoline (a selective α_1-adrenoceptor agonist) was studied in fura-2 loaded freshly dispersed single smooth muscle cells from rat tail artery. Repeated stimulation with cirazoline (0.1 μM) induced time-dependent and progressive reduction in the rapid, and transient (nifedipine-resistant) increase in $[Ca^{2+}]_i$ (the "phasic" response), without significant changes in the maintained increase in $[Ca^{2+}]_i$ (the "tonic" response). Pretreatment with L-arginine (1 mM) enhanced the reduction in phasic $[Ca^{2+}]_i$ response to repeated cirazoline exposure. However, pretreatment with L-NAME (50 μM) significantly reduced the desensitization in the phasic $[Ca^{2+}]_i$ response to repeated cirazoline exposure. Furthermore, pretreatment with 50 μM Rp-8-Br-cGMPs (a cyclic GMP-dependent protein kinase inhibitor) or 0.5 μM dexamethasone either significantly reduced desensitization to cirazoline; or modified the phasic response to cirazoline such that a substantial elevation (tonic response) of $[Ca^{2+}]_i$ was observed (about 30% of cells). In dexamethasone treated cells, applying exogenous nitric oxide (NO) (at μM concentrations) facilitated the decline of cirazoline induced tonic $[Ca^{2+}]_i$ responses and abolished the subsequent exposure to cirazoline induced increases in $[Ca^{2+}]_i$. Our data indicate that the desensitization of cirazoline induced increases in $[Ca^{2+}]_i$ in single smooth muscle cells from the rat tail artery results from NO synthesis; probably an induction of the inducible NO synthase occurs during cell isolation. Supported by AHSF & MRC.

Th-Pos123

AGONIST-INDUCED CONTRACTIONS ARE RELAXED BY NITRIC OXIDE IN AN AGONIST- AND TISSUE-SPECIFIC MANNER IN PREGNANT AND NONPREGNANT GUINEA PIG UTERUS. ((K.A. Kuenzli, M.E. Bradley, and I.L.O. Buxton)) Department of Pharmacology, University of Nevada School of Medicine, Reno, NV 89557 (Spons. by Judith Airey)

The ability of exogenous nitric oxide to relax full-thickness uterine strips or isolated myometrium obtained from both pregnant and nonpregnant guinea pigs was evaluated. NO had no effect upon the frequency or amplitude of spontaneous contractions in either pregnant or nonpregnant full-thickness or isolated tissues. Addition of 100 μM NO to full-thickness uterine tissue strips precontracted with a variety of concentrations of the uterotonic oxytocin resulted in significant reductions in tissue tension in both pregnant ($P<0.05$) and nonpregnant ($P<0.001$) tissues. NO did not relax prostaglandin-induced contractions in either full-thickness or isolated uterine tissue obtained from either pregnant or nonpregnant guinea pigs. The addition of NO to full-thickness nonpregnant tissue strips precontracted with acetylcholine caused tissue tension to be reduced significantly ($P<0.05$). A number of experiments were performed in which NO was added to organ baths containing strips of isolated (endometrium-free) guinea pig myometrium which had been precontracted with agonists such as oxytocin. The removal of the endometrium completely and reproducibly reversed the relaxing effect of NO seen in intact, full-thickness pregnant and nonpregnant tissue strips. These findings are the first to describe the effects of nitric oxide upon spontaneous as well as agonist-evoked contractions in guinea pig uterine tissues, and suggest that the ability of nitric oxide to relax precontracted uterine smooth muscle is not only agonist-specific, but also dependent upon the presence of non-muscle tissue layers.

Th-Pos124

ROLE OF Na/H EXCHANGE IN MEDIATING POSITIVE INOTROPIC EFFECTS OF ENDOTHELIN IN CARDIAC MYOCYTES ((C.A. Ward and M.P. Moffat)) Dept. Pharmacology and Toxicology, University of Western Ontario, London, ON, CANADA N6A 5C1. (Spon. by S.M. Sims)

We examined the mechanisms of the positive inotropic effect of endothelin-1 (ET1) during 10 min exposure in isolated rabbit ventricular myocytes. Myocytes were loaded with fura2 or BCECF to measure fluorescence changes in intracellular calcium and pH, respectively. Unloaded cell shortening was measured simultaneously with intracellular calcium. Exposure to ET1 (1 nM) caused an intracellular alkalinization of 0.1 pH unit which was prevented by pretreatment with 1 μM methylisobutylamiloride (MIA), an inhibitor of Na/H-exchange. ET1 significantly increased calcium transient amplitudes (systolic$_{340/380}$ - diastolic$_{340/380}$) to 155±5% of pre-ET1 values. Pretreatment of myocytes with 20 nM bisindolylmaleamide (BIS), an inhibitor of PKC, or MIA significantly attenuated this increase to 137±3% and 128±5%, respectively. Ryanodine (10 μM) delayed and significantly attenuated ET1 induced increases in calcium transient amplitude to 125±3%. With respect to unloaded cell shortening, ET1 caused an increase to 214±6% of pre-ET1 values. In the presence of BIS and MIA, these increases were significantly attenuated to 156±10% and 163±17%, respectively. Ryanodine failed to modulate the ET1 induced increase in cell shortening. The results of this study demonstrate that the positive inotropic effect of ET1 can be dissociated from changes in intracellular calcium and is likely related to activation of Na/H-exchange.

Supported by the Medical Research Council of Canada.

Th-Pos125

NITRIC OXIDE-INDUCED CHANGES IN cGMP AND TENSION IN HUMAN AND MONKEY MYOMETRIUM. ((M.E. Bradley, K.A. Kuenzli, J.E. Barber, and I.L.O. Buxton)) Department of Pharmacology, Univ. Nevada, Reno, NV 89557.

We have examined the effects of the endogenous smooth muscle relaxing agent nitric oxide (NO) on tissue tension and intracellular cGMP concentrations ([cGMP]$_i$) in pregnant and nonpregnant primate uterine smooth muscle. Simultaneous determinations of tissue tension and [cGMP]$_i$ was accomplished by flash-freezing myometrial tissue strips obtained from women or monkeys at specific points during spontaneous contractions; effects of addition of NO or the native substrate for nitric oxide synthase (NOS) -- L-arginine -- were evaluated by integration of contractile recordings and enzyme-linked immunoabsorbant assay for cGMP. Exogenous NO addition (100 μM final concentration) resulted in statistically-significant ($P<0.05$) reductions in human pregnant (83%) and nonpregnant (68%) tissues, and also in nonpregnant monkey myometrium (93%). These reductions in tissue tension were associated with significant ($P<0.05$) elevations in human myometrial [cGMP]$_i$: compared to either basal values or those seen at the peak of spontaneous contractions, [cGMP]$_i$ in pregnant and nonpregnant human tissues treated with 100 μM NO were elevated approx. 7-fold and 2-fold, respectively. An even larger increase in [cGMP]$_i$ was observed in NO-treated monkey myometrium, which exhibited a 25-fold increase over basal levels ($P<0.05$). Addition of *L*-arginine (1 mM) to spontaneously active tissues resulted in a highly significant ($P<0.001$) reduction in average tissue tension in nonpregnant monkey myometrium. These results suggest that primate myometrial cells are capable of relaxing in response to NO addition *in vitro*, and that generation of intracellular cGMP may mediate this effect; stimulation of endogenous NOS with L-arginine also provides evidence for the existence of this enzyme in primate uterine smooth muscle, and supports a role for NO in the regulation of uterine contractility in both the nonpregnant and pregnant woman. (Supported by NIH HD26227.)

Th-Pos126

NITRIC OXIDE MODULATES SIGNALLING BETWEEN CULTURED ADULT CARDIOMYOCYTES AND INTRINSIC CARDIAC OR STELLATE GANGLION NEURONS. ((M.Horackova, J.A.Armour)) Department of Physiology & Biophysics, School of Medicine, Dalhousie University, Halifax, NS B3H 4H7 Canada

To determine whether nitric oxide (NO) modifies cardiomyocytes directly or indirectly via peripheral autonomic neurons, the effects of NO were studied in long-term cultures of adult guinea-pig ventricular myocytes alone or cocultured with adult extracardiac (stellate ganglion) or intrinsic cardiac neurons. Adult ventricular myocytes and cardiac neurons were enzymatically dissociated and plated together or separately. Cultures so derived were used for experiments after 3-10 weeks, the contractile properties of cultured myocytes with or without associated neurons were investigated. NADPH diaphorase (NADPH-d) activity indicated NOS activity associated with cultured intrinsic and, to a much lesser extent, stellate ganglion neurons. The beating frequency of ventricular myocytes cocultured with intrinsic neurons (M-intrinsic) or stellate ganglion neurons (M-stellate) increased by 20-30% ($P <$ 0.001) following the administration of the NO donor SNAP; the beating frequency of noninnervated myocyte cultures was not affected by SNAP. The guanylate cyclase inhibitor LY 83583 abolished the SNAP-induced effects on cultured myocytes. L-arginine (a precursor of NO) increased the beating rate (~20%; $P < 0.05$) of M-intrinsic cocultures, but it did not affect the beating of M-stellate cocultures or that of noninnervated myocyte cultures. The effects induced by SNAP were reduced in presence of TTX, but they were not affected by β-adrenergic or muscarinic receptor blockade. Thus, it is concluded (1) that NO-sensitive neurons are present in both types of cocultures: in the presence of NO these neurons increased the beating rate of cardiomyocytes; (2) that NO-synthesizing neurons are present only in M-intrinsic cocultures: L-arginine increased the beating frequency significantly only in these cocultures; and (3) that populations of intrinsic cardiac and stellate neurons influence cardiomyocytes' contractility via NO-dependent mechanisms. Supported by MRC Canada.

Th-Pos127

ACUTE NEGATIVE INOTROPIC EFFECT OF TUMOR NECROSIS FACTOR-α IN ISOLATED MYOCYTES MEDIATED BY NITRIC OXIDE. ((J.I. Goldhaber, K.H. Kim, P. Natterson, T. Lawrence, P. Yang and J.N. Weiss)) UCLA School of Medicine, Division of Cardiology and the Cardiovascular Research Laboratory, Los Angeles, CA 90024.

Tumor necrosis factor-α (TNF) is a pro-inflammatory cytokine which may contribute to the contractile abnormalities observed in myocardial ischemia and septic shock. To determine whether TNF can act directly on myocytes, and to elucidate its mechanism of action, we simultaneously measured cytosolic calcium ([Ca^{2+}]$_i$), active cell shortening, and diastolic cell length, in enzymatically isolated adult rabbit ventricular myocytes loaded with INDO-1-AM and field stimulated at 0.2 Hz at 22°C. Compared with 7 controls, 5 myocytes exposed to TNF (10,000 U/ml) for 20 minutes exhibited a reduction in contraction amplitude without a decrease in the amplitude of the [Ca^{2+}]$_i$ transient (21.5 ± 6.5 and 1.0 ± 5.7%, respectively). Diastolic cell length increased modestly by 1.7 ± 0.3%. Phase-plane plots of cell length vs. [Ca^{2+}]$_i$ showed a downward shift, indicating a reduction in the dynamic myofilament contractile response to [Ca^{2+}]$_i$. The effects of TNF could be blocked by concurrent exposure to the nitric oxide (NO) synthase inhibitor L-NAME (10 μM), but not its inactive enantiomer D-NAME. Our results suggest that altered myofilament [Ca^{2+}]$_i$ responsiveness due to TNF-mediated induction of NO synthesis underlies the acute negative inotropic effect of TNF in isolated myocytes.

Th-Pos128

DO ANIONS INFLUENCE ENDOTHELIAL PERMEABILITY? ((M. Pamela Griffin, J. Randall Moorman)) Pediatrics and Medicine, University of Virginia, Charlottesville, VA 22908.

β-adrenergic stimulation reduces albumin permeation across pulmonary artery endothelial monolayers, and induces Cl-mediated changes in cell morphology. To test the hypothesis that these anion-mediated changes in endothelial cells underlie endothelial permeability, we have measured permeation of radiolabeled albumin across endothelial monolayers in the presence of 110 mM Cl, Br, I, F, acetate (Ac), gluconate (G), and propionate (Pr). Permeability coefficients (PC) were calculated before and after addition of 200 μM IBMX, which reduces permeability. The plot shows the effect of IBMX, $PC_{ibmx}/PC_{control}$, as a function of initial PC - for example, in Cl the PC is 2.5×10^{-6} cm/sec and falls by 70% in IBMX. The sequence of halides - Cl-Br-I-F - suggests an intermediate affinity anion binding site. Varying [Ca^{2+}]$_o$ from 0.2 mM to 2.8 mM had no effect on PC or the IBMX effect. The anion channel blockers SITS (0.25 mM) and 9AC (0.5 mM) significantly increased baseline PC and reduced the IBMX effect, but the anion transport blockers bumetanide (0.2 mM) and furosemide (1 mM) did not. We conclude that anions play a role in pulmonary capillary endothelial permeability, perhaps by modulating endothelial cell size and shape.

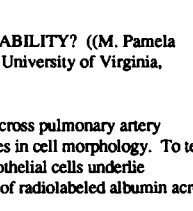

Th-Pos129

ALTERATIONS IN ENDOTHELIAL PERMEABILITY, CALCIUM MOBILIZATION AND CYTOSKELETAL F-ACTIN IN RESPONSE TO α-THROMBIN, BRADYKININ AND HISTAMINE. ((William D. Ehringer[1], Michael J. Edwards[2], and Frederick N. Miller[1,3])). Center of Excellence for Applied Microcirculatory Research[1], Department of Surgery[2], and the Department of Physiology[3], University of Louisville School of Medicine, Louisville, KY 40292.

The vasoactive mediators, α-thrombin (AT), bradykinin (BK) and histamine (HT) are endogenous proteins that modulate a variety of vascular processes by interacting with endothelium. Previous *in vivo* and *in vitro* work has demonstrated that each of these compounds, when given at near equivalent doses, can increase endothelial permeability. However it is not known if the mechanisms for the increased permeability induced by these compounds are similar. This study examined the *in vitro* effect of equivalent concentrations (10^{-6} M) of the three vasoactive mediators on human umbilical vein endothelial cells (HUVEC). Permeability to albumin, alterations in intracellular calcium mobilization and cytoskeletal f-actin localization were determined. HUVEC were grown to confluence on Transwell membranes and the flux of fluorescein isothiocyanate-labeled human serum albumin from the luminal to abluminal side of the membrane was monitored. Addition of AT, BK or HT increased the permeability coefficient of the HUVEC monolayer relative to control ($p<0.05$) with a temporal difference in the magnitude of the permeability coefficient. AT and BK induced rapid permeability alterations that declined over the course of the two hour experiment. In contrast, HT induced an attenuated change in the permeability coefficient of the HUVEC compared to AT and BK, but sustained the alteration for a longer period of time. In order to determine a possible mechanism for the differences in the permeability coefficients, HUVEC were labeled with FURA-2 and intracellular calcium was monitored by digital fluorescence ratio imaging. The results of this study indicated that intracellular calcium was mobilized by AT and to a lesser extent by HT but was unaffected by stimulation with BK. Fluorescent photomicrographs of BODIPY stained HUVEC, indicated that at 30 minutes AT and HT substantially altered f-actin content, while BK had no effect. The results of this study suggest that permeability may be increased by the three agonists, but that the intracellular mechanisms by which the permeability arises is different. Supported in part by the American Heart Association, Kentucky Affiliate.

Th-Pos130

MODEL OF CHANGES IN INTRACELLULAR $[Ca^{2+}]$ OF ENDOTHELIAL CELLS

((Annemarie Bartels, John W. Clark, Luis Vaca* and, Diana L. Kunze*))
Department of Electrical and Computer Engineering, Rice University, Houston, Tx 77030. *Department of Molecular Physiology and Biophysics, Baylor College of Medicine, Houston, Tx 77030

The endothelium is a monolayer of cells which lines the inside of blood vessels. It responds to several different kinds of agonists by increasing cytoplasmic $[Ca^{2+}]$. The increase in $[Ca^{2+}]$ will then trigger the synthesis and/or release of various vasoactive substances. In order to better understand the mechanisms involved in the modulation of cytoplasmic $[Ca^{2+}]$, a mathematical model has been developed. This model includes equivalent circuit descriptions of the plasmalemma and endoplasmic reticulum membranes along with material balance equations for $[Ca^{2+}]$, inositol 1,4,5-triphosphate and diacylglycerol. The emphasis of the equivalent circuit membrane models is primarily on describing the Ca^{2+} permeable channels and the Ca^{2+} pumps. The model produces good fits to data obtained from four different types of experiments in which intracellular $[Ca^{2+}]$ is modulated by: 1. increased phosphatidylinositol turnover due to agonist binding 2.block of the Ca^{2+}-ATPase pump of the endoplasmic reticulum 3.changes in the extracellular $[Ca^{2+}]$ 4.and block of the plasmalemmal Ca^{2+} influx pathway by SKF96365.
This research was funded by a Texas ATP grant awarded to DLK.

Th-Pos131

ENDOTHELIN AS A COMPONENT OF AN INTERCELLULAR SIGNALING SYSTEM THAT AUTOREGULATES CONTRACTILITY OF MAMMALIAN HEART. ((G. McClellan, A. Weisberg, and S. Winegrad)), Department of Physiology, School of Medicine, University of Pennsylvania, Phila., PA, 19104-6085

Endothelin, a peptide originally identified by its ability to cause contraction of smooth muscle, can also produce substantial changes in the contractility of heart muscle. The response and the sensitivity of isolated heart muscle to endothelin can vary considerably, with threshold concentrations from 1 pM to 1 nM. This variability appears to depend on the activity of endothelial cells in the heart and the magnitude of two other intercellular signals, nitric oxide (NO) and a cardiac myocyte derived regulator of endothelium (MDRE). In the absence of functioning endothelial cells, 1 pM endothelin raises cardiac contractility and actomyosin ATPase activity, while in their presence 0.1-1 nM is required. Inhibition of the action of NO by methyl nitro-L-arginine or methylene blue increases the sensitivity of the contraction to endothelin in the presence of endothelial cells by about 50 fold and generally produces instability in the amplitude of the isometric contraction. Addition of MDRE raises contractility by increasing endothelial cell secretion of endothelin. Together, the three intercellular signals, endothelin, NO, and MDRE form a feedback system that stabilizes cardiac contractility. With the cardiac myocyte serving as the oxygen sensor, the mechanism stabilizes contractility at levels dependent on oxygen tension and maintains a balance between oxygen supplied to the heart and work performed by the heart. The stabilization can be overridden by beta adrenergic stimulation, which partially bypasses the feedback loop.
(Supported by NIH grant HL 16010)

Th-Pos132

SIMULTANEOUS REGULATION OF CORONARY VASCULAR SMOOTH MUSCLE AND CARDIAC MYOCYTES BY ENDOTHELIA. ((A. Weisberg, G. McClellan, S. Winegrad)) Dept of Physiol, Univ of Penna., Phila, PA 19104-6085.

Endothelin increases the tone of vascular smooth muscle and increases the force of contraction of cardiac myocytes. These two contractile responses, if they occur simultaneously, are incompatible with healthy functioning of the intact heart because increased contractility of the heart would occur where coronary blood flow is reduced. Three general types of mechanisms might obviate this potential incompatibility: 1) a difference in the dose response relation of coronary vascular smooth muscle and cardiac myocytes to endothelin; 2) differences in the diffusion pathways of endothelin from vascular endothelial cells for the stimulation of the two different population of muscle cells; or 3) a differential response to another substance such as nitric oxide that modulates the endothelial effect. In order to test this hypothesis, the effect of endothelin on the actomyosin ATPase activity of coronary vascular smooth muscle and cardiac myocytes has been measured in cryostatic sections of quickly frozen rat hearts by quantitative histochemistry, which has the advantage of distinguishing between the activity in the two cell types in the same tissue and in smooth muscle among the various types of blood vessels. Actomyosin ATPase activity is increased in both cardiac myocytes and the smooth muscle of the arterioles (small thick-walled blood vessels) by 10 pM endothelin with a maximum increase at 1 nM. A 50% increase occurs in both types of cells with 50 pM. ATPase activity in smooth muscle cells in the large arteries is not increased at concentrations of endothelin up to 1 nM, and only a small increase is produced by 10 nM. Therefore actomyosin in arteriolar smooth muscle and cardiac myocytes have the same dose response curves to endothelin. A model for differential regulation of the response to endothelin based on modulation of diffusion pathways will be presented. (Supported by grant HL16010 from NIH)

Th-Pos133

VENTRICULAR EXPRESSION OF MESSENGER RNA FOR ENDOTHELIN-1 AND ATRIAL NATRIURETIC FACTOR *IN VIVO* DURING NOREPINEPHRINE INFUSION. ((S. Kaddoura and P. H. Sugden)) National Heart & Lung Institute, London, SW3 6LY, England.

The powerful vasoconstrictor endothelin-1 (ET-1) has potent effects upon cell growth and induces hypertrophy of cardiac myocytes in culture. Endothelin-1 produced by the myocardium *in vivo* may act in an autocrine/paracrine fashion to mediate the effects of hypertrophic stimuli. We have examined the effects of infusion of norepinephrine (NE) by osmotic minipumps at a dose of 600μg/kg/h in rats over a 7-day period, on ventricular myocardial expression of ET-1 mRNA, constitutive glyceraldehyde 3-phosphate dehydrogenase (GAPDH) mRNA and atrial natriuretic peptide (ANF) mRNA, expression of the last by adult ventricular myocardium being a marker for hypertrophy. mRNAs were measured by quantitative ribonuclease protection assays. Ventricular weight:body weight ratios and ventricular RNA:protein ratios were also measured as indicators of hypertrophy. The ventricular weight:body weight ratio increased (for controls and NE-infused groups, respectively, at day 1: 0.41 ± 0.02% vs. 0.47 ± 0.02% and at day 7: 0.36 ± 0.01% vs. 0.54 ± 0.03, $p < 0.05$, $n = 3 - 5$) and ventricular RNA:protein ratios also increased. There was a significant early increase in ventricular [ET-1 mRNA]:[GAPDH mRNA] in the NE-infused group relative to controls (at 1 day: 0.193 ± 0.018 vs. 0.003 ± 0.002, respectively, $p < 0.001$, and at 3 days: 0.061 ± 0.007 vs. 0.003 ± 0.001, respectively, $p = 0.001$, $n = 3 - 5$). At 5 and 7 days, ET-1 mRNA expression in the NE-infused group had fallen to control levels. ANF mRNA expression also increased significantly with NE infusion (mean increase above control expression at 1 day: 1.83-fold, at 3 days: 7.61-fold and at 7 days: 58.8-fold). Thus, in this *in vivo* model, norepinephrine-infusion induces ventricular hypertrophy, and is associated with an early rise in ventricular [ET-1 mRNA]. Endothelin-1 may be acting as an autocrine/paracrine mediator in this system.

CALCIUM WAVES AND OSCILLATIONS

Th-Pos134

THE ROLE OF GAP JUNCTIONS IN TRIGGERED PROPAGATED CONTRACTIONS IN RAT CARDIAC TRABECULAE.
((Yingming Zhang, Henk E.D.J. ter Keurs)) University of Calgary, Calgary, AB, Canada

Triggered arrhythmias in cardiac muscle can be elicited by triggered propagated contractions (TPCs). TPCs in rat trabeculae are triggered in damaged ends of trabeculae by preceding twitches; the local contractions propagate along the trabeculae at constant velocity. We hypothesized that propagation of TPCs depends on Ca^{2+} induced Ca^{2+} release (CICR) from the sarcoplasmic reticulum (SR) mediated by Ca^{2+} diffusion to adjacent SR and adjacent cell through gap junctions (GJs). We investigated the effects of GJ blockers octanol (OT) and heptanol (HT) on twitch force (Ft), TPC force (Fpc), propagation velocity (Vp) and time for triggering of TPCs (Tt). Trabeculae from rat hearts were superfused with Krebs-Henseleit solution. TPCs were elicited by trains of 15 stimuli (2Hz, 15-s intervals) at 20°C, 0.7-1.7 mM $[Ca^{2+}]_o$. Laser diffraction was used to measure Vp by testing sarcomere shortening at two sites along the trabecula; force was measured with a silicon strain gauge. 3-300 μM OT and HT decreased Fpc, Vp and increased Tt in a dose-dependent manner. 300 μM OT and HT decreased Fpc to 21.25% and 25.66%, decreased Vp to 15.36% and 12.98%, and increased Tt to 325.17±43.33% (mean±sem, n=8) and 436.72±76.36% (mean±sem, n=6), but decreased Ft only to 79.01% and 77.80% respectively. These results suggest that blocking of GJs decreases propagation of TPCs. The decrease of Vp reduces the number of sarcomeres activated along the trabeculae in any given moment and thus reduces Fpc. OT and HT increase Tt, indicating that they reduce the triggering rate of TPCs probably by decreasing Ca^{2+} diffusion from damaged parts to healthy parts of trabeculae. All of the observations support the hypothesis that propagation of TPCs is due to CICR from the SR mediated by Ca^{2+} diffusion through GJs.

Th-Pos135

NONLINEAR PROPAGATION OF Ca^{2+}-WAVES IN RAT CARDIAC MYOCYTES

((M.H.P. Wussling))
Institute of Physiology, 06097 Halle, Germany

Spontaneous Ca^{2+}-waves in enzymatically isolated rat cardiac myocytes were investigated by confocal microscopy using the fluorescent Ca^{2+}-indicator Fluo-3. As recently shown the origin of a Ca^{2+}-wave is a spark-like focus within the sarcoplasmic reticulum. The propagation velocity was found to be nearly constant determined at different points along the cell by conventional fluorescence microscopy . More precise measurements with a confocal microscope (Meridian) resulted in a nonlinear propagation of the Ca^{2+}-wave with time. The velocity of the wave was low near the focus and increased exponentially. This result was surprising inasmuch as for geometrical reasons a decrease of the propagation velocity might be expected if the confocal plane is not identical with that plane where the focus of the Ca^{2+}-wave was located. It is supposed that the observed nonlinearity of the propagation velocity is dependent on the calcium induced calcium release mechanism that becomes more effective with increasing cytosolic Ca^{2+}-concentration during the propagation of the spontaneous Ca^{2+}-wave along the cardiac cell.

Th-Pos136

CALCIUM WAVES IN CARDIOMYOCYTES: WAVE TYPES, ANISOTROPY, AND TEMPERATURE DEPENDENCE OF WAVE PARAMETERS ((J. Engel[1], A. J. Sowerby, S.A.E. Finch, M. Fechner and A. Stier)) Max Planck Inst. f. Biophys. Chemistry, 37018 Göttingen; [1]Inst. Physiology, Humboldtallee 23, 37073 Göttingen, F.R. Germany

Calcium waves were studied in isolated adult rat cardiomyocytes using the dye fluo-3 and a video imaging system. Different types of waves could be classified and specifically evoked using various drugs. Digitized images were analyzed with image processing software, and direction-dependent velocities were determined in spontaneous waves. Waves propagated at constant speed in both, transverse and longitudinal direction; however, waves were about 50 % faster in the longitudinal direction. This anisotropic propagation was attributed to the anisotropic arrangement of obstacles for Ca^{2+} diffusion such as myofilaments and mitochondria. We also investigated the temperature dependence of wave velocity, local Ca^{2+} release and local Ca^{2+} removal. Apparent activation energies of these processes were -23, -28, and -46 kJ/mol, respectively. The high activation energy of Ca^{2+} removal arising from the activity of the SR Ca^{2+} pump relative to those of wave propagation and local Ca^{2+} release excludes a 'release from the inside' mechanism in which Ca^{2+} that has been taken up by the SR from the approaching wavefront triggers Ca^{2+} release. It is, however, consistent with the hypothesis that CICR is triggered at the outer face of the SR.

Th-Pos137

CALCIUM WAVES AND IP_3 RECEPTORS IN CULTURED SKELETAL MUSCLE. (E. Jaimovich, J. L. Liberona, T. Pérez, J. Hidalgo and R. Caviedes). Depto. Fisiología y Biofísica, Fac. de Medicina, Universidad de Chile and Centro de Estudios Científicos de Santiago, Casilla 70005 Santiago, Chile.

Calcium images by confocal microscopy and binding of ^3H-IP_3 and ^3H-Ryanodine were studied both in RCMH, human skeletal muscle cell line and in both rat myoblasts and myotubes in primary culture. Upon potassium depolarization, mononucleated undifferentiated RCMH cells respond with a transient rise in $[Ca^{2+}]e$. Rat myotubes on the other hand, dyplay both a fast (>200 μm/s) propagated $[Ca^{2+}]i$ signal and a slow (10-50 μm/s) $[Ca^{2+}]i$ wave. The fact that both signals can be added, suggests that they are mediated by different mechanisms. The presence of possible Ca release channels was studied as expresion of ryanodine and IP_3 receptors. Undifferentiated RCMH cells express 0.1 pmol/mg protein ryanodine receptors that increase to 0.7 pmol/mg upon differentiation while 3.1 pmol/mg of IP_3 receptors are already present in undifferentiated cells. Rat myoblasts do not express IP_3 receptors and they reach 4.6 pmol/mg in 7 day old myotubes. A role for at least two types of calcium release channels in cultured skeletal muscle is proposed.
Financed by Fondecyt 1931089, DTI B3390.

Th-Pos138

ON THE ROLES OF Ca^{2+} DIFFUSION, Ca^{2+} BUFFERS, AND THE ENDOPLASMIC RETICULUM IN IP_3-INDUCED Ca^{2+} WAVES. ((M. S. Jafri and J. Keizer)) Institute of Theoretical Dynamics and Section of Neurobiology, Physiology, and Behavior, Univ. of Calif., Davis, CA 95616.

Using a mathematical model, we have investigated the effects of Ca^{2+} diffusion, cytosolic mobile and stationary Ca^{2+} buffers, and Ca^{2+} handling by the endoplasmic reticulum (ER) on inositol 1,4,5-trisphosphate-induced Ca^{2+} wave propagation. Although buffers severely limit Ca^{2+} diffusion, for conditions just below the threshold for Ca^{2+} oscillations a pulse of IP_3 or Ca^{2+} results in a solitary trigger wave that requires Ca^{2+} diffusion for its propagation. On the other hand, for repetitive wave trains found in the oscillatory regime, neither the wave shape nor the speed are strongly dependent on diffusion of Ca^{2+}. Local phase differences lead to waves that are *kinematic* in nature, with the wave speed (c) related to the wavelength (λ) and period of the oscillations (τ) by $c = \lambda/\tau$. The period is determined by features that control the oscillations, including $[IP_3]$ and pump activity, which are related to recent experiments. Both solitary waves and wave trains are accompanied by a Ca^{2+} *depletion wave* in the ER lumen. We explore the effect of endogenous and exogenous Ca^{2+} buffers on wave speed and wave shape, which can be explained in terms of three distinct effects of buffering, and show that exogenous buffers or Ca^{2+} dyes can have considerable influence on the amplitude and width of the waves.

Th-Pos139

CONDITIONS FOR THE VALIDITY OF THE RAPID BUFFERING APPROXIMATION NEAR A POINT SOURCE FOR FREE CALCIUM. ((J. M. Wagner, G. D. Smith, J. Keizer)) Institute of Theoretical Dynamics; Graduate Group in Applied Mathematics, Biophysics Graduate Group, and Section of Neurobiology, Physiology, and Behavior, U.C. Davis, Davis, CA 95616.

Wagner and Keizer (1994 *Biophys. J.* 67:447–456) presented a set of reaction-diffusion equations describing calcium diffusion in the presence of stationary and mobile calcium buffers. They further showed that in the case of rapid buffers, this set of equations reduced to a single transport equation for calcium which contains the effects of both stationary and mobile buffers. Here we examine the full and reduced models in detail, revealing the conditions necessary for the validity of the fast buffering approximation near a point source, for example, near the opening of a single calcium channel. Numerical simulations of the full and reduced models are analyzed, and the results compared to previous models for calcium diffusion near a channel pore.

Th-Pos140

PURINERGIC RECEPTORS ACTIVATE OSCILLATIONS IN INTRACELLULAR Ca^{2+} AND CONTRACTION IN ADULT VENTRICULAR MYOCYTES ((Bin-Xian Zhang, Derek S. Damron, Xiuye Ma and Meredith Bond)) Dept. of Molecular Cardiology and The Center for Anesthesiology Research, The Cleveland Clinic Foundation, Cleveland, OH 44195

ATP is co-released with catecholamines in response to various physiological and pathological stimuli. ATP activation of purinergic receptors has been shown to increase intracellular Ca^{2+} ($[Ca^{2+}]_i$) in cardiac myocytes and its effects on $[Ca^{2+}]_i$ may be an important factor in the generation of ventricular arrhythmias. In this study, we used 2-methylthio-ATP (2-m-ATP) to investigate the effects of purinergic receptor activation on $[Ca^{2+}]_i$ and contraction in acutely isolated adult rat ventricular myocytes. $[Ca^{2+}]_i$ was measured in single myocytes using fura-2 and contraction was assessed by measuring the amplitude of individual cell shortening using video edge detection. Superfusion of individual myocytes with 2-m-ATP (0.1-25 uM) resulted in oscillations in both $[Ca^{2+}]_i$ and contraction. The amplitude of the contraction varied with individual myocytes and was independent of the concentration of 2-m-ATP. The frequency of contraction increased with increasing concentrations of 2-m-ATP. These oscillations in contraction were reduced or abolished when myocytes were pretreated with thapsigargin (Tg; 0.1-8 uM) and abolished following pretreatment with caffeine (4 mM). These data provide the first evidence that purinergic receptor activation is sufficient to stimulate myocyte contractions and that these contractions result from oscillations in $[Ca^{2+}]_i$. The experiments also indicate that Ca^{2+} release from the sarcoplasmic reticulum is involved in the oscillatory contractions.

Th-Pos141

ISOLATION OF A SOLUBLE, LOW M_r SPERM PROTEIN THAT SPECIFICALLY COMIGRATES WITH CALCIUM OSCILLATION-INDUCING ACTIVITY IN MOUSE EGGS. ((John Parrington[1,2], Karl Swann[2,3] and F. Anthony Lai[1])) [1]MRC National Institute for Medical Research, Mill Hill, London NW7 1AA; [2]MRC Experimental Embryology and Teratology Unit, St. George's Hospital, London SW17 0RE; [3]Anatomy and Developmental Biology, University College, London WC1E 6BT.

At fertilisation in mammals, the sperm activates the egg by producing a series of oscillations in intracellular free calcium. A sperm protein factor that causes calcium oscillations when injected into mouse and hamster eggs has previously been described (Swann, 1990, Development 110, 1295-1302). We have identified a low molecular weight protein that specifically comigrates with calcium oscillation-inducing (oscillogen) activity in eggs. Cytosolic proteins extracted from hamster sperm were subjected to sequential column chromatography and eluted fractions assayed for their ability to produce calcium oscillations after microinjection into mouse eggs. Fluctuations in cytoplasmic free calcium concentration were monitored in individual mouse eggs with the calcium-sensitive fluorescent dye, fluo-3, before and after sample microinjection. A 2,500 fold protein enrichment was achieved following separation by Cibacron blue, MonoQ and hydroxyapatite column chromatography for the fractions comprising oscillogen activity, using this microinjection assay. Oscillogen-containing fractions from the hydroxyapatite column were observed to co-elute specifically with a low molecular weight protein. These observations suggest that this low M_r protein may be a critical component of the cytosolic sperm factor.

Th-Pos142

THE DYNAMIC PROPERTIES OF MECHANOSENSORY NEURONS IN A SPIDER SLIT SENSE ORGAN

((M.I. Juusola and A.S. French)) Department of Physiology, University of Alberta, Edmonton, Alberta, Canada.

Intracellular recordings were made from primary sensory neurons of the anterior lyriform organ on the patella of the wandering spider (*Cupiennius salei*). The organ has 7-8 slits, each innervated by a pair of large bipolar sensory neurons. Recordings were made using the discontinuous current- and voltage-clamp techniques during mechanical stimulation of the slits. The stimulation was applied by a probe attached to a small loudspeaker, with an optical position indicator and servo-controlled position. Both step stimuli and pseudo-random noise stimulation were used. Tetrodotoxin was used to suppress the fast voltage-activated inward currents. Mechanical stimulation produced a graded receptor current which reversed close to the Na^+ equilibrium potential. Positive and negative step movements added to a fixed indentation produced asymmetric responses, with a larger, adapting component following additional indentation of the slits. The frequency response function of the receptor current did not decline significantly up to the highest frequency tested (~300 Hz), in agreement with the electrical behavior of the neurons, which suggests that they detect rapid vibrations.

Supported by the Medical Research Council of Canada, the Alberta Heritage Foundation for Medical Research and the Academy of Finland.

Th-Pos143

MECHANICAL PROPERTIES OF ISOLATED AUDITORY OUTER HAIR CELLS.

((M. Ulfendahl, W.B. McConnaughey and E.L. Elson)) Dept. of Physiology and Pharmacology, Div. Physiology II, Karolinska Institutet, S-171 77 Stockholm, Sweden, and Dept. of Biochemistry and Molecular Biophysics, Washington University School of Medicine, St. Louis, Missouri 63110, U.S.A.

The function of the hearing organ is based on several mechanical processes occurring at the cellular level. The mechanical characteristics of the sensory hair cells are thus of great importance to the hearing process.

Using the "cell poker" (Petersen et al., Proc. Natl. Acad. Sci. USA 79:5327-5331, 1982) which measures the force required to indent the cell membrane we have investigated mechanical properties of isolated guinea pig auditory sensory cells. The outer hair cells are tube-like structures with a diameter of approximately 10 µm and a length in the range of 10-100 µm. The initial stiffness of the cell membrane in a direction perpendicular to the long axis was approximately 0.3 millidynes/micrometer. Measurements were obtained from cells of different lengths and at various cellular locations (at the nucleus, the cuticular plate etc.).

(Supported by the NIH and the Swedish Society of Medicine)

Th-Pos144

MECHANICAL HIGH-PASS FILTER OF THE OUTER HAIR CELL MOTILITY

((K. H. Iwasa)) NIDCD, NIH, Bethesda, MD 20892-0920

The outer hair cell has a membrane-potential motility, which is important for the tuning of the mammalian ear, presumably functioning as a feedback motor in the cochlear mechanics. It has been previously shown that this motility is explained by a combination of a 'membrane motor,' which is driven by the membrane potential due to its gating charge, and the cell mechanics based on the membrane elasticity (Biophys. J, 65 (1993) 492; J. Acoust. Soc. Am. October 1994 issue). It predicts that the response amplitude under voltage clamp conditions is dependent on the membrane tension and thus the pressure difference across the plasma membrane. We tried to test this prediction by measuring the length changes elicited by voltage pulses under voltage clamp condition while letting the cell volume expand slowly. We found that the ratio of the amplitude to the cell length remained constant while the length underwent 30 % reduction in about 5 min. If this slow length change of the cell were due to the elastic response to a pressure build-up, the risen tension would have forced the motor into the extended state, resulting in a significant reduction of the ratio. The absence of such an effect indicates the presence of a plastic element in the membrane, eliminating slow tension changes (thus resulting in a mechanical high-pass filter). The existence of such a plastic element implies that while the presence of a turgor pressure is important, the turgor pressure is not significantly larger than the pressure changes during the maximum voltage-induced length changes. The time constant of this filter would be longer than 10 s, but shorter than 1 min.

Th-Pos145

NON-LINEAR CAPACITANCE IN ISOLATED PATCHES OF THE LATERAL MEMBRANE OF COCHLEAR OUTER HAIR CELLS.

((J E Gale and J F Ashmore)) Dept. of Physiology, School of Medical Sciences, University of Bristol, Bristol BS8 1TD, UK.

The elementary unit of the cochlear amplifier is a voltage-sensing motor molecule distributed at high density along the lateral membrane of the outer hair cell. Gating charge associated with the motor's conformational change (approx 100fC/pF) can be measured as a non-linear voltage-dependent capacitance under whole-cell recording conditions. We have used a software lock-in amplifier to measure capacitance in both cell-attached and excised patches. Using 3-4MΩ pipettes (i.d. 1.5-3μm), patch capacitance changed by up to 80fF during a voltage ramp from -130 to +100mV. In cell-attached patches the capacitance peaked at -42 ± 14mV (n = 6) assuming the resting potential of the cell to be -20mV. In excised patches the capacitance peaked at -43 ± 13mV (n = 3). The inferred maximum charge movement was 6.6 ± 2.3fC (n = 6). Assuming a patch diameter of 2.5μm (and taking z = 1 from the voltage-dependence of the charge movement) the estimated charge density was 2000 and 8000e/μm^2, for hemi-spherical and non-spherical patches respectively. Negative pressure applied to the pipette shifted the capacitance peak to more positive potentials, in agreement with results from whole-cell recordings (*Proc.R.Soc.Lond.*B 1994, 255, 243-249). Positive pressure shifted the peak to more negative potentials. No capacitance changes were observed in patches taken from the basal pole of the cell, where patch conductance was significantly greater. This method provides data on the properties of the outer hair cell motor molecule and allows observations to be made under conditions of isotropic membrane stress.

(Supported by Hearing Research Trust and the Colt Foundation)

Th-Pos146

A LOW-VOLTAGE-ACTIVATING DELAYED RECTIFIER IN MAMMALIAN TYPE I HAIR CELLS AT DIFFERENT TEMPERATURES

((A. Rüsch and R. A. Eatock)) Otolaryng., Baylor College, Houston, TX 77030

Voltage-activated currents of type I hair cells from mouse utricles were recorded in whole-cell voltage clamp mode between 23 and 36 °C. Cells were identified by their shape and large input conductances (>20 nS at -64 mV).

Type I hair cells had two delayed rectifiers. One activated positive to -60 mV and was not blocked by 20 mM extracellular Ba^{2+}. A second, which we call $g_{K,L}$ for low-voltage-activating potassium conductance, activated positive to -95 mV. At rest (-77 mV) about 40 % of the maximally available $g_{K,L}$ conductance (85 nS at -54 mV) was activated. $g_{K,L}$ was half-blocked by 2 mM Ba^{2+} or 43 µM extracellular 4-aminopyridine. It was independent of extracellular calcium and not blocked by intracellular Cs^+ (permeability ratio P_{Cs^+}/P_{K^+}: 0.35).

$g_{K,L}$ activated with slow sigmoidal kinetics. Between -95 and -55 mV, the principal activation time constants were 800 - 100 ms at 23 °C. These values decreased with a Q_{10} of 3.5 (n=5) upon heating to 36 °C. Inactivation of $g_{K,L}$ was partial at all temperatures. Its time course was very slow (seconds) at 23 °C but considerably faster at higher temperatures (Q_{10} = 5). $g_{K,L}$ deactivated with a double exponential time course which was only moderately temperature-sensitive. The dominant fast component had a Q_{10} of 1.4. The $g_{K,L}$ data are consistent with a single channel type with a gating scheme similar to that of noninactivated *Shaker* K^+ channels (Bezanilla et al., Biophysical J. 66, 1011, 94).

Th-Pos147

STRETCH CHANNELS IN NEONATAL RAT ATRIOCYTES ENHANCED BY TRIIODOTHYRONINE.

V.Chen, C.A.Shuman and W.L.Green, Veterans Affairs Medical Center and SUNY/Brooklyn, Brooklyn, NY.

Atrial myocytes isolated from 0-2 day old Sprague-Dawley rats were examined by cell-attached patch clamp techniques, with varying amounts of triiodothyronine (T3) in the potassium containing recording pipet. Holding voltages varied from -100 to +50 mV. A stretch stimulus was created by applying suction, 20-40 mm Hg, to the recording pipette. In the presence of 100 nM T3, an ion channel with conductance of 90 pS was activated by suction; the channel was not evident without stretch, and showed only rare openings in the absence of T3. At very high T3 (1 µM), activation had a lower voltage threshold, and conductance was greater,compatible with multiple simultaneous channel openings. Frequent channel openings were also seen when the pipet contained 0.5% bovine serum albumin plus 1 µM T3 (estimated free T3 concentration, 30 nM). Characteristics of this channel were prompt opening with suction, delayed closing after release of suction, dependence on low concentrations of ATP and on presence of potassium In the presences of pinacidil or minoxidol in the recording pipette single channel open probability was increased and multiple conductance levels appeared more frequently. Actions of T3 on the atrium include positive chronotropism and increased synthesis and secretion of atrial natriuretic factor, processes which may also respond to stretch. Thus, we hypothesize that T3 may influence these functions by increasing sensitivity to the stretch stimulus. Studies to define other characteristics of the T3 sensitive channel, and its possible role in mediating T3's cardiac effects, are in progress.

Th-Pos148

Ca^{2+} ENTRY THROUGH STRETCH-ACTIVATED CHANNELS IS AMPLIFIED BY Ca^{2+} RELEASE FROM INTRACELLULAR STORES ((Michael T. Kirber, Agustin Guerrero, Richard A. Tuft, Douglas S. Bowman, Fredric S. Fay, & Joshua J. Singer)), Dept. of Physiology, Biomedical Imaging Group, Univ. of Mass. Med. School, Worcester, MA 01605.

Using patch clamp techniques combined with a UV laser based ultrafast imaging microscope, we investigated the relationship between the activity of stretch-activated ion channels (SACS) in cell-attached patches and the time course of the spatial distribution of changes in cytosolic Ca^{2+}. We found that inward currents through the SACS in the patch (1) could depolarize the cell membrane, opening voltage-gated Ca^{2+} channels causing an increase in Ca^{2+} throughout the cell and (2) cause a localized increase in Ca^{2+} in a region near the tip of the patch pipette which appeared to depend to a large extent on release of calcium from intracellular stores. Evidence for the latter is as follows: (1) When cells were incubated in ryanodine and caffeine (100 uM, 0.5 mM respectively) for longer than one-half hour, this response was abolished. 2) Setting the potential across the patch to a level near E_{ca++} virtually abolished the response. 3) Under conditions where we were able to monitor this response for an extended period of time, it appeared to run down with time when channels were repeatedly activated with the cells bathed in calcium free solutions. 4) When channel activity was blocked by including Gd^{+3} in the patch pipette solution or when patches contained no SACS, no changes in cytosolic Ca^{2+} were seen in response to applying stretch to the membrane patch. 5) In a few cases, the rise in cytosolic Ca^{2+} continued after all applied stretch and channel activity had ceased. These findings point to a calcium dependent amplification of calcium influx through SACS.

Th-Pos149

Gd^{3+} REDUCES A CATION CURRENT AND CELL SWELLING IN OSMOTICALLY CHALLENGED ADULT RABBIT VENTRICULAR MYOCYTES.

((HF Clemo and CM Baumgarten)) Medical College of Virginia, Richmond,VA 23298

The effect of Gd^{3+}, a blocker of stretch-activated channels (SAC), on current and relative cell volume (vol_{TEST}/vol_{1T}) was studied in osmotically stressed (± mannitol) myocytes using the amphotericin perforated-patch method. Voltage ramps (28 mV/s) were applied concurrently with digital video microscopy, and each cell served as its own control. Gd^{3+}-sensitive difference currents were obtained in Cl^--free (methanesulfonate) isotonic (1T) and hypotonic (0.6T) media (n=5). In 1T media, 10 μM Gd^{3+} did not significantly alter current (a-c) or volume. In 0.6T media, an inwardly rectifying Gd^{3+}-sensitive current (b-d) was seen, and concurrently Gd^{3+} reduced cell swelling from 1.250 ± 0.032 to 1.160 ± 0.031. Gd^{3+} did not affect current or volume in Cl^--containing 0.6T media when Na^+, K^+, and Ca^{2+} were replaced with N-methyl-D-glucamine. Based on E_{REV}, the P_K/P_{Na} ratio of the Gd^{3+}-sensitive current was 6:1. These results suggest that Gd^{3+} blocks a stretch-activated cation current and alters the cell volume response to osmotic stress in the adult mammalian myocyte.

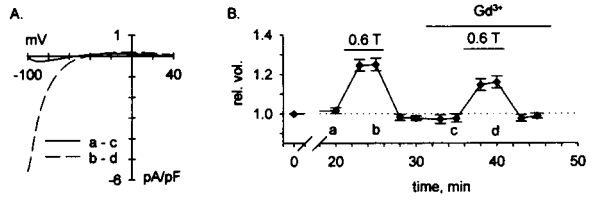

Th-Pos150

Hg^{2+} BLOCKS CELL VOLUME CHANGES IN OSMOTICALLY CHALLENGED RABBIT VENTRICULAR MYOCYTES.

((M.A. Suleymanian and C.M. Baumgarten))

Medical College of Virginia, Richmond VA & Armenian Academy of Sciences, Yerevan.

Hg^{2+} blocks water channels in some cells. Digital video microscopy was used to examine the effect of 3 mM $HgCl_2$ on relative cell volume ($VOL_{test}/VOL_{control}$) in myocytes and the response to hypo- (0.5T) and hyperosmotic (2T) media. Myocytes normally swell to 1.451±0.025 (n=7; SE) in 0.5T and shrink to 0.706±0.010 (n=10) in 2T. Adding Hg^{2+} to isosmotic 1T media caused a transient swelling to 1.053±0.014 followed by shrinkage to 0.922±0.011 in 25 min. Relative to volume in 1T+Hg^{2+}, cells swelled only to 1.019±0.004 (n=7) in 0.5T+Hg^{2+} (4% of control swelling) and shrank to 0.868±0.027 (n=10) in 2T+Hg^{2+} (45% of control shrinkage). Hg^{2+} induced a distinct RVI in 2T. The unequal block of swelling and shrinkage and RVI suggest Hg^{2+} alters ion transport rather than simply blocking water channels, whose existance in rabbit myocytes is uncertain because of the high Q_{10} of hydraulic conductivity (*Biophys. J.* 66:A168, 1994).

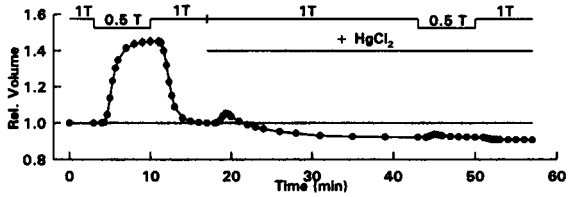

Th-Pos151

WHOLE CELL MECHANOSENSITIVE CURRENTS IN ACUTELY ISOLATED CHICK HEART CELLS: CORRELATION WITH MECHANOSENSITIVE CHANNELS. ((Hai Hu and Frederick Sachs)) Biophysical Sciences, SUNY at Buffalo, Buffalo, NY 14214.

Whole-cell mechanosensitive currents (MSC) can be recorded from acutely isolated embryonic chick heart cells, using perforated patches and a second micropipette to press on the cells (Hu and Sachs, Bioph. J., 66:A170). The MS channel inhibitor, Gd^{3+} at 30 µM completely blocked the current (n=3). The currents had a linear I-V relationship, with a reversal potential of -16.4±1.3 mV (n=5).

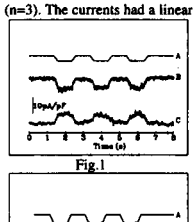

Fig.1

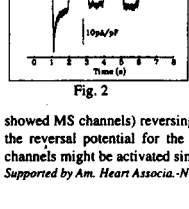

Fig. 2

The current was not carried by Cl^-. Using isethionate to substitute for bath Cl^-, we found that the reversal potential of the currents was basically unchanged (-14.0±3.3 mV, n=3), and that the outward currents at positive membrane potentials were similar to those before substitution (Fig. 1. **A**, trace of displacements of the stimulation pipette, 2.5 µm for B and 1.7 µm for C; **B**, current at -40 mV; **C**, +25 mV). Substituting K^+ for Na^+, we found that the MS conductance was increased by several fold, suggesting that the channels favor K^+ over Na^+. Ca^{2+} was not necessary to observe the MSC.

Most cells showed a steady response to deformation. But 15 of the 84 cells studied showed adaptation, in which the current decayed with time during a stimulus reaching a finite steady state value (Fig. 2. **A**, 3.4 µm displacement; **B**, current). In some cells the current adapted to almost 0 and took more than 12 seconds to recover, in others recovery was fast requiring less than 1 second.

In single channel studies on these cells, we observed two types of MS channels: a 100 pS channel (in 38% of patches that showed MS channels) reversing at ~ -70 mV, and a 25 pS channel (85%) reversing at -2 mV. Since the reversal potential for the whole cell MSC was between these two potentials, both types of channels might be activated simultaneously.

Supported by Am. Heart Associa.-NY Affiliate grant #93-338 to FS and MDRF of SUNYAB grant #S-94-10 to HH.

Th-Pos152

SINGLE-STEP PURIFICATION OF LARGE MECHANOSENSITIVE ION CHANNELS (MscL) OF *E COLI* AS FUSION PROTEINS WITH GLUTATHIONE S-TRANSFERASE. ((Claudia C Häse, Alexander C Le Dain, and Boris Martinac)). Dept of Pharmacology, University of Western Australia, Nedlands WA 6009, Australia.

Expression of recombinant proteins in *E coli* as fusion proteins with glutathione S-transferase (GST) is a common method to produce and purify proteins in bacteria. Using this method we constructed a fusion protein between GST and the large mechanosensitive channel (MscL) of *E coli*. After expression, purification, cleavage of the fusion protein by thrombin and solubilization in 2% octyglucoside, we obtained substantial amounts of purified MscL. The purified channel protein was reconstituted into artificial liposomes and examined with the patch-clamp technique. The reconstituted channels were fully functional, exhibiting characteristic large conductance (~ 3 nS in 200mM KCl), non selective permeability for cations and anions, and activation by stretching of the liposome membrane. When plotted against negative pressure, the open probability was described by a Boltzmann distribution with an e-fold change in open probability per ca. 7mm Hg, similar to that of the small mechanosensitive channel (MscS) in *E coli*. In giant spheroplasts the MscL exhibited voltage dependence, with increased activity at negative rather than positive pipette potentials. The voltage dependence of the MscL was preserved following reconstitution. Also, the reconstituted channel was blocked by submillimolar concentrations of Gd^{3+}. At present, the purified MscL protein is being used to generate antibodies in rabbits which will be useful for further study of channel voltage dependence and mechanosensitivity.

Supported by grants from the Australian Research Council and the Raine Foundation.

Th-Pos153

MEMBRANE TOPOLOGY OF THE PENICILLIN RECEPTOR BLAR1 OF BACILLUS LICHENIFORMIS. ((K. Hardt, A.L. Fink† and B. Joris)) University of Liège, Enzymology, B6, 4000-Belgium, †University of California at Santa Cruz, Department of Chemistry and Biochemistry, Santa Cruz, CA 95064.

The BlaR1 is involved in the induction of the *Bacillus licheniformis* ß-lactamase. The polypeptide (601 AA) has two domains : the extracellular domain (261 AA) carries the conserved motifs of the penicilloyl serine transferases and functions as the penicillin sensor; the transmembrane domain (340 AA) must function as the transducer of the signal received by the sensor. Analysis of the transducer has identified 5 hydrophobic segments (S1 to S5). To probe the predicted topology, truncated portions of the blaR1 gene were fused to the reporter gene blaM and cellular localization of the BlaM activity was determined. The results show four of the hydrophobic segments as being membrane spanning (S1, S2, S3 and S5). They also allowed identification of a intracellular domain (189 AA) between S3 and S5. This domain has no sites of methylation and no sites of phosphorylation/ dephosphorylation, but it possesses the signature of a neutral zinc metallopeptidase. This signature is conserved in the three known proteins of the BlaR family, BlaR of *B. licheniformis*, BlaR of *Staphylococcus aureus* and MecR of *S. aureus*. The intracellular domain is most likely responsible for the transmission of the signal received by the sensor (binding of penicillin) by generating an intracellular signal (peptidase activity) and the BlaR family probably forms a new class of bacterial receptors.

Th-Pos154

VESICLE TO PLASMA MEMBRANE TRANSFER OF A HYDROPHOBIC RAM SPERM PROTEIN ESA152 TO HETEROLOGOUS SPERM LEADS TO ACTIVATION OF ACROSOMAL EXOCYTOSIS UPON ANTIBODY CROSSLINKING ((C.A. McKinnon, E. Browne, F. Weaver, O. Braha, and D.E. Wolf)) Worcester Foundation for Experimental Biology Shrewsbury, MA 01545 (Spon. by Yu-li Wang)

ESA152 is a highly hydrophobic 18 KDa ram sperm glycoprotein which is secreted by the epididymis and integrates in the sperm plasma membrane at a critical juncture in epididymal maturation. Crosslinking of this antigen with bivalent antibodies induces the acrosome reaction. We have found that this protein is also present in a vesicle fraction of ram semen and that it becomes associated with the plasma membrane of sperm of heterologous species upon incubation with ram semen or with the high speed vesicle fraction of this semen. Following such incubation anti-ESA152 will induce the acrosome reaction in these heterologous sperm. Preliminary peptide and DNA sequencing results indicate theat ESA152 is a unique glycoprotein.

Th-Pos155

MODULATORY EFFECTS OF TEMPERATURE ON THE CA CURRENTS OF INSULIN-SECRETING CELLS. L.S. Satin, T.A. Kinard and P.D. Smolen. Dept. of Pharm. and Tox., Med. Coll. of VA., Richmond, VA. 23298 and Math. Res. Branch, NIDDK, Bethesda, MD. 20892

Pancreatic islets burst when [glucose] is > 7 mM, which is an important part of islet stimulus-secretion coupling (see Satin and Smolen, 1994; Endocrine 2:677-87). It has been proposed that slow inactivation of Ca channels by membrane depolarization mediates bursting (Cook et al, 1991;TINS 14:411-14), but simulations based on voltage-clamp studies of Ca current (Satin and Cook, 1989; Pflugers Archiv 411:401-9) do not show bursting unless several model parameters are modified (Keizer and Smolen, 1991; PNAS 88:3897-3901). To test whether the lack of bursting resulted from use of parameters based on Ca current data collected at 20°C (Satin et al, 1994; Biophys. J. 66:141-48), we studied the effects of raising temperature on the Ca currents of insulin-secreting HIT cells. Currents were measured in 3 mM Ca-containing solutions using standard whole-cell techniques. Increasing temperature from 20°C to 35°C increased peak Ca current by as much as 3-fold, increased the rate of fast, Ca-dependent inactivation, decreased time-to-peak, and shifted the activation threshold from -40 mV to -60 mV. Modifying the Keizer-Smolen model to account for increased Ca current and changes in the IV parameters observed at 35°C still failed to produce physiological bursting, all else being equal. Thus, although raising temperature strongly modified HIT cell Ca current, these effects cannot completely account for the inadequacies of the Keizer-Smolen model. Temperature must either modify other key currents or some other process is required which is missing or down-regulated in HIT cells.

Th-Pos156

CHARACTERIZATION OF LOW VOLTAGE-ACTIVATED CALCIUM CURRENTS IN A NON-OBESE DIABETIC MOUSE PANCREATIC ß CELL LINE. ((L. Wang, J. Fu and M. Li)) Department of Pharmacology, University of South Alabama College of Medicine, Mobile, AL 36688. (Spon. by A.E.Taylor)

The non-obese diabetic (NOD) mouse, a murine model for human insulin-dependent diabetes mellitus (IDDM), is characterized by an infiltration of lymphocytes into pancreatic islets and the complete destruction of islet ß cells. We have characterized calcium currents in NOD insulinoma tumor (NIT-1) cells. This cell line was developed from pancreatic ß cells of transgenic NOD mouse (Hamaguchi, K. et al., Diabetes 40:842, 1991). We found high voltage-activated calcium currents (L-type) and high levels of fast inactivating, low voltage-activated (LVA) calcium currents. In contrast, similar LVA currents were not observed in primary cultured normal mouse islet cells or in the ßTC-3 cells, which were developed from normal mouse pancreatic ß cells. In 40 mM external Ba^{2+}, the threshold of voltage-dependent activation of the LVA calcium current was approximately -50 mV and peaked at -10 mV. Half maximum steady-state inactivation was around -60 mV. The inactivation rate (τ) at -10 mV was around 30-35 ms. Although the biophysical properties of the LVA calcium channels in NIT-1 resembled typical T-type calcium channels, the pharmacological characteristics were not identical. Both nimodipine (500 nM) and nifedipine (3 µM) partially inhibited the LVA currents at -30 mV (holding potential -70 mV and -60 mV, respectively). Nickel (50 µM) significantly decreased the peak of the LVA currents. Administration of an N-type calcium channel blocker ω-CTx-GVIA (1µM) produced no appreciable effect. We conclude that LVA calcium channels predominate in NIT-1 cells. These results suggest that the altered cytosolic free calcium concentration may contribute to the pathogenesis of IDDM. Supported by a Research Starter Grant and Faculty Development Award to M. Li from the PhRMA Foundation.

Th-Pos157

CHARACTERIZATION OF VOLTAGE-DEPENDENT CALCIUM (Ca-V) CHANNELS IN CELL-ATTACHED PATCHES OF PANCREATIC β-CELLS ((M.-L. Kohler and C. L. Stokes)) Univ. of Houston, Houston, TX 77204.

Oscillations of the membrane potential (V_m), termed bursting, regulate the influx of calcium ions into pancreatic β-cells. Although Ca^{2+} is a critical activator of many intracellular events leading to the release of insulin, the regulation of bursting remains poorly understood. Others have proposed that slow inactivation of the Ca-V channel by voltage or Ca^{2+} might have a regulating function, motivating this investigation. We are interested in the endogenous regulation of the channel and the mechanisms by which glucose modulates that regulation. Hence, we used the cell-attached patch arrangement of the patch clamp technique rather than the excised-patch configurations preferred in previous work. The data were collected from rat β-cells (Harlan Sprague-Dawley), at 37 °C, in 2.8 and 11.1 mM glucose, and in "zero" (1 mM Ca^{2+} plus 5 mM EGTA) and high (10 mM) extracellular Ca^{2+}. 400-ms depolarizing pulses to -10 or -30 mV from a holding potential of -70 mV were repeatedly delivered to the cell every 4 s. The objective was to characterize the Ca-V channel by its mean open and closed times, open probability (P_o), and rate of inactivation by Ca^{2+} and voltage. Our results show that, in zero Ca^{2+}, the Ca-V channel opens with a higher probability in 11.1 mM glucose than in substimulatory 2.8 mM. P_o is also greater at -10 mV than -30 mV. In 11.1 mM glucose, the channels exhibit several modes of activity; some sweeps have a high P_o and others a low P_o. In 2.8 mM glucose, the channel rarely opens, in zero or high Ca^{2+}, at -30 or -10 mV. These results correlate the graded increases of Ca-V channel activity and insulin release in response to glucose. Continuing studies of how glucose and Ca^{2+} mediate channel activity should elucidate whether the modal changes in P_o represent alternating activation and inactivation on the burst time scale.

Th-Pos158

REGULATION OF INTRACELLULAR CA^{2+} BY cAMP IN THE PANCREATIC β-CELL. ((L. Xu and C. L. Stokes)) University of Houston, Houston, TX 77204. (Spon. by C. A. Tate)

The pancreatic β-cell secretes insulin in response to glucose, a behavior mediated through an increase in cytosolic Ca^{2+} concentration (Ca_i). Insulin release is modulated by several substances that stimulate production of cAMP such as glucagon and forskolin. These modulators also increase Ca_i; the sources of Ca^{2+} appear to be both extracellular (influx via voltage-dependent or other Ca^{2+} channels) and intracellular stores (possibly mitochondria, IP_3-sensitive stores or ryanodine-sensitive stores). To better understand the biochemical pathways by which cAMP modulates Ca_i and insulin release, we have done a systematic pharmacologic study to identify the Ca^{2+} sources. Using fluorescence microscopy, we measured Ca_i in single rat β-cells as a function of time under various conditions using fura-2 as the a Ca^{2+}-indicator. Increasing glucose from 2.8 to 11.5 to 20 mM caused sequential rises and sometimes oscillations in Ca_i. We stimulated cAMP production by exposing the cell to glucagon or forskolin. Either agent increased Ca_i, even when Ca^{2+} influx via membrane channels was eliminated by addition of 10 mM EGTA or diazoxide (to open K_{ATP} channels and hyperpolarize the membrane). To pinpoint the intracellular Ca^{2+} sources, we applied various pharmacologic agents to modulate the release or sequestration of Ca^{2+} from mitochondria (NaN_3, mannoheptulose), IP_3-sensitive stores (carbachol, thapsigargin) and ryanodine-sensitive stores (caffiene, thapsigargin), and again applied forskolin. We conclude that cAMP modulates cytosolic Ca^{2+} by (i) an influx through voltage-dependent Ca^{2+} channels, and (ii) a release from a nonmitochondrial intracellular store(s); the store is depletable by high extracellular [EGTA] and may include but is not exclusively the ryanodine-sensitive store.

Th-Pos159

INPUT RESISTANCE AND COUPLING CONDUCTANCE EVOLUTION DURING GLUCOSE-INDUCED ELECTRICAL ACTIVITY IN PANCREATIC B-CELLS. ((E. Andreu, B. Soria and J.V. Sanchez-Andres)) Dept. of Physiology, Institute of Neurosciences, University of Alicante, SPAIN. (Spon. by F. Sala)

It has been previously found that membrane potential of β-cells challenged with glucose respond in a byphasic mode. The aim of the present work is to follow the input resistance and the coupling conductance changes during the transition between the resting situation (Vm=-70 mV), the first phase (continuous spikes for 30-120 s.) and the steady-state situation (oscillations between a depolarized active phase and an hyperpolarized silent phase, -35 to -50 mV).

Methods: Intracellular electrical activity and input resistance from single cells and from pairs of β-cells within an islet was recorded with a bridge amplifier. Coupling conductance was estimated through the application of current pulses in one cell and recording the voltage drop in the other cell.

Results: 1) Glucose caused a depolarization paralleled by an increase in the input resistance (from a resting value of 80 MΩ, until a maximum peak value, 160 MΩ). 2)As the cell potential began to oscillate the resistance decreased and followed membrane potential oscillations (active phase: 130 MΩ, silent phase: 110 MΩ). 3)When higher glucose concentrations were applied (>20mM)the initial phase was prolonged while glucose was present with no oscillations of the membrane potential. Consequently, input resistance reached the maximum and did not decay. 4) 50 µM tolbutamide caused a similar effect. 5) Coupling conductance between a pair of cells in an islet followed a pattern similar to that of the input resistance.

It is concluded that, in addition with the effects of the input resistance (K_{ATP} channels?), glucose induces oscillations of the coupling resistance.

Th-Pos160

MOBILE CHELATORS ENHANCE THE PRESENTATION OF FREE CALCIUM AT TRANSPORT SITE OF ER CALCIUM PUMP.
((J. E. Moore, N.F. Al-Baldawi, and R. F. Abercrombie)) Department of Physiology, Emory University, Atlanta, GA 30322.

ATP-dependent ^{45}Ca accumulation into rat brain microsomes was measured at different free calcium concentrations [Ca^{2+}], at different pH, and with different concentrations of mobile chelator. At pH 6.8, 7.4, and 8.0 the V_{max} of the initial rate of ^{45}Ca accumulation was 0.04, 0.5, and 0.35 μmole (g protein)$^{-1}$ s^{-1} with or without a Ca chelator. In the absence of chelator, half-maximum rate was achieved for [Ca^{2+}] $\geq$ 25 μM while in the presence of 100 μM EGTA, this was achieved for [Ca^{2+}] $\leq$ 1 μM . If uptake was below V_{max}, it could be increased either by increasing the free calcium or by increasing the total EGTA at a fixed free calcium. Adding Ni-EGTA, a complex more stable than Ca-EGTA did not enhance ^{45}Ca accumulation. These results imply that mobile chelators bound with Ca may increase the calcium activity at the transport site. If this occurs, then the Ca-EGTA complex must remain in the vicinity of the transport site much longer than would be expected from its free solution diffusion coefficient and/or the off rate constant of calcium from chelator must be greater near the transport site than in free solution. Supported by NIH NS-19194.

Th-Pos161

PROTEIN KINASE MODULATION OF Ca^{2+} CHANNEL CURRENTS AND VOLTAGE-DEPENDENT EXOCYTOSIS IN RAT LACTOTROPHS. ((A.F. Fomina and E.S. Levitan)) Dept. of Pharmacology, University of Pittsburgh, Pittsburgh, PA 15261.

Ca^{2+} influx through voltage-gated channels triggers exocytosis by single rat lactotrophs (Biophys. J. 66:2, A248, 1994). Here we studied modulation of Ca^{2+} currents and exocytotic responses using the perforated-patch method and time-domain membrane capacitance measurements. Modulation of Ca^{2+} influx by varying the duration of depolarization or extracellular Ca^{2+} concentration leads to changes in amplitude of exocytotic responses. The relationship between Ca^{2+} influx and exocytosis can be described by power function with an exponent of ~ 3. Extracellular application of the protein kinase C activator TPA (100-500 μM), the protein kinase A activator 8-(4-chlorophenylthio)-cAMP (5 μM) or the Ca^{2+}-activated phosphatase (calcineurin) inhibitor cyclosporine A (1 μg/ml) enhanced voltage-gated Ca^{2+} currents and depolarization-evoked exocytosis. Extracellular application of the protein kinases inhibitors H7, staurosporine, calphostin C, chelerythrine or Ro 31-8220 gradually inhibited Ca^{2+} channel currents.
These findings suggests that (i) exocytosis by lactotrophs is steeply dependent on Ca^{2+} influx through voltage-gated Ca^{2+} channels; (ii) voltage-gated Ca^{2+} channels are targets for phosphorylation by different protein kinases; (iii) modulation of voltage-gated Ca^{2+} channels by changes in phosphorylation is an important feature in regulation of depolarization-induced exocytosis.

Th-Pos162

REAL-TIME CORRELATION OF INTRACELLULAR Ca^{2+} AND EXOCYTOSIS AT SINGLE BOVINE AND RAT CHROMAFFIN CELLS. ((Jennifer M. Finnegan and R. Mark Wightman)) Department of Chemistry, University of North Carolina, Chapel Hill, NC 27599-3290.

Catecholamine secretion from chromaffin cells has been used as a model for neurotransmitter exocytosis for many years. Typically, investigations of the role of Ca^{2+} in stimulus-secretion coupling have been undertaken in populations of chromaffin cells. Single-cell techniques have now been developed to measure intracellular Ca^{2+}, using the fluorescent probe fura-2, and catecholamine release, using a carbon-fiber microelectrode. Combination of these techniques allows real-time correlation of the Ca^{2+} trigger and resultant catecholamine secretion. Single-cell level measurements also permit study of cultured cells from small animals (with inherent low yields) and detection of heterogeneity within cell populations. Results from classic depolarizing stimuli, high K^+ and DMPP, show a dependence of maximal cytosolic Ca^{2+} concentration and catecholamine release on secretagogue concentration in both bovine and rat chromaffin cells. Mobilization of intracellular Ca^{2+} stores elicits different responses from each species indicating larger or more accessible stores in rat cells, although individual vesicular quantity and release time course appear to be conserved. Single-cell measurement of exocytosis and cytosolic Ca^{2+} rise induced by bradykinin-activated intracellular stores reveal cell-to-cell variability in bovine and oscillatory responses in rat chromaffin cells.

Th-Pos163

SYNAPTOPHYSIN ANTIBODY SPECIFICALLY AFFECTS BOTH A NEUROSECRETORY GRANULE CHANNEL AND PEPTIDE RELEASE. ((Y. Yin, C.J. Lee, G. Dayanithi, J.J. Nordmann and J.R. Lemos)) Worcester Found. Exp. Biol., Shrewsbury, MA 01545.

Isolated neurosecretory granules (NSG) from bovine neurohypophyses were reconstituted into lipid bilayers. The large NSG cation channel has a primary conductance of about 130 pS, but shows multiple sub-conductance states. It opens only in the presence of greater than 30 nM free [Ca^{2+}] but is inhibited by relatively high (>10 μM) [Ca^{2+}]. Release of vasopressin (AVP) from permeabilized neurohypophysial terminals also shows a similar biphasic dependence on Ca^{2+}. In order to try to determine if this channel corresponds to any known synaptic vesicle protein a number of antibodies were tested. SY-38, a monoclonal antibody which binds to the cytoplasmic tail of synaptophysin, could specifically alter the gating of the NSG channel, inhibiting the larger conductances and promoting smaller sub-conductance states. Similar effects can be observed on purified synaptophysin. Furthermore, this antibody could specifically inhibit AVP release in a Ca^{2+}-dependent manner. Other synaptic vesicle protein antibodies did not have these effects. The close correlations between channel and release properties lead us to conclude that the synaptophysin-like NSG channel may be involved in peptide secretion. (Supported by MDA and NIH grants)

Th-Pos164

CALCIUM SEQUESTERING STORES ARE CRITICAL FOR EXOCYTOSIS TRIGGERED BY NICOTINIC CURRENTS IN CHROMAFFIN CELLS AT HYPERPOLARIZED POTENTIALS . ((P. Mollard, E.P. Seward and M.C. Nowycky.)) Dept. Anat. & Neurobiol., Med.Coll.Penn., Philadel. PA 19129.

Neuronal nicotinic receptors (nAChR) are weakly permeant to Ca. Using plasma membrane capacitance measurements (C_m) in bovine chromaffin cells voltage clamped to -60 or -90 mV, we found that cationic currents carried by nAChR (I_{nic}) caused Ca-dependent jumps in C_m (ΔC_m). ΔC_m was high (123 ± 17 fF/nC) despite the small "fractional" Ca current flowing through nAChR (~3%). Measurements of averaged cytosolic Ca showed that I_{nic} caused a slowly rising and falling Ca_i. We investigated the role of internal Ca sequestering stores in I_{nic}-induced exocytosis by pretreating cells with thapsigargin (TG, 1 μM, 30 min) to block microsomal Ca-ATPases and deplete non-mitochondrial Ca stores. TG treatment alone did not trigger ΔC_m, but caused a substantial decrease in I_{nic}-induced ΔC_m (33 ± 9 fF/nC, n=17). Importantly, TG did not change I_{nic} triggered Ca signals, indicating that nAChR-induced Ca release from TG-sensitive stores must be localized and therefore not detected by global Ca measurements. This Ca-releasing mechanism is not recruited by voltage-gated Ca entry since TG did not alter the Ca signals and ΔC_m triggered by a series of depolarizing steps. nAChR activation of exocytosis adds to the growing list of Ca events that are restricted to highly localized areas of the cell.

Th-Pos165

DIVALENT CATION AND MG-ATP DEPENDENCE OF EXOCYTOSIS IN BOVINE CHROMAFFIN CELLS. ((N.I. Chernevskaya, E.P. Seward and M.C. Nowycky)) Dept. Anat. &Neurobiol. Med. Coll. Penn. Philadelphia, PA 19129. (Spon. by G. Oxford).

Stimulus-secretion coupling was studied under voltage-clamp with the capacitance detection technique. Ca influx through voltage-gated Ca channels predominantly elicited C_m jumps coupled to periods of Ca entry. Barium (Ba) influx elicited stimulus-decoupled secretion, characterized by slow (20-40 fF/sec), prolonged C_m increases that outlasted stimulating pulse trains by 10-50 sec. When the pipette solution contained 1 mM Ba, C_m increased at the same slow rate until several pF were added to the plasma membrane. Even after Ba-induced exocytosis was exhausted, Ca influx through channels elicited normal stimulus-coupled secretion for several more trials. This suggests that stimulus-coupled secretion operates through pathways that are not occluded by stimulus-decoupled exocytosis.
In 0 Mg-ATP, the first stimulating train in Ca caused stimulus-coupled exocytosis of ~200-500 fF. Subsequent trains caused no further C_m increases even if Ca current had not yet rundown. Under similar conditions, Ba influx through Ca channels substituted weakly for Ca, but did not elicit stimulus-decoupled exocytosis. Mg-ATP appears to be necessary for both stimulus-coupled and -decoupled pathways, with the exception of a small pool of vesicles that is already primed with Mg-ATP.

Th-Pos166

A PHORBOL ESTER INCREASES DEPOLARIZATION-EVOKED EXOCYTOSIS WHILE DECREASING CALCIUM CURRENT IN INDIVIDUAL BOVINE ADRENAL CHROMAFFIN CELLS ((K. D. Gillis and E. Neher)), Max-Planck-Institute for Biophysical Chemistry, 37077 Göttingen, Germany

Phorbol myristate acetate (PMA), an activator of protein kinase C (PKC), has been reported to increase catecholamine secretion from intact and permeabilized adrenal chromaffin cells. We have used membrane capacitance measurements to assay depolarization-evoked exocytosis (ΔC_m) while concurrently recording calcium currents (I_{Ca}) using the "perforated patch" variant of whole cell recording. In most cells, bath application of 50 nM PMA results within minutes in a several-fold enhancement of ΔC_ms despite a *reduction* in the amount of calcium influx (Q_{Ca}) during the pulse. Preliminary analysis suggests PMA increases the size of the "readily-releasable pool" (RRP) of vesicles. The inhibition of Q_{Ca} by PMA occurs through both a reduction in the peak amplitude of I_{Ca} (10-15% after a 5 minute exposure) and a prominent increase in the inactivation rate (e.g. 5 min. after exposure, I_{Ca} at the end of a 80 ms pulse is reduced 25-35% relative to control). 4a-phorbol didecanoate (50 nM), a phorbol ester which does not activate PKC, has no effect on I_{Ca} or ΔC_m. Since global increases in $[Ca]_i$ have also been previously shown to increase the size of the RRP, these experiments suggest activation of the phospholipase C cascade can augment secretion through both release of calcium from internal stores and activation of PKC.

Th-Pos167

CHANNEL CLUSTERING CAN LEAD TO TWO FUNCTIONALLY DISTINCT POOLS OF RELEASE-READY GRANULES IN BOVINE CHROMAFFIN CELLS ((J. Klingauf, R.H. Chow, and E. Neher)) MPI für biophysikal. Chemie, Abt. Membranbiophysik, Göttingen, Germany

We have inferred the mean $[Ca^{2+}]_i$ time course at the fusion sites during short step depolarizations from combined electrochemical and capacitance measurements, based on a previous characterization of the kinetics of Ca action at the fusion machinery (Chow et al., 1994, *PNAS*, in press). $[Ca^{2+}]_i$ rises to levels of about 5 µM during 20 ms-depolarizations, and then decays over 10's of msec's. To check whether the inferred time course is consistent with diffusion theory, we modeled buffered Ca diffusion in the vicinity of a channel pore. Peak $[Ca^{2+}]_i$ and the slow decay are well simulated when both vesicles and channels are assumed to be randomly distributed at mean interchannel distances of 200 to 400 nm. The initial rise in $[Ca^{2+}]_i$, however, is severely under-estimated. We furthermore explored how channel clustering influences this result. To do so, we assumed channel clusters of 300 nm diameter and a center to center separation of 2 µm, with vesicles located at random positions. This clustering leaves the peak of the predicted $[Ca^{2+}]_i$ as well as the decay time course unaffected. However, it accelerates the rising phase of predicted $[Ca^{2+}]_i$, because a small number ($\approx$ 10) of vesicles will be near or within channel clusters, where they will experience much higher $[Ca^{2+}]_i$ and are released quickly. But most of them (> 100) experience low $[Ca^{2+}]_i$ and are released slowly only after repetitive or longer pulses. These simulations suggest channel clustering, rather than channel-vesicle colocalization can account for observed patterns of secretion under a wide spectrum of stimuli intensity (see e.g. Horrigan & Bookman, Soc. Neorosci. Abstr., Vol.20, Part 1, p.59, 1994).

Th-Pos168

CALCIUM-ACTIVATED K CHANNELS IN PITUITARY NERVE TERMINALS AS A PROBE FOR MEMBRANE CALCIUM. ((G. Kilic and M. Lindau)) Abt. Molekulare Zellforschung, MPI f. Med. Forschung, D-69120 Heidelberg, Germany.

In pituitary nerve terminals during depolarization the Ca^{2+} concentration at the inner surface of the plasma membrane $[Ca^{2+}]_m$ may be significantly higher than the average Ca^{2+} concentration as measured by fura-2 [Rosenboom & Lindau (1994) *PNAS* 91:5267]. Fluctuation analysis of Ca^{2+}-activated K currents $I_{K(Ca)}$ may be used as a probe to estimate $[Ca^{2+}]_m$ [Roberts et al. (1990) *J.Neurosci.* 10:3664]. In whole terminal patch clamp experiments, internal perfusion of nerve terminals with free $[Ca^{2+}]$ buffered around 10 µM activated $I_{K(Ca)}$ at potentials above -25 mV. Following step depolarization, $I_{K(Ca)}$ activates slowly ($\tau \approx 100$ ms) and a corresponding corner frequency of 1-2 Hz is contained in the power spectra. In the potential range from -20 to +20 mV noise analysis provided single channel currents increasing from 1 to 4 pA, open probabilities from 0.1 to >0.9, and 20-100 channels/pF in agreement with single channel data [Wang et al. (1992) *J.Physiol.* 457:47; Bielefeldt & Jackson (1994) *Biophys.J.* 66: 1994]. During depolarization stimulating exocytosis and activation of $I_{K(Ca)}$, a mean $[Ca^{2+}]$ of 1-2 µM is indicated by fura-2 [Lindau et al. (1992) *Biophys.J.* 61:19]. However, at internal perfusion with $[Ca^{2+}]$ = 1-2 µM the channels did not activate. $[Ca^{2+}]_m$ during depolarization is thus much higher than the value indicated by fura-2. Fluctuation analysis of $I_{K(Ca)}$ may be used to follow the time course of $[Ca^{2+}]_m$ during depolarization.

SYNAPTIC TRANSMISSION

Th-Pos169

CALCIUM/CALMODULIN-DEPENDENT PROTEIN KINASE II AND CALYCULIN A ENHANCE $GABA_A$ RECEPTOR WHOLE-CELL CURRENTS. ((R.A. Wang, M. Kolaj, G. Cheng, D.A. Brickey and M. Randić)) Iowa State University, Ames, IA 50011 and Vollum Institute, Oregon Health Sciences University, Portland, Oregon 97201 (Spon. by J. Johansen)

γ-Aminobutyric acid type A ($GABA_A$) receptors are the receptors for the major inhibitory neurotransmitter in the central nervous system. Evidence exists for the regulation of $GABA_A$ receptor function by protein kinase A and protein kinase C. Phosphorylation of intracellular domains of $GABA_A$ receptor subunits by calcium/calmodulin-dependent protein kinase II (CaM-KII) has been recently demonstrated (J. Biol. Chem. 269:18111, 1994), suggesting a role for this kinase in modulating $GABA_A$ receptor function *in vivo*. Here we report that in acutely isolated rat spinal dorsal horn (DH) neurons, intracellularly applied the α-subunit of CaM-KII increased the amplitude of GABA (5-20µM)- and muscimol (2-5µM)-activated currents (GABA: to 169.6 ± 9.4% of control, n=13; muscimol: to 150.6 ± 6.3%, n=4) recorded with the whole-cell patch-clamp technique. Heat-inactivated CaM-KII (n=7) did not alter the GABA responses. In perforated patch recordings calyculin A (100nM), an inhibitor of serine/threonine protein phosphatases-1 and 2A, also enhanced the GABA responses. In addition, pharmacologically isolated $GABA_A$-mediated inhibitory postsynaptic potentials recorded from the rat hippocampal CA1 neurons were enhanced by CaM-KII. These results indicate that the function of postsynaptic $GABA_A$ receptors of DH neurons can be regulated by the activity of CaM-KII and that this regulation may contribute to control excitability of spinal DH neurons and plasticity of synaptic transmission. (Supported by NS-26352 and IBN-9209462).

Th-Pos170

The Single Domain/Bound Calcium Hypothesis of Transmitter Release and Facilitation

R. Bertram*, A. Sherman*, E. Stanley†, *MRB NIDDK, †SSM NINDS, NIH Bethesda, MD.

The finding that transmitter release can be gated during the opening of individual Ca channels suggests that the release site can be activated by the Ca domain under a single channel [Neuron 11:1007]. We have used this observation as the basis of a model of transmitter release in which secretion is dominated by single domains. Synaptic dynamics are governed by the kinetics of Ca binding and unbinding from release sites, not Ca diffusion. We assume four independent binding sites with kinetics graded from slow, high affinity to fast, low affinity. Values were derived from steps in the frequency-dependence of fast facilitation [Neurosci. 6:782]. This model can account for key features of release, including cooperativity with respect to external Ca, invariance of the time course of release evoked by successive action potentials, fast facilitation, and the above frequency-dependent steps. Facilitation occurs when an action potential invades a terminal with one or more ions remaining bound to the release sites. Residual free Ca is not necessary for this mechanism, but, if present, would enhance facilitation by binding to high-affinity sites between pulses.

Th-Pos171

CALCIUM RECOVERY AFTER DEPOLARIZATION IN A SYNAPTIC TERMINAL. ((D. Zenisek and G. Matthews)) Dept. Neurobiology, SUNY, Stony Brook, NY 11794

Changes in intracellular calcium within the synaptic terminals of retinal bipolar cells were investigated using the calcium indicator calcium green-1. Calcium green-1 and exogenous buffers were introduced by dialysis via a whole-cell patch pipette. Presynaptic calcium current was activated by brief depolarizing pulses from -60 to -20 mV, while fluorescence changes were monitored using an intensified ccd camera operating at 30 frames per second. The average fluorescence over an area of interest encompassing the synaptic terminal was used as an index of temporal changes in calcium concentration. Brief depolarization elicited a step increase in calcium-green fluorescence, which returned to baseline with two components of decay (see Fig.). The fast component (with an exponential time constant ≈ 50 ms) was saturated by depolarizing pulses longer than 100 msec, and was only present when EGTA was included in the recording solution. When EGTA was omitted or replaced with BAPTA, the fast time component was absent. The fast component can be explained by the rapid redistribution of calcium between the two exogenously added calcium buffers, calcium green-1 and EGTA. In addition to the fast component, a slower component of fluorescence decay was observed (see Fig.). The time constant of this component was dependent on exogenous buffer concentration. Higher concentrations of EGTA and BAPTA prolonged the decay. (Supported by NIH grant EY03821.)

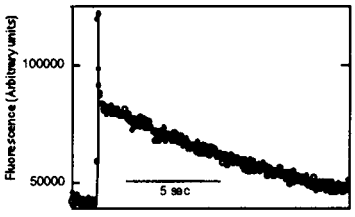

Th-Pos172

MILLISECOND SYNAPTIC AND SPIKE-INDUCED CALCIUM DYNAMICS IMAGED IN DENDRITIC SPINES WITH TWO-PHOTON LASER SCANNING MICROSCOPY. ((R. Yuste and W. Denk)) Biological Computation Research Dept., AT&T Bell Laboratories, Murray Hill, NJ 07974.

Dendritic spines are of considerable interest because of their potential role as functional compartments for information processing in the nervous system. Optical studies of the calcium dynamics of spines in brain slices have been hampered by their small size (1 μm^3) and by strong scattering of light by brain tissue. We have taken advantage of the improved tissue penetration provided by two-photon excitation of visible fluorophores with infrared light (Denk et al., Science 248: 73-76, 1990) to image calcium concentration in spines from CA1 pyramidal neurons in slices of rat hippocampus. Cells were filled with the calcium indicators Calcium Green 1 or 5N (250 μM), using whole-cell perfusion. Laser scanning was performed using a modified confocal microscope with a mode locked Ti:Saphire laser (λ≈850 nm) as the excitation source.

In response to single action potentials, initiated at the soma, the $[Ca^{2+}]_i$ rose in spines and dendritic shafts within a few msec and decayed as fast as 16 msec in spines. In contrast, focal subthreshold synaptic stimulation produced localized calcium accumulations, sometimes limited to individual spines. These accumulations were reversibly abolished by postsynaptic blockers (APV and CNQX). We also observed stochastic failures of synaptically induced $[Ca^{2+}]_i$ increases. Preliminary results suggest a nonlinear interaction between synaptic stimulation and postsynaptic action potentials. (Supported by the ONR)

Th-Pos173

Ca^{++}-PERMEABLE AMPA RECEPTORS MEDIATE AUDITORY NERVE SYNAPTIC TRANSMISSION. ((T.S. Otis, I.M. Raman, & L.O. Trussell)) Dept. of Neurophysiology, University of Wisconsin Medical School, Madison WI, 53706.

A rapidly desensitizing, outwardly rectifying, glutamate receptor of the AMPA subtype is present at high density on neurons of the chick cochlear nucleus (nucleus magnocellularis or NM). We measured the Ca^{++} permeability of NM AMPA receptors in response to exogenous glutamate applications or to synaptically released transmitter by analyzing reversal potentials (E_{rev}) in the presence of different extracellular cation activities. Fast-flow glutamate application to patches excised from acutely isolated neurons and subsequent fitting of E_{rev} vs. Ca^{++} activity with the constant-field equation uncovered a $P_{Ca^{++}}/P_{Cs^+}$ of 3.3, and a $P_{Ca^{++}}/P_{Na^+}$ of 5. Other ionic substitutions allowed us to characterize a permeability sequence of $Ca^{++} > Mg^{++} > Cs^+ > K^+ > Na^+$, and to estimate that Ca^{++} accounts for ~18% of AMPA receptor current at -60 mV. Using a brain slice preparation, AMPA receptor-mediated synaptic currents were isolated by inclusion of 50 μM AP5 and 50 μM bicuculline in the bath; the remaining synaptic current is abolished by 10 μM CNQX. We took advantage of the calyceal synapses made by VIIIth nerve endings onto NM somata to change extracellular solution at the synapse with a pressure pipette while examining synaptic currents evoked by single auditory nerve fiber stimulation. Control experiments with 300 mM sucrose/low Na^+ solutions showed large negative shifts (-16 to -30 mV) in E_{rev} of evoked synaptic currents, demonstrating that extracellular solution at the synaptic receptors could be altered. By contrast with the low Na^+ data, application of 110 mM $[Ca^{++}]_o$ solution shifted E_{rev} for the evoked synaptic current in the positive direction (11.4±2.8 mV, mean ± SD, n=4). In summary, signal transmission between the auditory nerve and cochlear nucleus uses Ca^{++}-permeable AMPA receptors. Based on the volume of spherical NM neurons and the large quantal content inputs, the increase in *total* cytosolic $[Ca^{++}]$ imposed by a single VIIIth nerve input is predicted to be ~4 μM. Moreover, Ca^{++}-activated ionic currents and second messenger processes in NM neurons may be exposed to high-frequency Ca^{++} dynamics with activity-dependent temporal patterns.

Th-Pos174

MECHANISMS MEDIATING STRETCH-INDUCED DELAYED DEPOLARIZATION. ((S.J. Tavalin, E.F. Ellis, and L.S. Satin)) Department of Pharmacology and Toxicology, Medical College of Virginia, Richmond, VA 23298.

We have previously shown that mechanical deformation of cultured cortical neurons leads to a delayed depolarization of their resting membrane potential that can last for hours. This stretch-induced delayed depolarization, which we call SIDD requires activation of NMDA receptors and Ca^{2+} influx for its induction. In order to test whether SIDD is due to alterations in membrane conductances, neonatal cortical neurons were grown in culture (day 12- 16) on a silastic membrane substrate that could be deformed by a single 50 ms pressure pulse of varying amplitude (5.7 mm maximum deformation). Cells were then incubated at 37° C for 1 hour. Resting membrane potentials and input resistances were measured using standard whole-cell patch clamp methods. Cortical neurons subjected to injury were significantly depolarized as compared to controls (-48.2 ± 3.8 mV vs. -60.8 ± 1.9 mV, n=8, $p < 0.05$) when pipettes contained 140 mM K-aspartate. No significant change in input resistance was observed (292 ± 33 MΩ vs. 313 ±38 MΩ). The magnitude of the depolarization was not significantly altered by dialyzing the cells with 140 mM KCl instead of K-aspartate (-43.6 ± 2.4 mV, n=8 vs. -57.0 ± 3.6 mV, n=7). This suggests that chloride ions did not contribute to the observed depolarization. Acute application of TTX (1 μM) or Ca-free external failed to repolarize neurons once they were depolarized by stretch, suggesting that tonic Na or Ca channel activity was not required for SIDD. It is also unlikely that SIDD requires tonic synaptic activation. Since there was no significant alteration of membrane conductance in stretched cells,we tested whether SIDD could result from inhibition of an electrogenic Na-K-ATPase. Ouabain (1mM) application depolarized control cells to a significantly greater extent than stretched cells (ΔRMP 7.2 ± 1.2 mV, n=5 vs. 2.5 ± 1.7 mV, n=4, $p \leq 0.05$), as expected if the Na-K-ATPases of stretched cells were already inhibited.

Th-Pos175

SIGNAL PROPAGATION IN SQUID OPTIC LOBE AND UNDERLYING CHANNEL ACTIVITIES. ((M. Ichikawa, Y. Hanyu*, W.-S. D. Griggs, R. Williamson** and G. Matsumoto)) Electrotechnical Laboratory, Tsukuba 305, Japan. *PRESTO(JRDC) and Electrotechnical Laboratory, **The Marine Laboratory, Plymouse, UK.

Neural activities in squid (*Loligo* bleekeri) optic lobe slice were monitored by high resolution optical method with voltage sensitive dyes. Observations with high spatial resolution show that action potential can be evoked in optic fibers by electric stimulation and it subsequently propagates into the inside of the lobe. This action potential induced the depolarization in outer granule cell layer and subsequently in inner granule cell layer, with delay of 5msec and 10msec respectively. Deletion of Ca^{2+} ions from external solution blocked this propagation. When optic fibers were stimulated by a train of pulses, the sustained depolarization was induced instead. This long-lasting depolarization was over 100msec in both layers. To study the mechanism of these neural activities, we tried to identify the channels in the synaptic part of the optic lobe. Channels in purified synaptosomes from the lobe were reconstituted in planar lipid bilayer and there single channel activities were monitored by voltage clamp method. Specific potassium and chloride channels were found. The kinetics of these channels and the relation to transmission properties in the lobe are discussed.

Th-Pos176

EXCITATORY SYNAPTIC POTENTIALS IN THE GLOMERULAR TRIAD OF FROG OLFACTORY BULB. ((O. Belluzzi, R. Bardoni and P.C. Magherini)) Dip. Scienze Biomediche, Sez. Fisiologia, Via Campi 287, 41100 Modena, Italy. (Spon. by O. Sacchi)

Whole-cell patch clamp recording techniques were applied to periglomerular (PG) and mitral/tufted (MT) cells in slices of frog olfactory bulb (OB) preparation to study the nature and pharmacology of post-synaptic responses to electrical stimulation of either the olfactory nerve (ON) or lateral and medial olfactory tract (LOT and MOT). Finely graded, prolonged (200-300 ms) depolarizing responses were observed in virtually all PG cells upon ON stimulation. The response was monophasic and no delayed hyperpolarisation were observed. The EPSP evoked in PG and MT cells by ON stimulation was blocked by the glutamate (Glu) receptor antagonist kynurenic acid. In both cell types post-synaptic potentials had a slow component, sensitive to the NMDA receptor antagonist AP5, and a fast component sensitive to the non-NMDA receptor antagonist CNQX. The co-application of the two drugs completely abolished any post-synaptic response. Fast and slow components had on average similar amplitudes. About 5% of PG cells could be synaptically activated by antidromic stimulation of LOT and MOT. The excitatory synaptic potentials had amplitude and duration comparable to that obtained by ON stimulation but were much less gradable.The block of NMDA receptors with AP5 abolished most of the post-synaptic depolarization evoked in PG cells by antidromic stimulation of MT cells; the small fast residual component was blocked by CNQX. These results suggest that Glu is the only excitatory neurotransmitter in the synaptic triad between ON, MT cells and PG cells, and that slow NMDA and fast non-NMDA component can be separated in post-synaptic potentials. However, whereas the two components have similar amplitudes in the axo-dendritic synapses, there is a clear dominance of the slow NMDA component in the dendro-dendritic synapse.

Th-Pos177

ELECTRICAL OSCILLATIONS OCCUR IN THE BASAL MEMBRANES OF ELECTRORECEPTIVE AMPULLARY EPITHELIUM FROM SKATES. ((Jin Lu and Harvey M. Fishman)) Dept. of Physiology & Biophysics, Univ. of Texas Medical Branch Galveston, TX 77555-0641

Steady, spontaneous oscillations (1 nA p-p) occur in the current through the voltage clamped epithelium of ampullary organs (canal,ampulla and nerve) isolated from skates (*Raja*). Spectral analysis showed that energy in these oscillations is confined to a narrow band (3 Hz) about a fundamental frequency (32 Hz @ 20°C) and in harmonics. The frequency of oscillations was temperature (T) dependent (increased from 21 to 33 Hz for increases in T from 13°C to 21°C). Addition of 0.5 μM TTX to the basal side of the ampullary epithelium eliminated afferent nerve activity but had no effect on the epithelial oscillations, indicating that the oscillations are not generated or induced by afferent nerve activity. Adding nitrendipine (2 μM) to the solution bathing the basal side of the ampullary epithelium abolished the oscillations within minutes, but the steady state negative conductance (NC) in the apical membranes (Lu and Fishman, BJ, 64:219, 1994) remained for 20-60 min. Perfusion of the apical side with saline + nitrendipine (50 μM) eliminated the NC within 20 min and had no effect on the spontaneous oscillations for > 1 hr. The rapid elimination of spontaneous oscillations from the basal side without an immediate effect on the apical NC indicates that the oscillations are generated in the basal membranes of the ampullary epithelium. Further, after elimination of spontaneous oscillations by 2 mM TEA and other blockers, postsynaptic potentials were eliminated or greatly reduced for voltage clamps of the epithelium of up to 500 μV. These results suggest that the spontaneous oscillation plays an essential role in transmitter release from presynaptic basal membranes of epithelial receptor cells. [Supported by ONR Grant N00014-90-J-1137]

Th-Pos178

A ROLE FOR BK CHANNELS IN CENTRAL NEURONAL SYNAPTIC TRANSMISSION. ((D.J. Post-Munson, C.G. Boissard, J.T. Lum-Ragan, M.C. McKay, S.I. Dworetzky and V.K. Gribkoff)) CNS Drug Discovery, Dept. 405, Bristol-Myers Squibb Co., Wallingford, CT 06492

Large-conductance Ca^{2+}-activated K^+ channels (BK channels) appear to be involved in the regulation of membrane repolarization and stimulus-secretion coupling in a variety of excitable cells. The present study used recently developed pharmacological tools to examine the involvement of BK channels in the regulation of central synaptic transmission. BK channels have been identified in primary cultures of rat hippocampal neurons and the BK channel opener NS004 increased the single channel P_o. The specific BK channel blocker iberiotoxin (IBTX) decreased whole-cell outward currents in these cells. Excitatory postsynaptic currents (EPSCs) recorded in the whole-cell patch clamp configuration from tetrodotoxin (TTX)-treated cultured neurons were unchanged (in frequency and total current) by NS004; however, NS004 substantially decreased EPSC frequency and total current in untreated cells. Extracellular field potentials were recorded from rat hippocampal slices; the slope of orthodromically-evoked excitatory postsynaptic potentials (EPSPs) and the population spike amplitude were decreased in a concentration-dependent manner by NS004. IBTX increased EPSP slope and population spike amplitude when applied alone and greatly reduced the effect of NS004 when applied with the opener. Population spikes elicited via antidromic stimulation were much less sensitive to the actions of NS004 and IBTX. Taken together, these data suggest that NS004 exerts its effects presynaptically, and therefore BK channels may be important regulators of central neurotransmission.

Th-Pos179

Ion Channel Blockers Restore Synaptic Plasticity in *shaker* and *dunce* Larval Motor End-Plates. Ricardo Delgado, Ramón Latorre and Pedro Labarca. Centro de Estudios Científicos de Santiago and Dpto. de Biología, Fac. de Ciencias, Universidad de Chile.

Nerve-evoked end-plate currents (neepcs) were recorded from larval neuromuscular junction of *Drosophila* on wild type (*Canton-S*), *Shaker* and *dunce* mutants, using the two electrode voltage-clamp. *Shaker* (*Shaker*$^{KS-133}$, *Shaker*$^{KS-102}$,β^3*Shaker*^{5}) lack the A-type currents and exhibit prolonged action potentials. *dunce* are defficient in a form of phosphodiesterase and exhibit elevated levels of cAMP. In *Canton-S* motor end-plates, a tetanic stimulation gave place to facilitation and post-tetanic potentiation (PTP). In *Shaker*, larval motor end-plates exhibited facilitation, but lacked PTP. Furthermore, exposure of *Canton-S* motor end-plates to 4-aminopyridine (0.5-2 mM), a blocker of A-type currents, abolished PTP but had no effect on facilitation. Thus, a lost of *Shaker* channels affects specifically PTP at the *Drosophila* larval motor end-plates. Micromolar concentration of the calcium channel blockers Co^{2+} and Cd^{2+}, and millimolar Mg^{2+}, were effective in restoring PTP in *Shaker* larval neuromuscular junctions. *Dunce* (*dunce*^{1}, *dunce*^{M14}) end-plates did not undergo facilitation and PTP in response to tetanic stimuli. Furthermore, exposure of *Canton-S* end plates to 8Br-cAMP abolished facilitation and PTP. PTP could be restored in *dunce* by the K^+-channel blockers 3,4 diaminopyridine (3,4 DAP) and tetraethylammonium (TEA) at micromolar concentrations and over a narrow range of concentrations. Moreover, 3,4 DAP and TEA restored plasticity in normal motor end-plates in wich facilitation and PTP had been abolished by exposure to 8Br-cAMP. The above observations suggest that a specific K^+-selective conductance might be relevant to the lack of facilitation and PTP at the *dunce* neuromuscular synapse. It remains to be established whether or not the synaptic anomalies found in *Shaker* and *dunce* larval motor end-plates are present in adults end-plates and in the nervous system. (Supported by HFSP and FONDECYT 1940169)

Th-Pos180

PHOTOACTIVATABLE PRECURSORS OF NMDA AND KAINATE. NEUROTRANSMITTER RELEASE IN THE MICROSECOND TIME REGION. ((K.R. Gee,[†] L. Niu,[‡] K. Schaper,[‡†] G.P. Hess[‡†])) [†]*Molecular Probes, Inc., Eugene, OR 97402.* [‡]*Division of Biochemistry, Molecular & Cell Biology, Cornell University, Ithaca, NY 14853.* (Spon. by R.P. Haugland)

We report the synthesis and biological characterization of α-carboxy-2-nitrobenzyl (CNB)-caged versions (**1**,**2**) of the exogenous neurotransmitters *N*-methyl-D-aspartic acid (NMDA) and kainic acid, the prototypical agonists for two of the major ionotropic glutamate receptor subtypes in the central nervous system. Photolysis in the near UV region of **1** & **2** at pH 6.8 provides free neurotransmitter with first-order rate constants of $3.2{*}10^4\ s^{-1}$ & $1.6{*}10^4\ s^{-1}$, respectively. These rate constants correspond to half lives for the production of NMDA and kainate of 22 and 43 μs, respectively. The photolysis rates appear to be maximal at pH 5.5, dropping off at pH < 5.5 and pH > 9. In cultured neonatal rat hippocampal neurons at pH 7.4, **1** does not elicit an agonist response. However, it is somewhat inhibitory in that it blocks some of the response to free NMDA, as measured by whole-cell patch-clamp recording of the associated transmembrane ion current. The degree of inhibition appears to be a function of the preincubation time. For example, when cells are preincubated with 300 μM **1** for 5 s, the response to 300 μM NMDA is inhibited by 40%; the response is inhibited by ≤10% without the preincubation period. Thus it appears that **1** will not be as useful for rapid kinetic investigations of the NMDA receptor. Cell studies with **2** show that it is neither an agonist nor an inhibitor at the kainate receptor. Whereas 50 μM free kainate slowly induces a membrane current of 30-40 picoamps (pA), photolysis of a neuron bathed in 750 μM **2** rapidly (ms) generates about 100 μM free kainate, which induces a 100 pA current. Photolysis quantum yields of **1** and **2** are ca. 0.4. Thus it appears that **2** will be useful for kinetic and mechanistic studies of activation of the kainate receptor.

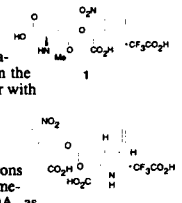

†Supported by a postdoctoral fellowship from Verband der Chemischen Industrie. ‡Supported by NIH grant GM 04892-38.

Th-Pos181

DETECTION OF QUANTAL RELEASE OF CATECHOLAMINES FROM DEVELOPING NEURONS IN CULTURE BY AMPEROMETRY. ((Z. Zhou and S. Misler)) Washington Univ. Med. Ctr., St. Louis, MO 63110

Amperometry has been used for electrochemical detection of quantal release of catecholamine (CA) from large (250 nm diam) granules in chromaffin cells. Application of this technique to CA-releasing nerve terminals containing smaller (50-90 nm diam) vesicles might permit monitoring of release independent of the function of post-synaptic receptors. Using improved-sensitivity polyethethylene coated carbon fiber electrodes (pCFEs), we have detected quantal CA release from developing nerve terminals abutting on somas of neonatal superior cervical ganglion neurons (SCGNs) cultured for 3-10 days. pCFEs were positioned into clefts between somas of SCGNs in clumps. Application of 60 mM K^+ Ringer (see figure) or crude latrotoxin evoked barrages of small amplitude (2-20pA), short duration (0.5-3ms) amperometric spikes (ASs), only when the pCFE was held at a voltage promoting CA oxidation. The charge per AS averaged 12.4 fC, corresponding to $4x10^4$ molecules (or ~ 1% that of a chromaffin granule). During the first 6 days in culture, the rate of detection of "hot spots" of release increases with culture age. Concurrent increases in punctate fluorescence staining for the synaptic vesicle antigen SV-2, at the perimeter of somas, confirms the proliferation of nerve terminals. (Support: AHA).

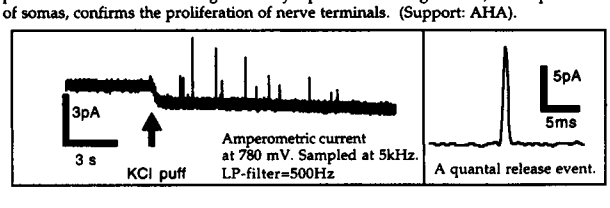

Th-Pos182

INHIBITION OF TWO NON-INACTIVATING K+ CHANNELS BY METABOTROPIC GLUTAMATE RECEPTORS IN CA3 PYRAMIDAL NEURONS ((David M. Lovinger)) Dept. Mol. Physiol./Biophys., Vanderbilt Univ. Medical School, Nashville, TN 37232

Metabotropic glutamate receptors (mGluRs) are G-protein-coupled receptors for glutamate, a major CNS neurotransmitter. mGluR activation depolarizes neurons in many brain regions. Application of mGluR agonists to the hippocampal slice produces a slowly-activating depolarization of CA3 pyramidal neurons, and an increase in the frequency of occurrence of spontaneous synaptic potentials. Voltage-clamp recordings reveal that receptor activation produces an inward current associated with increased input resistance. mGluR-mediated inward current can also be observed in acutely isolated CA3 neurons (medium to large pyramidal neurons) prepared from 1-3 week old rat. In a subgroup of neurons, application of mGluR agonist (2μM quisqualate in the presence of the AMPA/kainate receptor antagonist DNQX, or 50μM t-ACPD alone) elicits an inward current at membrane potentials of -50 to -60 mV. This current is accompanied by increased input resistance and reverses polarity near E_K. In another subgroup of neurons, mGluR agonists elicit an inward current at -30 mV but relatively little current at -60 mV. In these neurons, hyperpolarization from -30 to -60 mV elicits a time-dependent inward relaxation that reverses polarity near E_K. These observations suggest the presence of the M-type K+ current. Application of 2mM $BaCl_2$ at -30 mV elicits an inward current and blocks the time-dependent relaxation at -60 mV. mGluR agonists also reduce the amplitude of the relaxation component of current. The effect of mGluR agonists is occluded in the presence of $BaCl_2$. These observations suggest that quisqualate-sensitive mGluRs can inhibit a "leak" K+ current as well as the M-current in CA3 pyramidal neurons. Supported by NS 30470.

Th-Pos183

Evidence that *comatose*, a gene required for synaptic transmission, encodes *Drosophila* NSF. ((Richard W. Ordway, Leo Pallanck, and Barry Ganetzky)). Laboratory of Genetics, University of Wisconsin, Madison WI 53706.

To initiate a genetic analysis of NSF and SNAP secretory protein function in neurotransmitter release, we have previously cloned and characterized *Drosophila* genes encoding homologs of these proteins [Ordway, et al. Proc. Nat. Acad. Sci. USA 91: 5715 (1994)]. Several candidate mutations for Drosophila NSF (dNSF) or SNAP (dSNAP) were identified from among pre-existing mutations on the basis that their recessive phenotypes (e.g. lethality) were uncovered when the mutations were made heterozygous with dNSF or dSNAP deletions. For dNSF, one of the candidate mutations is *comatose*, which causes a temperature-sensitive paralytic phenotype. This is of particular interest since *comatose* was previously found to exhibit a temperature-dependent defect in synaptic transmission [Siddiqi and Benzer, Proc. Nat. Acad. Sci. USA 73: 3253 (1976)]. Since dNSF and *comatose* could not be separated by extensive deletion mapping, molecular analysis was initiated to determine whether *comatose* mutations are in dNSF. cDNA clones of dNSF from two different alleles of *comatose*, as well as from wild type flies, were obtained by RT-PCR and sequenced. dNSF in both *comatose* alleles contained point mutations leading to amino acid changes, while wild type flies lacked any such polymorphism. These results provide strong evidence that mutations in dNSF are responsible for the *comatose* phenotype and that NSF functions in synaptic transmission.

MITOCHONDRIA

Th-Pos184

RELATIONSHIP BETWEEN Mg^{2+} CONTENT AND SUBSTRATE UTILIZATION OF RAT LIVER MITOCHONDRIA ((A. Panov, A. Scarpa)) Dept. Physiol. & Biophys., CWRU, Cleveland, OH 44106

Rat liver mitochondria (RLM) isolated in the presence of 1 mM EGTA and further purified using a percoll gradient display higher total and A23187-insensitive magnesium pools(37.5 ± 3.4 nmol/mg and 6.5 ± 0.2 nmol/mg RLM respectively), and lower content of Ca^{2+} (0.28 ± 0.05 nmol/mg), as compared with non-purified mitochondria. Mg^{2+} depletion of RLM affected different states of mitochondrial respiration in a substrate-dependent fashion. The table below shows the effects of A23187 and Ruthenium Red (RR) on various substrates oxidation by RLM. Data are expressed as % of control activities of RLM respiring in a medium containing 125 mM KCl, 20 mM MOPS, 2 mM Pi, 1 mM EGTA, pH 7.2.

	1 μM A23187			A23187+RR 5 μM		
Substrate	State-4	State-3	Uncoupled	State-4	State-3	Uncoupled
Succinate 10 mM+Rotenone	127%	34%	80%	302%	67%	70%
Glutam.10 mM+Mal. 2mM	100%	73%	77%	397%	80%	75%
2-Oxogl.10 mM+Mal.2 mM	45%	10%	6%	-	-	-

Unlike RR, 10 μM La^{3+} added after A23187 had no effect on respiration of RLM. A23187 or A23187+RR (La^{3+}) do not stimulate mitochondrial swelling under these conditions. However, in 100 mM KNO_3 medium La^{3+} added after A23187 to deenergized RLM induced a dramatic increase in K^+ permeability, whereas RR was much less effective. The effects of La^{3+} and RR on the A23187 treated RLM could be explained either by their binding to some Mg^{2+}-dependent specific sites on the inner membrane of mitochondria, or by changing the properties of A23187. It is concluded that the substrate specific uncoupling effect of A23187 is not caused by calcium cycling (P.W. Reed, H.A. Lardy, J. Biol. Chem., 247 (1972) 6970) but is directly related to Mg^{2+} depletion of the RLM. *Supported by the NIH grant 18708.*

Th-Pos185

OXIDATIVE STRESS-INDUCED MITOCHONDRIAL PERMEABILITY TRANSITION IN RAT HEPATOCYTES: ROLE OF MITOCHONDRIAL NAD(P)H, Ca^{2+} AND REACTIVE OXYGEN SPECIES (A.-L. Nieminen, A.K. Saylor, S.A. Tesfai, B. Herman and J.J. Lemasters) Dept. of Cell Biology & Anatomy, University of North Carolina, Chapel Hill, NC 27599-7090.

Previously, we showed that the oxidant chemical, *tert*-butylhydroperoxide (*t*-BuOOH), induces a mitochondrial permeability transition (MPT) in intact hepatocytes leading to lethal cell injury. Here, we attempted to visualize the critical events preceding the MPT induced by *t*-BuOOH. Mitochondrial NAD(P)H was measured using UV/visible laser scanning confocal microscopy by autofluorescence excited at 351 nm. Mitochondrial Ca^{2+} was measured by Rhod-2. Mitochondrial membrane potential, reactive oxygen species (ROS), MPT and cell viability were monitored by rhodamine 123, 2',7'-dichlorofluorescin, calcein and propidium iodide uptake, respectively. *t*-BuOOH caused a 50% oxidation of NAD(P)H in 5 minutes. Oxidation was followed closely by generation of mitochondrial ROS. Subsequently, mitochondrial Ca^{2+} increased, and mitochondrial depolarized with onset of the MPT. After depolarization, Ca^{2+} gradually leaked from mitochondria. Trifluoperazine partially inhibited NAD(P)H oxidation, completely prevented radical formation, inhibited the MPT, and preserved cellular ATP levels and viability. Desferal, an iron chelator, also prevented NAD(P)H oxidation, formation of mitochondrial ROS, and cell death. In conclusion, NAD(P)H oxidation, formation of ROS and increased mitochondrial Ca^{2+} may be critical events leading to the MPT during oxidative injury to hepatocytes.

Th-Pos186

THE PERMEABILITY OF MITOCHONDRIAL OUTER MEMBRANE IS REGULATED BY NADH, NADPH AND ONCOTIC PRESSURE. ((A. Lee, M.H. Heda, M. Colombini)) Dept. Zoology, Univ. Maryland, College Park, MD 20742.

We monitored the permeability of the mitochondrial outer membrane to ADP using a method, we recently developed, that allows us to do this with intact, respiring mitochondria. NADH has previously been shown to decrease the permeability of the mitochondrial outer membrane to ADP by 6-fold. The action of NADH has a K_D of 96 μM. NADPH can also reduce the permeability of the outer membrane but with a K_D of 640 μM. The maximal decrease in permeability caused by NADPH is the same as that induced by NADH indicating that they act through the same mechanism but NADPH has a much lower affinity. The experiments were performed in the presence of 0.1 mM EGTA so that no significant oxidation of these cofactors would occur. Thus, NADH may be the physiological regulator of the permeability pathway. This pathway is probably VDAC (mitochondrial porin) since it is the major pathway through the outer membrane and NADH has been shown to increase its voltage dependence. The polymers, dextran and polyethylene glycol (PEG), have been shown to favor VDAC closure. 15% solutions of dextran (40 k) and PEG (20 k) decreased the outer membrane permeability to ADP by a factor of 4. Therefore, oncotic pressure might also regulate the function of mitochondria in situ. (Supported by ONR grant # N00014-90-J-1024)

Th-Pos187

ADP REGENERATING ENZYME SYSTEMS IN MITOCHONDRIA OF THE GUINEA PIG MYOMETRIUM AND HEART. ((J.F. Clark, A.V. Kuznetsov, and G.K. Radda)) Dept. of Biochemistry, South Parks Rd. University of Oxford, OX1 3QU, England.

ADP stimulates respiration in coupled mitochondria. Enzymes that produce ADP in proximity to the mitochondria will therefore stimulate respiration. Hexokinase (HK), Adenylate Kinase (AK) and Mitochondrial Creatine Kinase (Mi-CK) are all such enzymes which are associated with the mitochondria. These ADP generating enzymes may consequently play a role in stimulating or modulating oxidative phosphorylation. We measured the respiratory responses and enzyme activities from mitochondria isolated from the gravid guinea pig uterus and heart. The ability of each enzyme system to generate ADP and stimulate respiration was examined. The apparent K_m for ADP was not significantly different between the two groups (9.6 ± 0.9 and 5.1 ± 1 respectively). HK and AK activities were significantly greater in the uterine mitochondria compared with the heart while the CK activity was less. The ability of the enzymes to generate ADP was correlated to the activity assayed, but interestingly in the uterine mitochondria, the AK present was sufficient to stimulate maximal respiration. There was also twice the activity of HK present in the uterine mitochondria. These data are consistent with the high glycolytic capacity found in smooth muscle. It is concluded that uterine mitochondria are capable of utilising HK and AK to enhance local [ADP]. These enzymes may aid in the mitochondrial responses to energetic demands.

Th-Pos188

THE SODIUM-CALCIUM ANTIPORT OF HEART MITOCHONDRIA IS NOT ELECTRONEUTRAL. ((D.W. Jung, K. Baysal & G. P. Brierley)) Dept. of Medical Biochemistry, The Ohio State University, Columbus, OH 43210 .

Heart mitochondria contain a nNa^+/Ca^{2+} antiport that participates in the regulation of matrix $[Ca^{2+}]$. Based largely on a single study (Brand, M.D. (1985) *Biochem. J.* 229:161-166), there has been a consensus that this antiport promotes the electroneutral exchange of $2Na^+$ for one Ca^{2+}. We have re-examined Brand's protocol using fluorescent probes instead of isotopes to monitor matrix pH and $[Ca^{2+}]$. Respiring heart mitochondria, suspended in KCl and treated with ruthenium red to block Ca^{2+} influx, extrude Ca^{2+} and establish a large $[Ca^{2+}]_{out}$:$[Ca^{2+}]_{matrix}$ gradient. The extrusion of Ca^{2+} under these conditions is Na-dependent and diltiazem-sensitive and can be attributed to the nNa^+/Ca^{2+} antiport. Addition of nigericin increases the membrane potential ($\Delta\Psi$) and decreases ΔpH to 0.1 or less, but has no significant effect on the magnitude of the $[Ca^{2+}]$ gradient. Under these conditions a gradient maintained by electroneutral $2Na^+/Ca^{2+}$ antiport should be abolished because the rapid mitochondrial Na^+/H^+ antiport keeps the $[Na^+]$ gradient equivalent to the $[H^+]$ gradient. The $[Ca^{2+}]$ gradient is abolished, however, when an uncoupler is added to dissipate $\Delta\Psi$ or when the exogenous electroneutral antiport BrA23187 is added. In addition, $[Ca^{2+}]$ influx via the nNa^+/Ca^{2+} antiport in nonrespiring mitochondria is enhanced when $\Delta\Psi$ is abolished. These results are consistent with an electrophoretic antiport that can respond to $\Delta\Psi$, with an exchange such as $3Na^+/Ca^{2+}$, but not with an electroneutral antiport. (Supported by USPHS Grant HL09364)

Th-Pos189

THE MITOCHONDRIAL UNIPORTER IS SPECIFICALLY DESIGNED TO RESPOND TO PULSED $[Ca^{2+}]$

((G.C. Sparagna, K.K. Gunter, T.E. Gunter, and S-S. Sheu))
Univ. of Rochester Dept. of Biophysics, Rochester, NY 14642

We have exposed isolated rat liver mitochondria to *in vitro* pulses of Ca^{2+} similar to those observed in the cytosol of many types of cells *in vivo*. These Ca^{2+} pulses are produced in a cylindrical fluorescence cuvette using a computer-controlled automatic pipettor system in conjunction with a fluorescence spectrometer. Buffered Ca^{2+} and Ca^{2+}-buffer are injected independently into the medium within the cuvette so that the intensity, duration, shape, and periodicity of the pulses can be controlled.

We have studied the Ca^{2+} uptake properties of the mitochondrial calcium uniporter by producing single and multiple square wave pulses of $^{45}Ca^{2+}$. For example, we have found that the uniporter becomes activated by a first Ca^{2+} pulse which allows the mitochondria to take up much more calcium from two pulses than they would from a single pulse which is twice as wide. These and other studies lead us to believe that the calcium uniporter of liver mitochondria functions more efficiently in response to *calcium pulses* than to a rise in the steady state level of $[Ca^{2+}]$.

Gunter, T.E., K.K. Gunter, S.-S. Sheu, and C.E. Gavin, "Mitochondrial calcium transport: Physiological and pathological relevance." *Am. J. Physiol.* 267:(Cell Vol. 36) C313-C339 (1994)

Sparagna, G.C., K.K. Gunter and T.E. Gunter, "A system for producing and monitoring *in vitro* calcium pulses similar to those observed *in vivo*." *Anal. Biochem.* 219: 96-103 (1994).

(Supported by NIGMS Grant GM-35550 and NIDA Grant 27334)

Th-Pos190

INTRACELLULAR LOCALIZATION OF CALCIUM INDICATORS. ((E.L. Holmuhamedov, J.A. Bacon, J.D. Lechleiter[1], R.G. Ulrich)) Upjohn Laboratories, Kalamazoo, MI 49007 and [1] Department of Neuroscience, University of Virginia, Charlottesville, VA 22908.

Confocal imaging and dual-loading techniques were used to study the intracellular distribution of different cytosolic calcium indicators in 3T3-L1 and Chang Human Liver Cell (CHLC) Lines. Neutral dyes in esterified form (Calcium Green-1am, Fura-2am, Fluo-3am, Indo-1am) were observed to be uniformly distributed in the cytosol and nucleus. The positively charged dye, Rhod-2am, was distributed mostly within organelles (mitochondria) but was also observed in nucleoli. Distribution of a zwitterionic dye, Calcium Crimson-am, in cytosol mimicked the distribution of the neutral species. Stimulation of 3T3-L1 and CHLC with nucleotides was followed by similar changes in fluorescence for the neutral calcium dyes (Calcium Green-1am, Fura-2am, Fluo-3am, Indo-1am) and showed uniform transient and/or synchronous oscillations of fluorescence in the cytosol and nucleus. Nucleotide stimulation of 3T3-L1 cells loaded with Rhod-2am resulted in a marked increase in fluorescence which appeared to be associated with a re-distribution of either dye or Ca^{++} within the cell. Imaging of 3T3-L1 and CHLC cells dual-loaded with Calcium Green-1am and Rhod-2am revealed that changes in fluorescence of mitochondria and nucleoli (Rhod-2 fluorescence) had the same time-course as cytosolic calcium (Calcium Green-1 fluorescence). This study indicates that the subcellular distribution of the various calcium dyes is dependent, at least in part, on the net charge of the esterified and de-esterified forms.

Th-Pos191

FUNCTIONAL IDENTIFICATION OF THE FCCP-SENSITIVE Ca^{2+} STORE IN MOUSE CORTICAL ASTROCYTES. ((V.A.Golovina, and M.P.Blaustein)) Dept. of Physiol., Univ. of Maryland Med. Sch., Baltimore, MD 21201.

The influence of the protonophore, carbonyl cyanide p-trifluoromethoxy-phenylhydrazone (FCCP), on cytosolic ($[Ca^{2+}]_{cyt}$) and stored ($[Ca^{2+}]_{st}$) free Ca^{2+} concentrations was studied in cultured mouse cortical astrocytes. $[Ca^{2+}]_{cyt}$ and $[Ca^{2+}]_{st}$ were determined, respectively, by digital imaging of fura-2 and furaptra fluorescence. At rest, $[Ca^{2+}]_{cyt}$ was 0.11 ± 0.01 μM (mean ± SE; n = 159 cells) and $[Ca^{2+}]_{st}$ was 110 ± 60 μM (n = 38). FCCP (5 μM), which inhibits mitochondrial Ca^{2+} sequestration, decreased $[Ca^{2+}]_{st}$ by 10-20 μM and transiently increased $[Ca^{2+}]_{cyt}$ to 0.45 ± 0.03 μM (n = 47). The responses were observed in Ca^{2+}- and Na^+-free medium containing 50 μM EGTA, where both entry of extracellular Ca^{2+} and Ca^{2+} extrusion via the Na/Ca exchanger were inhibited. FCCP-evoked Ca^{2+} responses were unaltered when the ER Ca^{2+} stores were depleted by caffeine (10 mM) and a specific inhibitor of the ER Ca^{2+} ATPase, cyclopiazonic acid (CPA, 10 μM). Conversely, the CPA-induced transient increases in $[Ca^{2+}]_{cyt}$ (to 0.50 ± 0.02 μM, n = 50) were not attenuated in the presence of FCCP. These findings indicate that FCCP and CPA affect different Ca^{2+} stores, presumably mitochondria and ER, respectively. Dissipation of the plasmalemmal Na^+ gradient by inhibition of the Na^+ pump with 1 mM ouabain for 15 min caused only a small rise in resting $[Ca^{2+}]_{cyt}$ (to 0.20 ± 0.01 μM; n = 37), but augmented $[Ca^{2+}]_{st}$ by 20-50 μM (n = 18) and FCCP-induced $[Ca^{2+}]_{cyt}$ responses to 1.41 ± 0.08 μM (n = 26). This implies that the FCCP-sensitive (mitochondrial) Ca^{2+} store is influenced by the plasmalemmal Na^+ gradient.

ASSEMBLY OF SUPRAMOLECULAR STRUCTURES

Th-Pos192

NMR STRUCTRURAL STUDIES OF VPU IN BIOLOGICAL MEMBRANES. ((Francesca M. Marassi and Stanley J. Opella)) Department of Chemistry, University of Pennsylvania, Philadelphia, PA 19104, ((Ulrich Schubert and Klaus Strebel)) Laboratory of Molecular Microbiology, NIAID, NIH, 4/312 Bethesda, MD 20892.

Vpu (virus protein u) is an 81 residue membrane-associated, accessory protein specific to human immunodeficiency virus type I (HIV-1) which appears to have both amphipathic and hydrophobic helices. Recent studies have demonstrated that Vpu induces both the degradation of the virus receptor CD4, as well as the instability of MHC class I complexes in HIV-I infected cells. A second independent function of Vpu is the acceleration of virus particle release from infected cells. These functions are believed to allow the virus to spread more rapidly and thus, to enhance its pathogenicity. We have expressed Vpu as a maltose binding fusion protein in E. coli. Since the fusion protein is inert, its synthesis does not disturb the growth behavior of the cells. This allows large scale fermentation of bacteria in both rich and isotopically labeled minimal media, yielding milligram quantities of pure, non-labeled and isotopically-labeled Vpu. The structure and dynamics of Vpu are being determined in membrane environments by high resolution NMR spectrum. Multidimensional solution NMR studies are conducted in micelles while solid state NMR studies are carried out in lipid bilayer membranes.

Th-Pos193

HUMAN IMMUNODEFICIENCY VIRUS INFECTION DECREASES INTRACELLULAR pH ((A. Makutonina, T. G. Voss, C. D. Fermin, R. F. Garry, and C. H. Norris)) Departments of Microbiology and Immunology, Pathology and Pharmacology, Tulane School of Medicine. New Orleans, LA. 70112

Infection with several viruses, including myxoviruses and alphaviruses, leads to a change in intracellular pH (pH_i). The surface envelope glycoprotein (gp120, SU) of human immunodeficiency virus type-1 (HIV-1), the retrovirus that causes acquired immune deficiency syndrome (AIDS), has been shown to increase pH_i in astrocytes (Benos *et al.*, PNAS **91**:494, 1994) . This alteration in pH_i may contribute to neurological dysfunctions in AIDS patients. To determine whether HIV might also alter pH_i in other cell types, lymphoblastoid cells (HUT 78) were infected with HIV-1, and pH_i was monitored using the pH-sensitive fluorescent probe 2,7-biscarboxyethyl-5,6-carboxyfluorescein. HIV infection of lymphocytes resulted in a continuous decrease of pH_i from 7.23 (day 1 post-infection) to 6.10 (day 4) followed by restoration of pH_i to 7.15 at day 7, a value close to but still below normal. Studies with UV-inactivated HIV suggested that active virus replication was required to induce the alteration in pH_i. In HIV persistently-infected cells, pH_i was estimated to be 6.75 for HIV-1 strain IIIB and 7.00 for HIV-1 strain LA1. Studies with amiloride suggest that HIV-induced intracellular acidification in lymphocytes is due to dysfunction of the cellular Na^+/H^+ exchange system.

Th-Pos194

TMV REVISITED: FOUR LAYER DISK AGGREGATE. ((Balaji Bhyravbhatla and Donald L.D. Caspar)) Brandeis University, Waltham, MA-02254-9110

To understand the protein-protein and protein-RNA interactions which stabilize the mobile inner loop of the Tobacco Mosaic Virus coat protein (TMVP) we carried out structural studies of TMVP using cryo-crystallography. The crystals of the four layer disk aggregate were grown at room temperature in 0.2M $(NH_4)_2SO_4$, 0.1M Tris at pH 8.0 . 30% glycerol in the solvent was used as a cryo-protectant. At -155°C, the crystals diffract to 2.4Å resolution compared to 5 Å at room temperature. The initial phasing was obtained from the 2.8 Å resolution model of Ann Bloomer et.al.(Nature, 276, 1978). XPLOR program was used for model building and subsequent phase extension to 2.4 Å resolution. The electron density maps were improved by five cycles of symmetry averaging. The model refinement is in progress, the current R-factors are 24% to 2.4Å, and 18% to 4Å resolution. We will calculate a low resolution (30-6 Å) electron density map with improved phases and attempt to trace the mobile inner loop which does not contribute to the high resolution scattering and, therefore, is not visible in the high resolution electron density maps. Comparison of the refined structure of the four layer disk aggregate with the published virus structure should provide better insights into the stabilising effects of protein-RNA interactions on the virus structure.

Th-Pos195

CONTRACTION OF FILAMENTOUS PHAGE BY CHLOROFORM: A SIMPLE MODEL FOR UNDERSTANDING VIRUS UNCOATING ((A. K. Dunker and J. Oh)) Department of Biochemistry & Biophysics, Washington State University, Pullman, WA 99164

Contact of the fd filamentous phage with a chloroform/water interface leads to contraction to rod-shaped, I-form particles. Further contraction to spheroidal-shaped, S-form particles is associated with DNA release. The conformational changes leading to the release of the phage DNA involve interactions between the phage and an interface, and thus share key elements with viral uncoating. Therefore, a deeper understanding of the chloroform-induced contraction may provide insight into the more complex phenomenon of virus uncoating. Contraction is also induced by contact with the water/solvent interfaces of several other organic molecules that are unlike chloroform in structure, but are similar in being immiscible with water, but yet being somewhat polar. Completely nonpolar solvents such as chloroform fail to induce contraction, suggesting that the contraction is caused by the biophysical characteristics of the interface between water and an immiscible, but somewhat polar solvent, not by precise interactions between the phage and solvent molecules. Several chloroform-resistant mutants have been isolated. All such mutants isolated so far map to the major coat protein (pVIII), suggesting that interactions between pVIII and chloroform along the entire phage length is required. Putting these observations together leads to the proposal that displacement of water at the phage surface by chloroform (or other polar solvent) is the critical event required to induce contraction. Experiments are being devised to test the surface-water displacement hypothesis and to understand in detail just how such displacement could induce phage contraction and DNA release.

Th-Pos196

ROLE OF TARGET MEMBRANE SIALIC ACID IN THE FUSION ACTIVITY OF INFLUENZA VIRUS ((J. Ramalho-Santos[a], N. Düzgünes[b], D. Flasher[b], S. Nir[b] & M. C. Pedroso de Lima[b,c])) [a]Dep. of Zoology and [c]Dep. of Biochemistry, Univ. of Coimbra, Portugal; [b]Dep. of Microbiology, School of Dentistry, Univ. of the Pacific, San Francisco, CA 94115, U.S.A..

Cell surface sialic acid residues are considered to be the primary receptors for influenza virus. Initial binding of the virus is followed by endocytosis, and concomitant fusion of the viral envelope with the endosomal membrane upon acidification. To examine whether the cell membrane sialic acid is also involved in the membrane fusion reaction we have studied the fusion activity of influenza virus (A/PR/8/34) towards cultured CEM cells. Fusion was monitored by the dequenching of the fluorescent probe octadecylrhodamine (R18) incorporated in the viral envelope. Removal of sialic acid from the cell surface by neuraminidase resulted in drastic reduction in both viral binding and fusion. In contrast to control cells virus-cell prebinding before triggering fusion did not greatly affect influenza virus fusion with neuraminidase-treated cells. Interestingly, the association of the virus with neuraminidase-treated cells was enhanced at pH 5, compared to that at neutral pH, probably due to an increase in virus hydrophobicity However, this association was most likely of a nonspecific nature, and not efficient in terms of virus fusion activity. Indeed, the fluorescence of the virus associated with neuraminidase-treated cells was greatly quenched, while that of the virus associated with control cells under the same low pH conditions was essencially dequenched. Analysis of the results with a mass-action kinetic model revealed a decrease in the influenza virus fusion rate constant and an increase in the inactivation rate constant when the target membrane consisted of neuraminidase-treated cells. These results indicate that binding of influenza virus to sialic acid on the cell surface leads to rapid and extensive fusion and partially inhibits viral inactivation.

Th-Pos197

STRUCTURE OF THE STACKED DISK AGGREGATE OF TMV PROTEIN. ((Rubén Díaz-Avalos and Donald L.D. Caspar)), Brandeis University.

The self-assembly of *Tobacco Mosaic Virus* (TMV) is known to start from a nucleating aggregate, which has been hypothesized to be a bilayered disk that dislocates into a helical aggregate at the appropriate conditions for viral growth. A requirement for this to happen, is that such a bilayered disk has to have a polar configuration. One of the pieces of evidence supporting this hypothesis, was an electron microscopy study that showed that long disk aggregates (*stacked disk*) were packed in a polar fashion. In our study, we found that in contrast to that previous result, the packing of the stacked disk aggregate is bipolar, and furthermore, that the structure is that of stacks of A-ring pairs, as seen in the disk crystal. The resolution achieved in this study is about 15Å in the equatorial direction, and in the order of 10Å in the meridional direction. These results were obtained by means of electron microscopy of frozen hydrated samples and image processing, which were then compared with a modelled filament built from the atomic coordinates of the disk crystal. The fact that the stacked disk possesses dihedral symmetry, as well as its inherent stability, makes it an ideal test particle to use in the development of techniques for high resolution electron crystallography of particles with helical symmetry. We have been able to obtain high resolution electron diffraction patterns which can be merged with the phases of the image reconstruction to obtain a high resolution electron density map.

Th-Pos198

INTERACTIONS OF WILD-TYPE AND MUTANT SCAFFOLDING SUBUNITS WITH THE PHAGE P22 PROCAPSID LATTICE. ((Barrie Greene and Jonathan King)) Dept. of Biology, MIT, Cambridge, MA 02139.

Assembly of the bacteriophage P22 precursor capsid requires approximately 300 molecules of scaffolding protein in addition to the 420 coat protein subunits. All 300 scaffolding molecules are released intact upon the commencement of DNA packaging, presumably through channels observed at the centers of the pentamers and hexamers [Prasad et al., (1993) *J. Mol. Biol.* **231**, 65-74.]. This release can be reproduced *in vitro* by the addition of low concentrations of guanidine hydrochloride. In the absence of denaturants, purified scaffolding protein can reassociate with the extracted coat protein shells to regenerate filled precursor capsids, as observed by sedimentation and electron microscopy. The kinetics of rebinding and the separation of intermediates by sedimentation suggest that the coat lattice contains two classes of binding sites for scaffolding molecules. Both classes of sites become lost or inaccessible upon transformation of the procapsid lattice to the mature lattice. A set of point mutations in the scaffolding protein are defective at different stages in capsid assembly and maturation. The mutant proteins are selectively altered in binding to one or the other class of sites. The mutant phenotypes suggest that scaffolding exit and capsid maturation involve sites distinct from those needed at the earlier stages of shell initiation and polymerization [Prevelige et al., (1993) *Biophys. J.* **64**, 824-835].

Th-Pos199

TRANSMEMBRANE SEGMENT OF M13 COAT PROTEIN AS A MODEL FOR DIMERIZATION/OLIGOMERIZATION OF SINGLE-SPANNING INTEGRAL MEMBRANE PROTEINS. ((Yvonne M.Y. Chen and Charles M. Deber)) Division of Biochemistry Research, Research Institute, Hospital for Sick Children, Toronto, Ontario M5G 1X8, Canada.

In addition to serving as anchors in lipid bilayers, transmembrane (TM) segments may be functionally involved in the assembly of multi-spanning membrane proteins as well as the oligomerization/dimerization of single-spanning integral proteins. Our laboratory has used M13 coat protein as a model system to study the specific side-chain requirements for these processes. Mutational and structural analysis of a library of viable M13 TM mutants has demonstrated that interactions between TM helices can be highly residue-specific [Deber *et al.*, *PNAS USA* 90, 11648-11652 (1993)]. To extend and compare these results with M13 coat proteins containing non-viable TM segments, two constructs were prepared in which the sequence of either mature wild type M13 coat protein or its effective TM segment (YIGYAWAMVVVIVGATIGI) were expressed as fusion proteins to the C-terminus of staphylococcal nuclease (SN). Fusion protein SN/M13 ran as a monomer on SDS-PAGE gels, while in contrast, fusion protein SN/TM ran as a ladder of oligomers (monomer, trimer, pentamer, heptamer, etc.). Corresponding studies on selected M13 TM Val → Ala and Val → Leu mutants were carried out to investigate potential sensitive loci for TM helix dimerization. Preliminary circular dichroism spectra showed that the two domains in the SN/M13 fusion protein fold into separate entities. [Supported, in part, by grants to C.M.D. from MRC and NCIC.]

Th-Pos200

TAU, TAXOL, TEMPERATURE, AND NUCLEOTIDE AFFECT MICROTUBULE RIGIDITY. ((Brian Mickey, Fred Gittes*, and Jonathon Howard)) Department of Physiology and Biophysics and *Center for Bioengineering, University of Washington, Seattle, WA 98195.

The high flexural rigidity (EI) of microtubules is essential for their structural roles in cells. Several factors – the antimitotic drug taxol, the microtubule-associated protein tau, the slowly-hydrolyzed GTP analogue GMPCPP, and elevated temperature – promote the assembly and stability of microtubules. We asked whether these agents also influence the flexural rigidity.

Rhodamine-labelled tubulin was polymerized at 37 °C with 1 mM MgGTP or MgGMPCPP in standard buffer (80 mM K-Pipes, 4 mM $MgCl_2$, 1 mM EGTA, pH 6.9). Persistence lengths ($L_p = EI/kT$) were measured from thermal fluctuations in shape of microtubules in standard buffer with an oxygen-scavenging system without reducing agents.

At 37 °C, microtubules grown in GTP and stabilized by (i) growing GMPCPP caps onto their ends, (ii) adding tau, or (iii) adding taxol had persistence lengths of 6.3 ± 0.7, 8.0 ± 0.7, and 8.0 ± 0.8 mm respectively; microtubules grown in GMPCPP were significantly more rigid (L_p = 15 ± 2 mm). Lowering the temperature to 25 °C decreased the flexural rigidity of taxol-stabilized microtubules by 40%. While the flexural rigidity of taxol-stabilized microtubules was not affected by addition of the reducing agent β-mercaptoethanol (1% v/v), capped microtubules became more flexible (L_p = 0.93 ± 0.05 mm at 25 °C, Biophys. J. 64: A261).

In conclusion, several factors that increase microtubule stability also increase rigidity. This correlation could be due to rigidity and stability arising from the same interdimer bonds; alternatively, dimers in an intrinsically rigid state could associate more stably in the polymer. (Supported by the NIH, Pew, and HFSP.)

Th-Pos201

IS WATER A REACTANT IN ACTIN POLYMERIZATION? ((R. P. Rand, N.L. Fuller)) Biological Sciences, Brock University, St. Catharines, Ontario, Canada, L2S 3A1.

Water has recently been shown to be a critical reactant in the conformational changes of many proteins, and in protein association. Osmotic stress, whereby the chemical potential of water is controlled with indifferent polymers, can be used to measure the contribution of solvation in almost any system (Science 1992 256:618). We are beginning to look for any contribution of water in reactions involved in cellular motors. We have begun with the polymerization reaction of actin, measuring the critical monomer concentration of G-ATP actin in the G-F reaction, using classical fluoresence methods. Initial results show that the critical monomer concentration is decreased in the presence of both PEG and dextran. This suggests that, in the polymerization of actin, water is part of the reaction. We are attempting to measure that amount of water, and to make the same measurement for G-ADP actin polymerization.

Th-Pos202

CROSS-LINKING OF MODEL CYTOSKELETAL ELEMENTS: CONTROL OF EXCLUDED-VOLUME DRIVEN BUNDLING ((Daniel T. Kulp, Boris A. Itin and Judith Herzfeld)) Department of Chemistry, Brandeis University, Waltham, MA 02254-9110.

It has previously been shown, theoretically[1] and experimentally,[2] that high concentrations of globular proteins will induce long protein filaments to spontaneously coalesce into filament bundles. This means that cross-linking proteins are not necessary for bundle formation. However, cross-linking proteins may serve several other purposes. Cross-linkers with the appropriate geometric specificity can preferentially stabilize polarity and registration in filament bundles. Cross-linkers with a contrary geometric specificity can frustrate bundling by stabilizing orthogonal contacts between filaments. In the present work we have considered the latter category of cross-linkers. The theory combines a phenomenological description of reversible filament self-assembly, and reversible cross-linking, with a scaled particle treatment of excluded volume. The equilibrium distributions of filament lengths, orientations and cross-links is calculated by free energy minimization. We find that cross-linking can stabilize an isotropic gel. The stronger the binding of the cross-linker the less cross-linker is required to prevent bundling. This work was supported by NIH grant HL36546.

1. T.L. Madden & J. Herzfeld (1993). Biophysical J. 65: 1147-1154.

2. A. Suzuki, M. Yamazaki & T. Ito (1989). Biochemistry 28: 6513-6518.

MOLECULAR RECOGNITION AND BINDING

Th-Pos203

STUDIES ON THE STRUCTURAL AND THERMAL STABILITY OF INFLUENZA VIRUS HEMAGGLUTININ. ((David P. Remeta[1], Mathias Krumbiegel[2], Robert Blumenthal[2], and Ann Ginsburg[1])) [1]NHLBI and [2]NCI, National Institutes of Health, Bethesda, MD 20892

Hemagglutinin (HA) is a membrane integrating trimeric protein (M_r 220,000) that is responsible for binding influenza virus to sialic-acid containing surface receptors in target cells. Fusogenic activity is triggered by a pH-dependent conformational change of HA in the acidic milieu of endosomes. The conformational and thermal stability of HA purified from influenza strain X31 has been investigated by circular dichroism (CD) and fluorescence spectroscopy, and differential scanning calorimetry (DSC). Comparison of CD spectra acquired as a function of pH reveals that there are significant losses in the overall tertiary structure of HA from pH 7.4 to 4.9, whereas the secondary structure remains essentially unchanged. The loss of tertiary structure has also been confirmed by a proton-induced decrease in the intrinsic tryptophanyl residue fluorescence and concomitant increase in hydrophobicity. These features are consistent with a structural model in which HA adopts a *molten globule* conformation under fusogenic conditions (pH 4.9, 37 °C). The thermal stability of HA is strongly pH dependent as one observes a significant decrease in both the T_m of the DSC endotherm (66 to 43 °C) and ΔH_{cal} of unfolding (980 to 100 kcal/mol) upon acidification (pH 7 to 5). The calorimetric data therefore reflect the overall loss of HA tertiary structure, as evidenced by the decreasing amplitude of temperature-induced changes in Trp fluorescence that are coupled to the marked reduction in unfolding enthalpy. Interestingly, temperature-dependent far UV CD measurements indicate that HA secondary structure is actually stabilized (66 to 90 °C) as the protein is acidified (pH 7 to 5). The proton-induced destabilization of tertiary structure (correlated with observed decreases in T_m and ΔH_{cal}) and the apparent stabilization of secondary structure are novel features of influenza virus HA.

Th-Pos204

PHOSPHORYLATION AT TYR-99 OF CALMODULIN DECREASES ITS AFFINITY FOR TARGETS. ((Shaobin Zhuang[2], David B. Sacks[1], Michael Newman[1], and C.-L. Albert Wang[2])) [1]Brigham and Women's Hospital, Harvard Medical School, Boston, MA, and [2]Muscle Research Group, Boston Biomedical Research Institute, Boston, MA 02114. (Spon. by S. Sarkar)

Calmodulin (CaM) is specifically phosphorylated by purified insulin receptor kinase (IRK) at both Tyr-99 and Tyr-138, and upon phosphorylation the affinity of CaM toward cyclic nucleotide phosphodiesterase is attenuated (Williams et al., Arch. Biochem. Biophys. in press, 1994). In order to determine which tyrosine residue being modified by IRK is responsible for the observed reduction in the biological activity of CaM, we have examined the effect of IRK treatment of wild-type recombinant CaM, wheat germ CaM (wgCaM, which contains only one tyrosine residue at position 139) and a CaM mutant CaMyf, of which Tyr at position 138 has been changed to Phe, and thus containing only Tyr-99. Binding of wild-type CaM, wgCaM and CaMyf, with or without IRK phosphorylation, to two selected target peptides, M13 and GS17C, corresponding, respectively, to the CaM-binding sequence of smooth muscle myosin light chain kinase and caldesmon, was monitored by measuring the changes in tryptophan fluorescence of the peptides. We found that phosphorylation of both wild-type CaM and CaMyf resulted in a 3- to 6-fold decrease in affinity toward both target peptides; in contrast, IRK-treatment of wgCaM showed no significant changes in the target binding affinity, although Tyr-139 did appear to be phosphorylated. These results clearly demonstrated that phosphorylation at Tyr-99, but not at Tyr-138, by IRK weakens the interaction between CaM and its targets in smooth muscle cells. Supported by grants from NIH.

Th-Pos205

MUTATIONAL PERTURBATION OF CALMODULIN STRUCTURE

((B. Sorensen and M. A. Shea))
Dept. of Biochemistry, U. of Iowa College of Medicine, Iowa City, IA 52242-1109 (madeline-shea@uiowa.edu)

On the basis of molecular dynamics studies, Weinstein *et al* (*Mol. Eng.* 1: 231-247, 1991) proposed R74, R86 and R90 in $Ca^{2+}{}_4$-calmoduin (CaM) are critical in a ratcheting mechanism of compaction. We began testing this hypothesis experimentally by mutating R90 to ala and gly and characterizing the structure of these mutants at pH 7.4, 100mM KCl using UV and CD spectroscopies, and gel permeation chromatography. The calcium-binding properties of these mutants were monitored using calcium-dependent changes in intrinsic tyrosine fluorescence and their stabilities characterized by chemical denaturation studies using GuHCl.

We have extended the testing of this hypothesis by mutating R74 to ala and characterizing the mutant using the techniques described above. These studies indicated R74A has appoximately the same percent increase in helical content upon binding calcium as wild type (WT). Gel permeation chromatography was performed at pH 7.4 and 5.0. At pH 7.4, $Ca^{2+}{}_4$-R74A has a larger Stokes' radius (R_S) than $Ca^{2+}{}_4$-WT; at pH 5.0, this difference significantly increased. In general, at pH 7.4, $Ca^{2+}{}_4$-CaM has a smaller R_S than apo-CaM; at pH 5.0, the opposite was observed. The stabilities of R74A, R90A, R90G and WT were compared by chemical denaturation; the raw data were fit for $\Delta G°$ (accounting for deviations in the folded and unfolded baselines and stabilization by ligand binding). The order of stability of $Ca^{2+}{}_4$-CaM was R90G > WT≈R74A≈R90A; for apo-CaM, it was R90G < R74A < R90A < WT. (NSF MCB 9057157, AHA 91014980)

Th-Pos206

ENERGETICS OF CALCIUM BINDING TO CALMODULIN

((Susan Pedigo and Madeline A. Shea)) Dept. of Biochemistry, Univ. of Iowa College of Medicine, Iowa City, IA 52242

Calmodulin (CaM) is the primary eukaryotic calcium receptor. When calcium levels rise in response to signaling events, CaM binds 2 calcium ions cooperatively in each of 2 domains. To understand the allosteric mechanism of this process, it is essential to determine microscopic and macroscopic free energies of calcium binding. In order to characterize the macroscopic binding properties of CaM, we have adapted the Molecular Binding Density Function method originally developed by Lohman and Bujalowski (*Methods in Enzymol.* (1991) 208: 258-290) for the study of protein-DNA interactions. This method allows resolution of the macroscopic Adair constants and the spectral signal change associated with each binding event without assuming a linear relationship between the spectral signal and ligand-binding. We used the intrinsic tyrosine fluorescence of rat CaM and the isolated C-domain of CaM to generate a family of stoichiometric calcium-binding isotherms that were analyzed to determine the signal change per binding event. This information was then used to resolve macroscopic Adair constants from equilibrium titrations. In order to investigate microscopic binding properties of CaM, we have cloned, overexpressed and purified the isolated N-terminal (residues 1-75) and C-terminal (residues 76-148) domains of rat CaM. We are characterizing the calcium-binding properties of the domains. Results from analysis of the calcium-binding properties of the isolated domains are compared to the domains in wt- CaM.

(NSF MCB 9057157, AHA 91014980, PHS 1 T32 GM08365-04)

Th-Pos207

ENHANCED CALCIUM AFFINITY OF A CALMODULIN-TARGET PEPTIDE HYBRID PROTEIN. ((S. R. Martin, P. M. Bayley, S. E. Brown, T. Porumb*, M. Zhang*, and M. Ikura*)). Div.Phys.Biochem., N.I.M.R., Mill Hill, London NW7 1AA, U.K. and (*) Ontario Cancer Inst., Univ. of Toronto, Ontario, Canada M4X 1K9. (Spon. D.B.Kell)

H-2 is a hybrid protein comprising the full length of the *Xenopus laevis* calmodulin (CaM) sequence, followed by a pentapeptide linker (GGGGS), and residues 3-26 of M13, the calmodulin binding region of myosin light chain kinase. The addition of calcium to H-2 produces pronounced changes in: (1) the tryptophan emission spectrum (of the single Trp in M13), (2) the near- and far-UV CD spectra, and (3) the accessibility of the tryptophan residue to acylamide quenching. These changes are consistent with the Trp residue being immobilised in a hydrophobic environment and with the hybrid protein adopting a more α-helical structure when calcium is bound. The increased α-helicity derives from changes in both the calmodulin and peptide regions of the hybrid protein. Changes in the circular dichroism and fluorescence properties of H-2 as a function of the calcium to H-2 ratio are consistent with the fact that these changes parallel the appearance of the Ca_4.H-2 species.

The hybrid protein shows greatly increased affinity for calcium compared with CaM itself. Macroscopic calcium binding constants (K_1 to K_4) were determined from calcium titrations performed in the presence of the calcium chelator, Quin 2. Values for $Log(K_1K_2)$ and $Log(K_3K_4)$ were determined to be 15.45 ± 0.2 and 15.65 ± 0.25 (20C). The corresponding values for CaM alone are 11.6 ± 0.15 and 9.7 ± 0.25. Consistent with this increased affinity for calcium, stopped-flow kinetic studies show that the dissociation rate for the N-terminal calcium ions is ≈ 0.5 s^{-1}, compared with ≈ 650 s^{-1} for calmodulin alone. H-2 is of interest both as an extremely high affinity calcium binding protein that can be used as a calcium-sensitive biosensing device, as well as providing a specific model for studying calmodulin:target interactions. [Supported by The Medical Research Council of Canada]

Th-Pos208

THE MECHANISM OF INTERACTION BETWEEN CALMODULIN AND MYOSIN LIGHT CHAIN KINASE TARGET SEQUENCES. ((S. E. Brown, P. M. Bayley, and S. R. Martin)). Div.Phys.Biochem., N.I.M.R., Mill Hill, London NW7 1AA, U.K.

The kinetics of dissociation of target peptides based on skeletal muscle myosin light chain kinase, (MLCK), from complexes with *Drosophila* calmodulin have been studied using fluorescence stopped-flow techniques with monitoring of signals from calmodulin tyrosine, peptide tryptophan, and Ca-Quin 2. All parameters show complex kinetic behaviour (related to calcium dissociation) which is generally resolved as two exponential processes. For the majority of the calmodulin:peptide complexes studied, dissociation of the N-terminal calcium ions is sufficiently rapid (10-30 s^{-1}, cf. 650 s^{-1} for calmodulin alone) to be significantly faster than dissociation from the complex of either the peptide or the C-terminal calcium ions. The scheme is:

$$C_{[NC]}P \rightarrow C_{[-C]}P + Ca, \quad C_{[-C]}P \rightleftharpoons C_{[-C]} + P, \quad C_{[-C]} \rightarrow C_{[--]} + Ca$$

where C is calmodulin, P is peptide, and [N,C] are the N- and C-terminal calcium ion pairs. Loss of the N-terminal caicium ions is followed by relaxation of the $C_{[-C]}P$ complex (rate limited by N-terminal calcium dissociation). The amplitude of this relaxation depends on the extent to which the binding of the peptide is weakened by loss of the N-terminal calcium ions. The final step is loss of the C-terminal calcium ions from $C_{[-C]}$. Although the rate constant for the last step occurring in isolation (i.e., $C_{[-C]} \rightarrow C_{[--]} + Ca$) is 8.5 s^{-1}, the observed rate for formation of apo calmodulin is slower owing to the kinetics of the preceding steps.

For some peptides, the dissociation of the N-terminal calcium ions is not significantly faster than dissociation of peptide from the $C_{[N,C]}P$ complex and the dissociation route follows a different multistep kinetic pathway. The results indicate that subtle changes in the peptide sequence can have significant effects on the kinetic pathway for dissociation of the calmodulin:target peptide complex.

Th-Pos209

ESTABLISHING SINGLE Ca^{2+} BINDING SITE PROTEIN MODELS FOR STRUCTURAL INVESTIGATIONS OF "EF-HAND" TYPE Ca^{2+} BINDING PROTEINS.

((Q. Li, G. Guzman, J. Dai, & J.D. Potter)) Dept. of Mol. & Cell. Pharm., Univ. of Miami Sch. of Med., Miami, FL 33136

The cDNA for the Carp parvalbumin (PV) whose crystal structure is known, has been synthesized and expressed in bacteria in our lab. We have chosen parvalbumin since it is a simple Ca^{2+} binding protein, with two Ca^{2+} binding sites, that is very well characterized in terms of its biochemical and biophysical properties. In order to create single Ca^{2+} binding site proteins, which are simpler to study than two Ca^{2+} site proteins, we have made two double mutants [$PV_{D51A,F102W}$ and $PV_{D90A,F102W}$], in which a PHE at position 102 and an ASP at positions 51 or 90, respectively were replaced with a unique TRP and ALA to introduce a fluorescent probe near the active Ca^{2+} binding site and alternately to inactivate either of the two Ca^{2+} binding sites. Utilizing the flow dialysis method, we demonstrated that both $PV_{D51A,F12W}$ and $PV_{D90A,F102W}$ bind only 1 Ca^{2+} with similar affinity constants relative to the parent mutant, PV_{F102W} (K_b=3.0±1.5 x 10^7M^{-1}). The TRP fluorescence spectra of the metal-free and Ca^{2+}-forms of $PV_{D51A,F102W}$ are very similar to those of PV_{F102W}, and the Ca^{2+} affinity of these proteins, determined from the Ca^{2+} dependence of their TRP fluorescence change were the same as those obtained with flow dialysis. Thus these single Ca^{2+} binding site proteins are ideally suited for structural investigations. Supported by NIH HL42325, AR37701 & AR40727.

Th-Pos210

VINBLASTINE–INDUCED ASSEMBLY OF βIII–TUBULIN ISOTYPE IS IDENTICAL TO THE ASSEMBLY OF NATIVE TUBULIN.

((S. Lobert†, J.J. Correia* and A. Frankfurter‡)) †School of Nursing and *Dept. of Biochemistry, Univ. of Miss. Medical Center, Jackson, MS. 39216 and ‡Dept. of Biology, Univ. of Virginia, Charlottesville, VA. 22901

A microtubule assembly–competent β3–tubulin isotype has been purified from an affinity column specific for βIII–tubulin (utilizing the monoclonal antibody TuJ1) by competitive elution with the β3–isotype defining peptide, YEDDDEESEAQGPK, at 1 mM in 0.1 M Pipes, 1 mM $MgSO_4$, 2 mM EGTA, 0.1 mM GTP, pH 6.9. Vinblastine–induced assembly of tubulin and purified βIII–tubulin were investigated by velocity sedimentation in a Beckman XLA analytical ultracentrifuge. Experiments were conducted as a function of temperature and in the presence of GDP or GTP. The diphosphate nucleotide stimulates assembly. The data are converted to a weight average $S_{20,w}$ by integration, $\int g(s)sds / \int g(s)ds$, and fit to a ligand–mediated plus ligand–facilitated isodesmic association model. The vinblastine–induced association of βIII–tubulin is identical to the drug–induced association of whole PC–tubulin. In addition, the thermodynamic parameters are identical, within error, to the results of Na and Timasheff (Biochemistry 1986, 25:6214 & 6223), even though our work was done at much lower protein concentrations, ie. 1–4 μM tubulin. The influence of heterodimer dissociation and the asymmetry of the vinblastine–tubulin coiled aggregate on the fitted parameters were also evaluated in the analysis. [Supported by NR00056 (S.L.), GM41117 (J.J.C.) and NS21142 (A.F.).]

Th-Pos211

SLOW LOADING OF BIOTIN-STREPTAVIDIN BONDS YIELDS UNEXPECTEDLY LOW DETACHMENT FORCES ((R. Merkel, K. Ritchie and E. Evans)) Univ. of British Columbia, Dept. of Physics, Vancouver BC, Canada, V6T 1Z1.

A new method to measure ultralow forces has been used to probe the strength of single biotin streptavidin (SA) bonds. Details of the method are described in a companion abstract at this meeting (K. Ritchie, R. Merkel and E. Evans). The transducer is sensitive to a wide range of force (0.1 pN to 1 nN) which enables both very soft contact to the surface ($\sim$ 1 pN) and subsequent rupture of molecular attachments at large forces ($>$ 100 pN). With this probe, attachments formed by biotin SA bonds were loaded under relatively slow rates (0.1 nN/sec) up to rupture. The experimental approach was to prepare both a glass coverslip and the transducer microbead probe with covalently linked biotin arrays, i. e. glutaraldehyde fixed (1) biotinylated bovine serum albumin (BBSA) physisorbed to the coverglass and (2) biotinylated lectin reacted with aldehydesulfate groups derivatized on the latex microbead. SA was bound to the crosslinked BBSA surface, washed, then tested with the transducer probe. Surprisingly we found that detachment forces ($\approx$ 50 pN) were a factor 4-5 smaller than values published in AFM studies (e. g. Moy et al, report 240 pN). Crosslinking of the biotin conjugated proteins should localize failure to the biotin-SA bond. Hence, we conclude that the low level of detachment force as compared to AFM values most likely originates from differences in loading rate because, attachments were broken 6000 times slower in our experiment than in the AFM studies. If tests in progress verify breakage of biotin-SA bonds in our system, the results expose strong dynamical features of bond dissociation.

Th-Pos212

THE ROLE OF TRYPTOPHAN CONTACTS IN THE STREPTAVIDIN-BIOTIN INTERACTION ((Patrick S. Stayton*, Ashutosh Chilkoti*, Mark Fisher°, and Philip Tan*)) *Center for Bioengineering, University of Washington, Seattle and °Department of Biochemistry and Molecular Biology, University of Kansas Medical Center, K.C.

The streptavidin and biotin system has found broad use in the laboratory and in industry, largely because of the extremely high-affinity binding interaction between protein and ligand ($K_a \approx 10^{13}$ M^{-1}). We have initiated a site-directed mutagenesis and biophysical study of the structure-function relationships governing this remarkable high-affinity couple. Our first target has been the set of aromatic tryptophan side-chains found at the base and lid of the biotin binding-site. Each tryptophan has been mutated to alanine, removing the aromatic side-chain, and phenylalanine, substituting the indole for an aromatic phenyl side-chain. We have quantitated the binding of the mutants to biotin and imino-biotin in an ELISA assay where relative affinities are measured via an EC_{50} determination. We have also determined the biotin off-rate kinetics for these mutants and find an important role for Trp120 at the lid of the binding pocket. The thermal dependence of the off-rates has been analyzed with van't Hoff formalism, and suggests that Trp120 operates with distinctly different activation enthalpy and entropy as compared to the binding pocket tryptophans. Titrating calorimetry experiments support these activation enthalpy assignments and provide direct determination of equilibrium binding enthalpies. These results provide a quantitative molecular dissection of the role of aromatic side-chains in the high-affinity streptavidin system.

Th-Pos213

STUDIES OF *ras*-p21 WITH CLASSICAL RAMAN SPECTROSCOPY. ((D. Xiao, D. Prettypaul, G. Weng, M. Webb*, D. Manor and R. Callender)) Department of Physics, City College of CUNY, NY10031; *National Institute for Medical Research, Mill Hill, London. NW7 1AA, U.K.

Many mutant p21 proteins (one exception is p21(G12P))have lower intrinsic GTPase activities than that of wild type p21 . We used Raman Difference Spectroscopy to obtain the phosphate vibrational spectra of bound GDP and GTP in the wild type and mutant proteins. The phosphate stretching modes are recognized and picked out from the overwhelming protein bands by the method of ^{18}O isotopic editing . The shift of phosphate stretching modes due to the binding to these different proteins reflect changes in P-O bond order of the bound phosphate groups. We found that the terminal phosphate stretching mode of GDP at 943 cm^{-1} in solution splits and shifts down to 914 cm^{-1} and 888 cm^{-1} when it is bound to p21. The shift of wild type p21 does not vary much from mutant proteins may imply that the binding environments around terminal phosphates at GDP state are similar in wild type p21, mutant p21(G12V), p21(G12D), p21(G12P). The mechanism of the GTP hydrolysis in protein p21 will be discussed based upon these phosphate modes studies.

Th-Pos214

HYDRODYNAMIC PROPERTIES OF THE ATP-DEPENDENT CLP-AP PROTEASE OF *E. COLI*. ((Michael R. Maurizi[1] and Ann Ginsburg[2])) NCI[1] and NHLBI[2], NIH, Bethesda, MD 20892.

ATP-dependent proteases from both prokaryotes and eukaryotes have protein unfolding, peptide bond cleaving, and ATP-hydrolyzing activities. The ClpAP protease from *E. coli* is composed of a proteolytic component (ClpP) and a regulatory ATPase component (ClpA). Ultracentrifugation was conducted at pH 7.5 (0.1 - 0.3 M KCl) and 4 or 20 °C. Without nucleotide, ClpA (subunit M_r of 84,150) exists in a monomer-dimer equilibrium with K = 10^5 M^{-1} ($s_{20,w}$ = 8.7 S). With nonhydrolyzable ATPγS present, ClpA associates to a hexamer with M_r = 505,000 and $s_{20,w}$ = 17.2 S (f/f_0 = 1.4). ClpP has identical subunits (21,544 M_r), sediments as a monodisperse species ($s_{20,w}$ = 12.1 S), and appears to have 7-fold symmetry (electron microscopic analysis of M. Kessel *et al.*). However, sedimentation equilibrium and gel filtration studies with ClpP have given molecular weights that range from 220,000 to 302,000 (10-mer to 14-mer). Nucleotide-bound, hexameric ClpA is required for its association with ClpP to form the active ClpAP protease. Sedimentation velocity studies in the presence of ATPγS and 2-fold excess $(ClpA)_6$ over $(ClpP)_{14}$ showed two complexes: $s_{20,w}$ = 30 S and 40 S. These correspond to 1:1 and 2:1 complexes of hexameric ClpA and oligomeric ClpP, with M_r ~8.1 x 10^5 (f/f_0 = 1.0) and M_r ~1.3 x 10^6 (f/f_0 = 1.1), respectively. Both complexes are active in protein degradation and both are seen in electron micrographs.

Th-Pos215

WATER SOLVENT AND INTERMOLECULAR RECOGNITION FOR THE HIV-1 PROTEASE INTERACTION WITH INHIBITORS. ((V.V. Nauchitel, C. Villaverde and F. Sussman)) R & E Computing, OUHSC, Oklahoma City, OK 73104, Protein Studies Section OMRF, Oklahoma City, OK 73104. (Spon. by R.L. Floyd)

We have developed an approach that allows evaluation of free energies of binding between macromolecules. The approach is based on the assumption that water solvent is the major factor governing interactions between such molecules. In this work we apply the approach to studying interactions between 14 inhibitors and the Human Immuno-defficiency Virus Protease (HIV-1 PR). The calculated free energies of binding for the set of inhibitors have average deviation of 0.86 kcal/mol from the observed ones. Our approach has enabled an assessment of the significance of different binding groups of the inhibitors and of the potential for binding of different pockets of the HIV-1 PR. The gained knowledge about binding specificity is of vital importance for rational drug design against AIDS.

This work was supported by NIH and OCAST grants.

Th-Pos216

EVALUATION OF BINDING FREE ENERGIES OF MHC CLASS I PROTEIN-PEPTIDE COMPLEXES. ((N. Froloff and B. Honig)) Dept. of Biophysics, Columbia University, New York, NY 10032.

Binding free energies of immune protein-peptide complexes are evaluated using a macroscopic solvent model. Crystal structures of two different viral peptides in complex with murine MHC Class I H-2Kb protein are studied. Solutes are treated as polarizable cavities of shapes defined by their molecular surfaces, containing point charges at the location of atomic nuclei.

Two different thermodynamic pathways were tested to evaluate the binding energy of a protein-peptide complex in water : in the first pathway, reactants are individually desolvated from water to vacuum, associated to form the final complex in vacuum, which is resolvated back to water ; in the alternate pathway, reactants are individually discharged in water, associated as purely nonpolar entities, and the final complex is recharged. Electrostatic contributions to solvation are derived from finite difference solutions of the Poisson equation (FDPB method). Electrostatic and van der Waals contributions to binding in vacuum are calculated using CHARMm parameters. Other nonpolar (cavity/van der Waals) energies are evaluated as surface area dependent terms, with two single surface tension coefficients derived from hydrocarbon solubility in water, and hydrocarbon hexane-water transfer energy. An analysis of relative free energy contributions of peptide backbone and side chains to binding is presented.

Th-Pos217

PARTITION FUNCTION FOR HUMAN HEMOGLOBIN

(G.K. Ackers, J. Holt, Y. Huang, and A. Klinger) Dept. of Biochemistry and Molecular Biophysics, Washington University School of Medicine, St. Louis, MO 63110.

Studies over the last decade have resolved the energetics of cooperativity for the 10 ligation microstates of tetrameric human hemoglobin using a variety of ligands and ligand analogs which mimic oxygenated vs deoxygenated sites[cf. Science (1992) 255, 54-63, Trends Biochem. Sci. (1993); 18 385-390.]

Five ligation systems have been found to exhibit a common distribution of cooperative free energies from which a "consensus partition function" has been deduced. While magnitudes of the energetic effects vary with hemesite ligand, the qualitative relations between them are the same. This partition function has been evaluated as a function of temperature, pH and [NaCl] and its predictions found to be in accord with detailed measurements on oxygen binding. Hemoglobin thus appears to operate by a common allosteric mechanism (the "Symmetry Rule mechanism") regardless of the variations in hemesite ligands. Supported by NIH grant R37-GM24486.

Th-Pos218

ADENOVIRUS TYPE 5 HEXON: PURIFICATION AND X-RAY STRUCTURE ANALYSIS.

((John J. Rux and Roger M. Burnett))
The Wistar Institute, Philadelphia, PA 19104

Adenovirus type 5 (ad5) is associated with respiratory infections and is one of over forty types that infect humans. Hexon is the major protein component of the viral capsid and displays both group and type specific antigenic determinants.

Improvements have been made in the methods for purifying hexon and have been applied to both ad2 and ad5. These include the use of DEAE-Sepharose-CL and Mono-Q anion-exchange chromatography on a Pharmacia FPLC. The highly purified ad5 hexon crystallizes under the same conditions as ad2 hexon (0.5 M sodium citrate at pH 3.2). The crystals have a rhombic dodecahedral morphology with a maximum diameter of 0.3-0.6 mm. The ad5 crystals diffract to at least 2.5 Å resolution and the data collected to 2.7 Å is >95% complete. The ad5 hexon crystals belong to the cubic space group $P2_13$ with a unit cell edge of 150.5±0.1 Å.

Adenovirus types 5 and 2 are closely related and share 89% sequence homology. Since crystals of ad5 and ad2 hexon are isomorphous, features of the ad2 hexon structure that are common to ad5 hexon were used for the initial phasing of the ad5 model. Difference Fourier maps reveal the structural differences in the two hexon species. Supported by NIH (AI-17270).

Th-Pos219

SITE-DIRECTED MUTAGENESIS AND OPTIMIZATION OF PROTEIN EXPRESSION OF RECOMBINANT α-BUNGAROTOXIN.

((J.A. Rosenthal and E. Hawrot)) Department of Molecular Pharmacology and Biotechnology, Division of Biology and Medicine, Brown University, Providence, RI 02912.

Recombinant DNA techniques have previously allowed us to express a synthetic α-bungarotoxin (Bgtx) gene fused to the 3'-end of a gene for a T7 coat protein. An engineered Factor Xa protease site allows for cleavage and liberation of an active Bgtx protein as assessed by competition binding experiments with ^{125}I-labelled native Bgtx and nicotinic acetylcholine receptor (nAChR)-enriched membranes from *Torpedo californica*. Several residues near the tip of the central loop of Bgtx's three-looped structure have been implicated in nAChR recognition. To address this issue, we have chosen highly conserved residues in this region as targets for mutagenesis and looked for changes in the ability of these modified toxins to bind nAChRs. It has been proposed that the side chains of D30 and R36 interact so as to mimic the structure of the natural ligand, acetylcholine. We have previously shown that substitution of D30 with alanine has no effect on binding affinity as determined in competition assays. We show here that mutagenesis of D30's proposed counterpart, R36 to alanine, results in an approximately 500-fold reduction in binding the nAChR, supporting the hypothesis that this residue is important in receptor recognition.

A parallel goal in the study of the structure-function analysis of Bgtx and its mutants is to optimize expression levels. Currently we can produce ~450μg of active toxin/L of LB shaker culture media. To increase this value we have designed a 7-residue Histag sequence onto the N-terminus of Bgtx. This allows for greatly simplified purification of the fusion protein and cleaved Bgtx by Ni^{2+} affinity chromatography. Simultaneously we have added a thrombin cleavage site to allow for more economical cleavage of the toxin from the fusion partner.

Th-Pos220

EXPRESSION OF RECOMBINANT SAXIPHILIN AND LOCALIZATION OF THE SAXITOXIN-BINDING SITE TO THE C-LOBE DOMAIN WHICH IS HOMOLOGOUS TO THE C-LOBE OF TRANSFERRIN.

((M. Morabito, L. E. Llewellyn and E. G. Moczydlowski)) Dept of Pharmacology, Yale Univ. School of Medicine, New Haven, CT 05620.

Saxiphilin is a 91 kDa soluble protein that contains one high-affinity binding site for saxitoxin (STX) and STX derivatives. [^{3}H]STX binds to native saxiphilin with a K_D of 0.2 nM at 0° C and a dissociation half-time of 80 min. Binding of [^{3}H]STX to native saxiphilin is also inhibited by decreasing pH with an apparent pKa of 5.7. Saxiphilin is homologous to members of the transferrin family of Fe^{3+}-binding proteins (44% identity to human serum transferrin) but does not appear to bind Fe^{3+}. Members of the transferrin family including saxiphilin consist of a single polypeptide with an internal duplication. In transferrin, this feature corresponds to N-lobe and C-lobe domains that are structurally homologous at the three-dimensional level. A cDNA encoding saxiphilin was isolated from bullfrog liver and inserted into a baculovirus expression vector. Infection of cultured insect cells with this vector resulted in the secretion of saxiphilin activity. Recombinant saxiphilin isolated from the insect cell medium is virtually identical to native saxiphilin with respect to molecular mass, binding kinetics of [^{3}H]STX and pH dependence. To determine the location of the STX binding site, an expression vector for the C-lobe of saxiphilin was engineered by deletion of N-lobe sequence between the secretory signal sequence and the C-lobe domain. Cells infected with baculovirus containing the C-lobe gene also secrete STX-binding activity. Since titration data indicates that there is only one STX-binding site per saxiphilin molecule, this finding establishes that the STX binding site is located exclusively within the C-lobe domain. The recombinant C-lobe has a molecular mass of ~40kDa and binds [^{3}H]STX with 3-fold lower affinity and a 3-fold faster dissociation rate than native saxiphilin. (Supported by USAMRDC and NIH).

Th-Pos221

BIORECOGNITION, INTERNALIZATION AND SUBCELLULAR TRAFFICKING OF HPMA COPOLYMER-ANTIBODY-DRUGS CONJUGATES: A FLUORESCENCE AND CONFOCAL STUDY.

((V.Omelyanenko[1], P.Kopečková[1], L.Poels[2], J.Kopeček[1]))
[1]University of Utah, Salt Lake City, UT 84112
[2]University of Nijmegen, Nijmegen, The Netherlands

Targetable polymer - drug conjugates have to be biorecognizable on two levels. First, on the cellular level at the plasma membrane to be internalized by a subset of cells by receptor-mediated endocytosis. Second, they have to be recognized intracellularly in the lysosomal compartment by enzymes to release the drug. We have been systematically evaluating the potential of N-(2-hydroxypropyl)methacrylamide (HPMA) copolymers as targetable anticancer drug carriers. Recently, we have been studying targetable HPMA copolymer - anticancer drug conjugates biorecognizable by ovarian cancer cells. The conjugates contain monoclonal antibody OVTL-16 as a targeting moiety, and adriamycin or chlorin e_6 as anticancer drugs. The affinity constants of the wild-type antibody and of the copolymer conjugated antibody were determined. The internalization and localization of the conjugates inside the cells was demonstrated by confocal fluorescence microscopy.

Th-Pos222

A MODEL FOR THE INTERACTION OF THE SULFONIC DISTAMYCIN A DERIVATIVES, ANGIOGENESIS-MODULATING AGENTS, WITH RECOMB-INANT HUMAN BASIC FIBROBLAST GROWTH FACTOR (bFGF).

((M. Zamai, A.H. Parola, V.R. Caiolfa[a], M. Grandi[a], F. Manetti[], F. Corelli[], M. Botta[] & N. Mongelli[a])) Dept. of Chemistry, B.G. University, Beer-Sheva, Israel; [a]PHARMACIA Farmitalia, R&D BA/Oncology, Nerviano, Italy; []Dept. of Medicinal Chemistry & Technology, University of Siena, Siena, Italy. (Spon. by A.H. Parola).

In-vitro receptor binding and in-vivo studies (1) have suggested that the biological activity of sulfonic distamycin A derivatives might be due to their interaction with growth factors. In the effort of sustaining the clinical development of these novel agents and rationalizing the biological data, the binding equilibrium between a series of sulfonic distamycin A derivatives and bFGF was investigated in-vitro and in the absence of the bFGF cellular receptor. Sulfonated distamycin A derivatives, as suramin, were characterized for their steady-state and dynamic fluorescence features due to the common substituted-dansyl moiety. In fact, this class of molecules have a typical fluorescence lifetime of about 10 - 17 nsec Their binding to bFGF, in 20 mM phosphate buffer, 0.15 M NaCl, 10-40 μM EDTA, pH 7 and 22°C, was followed by the changes in anisotropy and lifetime. The experimental rotational correlation time indicated the formation of a complex with 1:1 stoichiometry, as it was suggested by the molecular modeling studies that were carried out on the bases of the published X-ray structure of the protein (2). For compounds that were active in-vivo as inhibitors of bFGF-induced angiogenesis, the affinity constants obtained, by fluorescence binding studies, ranged from $1 \cdot 10^6$ to $0.03 \cdot 10^6$ M^{-1}. (1) M. Ciomei, W. Pastori, M. Mariani, F. Sola, M. Grandi and N. Mongelli; Biochem. Pharm. 47, 295-302, 1994. (2) G. Biasoli, M. Botta, M. Ciomei, F. Corelli, M. Grandi, F. Manetti, N. Mongelli, A. Paio; Med. Chem. Res.4, 202-210, 1994.

Th-Poa223

DESENSITIZATION OF THE *TORPEDO* NICOTINIC ACETYLCHOLINE RECEPTOR (nAChR) LINKED TO MOVEMENT OF THE AGONIST SITE RESIDUES γTRP-55 AND δTRP-57. ((D.C. Chiara and J.B. Cohen)) Department of Neurobiology, Harvard Medical School, Boston, Ma. 02115.

The *Torpedo* nAChR is a ligand-gated ion channel consisting of a pentamer of four homologous subunits arranged as αγαδβ. There are two agonist/competitive antagonist binding sites on each receptor located at the α-γ and α-δ interfaces (Pedersen and Cohen, *PNAS* 87: 2785-2789, 1990) The competitive antagonist d-tubocurarine (dTC) specifically photoincorporates into residues in the α-, γ-, and δ-subunits. For the γ- and δ-subunits, the major sites of [^{3}H]dTC incorporation are γ Trp-55 and δTrp-57 (Chiara and Cohen, *Biophys. J.* 61: A106, 1992.) To investigate structural changes in the agonist sites due to the transition from the resting state to the desensitized state, nAChR-rich membranes were photolabeled with 5 μM [^{3}H]dTC (>99% occupancy of the α-γ dTC binding site and ~50% occupancy of the α-δ dTC site) in the presence of various concentrations of tetracaine or proadifen, non-competitive antagonists (channel blockers) that stabilize the resting and desensitized states of the nAChR, respectively. [^{3}H]dTC incorporation into the γ- and δ- subunits increased 2-fold in the presence of tetracaine ($EC_{50} \cong 1$ μM.) Proadifen caused a 50% reduction in the [^{3}H]dTC labeling of the γ-subunit ($EC_{50} \cong 100$ nM) with no detectable change in the δ-subunit incorporation level. These results indicate that the photoreactive region of dTC is sensitive to changes in the structure of the binding sites between resting and desensitized states, with enhanced reactivity at the non-alpha residues, γTrp-55 and δTrp-57, a property of the resting state.

Th-Poa224

CHARACTERIZATION OF THE AGONIST BINDING SITES IN THE *TORPEDO* nAChR: CONTRIBUTIONS BY THE NON-α SUBUNITS. ((Y. Xie and J.B. Cohen)) Department of Neurobiology, Harvard Medical School, MA 02115

The nicotinic acetylcholine receptor (nAChR) from *Torpedo* electric organ is composed of four homologous subunits ($\alpha_2\beta\gamma\delta$) and has two sites located at α-γ and α-δ interfaces that bind agonists, competitive antagonists and α-bungarotoxin (αBgt). Previous affinity labeling studies with [^{3}H]d-tubocurarine (dTC) identified γW55 and δW57 within these sites (Chiara and Cohen, *Biophys. J.* 61:A106, 1992). For nAChRs expressed in *Xenopus* oocytes, the mutation γW55L resulted in an 8-fold increase in EC_{50} of ACh activation and a 110-fold increase in IC_{50} of dTC inhibition, whereas the δW57L mutation had no effect (O'Leary et al., *Am. J. Physiol.* 266 (*Cell Physiol.* 35): C648-C653, 1994). To determine the effects of these mutations on ligand binding, we measured dose-dependent inhibition by dTC and ACh of ^{125}I-αBgt binding to nAChRs in membranes isolated from oocyte homogenates. Surprisingly, nAChRs containing either γW55L or δW57L have the same affinities for dTC as wild-type nAChR ($K_H = 50 \pm 10$ nM and $K_L = 4 \pm 1$ μM). In contrast, the γW55L mutation decreased the affinity for ACh at one site by 10^5! For wild-type nAChR, ACh bound with two affinities, $K_H = 30 \pm 10$ nM and $K_L = 2.6 \pm 0.6$ μM. For γW55L, $K_H = 2.6$ μM and $K_L = 5.3 \pm 1.7$ mM. For δW57L, $K_H = 30$ nM and $K_L = 1.3 \pm 0.8$ mM. Thus, the mutation γW55L has no effect on ACh binding at the α-δ site, while binding at the α-γ site is weakened by 10^5. Conversely, the δW57L mutant has no effect on ACh binding at the α-γ site, while weakening the binding at α-δ by 10^5. The tryptophans at γW55 and δW57 that are conserved in all γ- and δ-subunits are not important determinants of dTC binding affinity, but they are crucial in determining ACh binding affinity at equilibrium, a parameter determined both by the binding affinity of the desensitized conformation and the equilibrium constants for the conformational transitions between resting and desensitized states of the nAChR.

Th-Poa225

EQUILIBRIUM AND KINETICS OF MEMBRANE BINDING FOR BIVALENT AND MONOVALENT MONOCLONAL ANTIBODIES MEASURED USING TOTAL INTERNAL REFLECTION FLUORESCENCE MICROSCOPY ((Willem Vanden Broek and Nancy L. Thompson)) Department of Chemistry, University of North Carolina, Chapel Hill, NC, 27599-3299

Equilibrium and kinetic parameters for the binding of three anti-dinitrophenyl (DNP) monoclonal antibodies (ANO2, 1B7.11, and TIB142) to DNP-glycine in solution and to dinitrophenylated membranes have been measured and comparatively evaluated. The behaviors of both intact (bivalent) and Fab (monovalent) forms were investigated. Equilibrium association constants for the antibodies with DNP-glycine in solution were measured by tryptophan fluorescence quenching. Dinitrophenylated membranes were constructed by fusing small unilamellar vesicles composed of DNP-conjugated dipalmitoylphosphatidylethanolamine (25 mol%) and dipalmitoylphosphatidylcholine (75 mol%) at quartz surfaces. Apparent equilibrium association constants for membrane binding were measured using steady-state total internal reflection fluorescence microscopy (TIRFM). The kinetics of membrane binding were characterized using total internal reflection with fluorescence photobleaching recovery (TIR-FPR). The values of the measured parameters were interpreted with models that address several physical features of antibody-hapten binding: (1) the relationship of an antibody's ability to bind haptens in solution to its ability to recognize membrane-bound haptens; (2) the role of antibody bivalency in enhancing membrane binding; (3) interconversion between antibodies monovalently and bivalently bound to membrane surfaces; and (4) conditions for which antibodies might undergo transport across membrane surfaces via sequential detachment and attachment of single antigen binding regions. Supported by NIH GM-37145 and by NSF GER-9024028.

Th-Poa226

PRELIMINARY EVIDENCE FOR RECEPTOR-LIGAND BINDING DURING SIGNAL TRANSDUCTION AS AN INTERACTION SITE FOR 60Hz MAGNETIC FIELDS. ((Robert P. Liburdy & Valorie Eckert)) Cell & Molecular Biology Dept., Life Science Division, Lawrence Berkeley Laboratory, UC Berkeley, CA, USA 94720. (Spon. by R. P. Liburdy)

Early events in the signal transduction (ST) cascade in activated human T-lymphocytes (Jurkat E6.1 cells) have been investigated to identify a possible candidate for a primary interaction site responsible for elevated intracellular calcium in the presence of a magnetic field (1 Gauss, 50 Hz). When Jurkat cells are activated with anti-CD3(0.5ug/ml) in the presence of the magnetic field an increase in plateau phase $[Ca^{+2}]_i$ is observed compared to sham-exposed cells (t = 3.89, p = 3.90×10^{-4}, n=11 expts). To investigate receptor-ligand binding Scatchard analyses were performed using FITC-antiCD3 antibody in the presence or absence of the magnetic field. Preliminary data suggest (3 MF expts., 5 control expts) the x-intercept appears shifted to higher values for magnetic field exposed cells suggesting a greater number of receptor sites are available for binding. This is a plausible explanation for the observed increase in $[Ca^{+2}]_i$ since an increase in receptor-ligand binding would lead to a greater number of calcium channels opening and, thus, an increase in calcium influx. Support provided by the Office of Energy Management, Utilities Systems Division, U.S. Department of Energy under contract DE-AC03-76SF00098 and the NIEHS, Grant ES06401.

Th-Poa227

PEPTIDE RECOGNITION BY AN ANTI-IDIOTYPIC ANTIBODY AGAINST ANGIOTENSIN II: PEPTIDE LIBRARY SEARCH FOR PEPTIDES OTHER THAN ANGIOTENSIN II. ((Kon Ho Lee, Min Li and L. M. Amzel))The Johns Hopkins School of Medicine, Baltimore MD 21205

The understanding of hormone-receptor interactions is important in the design of small ligands which have similar interactions to the angiotensin II(AII) receptor. Small peptide hormones such as AII bind to their receptors with very high affinity although they have to overcome the high barrier of conformational entropy change. The crystal structure of bound AII was elucidated in the complex of anti-anti-idotypic antibody (MAb 131). Finding some other small peptides that bind to the antibody with high affinity is important in understanding the interaction between AII and the antibody MAb 131. These peptides were searched using a random sequence peptide library. The peptide library used here has octapeptides with cysteine on both ends displayed on the surface of filamentous phage M13. The peptide sequences inserted in the phage were made by randomly synthesized oligonucleotides. After three rounds of panning we found several clones that have very high specific binding to the MAb 131 as judged by ELISA. The peptide sequence of one high affinity binder showed large differences with AII sequence. Determination of the crystal structure of the peptides screened with the antibody is under way. (supported by NIH grant GM44692)

Th-Poa228

CHARACTERIZATION OF MONOCYTE CHEMOATTRACTANT PROTEIN-1 (MCP-1) BINDING TO SPECIFIC IgG AUTOANTIBODIES IN HUMAN SERUM ((J. R. Casas-Finet, I. Clark-Lewis, and E. J. Leonard)) Structural Biochemistry Program, PRI/DynCorp, NCI-FCRDC, Frederick, MD 21702, Biomedical Research Center, U. B. C., Vancouver, Canada, and Laboratory of Immunobiology, NCI-FCRDC, Frederick, MD 21702. (Spon. by C. A. Bush)

In normal human sera, MCP-1-IgG immune complexes are present at a concentration of 330 ± 33 pM for 48 subjects, free MCP-1 is below the 8 pM detection limit, and free anti-MCP-1 (8 ± 1 pM) can be detected in *ca.* 20% of sera. To gain insight into the functional significance of autoantibodies against the proinflammatory cytokine MCP-1, estimates of affinity were obtained. *In vitro* immunodepletion of free anti-MCP-1 in sera of 3 subjects upon addition of synthetic MCP-1 was determined by direct ELISA; the data were fit to a model of divalent binding of ligand to one or more antibody classes. The free anti-MCP-1 (termed Ab2) was of low affinity (Kd = 0.64 ± 0.11 μM/combining site). One serum had an additional low affinity antibody (Kd = 0.14 μM/combining site). The high [MCP-1-IgG] relative to [free MCP-1] suggests that the antibody in the immune complex is of high affinity, with an estimate of Kd = 1.1 ± 0.2 pM/combining site. Only 1-2% of this antibody (termed Ab1) was in the free form, and was near or below the anti-MCP-1 antibody detection limit. At least 90% of total (Ab1+Ab2) anti-MCP-1 antibody was Ab1, predominantly as immune complex. Conversely, in view of the low affinities of Ab2, formation of MCP-1-Ab2 complexes would not be expected at MCP-1 concentrations *in vivo*, either at basal levels (≤ 8 pM) or peak levels (330 ± 50 pM) resulting from i. v. administration of lipopolysaccharide (LPS). As predicted, neither a drop in [free anti-MCP-1] nor an increase in [MCP-1-IgG] was observed when MCP-1 secretion was induced by i. v. LPS challenge in healthy subjects. In all subjects that exhibited free anti-MCP-1 (Ab2) antibodies, comparable *in vitro* interaction was observed with either synthetic full-length MCP-1 (res. 1-76) or truncated MCP-1(10-76). As residues 1-10 are required for cellular MCP-1 binding, we suggest that the production of free Ab2 anti-MCP-1 antibodies is functionally irrelevant in terms of their potential for either MCP-1 binding or inactivation. The constancy of MCP-1-IgG immune complex levels in paired samples of human serum drawn at 30 day intervals lends support to the role of Ab1 autoantibodies in MCP-1 homeostatic control.

Th-Pos229

PHYSICAL CHARACTERIZATION OF RECOMBINANT ANTI-c-erbB-2 741F8 SINGLE CHAIN Fv ANTIBODY DIMER $(sFv')_2$ AND ANALYSIS OF ITS INTERACTION WITH RECOMBINANT EXTRACELLULAR DOMAIN OF c-erbB-2 ONCOGENE PRODUCT BY ANALYTICAL ULTRACENTRIFUGATION. ((S. Liu[1], M.-S. Tai[2], J. McCartney[2], H. Oppermann[2], R.M. Hudziak[2], L.L. Houston[3], L.M. Weiner[4], J.S. Huston[2], and W.F. Stafford[1])) [1]Boston Biomedical Research Institute, 20 Staniford Street, Boston MA 02114; [2]Creative Biomolecules Inc., Hopkinton, MA; [3]Prizm Pharmaceuticals Inc., San Diego, CA; [4]Fox Chase Cancer Center, Phila, PA.

The c-erbB-2 oncogene is over-expressed in about 25% of breast cancers and in other adenocarcinomas. The extracellular domain (ECD) of c-erbB-2 is antigenic and, therefore, can be made the target of various immuno-therapeutic agents. Recombinant anti-c-erbB-2 741F8 single chain Fv antibody dimer $(sFv')_2$ was prepared as described previously (Adams et al.(1993) Cancer Research 53, 4026-4034). The extracellular domain of c-erbB-2 was expressed in CHO cells. We have used velocity and equilibrium ultracentrifugation to characterize the ECD and $(sFv')_2$. By equilibrium sedimentation we show that ECD was essentially monodisperse with a molecular weight of about 83,000 and $s_{20,w}$ of 4.3S. The $(sFv')_2$ was also monodisperse with $s_{20,w}$ 3.4S. At high concentrations in the presence of excess ECD, we observed the formation of a complex with a sedimentation coefficient of about 8.1S corresponding to the doubly liganded complex. Sedimentation velocity analysis using signal averaging Rayleigh optics has allowed us to observe the reversible equilibrium between (sFv')2 and ECD in the 0.5-1.0x10^{-7}M range. The $(sFv')_2$ binds two moles of ECD with an intrinsic association constant of ~2x10^7M^{-1}.
Supported by the National Cancer Institute through NCDDG U01-CA51880

Th-Pos230

QUANTITATIVE DNASE I FOOTPRINTING EXPERIMENTS ON THE BINDING OF ECHINOMYCIN TO DNA FRAGMENT CONTAINING CLOSELY SPACED CpG SITES. ((C. Bailly, F. Hamy, M.J. Waring)) INSERM U124, 59045 Lille, France and Dept. of Pharmacology, University of Cambridge, Cambridge CB2 1QJ, UK. (Spon. by D. Graves)

Echinomycin is the chief compound in the series of quinoxaline antibiotics. Direct interaction with DNA is considered central to the molecular mechanism by which the drug exerts its antitumour activity. Spectroscopic and footprinting studies have clearly demonstrated that echinomycin opts preferentially for CpG sequences in DNA. The sequence selectivity is mediated to a large extent by hydrogen bonding between the alanine residues present in the ligand and the 2-amino group of the guanine nucleotides. However, the bases adjacent to the clamped CpG step powerfully influence the DNA recognition process. For example, echinomycin binds better to 5'-ACGT than to 5'-TCGA. Bases remote from the binding sites can also affect the binding to DNA. We have synthesized and cloned a series of 52-mer oligonucleotides each containing 4 CpG dinucleotide steps spaced by 2, 4 or 6 A•T base pairs. The use of DNA fragments containing well-defined echinomycin binding sites embedded in $(A•T)_n$ tracts of varying length provides an opportunity (i) to investigate the effect of flanking sequences on echinomycin-CpG recognition and (ii) to evaluate the accuracy and sensitivity of the footprinting probe as a means of identifying two closely-spaced ligand binding sites. We report the results of a quantitative footprinting study using DNAase I as principal probe.

Th-Pos231

Studying Tumorigenic Mutations of p53 Using a Peptide and DNA Model ((Julie A. Trulson and Glenn L. Millhauser)) Department of Chemistry and Biochemistry, University of California, Santa Cruz Santa Cruz, California, 95064

Mutations in the p53 tumor supressor protein have been implicated in about half of all human cancers. The protein consists of three regions, the transactivation region, the core region, and the oligomerization region. An X-ray crystal structure of the core region bound to a DNA oligonucleotide (Cho *et al., Science,* **254**: 346) revealed that a 9 residue helix is a major element in the binding of p53 to the DNA. We have synthesized this helical region with a N-terminal cysteine to allow labeling with the ESR probe MTSSL, and an alanine-rich C-terminal extension to lengthen the peptide. This peptide,

Ac-CPGRDRRTEEAAAAKA-NH_2

forms helices in physiological conditions. This is an excellent model system which will allow us to study tumorigenic mutations. The helicity of the peptide, in the presence as well as the absence of DNA, will be probed with circular dichroism.

Th-Pos232

CHEMICAL CROSSLINKING OF DAUNOMYCIN TO DNA ((F. Leng, R. Savkur & J. B. Chaires)) Dept. Biochemistry, Univ. Mississippi Med. Center, Jackson, MS 39216–4505; ((W. Priebe)) M. D. Anderson Cancer Center, Univ. Texas, Houston, TX 77030

Daunomycin, a potent anticancer drug, binds tightly to DNA by the process of intercalation. Formaldehyde was found to rapidly and efficiently crosslink the drug to DNA. The rate of the crosslinking reaction was found to be strongly dependent upon the formaldehyde concentration. Comparative crosslinking studies using a series of anthracycline derivatives showed that the 3' NH_2 group on the daunosamine moiety is absolutely required for crosslinking. Comparative crosslinking studies using synthetic polynucleotides showed that the N2 of guanine is absolutely required for crosslinking. Absorbance, fluorescence, and circular dichroic spectroscopies were used to show that the crosslinked drug remains intercalated into DNA. In studies that utilized pBR322 DNA as a substrate in a restriction enzyme assay, it was found that crosslinked daunomycin completely inhibited cutting by Nae I (recognition site 5'GCCGGC), but did not inhibit cleavage by Dra I (recognition site 5'TTTAAA). These studies extend into solution previously published observations from the Wang laboratory that reported crosslinking of daunomycin to oligonucleotides in crystals. *Supported by NCI Grants CA35635 (J.B.C) & CA55320 (W.P.).*

Th-Pos233

MOTIONAL AND EXCHANGE DYNAMICS OF SODIUM IONS BOUND TO DNA QUADRUPLEXES. ((Hong Deng and William H. Braunlin)) Department of Chemistry, University of Nebraska, Lincoln, NE 68588-0304

The binding environments of Na^+ ions on oligomeric DNA quadruplex structures have been examined by ^{23}Na and ^1H NMR. In the presence of Na^+, the dimeric G-quadruplex structure of the oligomer $d(G_4T_4G_4)$ is more stable than the parallel four-stranded complex of the short oligonucleotide $d(T_2G_4T)$. Lineshape analysis of ^{23}Na spectra demonstrate that on the nanosecond timescale of oligomer rotation, a small class of specifically bound Na^+ ions is tightly bound to and tumbles with the oligomer quadruplex. In contrast to the rapid exchange of specifically bound Na^+ ions from the tetrameric G-quadruplex structure of $d(T_2G_4T_2)$, exchange from the dimeric structure is slow on the millisecond timescale of the NMR relaxation. The unusually broad ^{23}Na peak of the Na^+ ions bound specifically to the strong sites of the G-quadruplex $d(G_4T_4G_4)$ indicates the loss of waters of hydration. Monitoring the decay of higher order quadrupolar coherences provides a useful means of determining kinetic rate constants for cation binding for this multiple-site exchange system.

Th-Pos234

CONFORMATIONAL DIFFERENCES IN SHORT AND LONG PIECES OF DNA VIA VIBRATIONAL CIRCULAR DICHROISM ((S.S.Birke and M.Diem)) City Univ New York, Hunter College, New York, NY 10021. (Spon.by S.S.Birke)

Vibrational Circular Dichroism (VCD) spectroscopy is a powerful tool which can be used to elucidate conformational information in both short oligonucleotides and in large polymeric DNA. These VCD features can be predicted qualitatively by use of the exciton model for infrared VCD intensities. There is qualitative agreement between the calculated and observed VCD spectra of poly(dG-dC)$_2$, a number of G and C containing self-complementary tetranucleotides such as 5'd(CGCG)3' or 5'd(CCGG)3', and the dinucleotide 5'd(CG)3' and 5'd(GC)3'. The VCD results of the smallest segments, the dinucleotides, were used to explain the origin of the VCD spectra in canonical B-form DNA segments.

Upon addition of the intercalative drug ethidium bromide to poly(dG-dC)$_2$ and poly(dA-dT)$_2$, the observed and calculated VCD spectra of the physical complexes are consistent with an expected increase in the distance between the bases. A non-intercalative drug, netropsin, appears to be causing a large change in the observed infrared absorption and VCD spectra of poly(dA-dT)$_2$, which may be indicative of a bend in the polymer which causes a difference in the dipolar coupling between the base transition moments.

Th-Pos235

SEQUENCE DEPENDENCE OF DNA HYBRIDIZATION KINETICS AND THERMODYNAMICS ON DNA CHIPS

((M. O. Trulson and R. P. Rava)) Affymetrix, 3380 Central Expressway, Santa Clara, CA 95051.

The kinetics and thermodynamics of hybridization of solution-borne DNA to immobilized DNA oligomer probes is being investigated. Photolithography is employed to synthesize large and highly diverse arrays of immobilized probes, allowing the length and sequence dependence of duplex formation to be elucidated in detail. This format also allows extensive investigation of the energetic cost of single-base mismatches and other defects. Hybridization at the supporting surface is detected by confocal fluorescence imaging microscopy. The measurement of absolute hybrid densities on the surface facilitates the extrapolation of measured duplex-formation energetics to solution values.

Th-Pos236

NA-23 NMR INVESTIGATION OF DNA HAIRPIN FORMATION. ((Srinivas Jampani and William H.Braunlin)) Dept. of Chemistry, Univ. of Nebraska-Lincoln, Lincoln, NE 68588-0304.

The dynamics of DNA hairpin formation by the oligomer d(CGCGTATACGCG) have been well studied. ^{1}H-NMR spectra revealed an equilibrium between a duplex and a loop structure that is sensitive to temperature, counterion(Na^+) and DNA strand concentration (Patel et al(1983):Cold Spring Harbor Symp.Quant.Bio.,47,197-206 and Wemmer et al(1985):Nucl. Acids Res.,13,3755-3772). Here we use ^{23}Na-NMR to probe the dynamics of Na^+ binding to DNA. It is our hypothesis that the conformation of the oligomer d(CGCGTATACGCG) is modulated by the binding of Na^+ ions at specific sites and their exchange with free ions in the aqueous phase. We are testing this idea by investigating the ^{23}Na nuclear magnetic relaxation behavior of Na^+ ions in a solution containing the oligomer d(CGCGTATACGCG). The relaxation behavior of Na^+ ions is being studied as a function of temperature, Na^+ ion and DNA strand concentrations.

Th-Pos237

SOLVATION EFFECTS ON DNA TOPOLOGY AND DRUG INTERCALATION. (J. Ruggiero, U.D.S. Covissi and M.F. Colombo) Dept. of Physics - IBILCE - UNESP S. José do Rio Preto SP 15054-000, Brazil. (Spon. by R. Sanches)

The effects of neutral solutes on the binding of actinomycin D (act D) to natural DNA and synthetic polydeoxynucleotides has been investigated by optical absorption, CD spectroscopy and by agarose gel eletrophoresis. Drug binding constants, obtained from spectroscopic titrations, permits us to group the different neutral solutes used in this study into two categories. a) Alcohols (methanol, ethanol, glycerol and ethylene glycol), decrease the act-D binding constants as the co-solvent concentration increases, wheras b) sugars (sucrose, fructose, glucose and sorbitol) have the opposite effect on binding constant. The titration of the superhelical density of pUC18 with actD, in the presence of alcohols and sugars, was followed by agarose gel eletrophoresis. These experiments indicate that the mode of act-D binding to DNA is still intercalative and independent of the presence or species of solute. The effect of glycerol and sucrose on the distribution of topoisomers, measured by gel eletrophoresis of DNA ligase closure reactions using DNAse nicked plasmids, indicated a pronounced unwind of DNA by glycerol while sucrose apparently does not affect DNA topology. These data emphasize a solute induced effect on DNA elastic properties and on drug and DNA hydration. Titrations carried out with synthetic polydeoxynucleotides have shown that the drug specificity to sequences GC and AC:GT is not altered by the solutes. Thus, an important role of solvation appears to be modulating actD-DNA intercalation, since under the same conditions actD shows no binding to AT polymers. Supported by:FAPESP, CNPq and PADCT.

Th-Pos238

THE WATER EFFECT ON ALLOSTERIC BEHAVIOR OF HEMOGLOBIN PROBED IN WATER\GLUCOSE AND WATER\GLYCINE SOLUTIONS. ((G.O. Bonilla and M.F. Colombo)). Depto. de Fisica, IBILCE-UNESP, São José do Rio Preto 15054-000, São Paulo, Brazil. (Spon.by D.C. Rau)

We have previously proposed a role of hydration in the allosteric control of hemoglobin based on the effect of varying concentrations of polyols and polyethers on the human hemoglobin oxygen affinity and on the solution water activity (Colombo et al., 1992, Science 256, 655). Here, the original analysis is extended, to include the possibility of concomitant solute and water allosteric binding and, by introducing the bulk dielectric constant as variable in our experiments.
We present data which indicate that glycine and glucose influence HbA oxygen affinity to the same extent, despite the fact that glycine increases and glucose decreases the bulk dielectric constant of the solution. Furthermore, we present a detailed derivation of an equation linking changes in O2 affinity to changes in differential solute and water binding, that permits us to critically test the possibility that a neutral solute behave as a heterotropic ligand. Applied to our data, these analyses support our original interpretation that neutral solutes such as sugars, polyethers and glycine indirectly regulate the allosteric behavior of hemoglobin by varying the chemical potential of water in solution, and consequently altering of the chemical potentials of each conformational state of the protein involved in the cooperative binding of oxygen in proportion to their hydration.
Supported by FAPESP and CNPq.

Th-Pos239

THEORETICAL CALCULATIONS OF DNA-CATALYZED REACTIONS: THE HYDROLYSIS OF BENZO[A]PYRENE DIOL EPOXIDE. ((George R. Pack, Linda Wong and Gene Lamm)) University of Illinois College of Medicine, Rockford, IL 61107.

DNA-catalysis of the hydrolysis of the diol epoxides of the procarcinogen benzo[a]pyrene has been studied for over a decade. Studies of others have shown that k_{obs}, the observed rate of hydrolysis (in the absence of DNA), can be represented as the sum of k_o, a spontaneous (pH-independent) contribution and k_H, an acid-catalyzed component: $k_{obs} = k_o + k_H [H^+]$. We have used the Poisson-Boltzmann (PB) equation to map the electrostatic potential and the hydronium ion concentration, $[H^+]$, near a B-form model of DNA. Monte Carlo calculations have been used to find the equilibrium distribution of benzo[a]pyrene diol epoxide (BPDE) in this PB-calculated electrostatic potential. Association constants for non-covalent, non-intercalative binding also have been computed. Structures of BPDE intercalated into the base-pair stack of an 11-mer helical duplex were calculated by energy minimization (AMBER with TIP3P water) and $[H^+]$ was mapped by PB for each of these conformations. From these quantities an estimation of the rate constant, $k_{calc} = \Sigma \{k_o + k_H [H^+]\} [BPDE] v_i / \Sigma [BPDE] v_i$, was made. A picture consistent with the experimental data emerged from these calculations, suggesting that about 90% of the DNA-catalyzed hydrolysis occurs when BPDE is intercalated into the DNA while an additional 10% results from the formation of externally-bound complexes. Maps showing regions in which carbocation formation is predicted to occur will be presented. The preference for formation of covalent adducts at the exocyclic amine group of guanine emerges from this model. (Supported by NIH GM29079.)

Th-Pos240

ON THE MOLECULAR MECHANISMS IN THE RECOGNITION OF THE LIGAND-BINDING POCKET OF HUMAN APOLIPOPROTEIN D

Patel, S.C.,[1] Asotra, K.,[2] Suresh, S.,[1] Dubey, I.,[3] Dubey, A.,[3] Patel, Y.C.,[4] McConathy, W.,[5] McKeown, K.L.[2] and Patel, R.C.[3]
[1]Neurolgy, UCHC, Farmington & Neurobiology Lab., VAMC, Newington, CT; [2]Neurology, UCHC & Signal Transduction Lab., VAMC, Newington, CT; [1]Chemistry, Clarkson Univ., Potsdam, NY; [4]Fraser Lab., McGill Univ., Montreal; [5]Medicine, Univ. North Texas, Fort Worth, TX.

Since our initial discovery of apolipoprotein D (apo D), this lipocalin has been found to be of critical importance in several physiological processes, such as the intracellular binding and transport of biologically important molecules including cholesterol, progesterone and heme-related compounds as well as in pathological processes such as nerve regeneration following injury and in breast and prostate cancer. We have found in cultured astrocytes from the Niemann-Pick type C mutant mouse that the characteristic intracellular accumulation of unesterified cholesterol within lysosomes is associated with defective secretion of apo D. To date, very little is known regarding the molecular details of apo D binding to its ligands. We have found that the fluorophore BIS binds very tightly with human apo D purified from breast cystic fluid, and is competitively displaced by cholesterol and cortisol, forming the basis for accurate determination of the kinetic and thermodynamic parameters using fluorescence spectroscopy. We have established that apo D-BIS complexing occurs with a stoichiometry of 2:1. A significant influence of metal ions on the binding constants has also been found, indicating perturbation of conformational states favoring association. Metal ions inhibit apo D-BIS binding and their chelation with EDTA increases the fluorescence signal of BIS when associated with purified apo D. Sequence analysis of the ligand-binding region of the apo D protein core has been compared with theoretical models. Finally, we have analyzed our experimental data in light of theoretical calculations of the calcium-binding pocket based on the available crystallographic coordinates. Preliminary kinetic data obtained from stopped-flow and termperature-jump experiments suggest that the binding specificity of BIS-apo D complexation is primarily controlled by the K_{off} for the differential transport of multiple ligands of apo D. Funded by the Medical Research Service of the VA & the NIH.

Th-Pos241

FLUORESCENCE STUDIES OF THE INTERACTION OF THIONIN WITH DIPALMITOYLPHOSPHATIDYLGLYCEROL LARGE UNILAMELLAR VESICLES. ((W. Huang and J.D. Bell)) Brigham Young University, Provo, Utah 84602.

The binding of the peptide toxin thionin from *Pyrularia pubera* to dipalmitoylphosphatidylcholine (DPPG) large unilamellar vesicles causes a two-fold increase in the intensity of the fluorescence of the single tryptophan residue of the protein. This increase in intensity is accompanied by a 10 nm blue shift in the emission maximum. The change in fluorescence intensity displayed saturation kinetics as a function of the concentration of vesicles. Furthermore, the apparent affinity of the interaction between thionin and the vesicles increased as a function of temperature in the region of the thermotropic phase transition of the DPPG (about 42 °C). These data were consistent with the conclusion that the tryptophan residue is inserted into the bilayer upon binding of thionin to the vesicle surface and that such is favored in the liquid crystalline phase of the DPPG. Fluorescent probes sensitive to the structure and dynamics of the membrane were used to assess the effect of thionin binding on the bilayer. The ratio of monomer to excimer fluorescence of the probe 1,3-bis-(1-pyrene)propane indicated that the binding of thionin increased the diffusion rate of the pyrene molecules (presumably in the region of the phospholipid acyl chains) below the thermotropic phase transition of the DPPG and decreased the diffusion rate above the phase transition. The fluorescence emission spectra of three probes sensitive to the polarity of their environment (PRODAN, PATMAN and LAURDAN) all showed spectral changes consistent with a decrease in the polarity of the region occupied by the probes. These apparent changes in polarity would be consistent with a decrease in solvent relaxation in response to the excited state of the probes due to the increase in bilayer viscosity provoked by thionin.

Th-Pos242

BINDING MECHANISM OF APOLIPOPHORIN-III TO A PHOSPHOLIPID BILAYER. A SURFACE PLASMON RESONANCE STUDY. ((J.L. Soulages*, Z. Salamon, M.A. Wells and G. Tollin)) Department of Biochemistry and Center for Insect Sciences, University of Arizona, Tucson, AZ 85721 (Spon. by G. Tollin)

The binding of the exchangeable apolipoprotein, apolipophorin-III (apoLp-III), to an egg phosphatidylcholine bilayer as a function of the concentration of diacylglycerol (DG) in the bilayer was studied by surface plasmon resonance spectroscopy. At a DG concentration of 2 mol% the binding of apoLp-III reached saturation. Under saturating conditions apoLp-III forms a closely packed monolayer of ≈ 55 Å thickness, where each molecule occupies ≈ 500 A^2 at the membrane surface. These dimensions are consistent with the molecular size of the apoLp-III molecule determined by X-ray crystallography, if apoLp-III binds to the bilayer in an orientation in which the long axis of the protein molecule lies normal to the membrane surface. In the absence of protein, the overall structure of the lipid bilayer was not significantly changed up to 2.5 mol % of DG. However, at 4 % and 6 % DG the presence of a non-bilayer structure was observed. The addition of apoLp-III to a membrane containing 6 mol % DG promoted the formation of large lipid-protein complexes. These data support a two-step sequential binding mechanism for binding of apoLp-III to a lipid surface. The first step in the binding process is a recognition-process, consisting of the adsorption of apoLp-III to a nascent hydrophobic defect in the PC bilayer caused by DG. This recognition process depends on the presence of a hydrophobic sensor located at one of the ends of the long axis of the apoLp-III molecule. Once the primary binding is achieved, subsequent enlargement of the hydrophobic defect in the lipid surface triggers the unfolding of the apolipoprotein and binding via the amphipathic α-helices. The two-step sequential binding mechanism could be a general mechanism for all exchangeable apolipoproteins.

Th-Pos243

PROTEIN ADSORPTION AND CELL ADHESION ON SURFACES CONTAINING PEG-CONJUGATED LIPIDS. ((Hong Du and S.W. Hui))
Biophysics Department, Roswell Park Cancer Institute, Buffalo, NY, 14263.

Poly-(ethylene glycol) (PEG) conjugated lipids has been used to prolong the circulation time of drug-carrier liposomes. We examined the properties of PEG-conjugated lipids in modulating protein adsorption and cell adhesion on lipid surfaces. Lipid bilayers containing various amount of PEG5000 conjugated phosphatidylethanolamine (PEG-PE) were deposited on solid supports. The adsorption of fluorescence labelled bovine serum albumin (BSA), fibronectin and laminin was measured as functions of concentration of PEG-PE. The adhesion of rabbit erythrocyte, lymphocyte and mouse macrophage to these types of bilayer surfaces were also measured. We found that the major effect of PEG5000 on preventing protein adsorption and cell adhesion is at the same grafting density of less than 1.0 mol% of DSPE-PEG. This holds for each type of protein or cell we tested, although the absolute efficiency is protein or cell dependent. The common threshold of approx. 0.7 mol% is believed to be related to the coverage of the surface area by PEG5000 molecules in the mushroom conformation. At higher grafting densities, the dependence of adsorption and adhesion prevention on grafted lipid concentration is small, indicating that the grafted PEG5000 changes from mushroom to brush conformation at this high concentration. We believe that the inhibition of protein adsorption and cell adhesion by grafted PEG may contribute to the stability and prevention of opsonization of liposomes containing an optimal amount of PEG-conjugated lipids. Lipid bilayers and monolayers deposits containing PEG-conjugated lipids may be used as non-fouling biocompatible surfaces.

Th-Pos244

PRESSURE- AND SALT-INDUCED PERTURBATIONS OF THE NEUROFIBROMIN•RASP21•GTP TERNARY COMPLEX. ((T.L. Hazlett and J.F. Eccleston*))
LFD, Univ. Il U.C., Urbana, Il, *Nat. Inst. Med. Res., London, Mill Hill, U.K.

The interaction between ras p21, GTP and the catalytic domain of neurofibromin, NF1-334, has been examined using hydrostatic pressure and time-resolved fluorescence methods. Neurofibromin activates the GTPase activity of wild type ras p21. To avoid catalysis of GTP in the ternary complex we used the Hras(Leu61) p21 mutant, which binds neurofibromin but is not activated, or the non-hydrolyzable GTP analogue Gpp[NH]p. Association of neurofibromin and ras p21 and the conformation of the ras p21 nucleotide site was monitored through the use of the fluorescent, 2'(3')-O-(N-methylanthraniloyl-) (mant-) derivatives of GTP, 2'-deoxyGTP, and Gpp[NH]p. Upon binding of neurofibromin to ras p21•mant-nucleotide (20°C) under low salt conditions the average fluorescence lifetime of the mant moiety lengthens from approximately 8.5 ns to 10.4 ns. The neurofibromin-induced lengthening of the fluorescence lifetime and the observed spectral blue shift are consistent with an increase in the apolar character of the mant probe, and thus the nucleotide, environment. Differential phase and modulation data show an increase in the slow rotational component of the mant reporter, as would be expected after ternary complex formation. The local motion of the mant probe was relatively unaffected suggesting little change in the nucleotide site flexibility. Application of hydrostatic pressure, to 2.4 kbar, on the ternary complex induced a reversible red shift of the mant fluorescence spectrum and decrease of the sample anisotropy indicating subunit dissociation. The affect of hydrostatic pressure and increasing NaCl concentrations on the ternary complex are examined. Data are discussed in terms of subunit contact sites and the nucleotide site conformational state. Supported by NIH grant RR03155 and the MRC, U.K.

Th-Pos245

THE ENERGETICS & DYNAMICS OF MOLECULAR RECOGNITION BY CALMODULIN. ((M. R. Ehrhardt, J. L. Urbauer & A. J. Wand)) Department of Biochemistry, University of Illinois at Urbana-Champaign, Urbana, Illinois, USA 61801

Calmodulin is a component of many calcium-triggered signal transduction pathways that control a number of critical cellular events. Regulation by calmodulin usually involves calcium-dependent binding to targeted proteins. The calmodulin-binding domains of regulated proteins are generally small, usually contiguous stretches of the primary sequence that bind with high affinity. All domains described thus far display clustering of basic and hydrophobic amino acid residues consistent with the formation of amphiphilic helical structure upon complexation with calmodulin. Though the structure of the final, compact complex is now known, little is known about how calmodulin initially recognizes the domain, how it collapses from an initial encounter complex to the final compact state, or the energetics of these events. We have used the technique of hydrogen exchange to probe the manifold of states accessible to the peptide while bound to calcium saturated calmodulin. The results provide insight into the energetics of collapse from the encounter complex to the final compact state. The pattern of slowing factors indicates that helix-coil transitions in the peptide occur in a more open, reorganized state of the complex, not the compact collapsed state. In this reorganized state, the peptide appears to be extensively solvated and helix-coil transitions create a manifold of states that lead to transient breakage of intrahelical hydrogen bonding. Free energies for the reorganization and the span of the helix-coil transitions are estimated to be 5.5 and 2.5 kcal/mole, respectively.

This work was supported by grant DK39806 from the NIH.

Th-Pos246

FLEXIBILITY AND CIRCULAR DICHROISM CHARACTERISTICS OF POLY-α (2→8)SIALIC ACIDS. Slavo Bystricky* and Shousun C. Szu, Unit on Molecular Biophysics & Biochemistry, LDMI, NICHD, NIH, Bethesda, MD 20892 and *Institute of Chemistry, Slovak Academic of Sciences, Slovakia.

The capsular polysaccharide of meningococcus group B and E. coli K1, poly-α(2→8) sialic acid (PSA), is an essential virulence factor for these pathogens. PSA also appears on the non-reducing end of mammalian neural cell adhesion molecule (N-CAM) with lower degree of polymerization. The linear charge distance between its carboxyls is ~ 6 A. The intrinsic viscosity of PSA showed that this polymer is more flexible than other polyelectrolyte such as double or single strand DNA. CD of PSA with high polymerization (n>50) showed no conformational transition between 4-60°C. Further, there was no observed salt-induced conformational jump of PSA -- a phenomenon common for polyanions with ordered structure. Compiled data of CD at 225nm for PSA oligosaccharides (n=2 to 17) showed the internal units become more flexible as the length increases. Cooperative conformational transition was not observed for PSA.

Th-Pos247

HARD AND SOFT SULFATE AND SULFONATE ANIONS IN PROTEIN PRECIPITATION-BIORECOGNITION. Rex Lovrien and Daumantas Matulis, Biochemistry Dept., Univ. Minnesota, St. Paul 55108

Proteins can be precipitated and coprecipitated out of solution by over a dozen different techniques. Selection of techniques determines cost, scaleability, unit process interfacing, feasibility of upstream vs. downstream operation. Molecular principles involved range from completely pushing methods (sulfate kosmotrope salting out) to completely pulling with matrix organic sulfonate ligands at the other extreme. Some methods are hybrids, both push and pull. In all cases how water is handled is an unseen but crucial factor in the overall equilibria. Sulfate salts and sulfate/sulfonate organic ligands exert themselves by mixtures of factors expressed by how hard vs. how soft they are in the Pearson sense. Water molecules, aliphatic hydrocarbons are hard, poorly polarizable. Aromatics are soft, and polarizable. Molecular volumes of large soft ligands get important when they displace water and lower average dielectric constants around ligands exerting electrostatic forces. The large (huge) differences in concentrations of compounds able to force precipitation indicate what several of the precipitation mechanisms rest on, vis a vis sulfate/sulfonate softness or hardness, their reliance on pushing vs. pulling mechanisms.

Th-Pos248

SELF-ASSOCIATION OF IL-8 AND ITS MUTANTS: EFFECTS OF IONIC STRENGTH AND PH((Jun Liu, Henry B. Lowman, Caroline A. Hébert and Steven J. Shire))Department of Pharm R&D, Protein Engineering and Immunology, Genentech, Inc., 460 Pt. San Bruno Blvd., South San Francisco, CA 94080.

IL-8 is a chemoattractant involved in many inflammation processes. The NMR and X-ray crystallography data show that it essentially exists as a non-covalent linked homodimer at high concentration (Clore, G. M. *et al.* (1990) *Biochemistry* **29**, 1689; Baldwin, E. T. *et al.*(1991) *Proc. Natl. Acad. Sci. USA* **88**, 502.). Although several in vitro studies suggest that IL-8 is exclusively monomeric at the nanomolar physiological concentrations at which it displays maximal chemotactic activity (Paolini, J. F. *et al.* (1994) *J. Immunol.* **153**, 2704.), it is still unclear whether the IL-8 is able to dimerize on the cell surface. In this study, the self-association of IL-8 and its mutants were examined in different buffer conditions by analytical ultracentrifugation. We show that IL-8 self-associates strongly to a dimer (Kd<10 nM) in 50 mM phosphate buffer at pH 5.3, whereas in 0.15 M PBS at pH 7.2, the self-association is considerably weaker with Kd on the order of μM. The effects of ionic strength and pH on thermodynamic properties of IL-8 dimerization and conformation changes were followed by analytical ultracentrifugation and CD. In addition, we have also generated several mutants with reduced hydrophobicity on the dimer interface. We show that these variants have much weaker association constants and appear to be independent on the change of buffer conditions.

SODIUM/CALCIUM EXCHANGER

Th-Pos249

CHARACTERIZATION OF THE Na/Ca EXCHANGER cDNA IN DROSOPHILA. ((C. Valdivia, P. Kofuji, W. J. Lederer and D. H. Schulze)) Departments of Physiology and Microbiology and Immunology, University of Maryland School of Medicine, Baltimore MD 21201.

Using classical approaches of homology screening we have cloned the full length cDNAs for the Na/Ca exchanger from Drosophila using a human cDNA as a probe. The Drosophila Na/Ca exchanger has many of the same characteristics of previously described mammalian exchanger, a series of N terminal and C terminal hydrophobic regions suggesting this protein to be a multipass membrane protein and a large intracellular loop between these transmembrane regions. The overall homology between the human and Drosophila is 44% identity and 60% including similar amino acid substitutions. The Drosophila cDNA is more similar to the Na/Ca exchanger found in most tissues (NCX1) than the recently described second Na/Ca exchanger (NCX2). Notable differences between the human and Drosophila sequences : the absence of an N-terminal glycosylation site in Drosophila, the Drosophila sequence is shorter than the human because of three sets of deletions in the intracellular loop region, one of these deletions (45AA) in the Drosophila sequence results in the loss of some of the region that contains the cassette type exons created by alternative splicing of exons in the mammalian gene. We have independent cDNA clones from Drosophila that display sequence variation at the equivalent position in the mammalian cDNAs where alternative splicing has been demonstrated, suggesting a further parallel between the Drosophila and mammalian Na/Ca exchanger cDNAs. We have also used the Drosophila cDNA to map the Na/Ca exchange gene to chromosome 3 (93A-B) using polytene chromosomes.

Th-Pos250

ANOMALOUS REGULATION OF THE Na^+-Ca^{2+} EXCHANGER FROM *DROSOPHILA*. ((L.V. Hryshko, D.A. Nicoll, S. Matsuoka, J.N. Weiss, E. Schwarz, S. Benzer, and K.D. Philipson)) UCLA Cardiovasc. Res. Labs, Los Angeles, CA 90024 and Div. Biology, CIT, Pasadena, CA 91825.

The Na^+-Ca^{2+} exchanger from *Drosophila* (Schwarz and Benzer, submitted) was expressed in *Xenopus* oocytes and characterized electrophysiologically using the giant excised patch technique. This protein shares 48% amino acid identity to the canine cardiac Na^+-Ca^{2+} exchanger, NCX1. The Na^+-Ca^{2+} exchanger from *Drosophila* exhibits similar properties to previously characterized Na^+-Ca^{2+} exchangers (NCX1 and NCX2) including Na_i affinities, IV relationships, and sensitivity to the peptide inhibitor, XIP. However, the Na^+-Ca^{2+} exchanger from *Drosophila* exhibits a completely opposite response to cytoplasmic Ca^{2+}. Both NCX1 and NCX2 are stimulated by cytoplasmic Ca^{2+} in the micromolar (0.1-10 μM) range. This stimulation of exchange current is mediated by occupancy of a regulatory Ca^{2+} binding site distinct from the Ca^{2+} transport site. In contrast, the Na^+-Ca^{2+} exchanger from *Drosophila* is inhibited by cytoplasmic Ca^{2+} over this same Ca^{2+} concentration range. The inhibition of exchange current is evident for both forward and reverse modes of transport. Pre-incubation of patches with micromolar cytoplasmic Ca^{2+} led to inhibition of subsequent currents whereas large initial currents were observed when patches were pre-incubated in zero Ca^{2+} containing solutions. Thus, occupancy of the putative regulatory Ca^{2+} binding site regulates exchange activity independent of Ca^{2+} at the transport site. These data should provide a rational basis for subsequent structure-function studies targeting the Ca_i regulatory mechanism.

Th-Pos251

IDENTIFICATION OF IMPORTANT AMINO ACID RESIDUES OF EXCHANGER INHIBITORY PEPTIDE XIP ((Z. He and K. D. Philipson)) Cardiovascular Research Laboratory, UCLA School of Medicine, Los Angeles, CA 90024. (Spon. by D. A. Nicoll)

The Na^+-Ca^{2+} exchanger plays an important role in cardiac contractility by extruding Ca^{2+} across the plasma membrane during excitation-contraction coupling. A 20 amino acid peptide, XIP, synthesized to mimic a region of the exchanger inhibits the activity of the exchanger (JBC 266:1014-1020). We are attempting to identify amino acids of the XIP peptide which are essential for inhibitory function. XIP peptides with various modifications were synthesized and Na^+-Ca^{2+} exchange activity was then assayed in the presence of these peptides as $^{45}Ca^{2+}$ uptake into Na^+-loaded cardiac sarcolemmal vesicles. Deletion of the first 5 residues at the N-terminus or the last 7 residues at the C-terminus, respectively, caused modest decreases in the inhibitory activity of XIP, whereas deletion of the first 8 residues at the N-terminus or the last 9 residues at the C-terminus completely eliminated inhibitory activity. In addition, replacement of tyrosines 6, 8, 10, and 13 with tryptophans did not change the inhibitory activity of XIP. However, XIP inhibitory activity was eliminated when all four tyrosine residues were replaced by alanine. Moreover, replacement of arginine 12 or 14 with alanine decreased inhibitory activity, while replacement of other positively-charged residues with alanine did not affect inhibitory activity. Our data suggest that positively-charged residues, arginines 12 and 14, and aromatic residues, tyrosines 6, 8, 10, and 13 play an important role in interactions with the exchanger.

Th-Pos252

TISSUE-SPECIFIC EXPRESSION OF THE SECOND ISOFORM OF THE Na/Ca EXCHANGER, NCX2 ((B.D. Quednau, N. Brecha, and K.D. Philipson)) Cardiovascular Research Laboratory, UCLA and V.A. Medical Center, Los Angeles, CA 90024

The Na/Ca exchanger NCX1 first cloned from heart is also present in several other tissues. Alternative splicing of NCX1 mRNA generates a wide variety of tissue-specific splicing isoforms. Recently, Li et al. (JBC 269: 17434, 1994) have cloned a second Na/Ca exchanger from rat brain, NCX2, which is most abundant in brain and skeletal muscle. In comparison to NCX1, the NCX2 mRNA lacks a stretch of 111 nts at a position where alternative splicing of NCX1 occurs. We have investigated the tissue-specific expression of NCX2 in rat by RT-PCR using primer pairs spanning the missing nucleotide sequence. We could detect NCX2-specific transcripts in almost all tissues without finding any alternatively spliced isoforms. Less sensitive Northern Blot analysis confirmed that NCX2-specific mRNA is abundant only in brain and skeletal muscle. To further investigate the expression of NCX2 in the brain we performed in situ hybridization and immunocytochemistry with rat brain sections. A NCX2-specific RNA-probe detected transcripts in the Purkinje cell and granular cell layers of the cerebellar cortex, the hippocampus, the midbrain, the cerebral cortex, and to a lesser extent in the olfactory bulb. Similar rat brain sections were analyzed by immunocytochemistry using a polyclonal antibody against a fusion protein which contained 302 aa of the loop region of NCX2. The staining shows a pattern of expressed protein that corresponds to the in situ hybridization data. The distinct distribution and high abundance of NCX2 in the brain suggests that the protein might play an important role in this tissue.